EVALUATION OF A GEOSYNTHETIC CAPILLARY BREAK

A Thesis Submitted to the College of

Graduate Studies and Research

In Partial Fulfillment of the Requirements

For the Degree of Master of Science

In the Department of Civil and Geological Engineering

University of Saskatchewan

Saskatoon

By

Kevin D. Park

Keywords: engineered soil cover, capillary break, geosynthetic

Permission to Use

In presenting this thesis in partial fulfilment of the requirements for a Postgraduate degree from the University of Saskatchewan, I agree that the Libraries of this University may make it freely available for inspection. I further agree that permission for copying of this thesis in any manner, in whole or in part, for scholarly purposes may be granted by the professor or professors who supervised my thesis work or, in their absence, by the Head of the Department or the Dean of the College in which my thesis work was done. It is understood that any copying or publication or use of this thesis or parts thereof for financial gain shall not be allowed without my written permission. It is also understood that due recognition shall be given to me and to the University of Saskatchewan in any scholarly use which may be made of any material in my thesis.

Requests for permission to copy or to make other use of material in this thesis in whole or part should be addressed to:

Head of the Department of Civil and Geological Engineering

University of Saskatchewan

Saskatoon, Saskatchewan

S7N 5A9

ABSTRACT

One of the major issues in the successful decommissioning of any waste disposal system is to mitigate the spread of contaminants into the surrounding environment. In many instances this is achieved by reducing amounts of net percolation and/or oxygen diffusion into the underlying waste. An engineered cover system incorporating a capillary break is a common solution to this problem. However, traditional soil capillary breaks can often be impractical for large facilities where desirable construction materials are not readily available.

The primary objectives of this research were to show the initial steps in the development of a new type of geosynthetic product, namely a geosynthetic capillary break (GCB). This new product, composed of a nonwoven geotextile coupled with a fine-grained rock flour, will function similar to, and has the possibility of replacing traditional, soil capillary breaks in many applications.

The specific objectives of this research were to: *i)* determine the pertinent material parameters of the materials used to evaluate the GCB; *ii)* examine one-dimensional column testing of a typical engineered soil cover system incorporating the GCB; and *iii)* model the cover systems to better understand current performance and predict long-term hydraulic performance of the GCB.

The GCB was evaluated based on the objectives outlined above. The material characterization consisted of the selection of suitable materials for the GCB, as well as the determination of unsaturated properties. The results indicated that a geotextile-rock flour combination would develop a capillary break within an engineered cover.

The one-dimensional column tests evaluated four cover systems. Soil thicknesses of 30 and 60 cm were utilized, with one column of each cover thickness incorporating the GCB. The columns were tested under both high evaporative fluxes and high infiltration rates over the course of 111 days. The measured results showed that there was less moisture movement in columns that incorporate the GCB.

A coupled soil-atmospheric finite element model was used to develop a predictive model for the cover systems. Analyses were performed to simulate the results of the column testing. The material properties obtained from this model were used to evaluate the hydraulic performance of an engineered cover system incorporating the GCB for a minesite in Flin Flon, MB. The results from the predictive modeling showed that moisture infiltration is reduced approximately 80% due to the inclusion of the GCB for the conditions simulated in this research. Oxygen diffusion was also reduced by 20 to 25% with the inclusion of the GCB under the simulated conditions.

ACKNOWLEDGEMENTS

I wish to express my sincere appreciation to my supervisor Dr. Ian Fleming. His wealth of knowledge as well as enthusiasm towards my work was invaluable. During my time as a graduate student I have come to consider him a friend as well as a mentor. My advisory committee, Dr. Sharma and Dr. Fredlund were also invaluable throughout my research program.

My studies were funded by O'Kane Consultants, NSERC, the University of Saskatchewan, as well as Terrafix Geosynthetics. Without this financial assistance my research would not have been possible.

The staff at O'Kane Consultants Inc. deserves recognition for their support and guidance throughout the course of my research.

Mr. Alex Kozlow and Mr. Dale Pavier also deserve recognition for the assistance that they gave me throughout the laboratory program of my research. I would also like to acknowledge the CANSIM at the University of Saskatchewan for use during the finite element portion of my research.

A special thank you to Alison Kirkpatrick for decreasing my workload by compiling large amounts of climate data and for looking after my columns when needed. My fellow graduate students also deserve acknowledgement for their friendship and assistance (Alexis and Heather, this includes you).

Lastly, I would like to thank my family and friends for their support during the completion of my research.

Dedication

This thesis is dedicated to my grandfather, Henry Clark. He passed away in the fall of 2003, shortly before the start of my research.

TABLE OF CONTENTS

LIST OF TABLES

LIST OF FIGURES

LIST OF APPENDICES

CHAPTER 1 INTRODUCTION

1.1 Background

A major problem facing the Canadian mining industry today is acid mine drainage. Tailings or waste rock containing sulphide minerals, which come into contact with oxygen and water, will generate sulphuric acid resulting in acid mine drainage (Nicholson et al., 1989). Therefore, one of the major issues in the successful decommissioning of any waste disposal system is to mitigate the spread of contaminants into the surrounding environment by limiting inward oxygen and moisture fluxes. In the past, flooding of the waste with water has been deemed acceptable in reducing the amount of oxygen diffusion, and therefore, acid generation. However, over the past few years, engineered soil covers have become increasingly acceptable as an alternative to flooding (Swanson et al., 2003).

An engineered cover system involves selective layering of different soils with the primary goals of reducing the inward transport of oxygen and reducing water infiltration into the waste material (O'Kane et al., 1998). Often, the soils are layered in such a manner that a capillary break develops within the system.

A capillary break is designed as an unsaturated system and involves the selective layering of materials with significantly different textures. A relatively coarse-grained material, such as a sand or gravel, is commonly placed below a fine-grained material, such as a silt or clay, to achieve such an objective (Nicholson et al., 1989). Since the elevation above the water table increases, the pressure head in the soils progress in a

negative direction and the air-entry value of the materials are approached. However, the pressure head in the overlying fine-grained layer will not become substantially more negative than that corresponding to the residual pressure head in the coarse layer (Nicholson et al., 1989). At this negative pressure head, the hydraulic conductivity of the coarse grained material is low and a transient condition is developed with no further decline in the pressure head, allowing the fine-grained material to remain saturated. Akindunni et al. (1991) examined this phenomenon numerically and concluded that it was hydraulically possible to maintain a near saturated layer of fine-grained material above a coarse-grained material, even with the water table at a depth below the surface of the waste.

Nicholson et al. (1989) showed that the effective diffusion coefficient for oxygen decreases up to four orders of magnitude as the degree of saturation increases from zero to one hundred percent for a given soil. Therefore, the inclusion of a capillary break as part of an engineered cover system will reduce inward oxygen transport due to the presence of a near saturated fine-grained layer of material above the waste.

Due to the increased degree of saturation of the overlying fine-grained layer, Stormont and Morris (1998) concluded that a capillary break was also a suitable means to prevent downward moisture movement. The water content of the fine-grained material was increased above what would be associated with free drainage due to the placement of the underlying coarse-grained material. This ability to sustain increased water content, thus, increased the storage capacity of the material. An increase in the storage capacity in the overlying material allowed more precipitation to remain stored in

the cover system and therefore, allowed less moisture to move downward into the waste material.

The initial steps in the development and evaluation of a new type of capillary break; namely a geosynthetic capillary break (GCB) were evaluated. The proposed GCB, composed of a layer of fine-grained rock flour sandwiched between two layers of nonwoven geotextile, functioned as a capillary break as part of an engineered cover system.

Nonwoven geotextiles are used in engineering practice as a drainage layer or to enhance the rate of dissipation of excess pore-water pressures due to increasing overburden stress. Due to high in-plane hydraulic conductivity, geotextiles perform well in supplying horizontal drainage. However, studies have shown that geotextiles have not always behaved as desirable drainage materials (Iryo and Rowe, 2003). After heavy rainfalls, and under unsaturated conditions, water has been known to pond to depths of 10 cm above a geotextile, increasing the pore-water pressures in the soil (Dierickx, 1996 and Richardson, 1997). Henry (1990 and 1995), Stormont and Morris (2000), and Henry and Holtz (2001) evaluated the concept of geotextiles used as moisture limiting barriers in unsaturated soils. The change in hydraulic behavior of an unsaturated, layered soil system due to the inclusion of a nonwoven geotextiles was examined and it was concluded that the placement of the geotextile was effective in mitigating moisture migration in unsaturated soils. Measurements of the unsaturated hydraulic properties of nonwoven geotextiles have shown that the behavior was consistent with that of a uniform, coarse material such as a pea gravel (Stormont and Morris, 2000).

The proposed capillary break combined the coarse-grained unsaturated hydraulic behavior of the nonwoven geotextile with fine-grained rock flour. The geotextile was placed beneath the rock flour, acted as the capillary break, and allowed the rock flour to remain at a higher degree of saturation than under free draining conditions. The near saturated rock flour will reduce inward oxygen transport, while the nonwoven geotextile inhibited moisture migration into the underlying waste.

1.2 Research Objectives

The main research objectives were to design and evaluate a geosynthetic capillary break (GCB) capable of limiting moisture and oxygen migration as part of an engineered soil cover system. To achieve the objectives the research was divided into three parts:

- Determination of the pertinent material parameters for materials used to evaluate the GCB;
- One-dimensional column testing of a typical engineered soil cover system incorporating the GCB; and
- Modeling of the cover systems to understand current performance and predict long-term hydraulic performance.

1.3 Scope

The scope of the thesis shall be limited to the design and evaluation of the geosynthetic capillary break (GCB). The design of the GCB included selection of suitable materials and measurements of pertinent physical properties. The evaluation of the GCB included one-dimensional column testing and analytical and numerical modeling. The GCB was evaluated based on its ability to reduce moisture movement and to potentially mitigate oxygen diffusion into underlying waste materials. The ability

of the GCB to reduce moisture movement in an engineered cover system was verified using the results of the one-dimensional column testing. The results of this testing program were used to construct a finite element model of an engineered cover system to predict and evaluate downward oxygen diffusion.

1.4 Organization of Thesis

The thesis was divided into seven chapters. Chapter 2 provides a literature review of past works that relate to this current research. The basic theoretical aspects related to the evaluation of the GCB are discussed in Chapter 3. Chapter 4 outlines the laboratory program that was undertaken in order to determine key material properties and to conduct field-scale testing, while Chapter 5 presents the results obtained from these tests. Chapter 6 includes the analytical and numerical modeling programs for the evaluation of the GCB and also the analysis and discussion of their results. Lastly, Chapter 7 presents conclusions that can be drawn from this work and outlines future research programs that may be undertaken.

CHAPTER 2 LITERATURE REVIEW

2.1 Introduction

Chapter 2 examined past works which were relevant to the evaluation of the geosynthetic capillary break. Literature regarding the determination of the unsaturated properties of nonwoven geotextiles, including testing methods and results were reviewed. The ability of an unsaturated geotextile to reduce moisture migration in soils was also examined. Lastly, pertinent research on the theory and implementation of engineered cover systems as barriers to oxygen and moisture movement into reactive wastes were summarized.

2.2 Unsaturated Hydraulic Properties of Geotextiles

2.2.1 General

An engineered cover system is an unsaturated system. Therefore, an understanding of the unsaturated properties of the materials used in the system was imperative to the success or failure of the cover design. For this work, nonwoven geotextiles were evaluated as possible materials included in the cover system design. The following section focused on the background on the determination of the unsaturated properties of geotextiles including water characteristic curves and hydraulic conductivity functions.

2.2.2 Nonwoven geotextiles

Past research on the determination of the unsaturated properties of geotextiles were conducted by Stormont et al. (1997), Stormont and Morris (2000), Lafleur et al. (2000), Knight and Kotha (2001), and Iryo and Rowe (2003). Test methods for the

determination of the water characteristic curve for nonwoven geotextiles were examined by the researchers. In general, the results showed that the geotextile-water characteristic curve (GWCC) were similar to that one might anticipate for uniform, coarse soil such as a pea gravel.

Stormont et al. (1997) examined four nonwoven polypropylene geotextiles (Table 2-1) with the Klute (1986) method (Figure 2-1) adapted to measure the geotextile-water characteristic curve (GWCC). The apparatus consisted of a 90 mm diameter ceramic porous plate with an air-entry value of 20 kPa. The plate was fitted into a filter funnel which was connected to a 110 mm diameter bottle. The suction head in the specimen was changed by raising or lowering the bottle to create a head differential between the porous plate and the elevation of the reservoir. The water in the specimen was allowed to equilibrate with the water in the porous plate, and the water content of the sample was determined (Stormont et al., 1997).

A dry, circular, 60 mm diameter specimen was placed on top of the porous plate and a 225 g mass was placed on top of the specimen to ensure hydraulic contact between the geotextile and the porous plate. A measurement was taken at an initial suction head of 600 mm, and decreased with subsequent increments of 150 mm until the geotextile absorbed an appreciable amount of water. The suction head increments were reduced to as low as 20 mm near zero suction. After the specimen reached equilibrium at zero suction the process was reversed and the bottle was lowered incrementally to the suction head of 600 mm (Stormont et al., 1997).

Table 2-1. Stormont et al. (1997) properties of specimens.

Product Designation	Manufacturing Process	Mass per Unit Area (g/m^2)	Apparent Opening Size (mm)
A1	Stable fibres	339	0.15
A2	Stable fibres	543	0.15
B1	Continuous fibres	340	0.18
B2	Continuous fibres	540	0.15

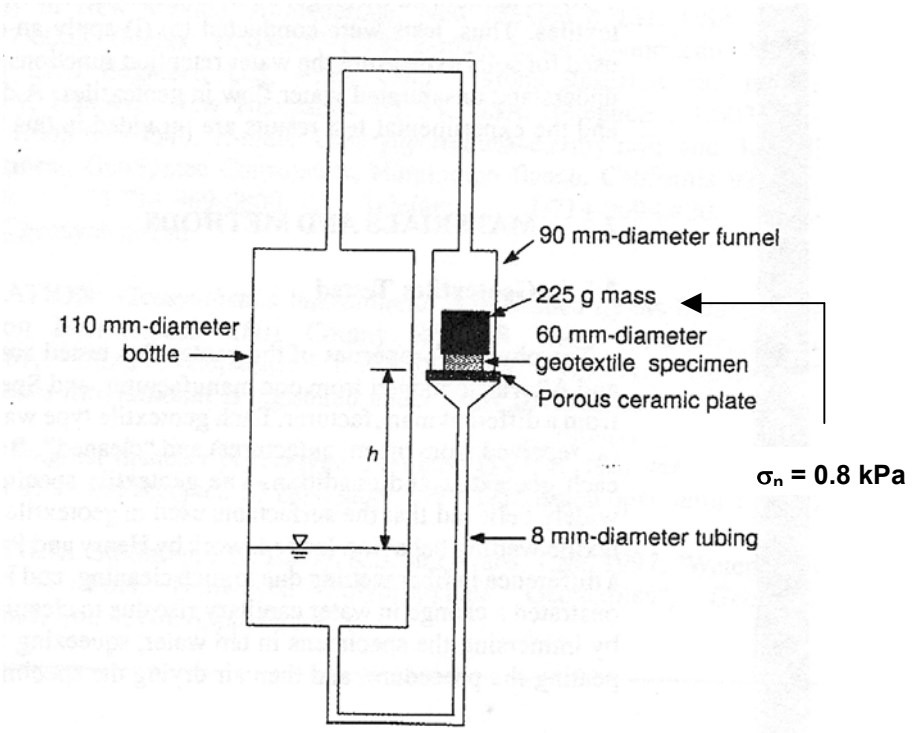

Figure 2-1. Klute (1986) test apparatus.

At each increment the specimen was removed from the funnel and weighed to determine its water content. Equilibrium periods were noted to range from 24 to an excess of 48 hours (Stormont et al., 1997).

Each geotextile in Table 2-1 was tested in two conditions; "new" and "cleaned". The "new" specimens were tested as received from the manufacturer, while the "cleaned" specimens were tested after immersing the specimens in tap water and squeezed by hand, followed by air drying the specimens. The specimens were cleaned in order to

examine the change in wetting behaviour of the geotextile after the removal of surfactants from the product used in the manufacturing process (Stormont et al., 1997). The measured GWCC are shown in Figures 2-2 and 2-3.

The results showed that the water-entry head for the geotextiles studied ranged from 0 to 0.3 kPa and that the air-entry head for the specimens were approximately 0.5 kPa; which was similar to the behaviour exhibited by pea gravel (Stormont et al., 1997). Stormont concluded that washed specimens contained more water at comparable suction heads than new specimens of the same product, which were attributed to the removal of possibly hydrophobic manufacturing surfactants.

Stormont and Morris (2000) examined both the water-characteristic curve as well as the unsaturated transmissivity function for two nonwoven geotextiles. The properties of the geotextiles tested are shown in Table 2-2. The Klute (1986) hanging column apparatus (Figure 2-1) was utilized to measure the water characteristic curves for the two specimens, following the test procedure outlined by Stormont et al. (1997). The geotextiles were tested as received from the manufacturer ("new"), with the results presented in Figure 2-4. The affect of the intrusion of soil particles on the unsaturated hydraulic conductivity of the geotextile was also examined. Geotextile A was tested along the wetting path with sand, silt, and clay sized particles intruded. The results are presented in Figure 2-5 with the data indicating that the intruded soil caused the specimens to wet at a higher suction head. The data was found not to be significantly affected by the type of soil intruded (Stormont and Morris, 2000).

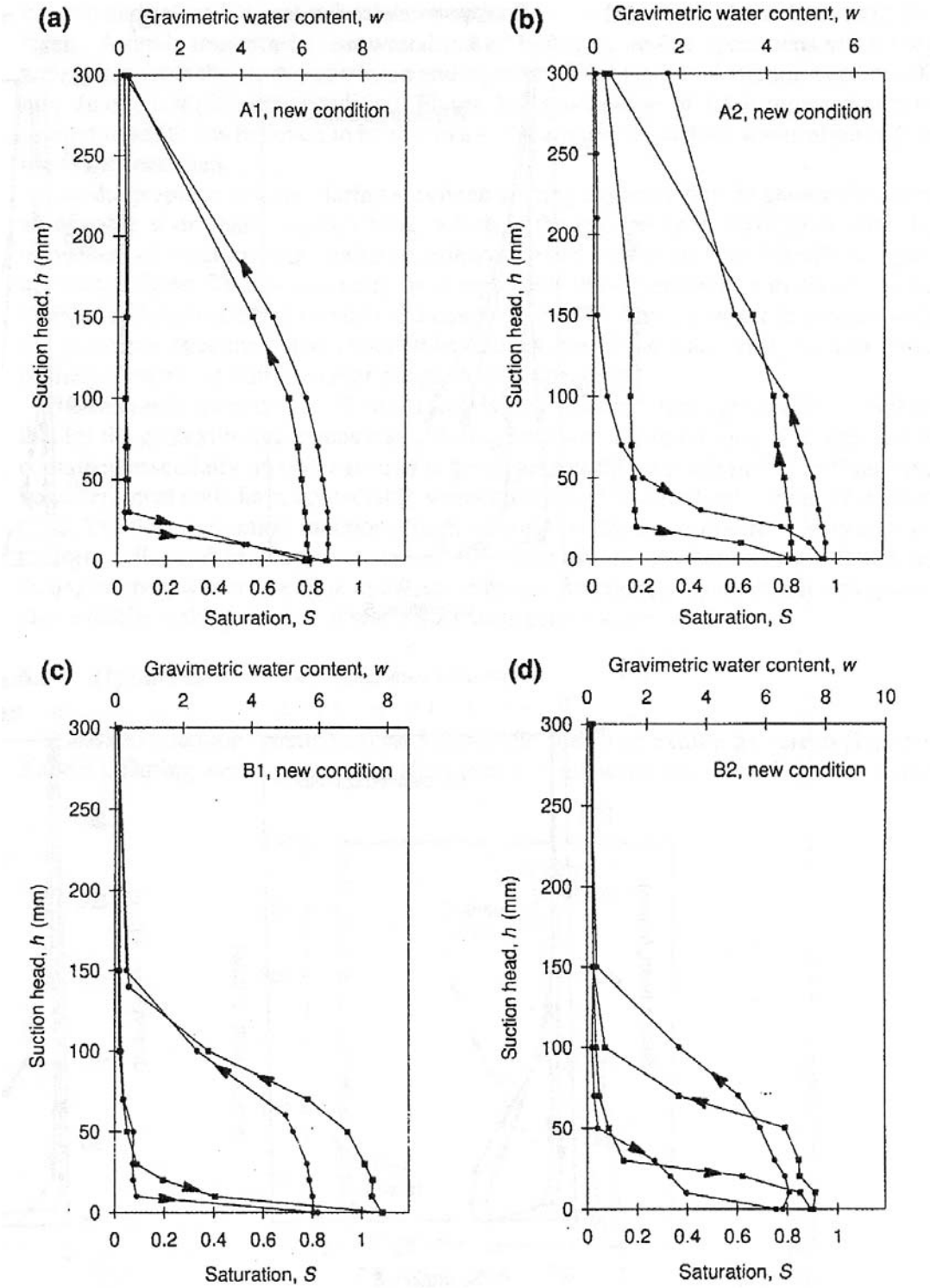

Figure 2-2. Geotextile-water characteristic curves for "new" specimens: (a) Geotextile A1; (b) Geotextile A2; (c) Geotextile B1; (d) Geotextile B2 (Stormont et al., 1997).

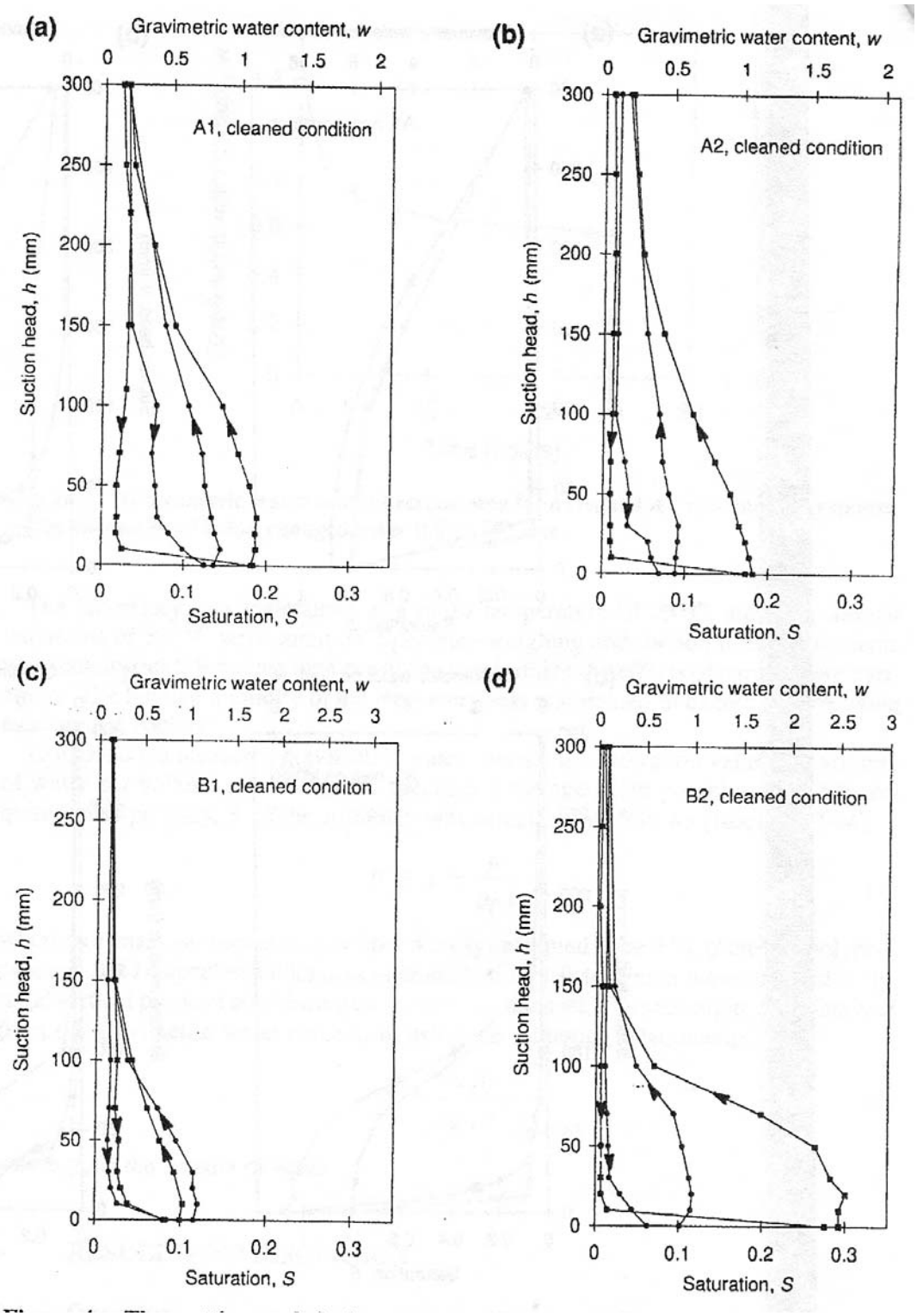

Figure 2-3. Geotextile-water characteristic curves for "cleaned" specimens: (a) Geotextile A1; (b) Geotextile A2; (c) Geotextile B1; (d) Geotextile B2 (Stormont et al, 1997).

Table 2-2. Stormont and Morris (2000) properties of specimens.

Product	Polymer Type	Mass per Unit Area (g/m^2)	Apparent Opening Size (mm)	Thickness (mm)	Saturated Transmissivity (mm^2/s)
A	Polyester	266	0.04	1.8	0.04
B	Polypropylene	340	0.18	5.9	0.18

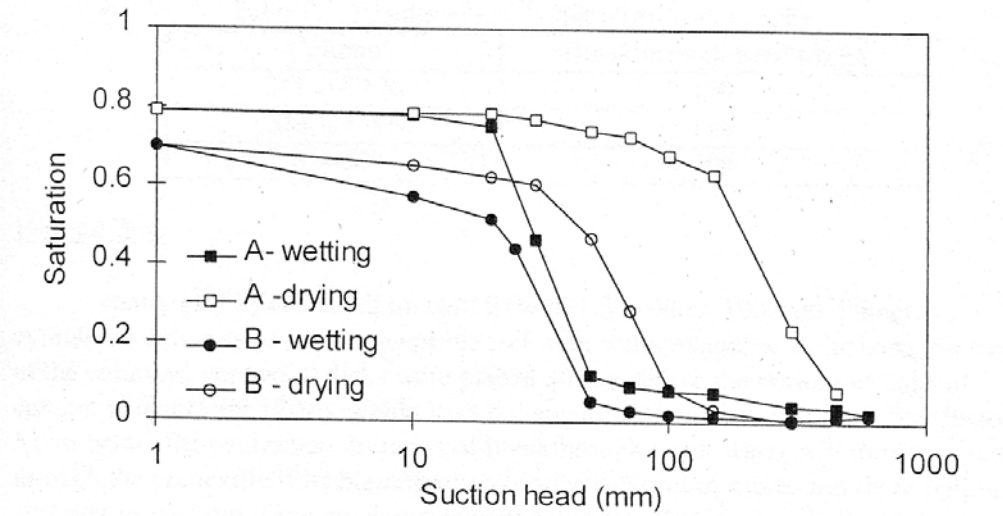

Figure 2-4. Geotextile-water characteristic curves for "new" specimens (Stormont and Morris, 2000).

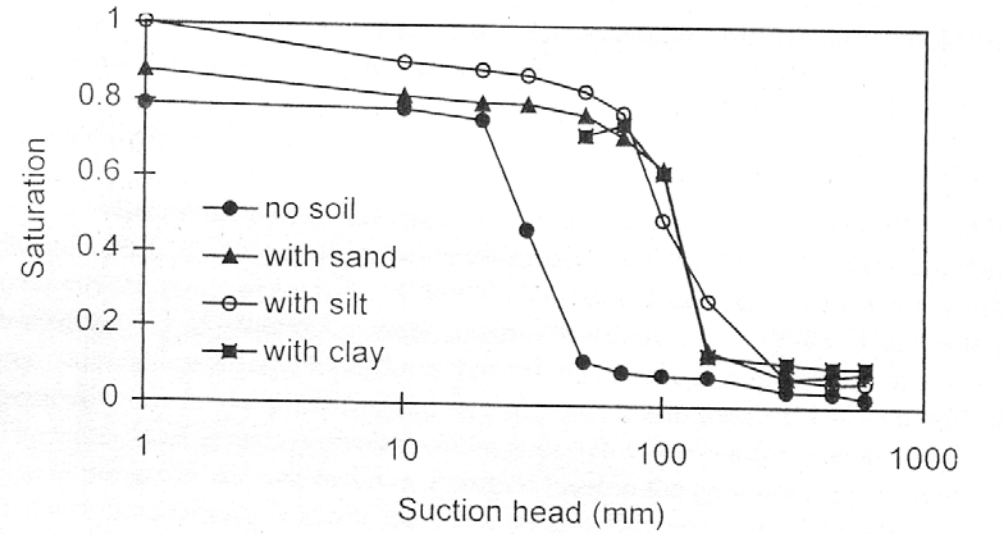

Figure 2-5. Geotextile-water characteristic curves for Geotextile A with intruded soil (Stormont and Morris, 2000).

Stormont and Morris (2000) measured the in-plane transmissivity of the geotextiles at suction increments along both the wetting and drying portions of the water characteristic curves in order to develop the unsaturated transmissivity function for the geotextiles. An unsaturated permeameter consisting of a platform extending above two reservoirs of water was used as the testing apparatus. The geotextile lied on the platform with the ends submerged in the reservoirs. The water in the reservoir was filled to, or below the elevation of the platform. The suction head in the geotextile was calculated using a steady-state solution used to calculate transmissivity under positive pressures (Stormont and Morris, 2000).

Figure 2-6 shows the measured transmissivities as a function of suction for the two geotextiles. The research study noted that, for initial wetting, the specimens were non-conductive until the suctions reached to 0.35 kPa and 0.25 kPa for Geotextiles A and B respectively. During the drying, the specimens remained transmissive to suctions over 1 kPa. The results suggested that the geotextiles wetted and became transmissive under suctions, but not until the reduction of suction head in the soil reached around 0.3 kPa (Stormont and Morris, 2000).

Lastly, Stormont and Morris fitted the results of the measured water characteristic curve tests with van Genuchten (1980) parameters and compared the predicted transmissivity function to that measured in the laboratory. The results showed good fit and suggested that it may be possible to apply functions commonly used for soils to nonwoven geotextiles.

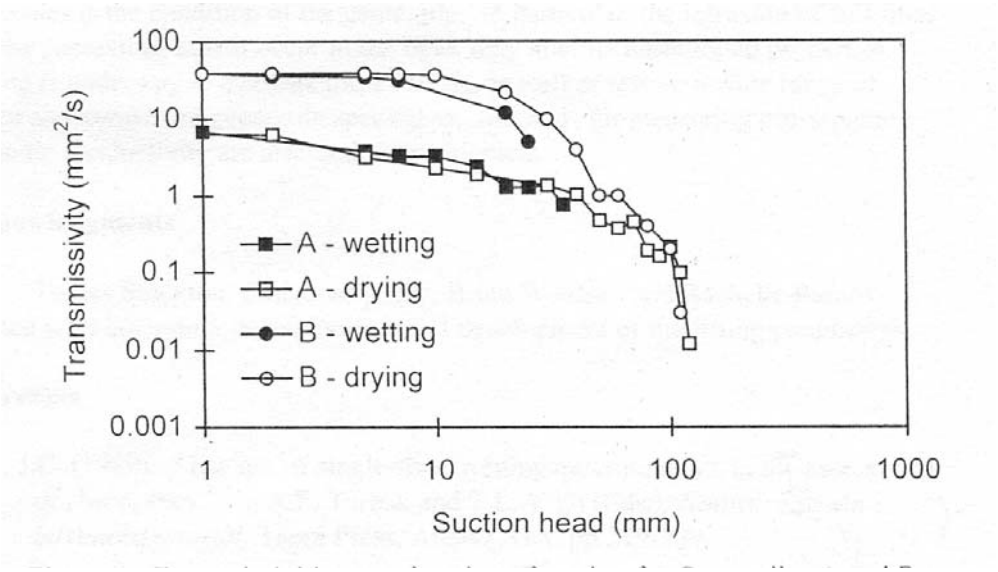

Figure 2-6. Measured transmissivity functions for nonwoven geotextiles (Stormont and Morris, 2000).

The research program of Lafleur et al. (2000) also looked at the application of functions for unsaturated hydraulic behaviour of soils to nonwoven geotextiles. The objectives of the research were to show the impact of fibre type on the hydraulic properties of unsaturated geotextiles and to evaluate the possibility of estimating the unsaturated hydraulic conductivity function of the geotextile from the more easily measured water retention data.

Lafleur et al. (2000) proposed a simple apparatus to measure the water characteristic curve for a nonwoven geotextiles (Figure 2-7).

Table 2-3. Lafleur et al. (2000) properties of specimens.

Product	Polymer Type	Fibre	Mass per Unit Area (g/m^2)	Thickness (mm)
A1	Polyester	Continuous	154	1.9
A2	Polyester	Continuous	333	3.5
B1	Polyester	Staple	276	2.3
C1	Polyester	Continuous	597	2.2

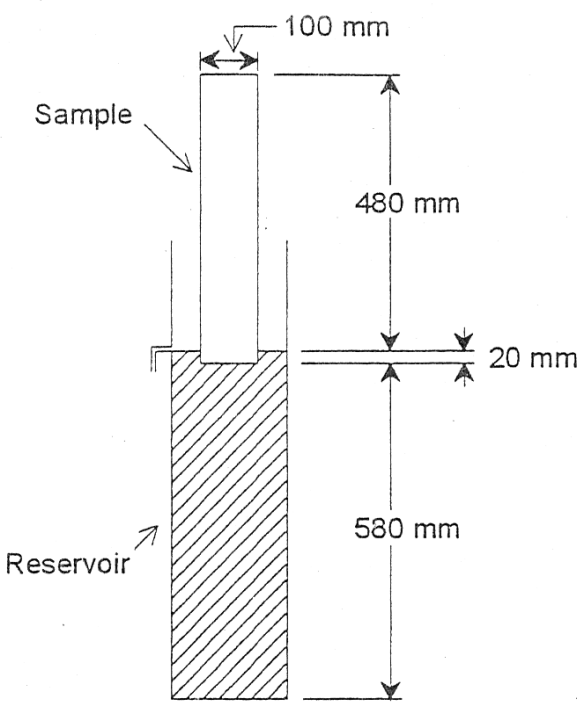

Figure 2-7. Lafleur et al. (2000) testing apparatus.

The test was performed by submerging one end of a 500 mm long geotextile strip in water. For the measurement of the drying curve the sample of geotextile was initially saturated, while for the wetting curve the sample was initially dry. The sample was allowed to equilibrate and the volumetric water content was determined at various points within the specimen. The water content profile was determined by cutting the specimen into 20 or 50 mm segments, and the volumetric water content of each strip was

determined by oven drying. The matric suction was determined by the elevation of each strip above the water level assuming the pore-air pressure at the air-water interface was equal to atmospheric (Lafleur et al., 2000).

The results from this test were similar to those presented Stormont et al. (1997) and Stormont and Morris (2000) with the measured air and water entry suction heads typical of a coarse, uniform material.

The in-plane hydraulic conductivity of the specimens were then determined using a steady-state flux control method (Klute, 1986). Again, the results were similar to those of Stormont and Morris (2000). The measurement of the hydraulic conductivity along the wetting path showed that the geotextile did not become conductive until suction heads of approximately 0.30 kPa. The research also showed that along the drying path, the geotextile remained conductive to suction heads of approximately 1.5 kPa.

The Fredlund and Xing (1994) equation was utilized to fit the measured water characteristic curves for the geotextile with curve fit parameters. The measured hydraulic conductivity functions were then compared to those predicted using the Fredlund et al. (1994) method. Lafleur et al. (2000) concluded that the hydraulic conductivity function of a geotextile specimen could be predicted using parameters fitted to the water characteristic curve.

The research of Knight and Kotha (2001) described the use of a controlled outflow capillary pressure cell (Figure 2-8) for the measurement of the GWCC. This method differed from the Klute (1986) method where the air and water pressures are set and flow from the specimen was monitored until equilibrium is reached. Table 2-4 shows the physical properties of the geotextile used for testing.

Table 2-4. Knight and Kotha (2001) properties of specimens.

Product	Apparent Opening Size (mm)	Permittivity (1/s)	Flow Rate (1/min/m^2)
A	0.15	0.7	34

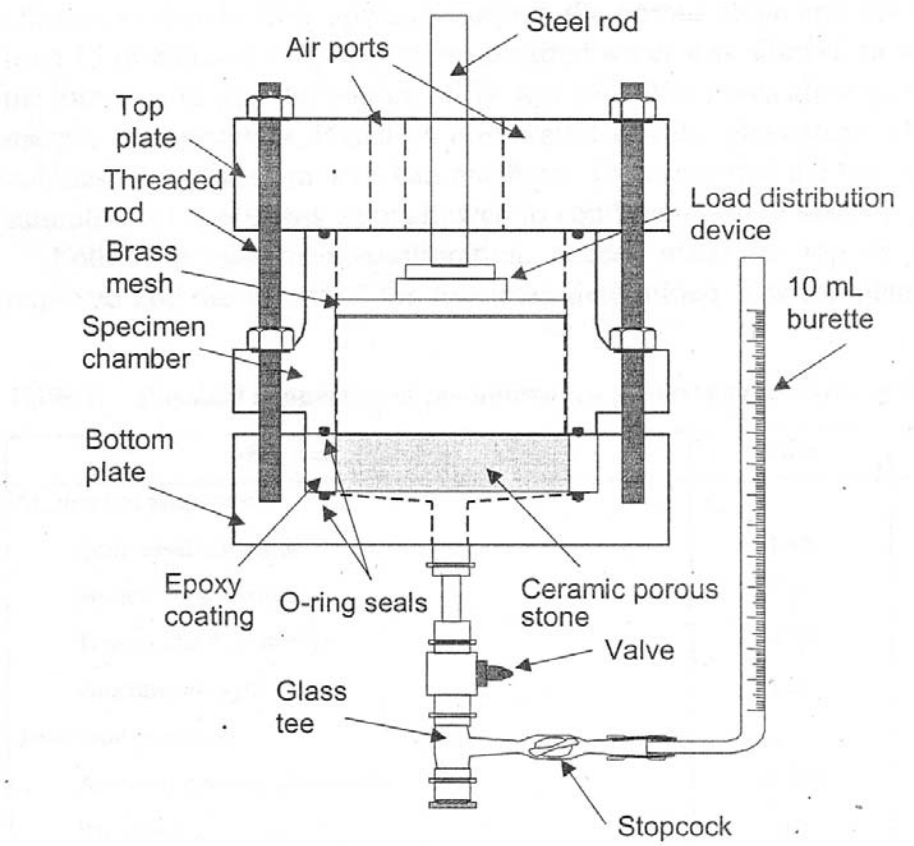

Figure 2-8. Controlled outflow capillary pressure cell (Knight and Kotha, 2001).

Lorentz et al. (1993) reported that water characteristic curves measured with the controlled outflow cell agree well with those measured from the Klute (1986) method. The controlled outflow cell consists of a 50 kPa air entry value porous stone sealed within a Plexiglass chamber. A 10 mL burette was attached to the cell and allowed for the measurement of water fluid volume changes. Cell water and air pressures were monitored using pressure transducers and water and mercury manometers.

A 63.5 mm specimen of geotextile was placed on the porous stone. Air pressure within the cell was increased or decreased (depending on the measurement of the drying or wetting portion of the curve) in order to force water in or out of the specimen. For each increment the pressure transducer was allowed to come to equilibrium and the pressure in the sample was determined. Prescribed amounts of water were allowed to drain or enter the specimen, and the measurement of pressure at these points described subsequent points on the GWCC (Knight and Kotha, 2001).

The research program showed that the controlled outflow cell can be used to measure the water characteristic curve for the geotextile. Test results obtained from the Klute (1986) method were consistent with those from the controlled outflow cell. However, compared to the Klute (1986) method, the controlled outflow cell required less time to complete and did not require the specimen to be removed from the apparatus to determine field saturation (Knight and Kotha, 2001).

Iryo and Rowe (2003) summarized published water characteristic curves and hydraulic conductivity functions of nonwoven geotextiles. In addition, Iryo and Rowe examined and discussed the application of the van Genuchten (1980) equations to unsaturated geotextiles.

The compiled water characteristic curves for the geotextiles are shown in Figure 2-9, while the measured hydraulic conductivity functions are shown in Figure 2-10.

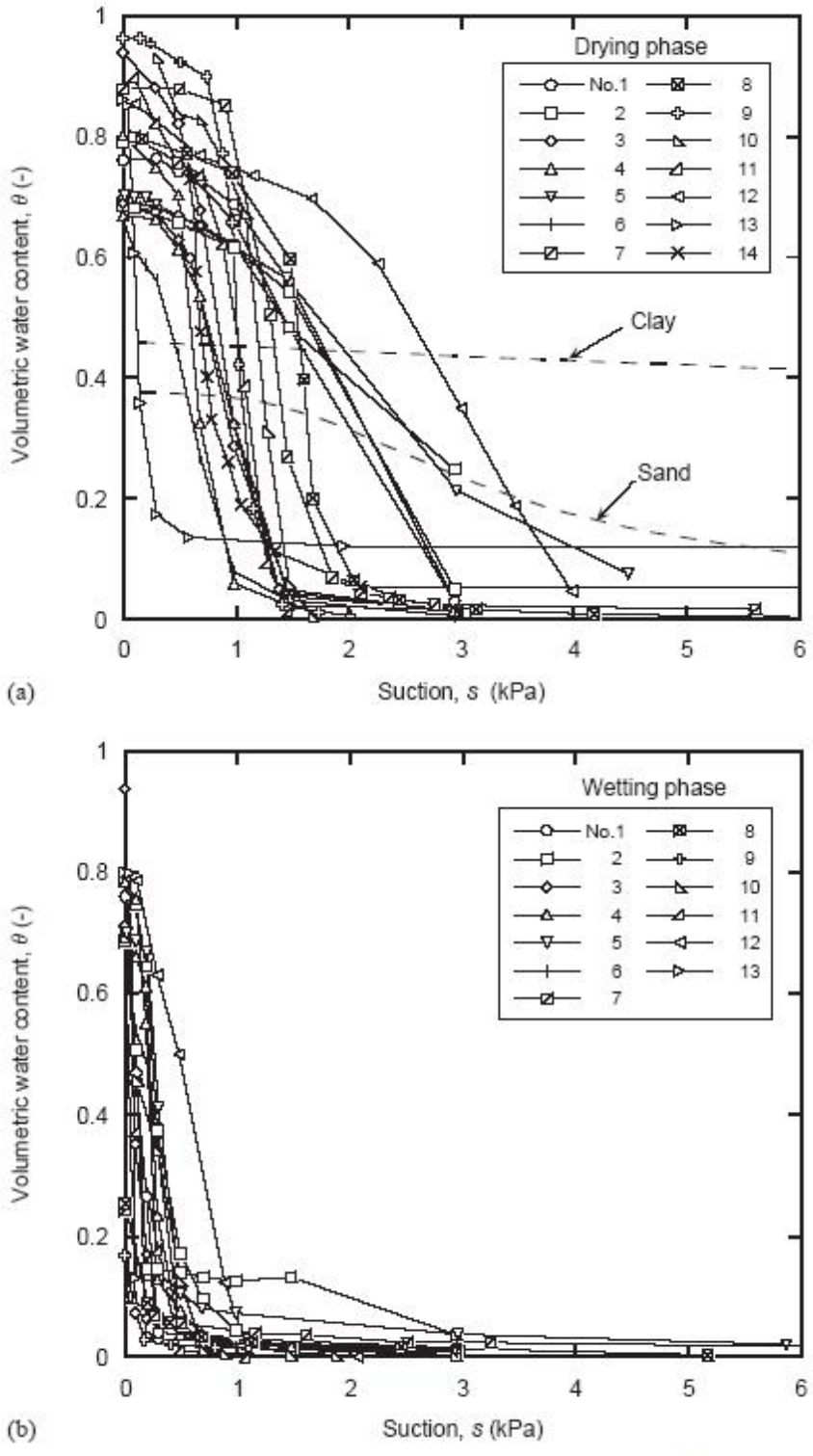

Figure 2-9. Nonwoven geotextile-water characteristic curves (a) drying phase; (b) wetting phase (Iryo and Rowe, 2003).

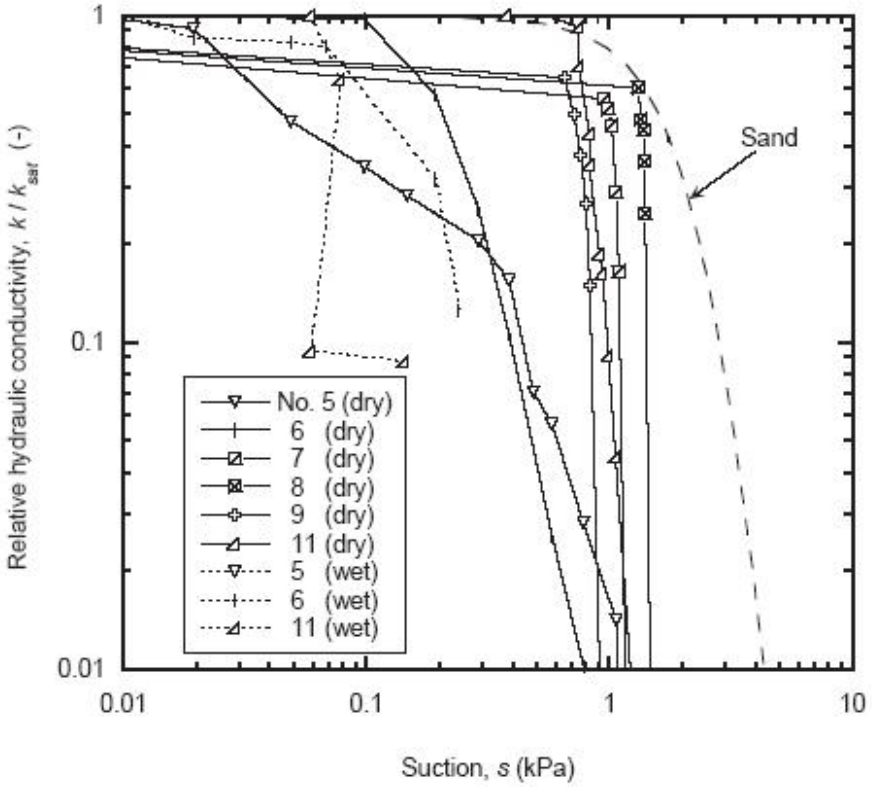

Figure 2-10. Measured geotextile hydraulic conductivity functions (Iryo and Rowe, 2003).

Iryo and Rowe (2003) examined, in detail, the measured GWCC and unsaturated hydraulic conductivity functions for Geotextile A measured by Stormont and Morris (2000). The measured water characteristic curves were fitted with van Genuchten (1980) parameters and the parameters were used to estimate the hydraulic conductivity function for the geotextile. The measured function for the geotextile was then compared to the calculated function and concluded that the van Genuchten (1980) equations modeled the water characteristic curve of the geotextiles relatively well. In general, the hydraulic conductivity functions measured by other researchers were also modeled well, but more experimental data and further investigation was needed.

2.3 Geotextiles as Moisture Limiting Barriers

2.3.1 General

Henry (1990 and 1995), Stormont and Morris (2000), as well as Henry and Holtz (2001) evaluated the concept of geotextiles used as moisture limiting barriers in unsaturated soils. The research programs examined the change in hydraulic behavior of an unsaturated, layered soil system due to the inclusion of a nonwoven geotextile.

2.3.2 Past Works

Henry (1990 and 1995) evaluated the use of a single layer of thin geotextile for reducing the moisture migration beneath roadway embankments. The geotextile used in the study was a needle-punched, polypropylene nonwoven with a thickness of approximately 2.8 mm, an apparent opening size (AOS) of 0.15 mm, and a saturated hydraulic conductivity of $3x10^{-3}$ m/s. The research focused on the reduction in the upward migration of pore water beneath the roadway embankment in order to reduce frost heave.

The research program concluded that a nonwoven geotextile placed above the water table and below the height of capillary rise significantly reduced the upward moisture migration due to capillary rise across the geotextile in response to hydraulic gradients. Vapor movement across the geotextile layer due to hydraulic gradients caused by evaporation or freezing was found to govern rather than liquid flow.

Stormont and Morris (2000) evaluated the effect of a single layer of geotextile on downward flow in soils. Infiltration tests were conducted in Plexiglass tubes in which a layer of nonwoven, polypropylene, geotextile was placed between an upper layer of silty

sand (SM) and a lower layer of coarse sand (SP). The geotextile used in this study was Geotextile B from Table 2-2. Two columns were constructed, one with the geotextile layer and one without in order to show the effect of the inclusion of the geotextile.

Suction heads above and below the soil interface were measured while a constant flow of 2.0×10^{-4} mm/s was added to the top of each column. Initially, suctions in both columns responded in a similar manner; suctions in the upper layer decreased, while suctions below remained constant. Eventually, suctions in the overlying soil decreased due to continuing infiltration and water moved across the interface into the underlying soil. However, in tubes containing the geotextile layer, the "breakthrough" suction was significantly lower than those columns without the geotextile (Stormont and Morris, 2000). For the column which did not have the geotextile, "breakthrough" occurred at a suction head of 3 kPa; for the column which incorporated the geotextile, the suction head was reduced to 1.6 kPa. A third column was then examined under the same flow rate in which the geotextile was placed between two layers of the silty sand (SM). For this case the "breakthrough" suction head was measured to be 1.5 kPa. From the results, Stormont and Morris (2000) concluded that the geotextile may serve as a better capillary break than the coarse sand.

Further testing by Henry and Holtz (2001) showed that geotextiles prepared to represent field conditions (containing fine soil particles) may, in some cases, not significantly reduce moisture migration within the tested soils. A geocomposite was considered in which layers of nonwoven, needle punched, polypropylene geotextiles sandwiched a drainage net. One-dimensional freeze-thaw testing was conducted to

quantify and compare the magnitude of frost heave within samples which incorporated the geocomposite and those which did not.

The results showed that in order for the geocomposite to be effective in developing a capillary break within the system, suctions of 18 kPa above the geocomposite were required. For suctions of 8 kPa or less, the testing concluded that the break would not develop. However, in cases where the geocomposite was effective in developing a capillary break within the soil, the amount of moisture migration was significantly reduced.

2.4 Engineered Cover Systems

2.4.1 General

Feasby et al. (1991) stated that the one of the largest environmental problem facing the Canadian mining industry today is acid mine drainage. Tailings or waste rock containing sulphide minerals which come into contact with oxygen and water will generate sulphuric acid which results in acid mine drainage (Nicholson et al., 1989). In the past, flooding of the waste with water has been deemed acceptable in reducing the amount of oxygen diffusion and therefore acid generation. However, over the past few years, engineered soil covers have become increasingly acceptable as an alternative to flooding (Swanson et al, 2003).

O'Kane et al. (1998) stated that the primary goals of an engineered cover system are to reduce the inward transport of oxygen and to reduce water infiltration into the waste material. The role of nonwoven geotextiles to reduce moisture movement in soils has been discussed in the previous section. Therefore, this section will focus on the criteria for the selection of a suitable system to limit inward transport of oxygen.

2.4.2 Oxygen Limiting Covers

Nicholson et al. (1989) showed that the effective diffusion coefficient for oxygen can decrease up to four orders of magnitude as the degree of saturation increases from zero to one hundred percent. In an engineered cover system, the underlying principle is that one of the material layers in the system remains at or near saturation and thus mitigates the diffusion of oxygen into the underlying waste.

Nicholson et al. (1989) hypothesized that by placing a fine-grained, nonreactive material onto the surface of the waste, acid generation could be reduced. The key process was described as the moisture retention characteristics of the cover material, such that the material could remain at or near saturation even at several meters above the water table. As the pressure progresses in a negative direction above the water table, the air-entry value of the cover material was approached. At this point the material was beginning to desaturate and effectiveness as an oxygen barrier was reduced. The effectiveness of this system was dependant on the depth of the water table as well as the air-entry value of the cover material (Nicholson et al., 1989).

An alternative approach was proposed by Nicholson et al. (1989) and involved the placement of a fine-grained layer of material over a coarse grained layer. The pressure head in the soils progressed in the negative direction as the elevation above the water table increases. However, the pressure head did not become substantially more negative than that corresponding to the residual pressure head in the coarse layer. At this negative pressure head, the hydraulic conductivity of the coarse grained layer was low and a transient condition was developed with no further decline in the pressure head, and the fine-grained material was allowed to remain saturated. Therefore, in principle, the

thickness of the saturated fine-grained layer was the difference between the air-entry value of the fine grained material and the residual pressure head of the coarse grained material (Nicholson et al., 1989).

Akindunni et al. (1991) utilized one-dimensional finite element flow modeling to examine the research program of Nicholson et al. (1989). Cases in which fine grained materials were placed above coarse grained materials were studied. A transient analysis was performed in which the water table was initially placed at the ground surface and lowered with time. The results showed a "static" case was reached in which the pressure profile in the coarse layer was such that the upper, fine grained layer remained saturated for water table depths below its air-entry value.

Barbour (1990), expressed concerns with the hypothesis proposed by Nicholson et al. (1989). Barbour stated that an assumption of steady-state equilibrium rather than "static" equilibrium was more appropriate. The research program showed that for cases of steady-state flow, the overlying fine-grained material may not remain saturated. Barbour (1990) concluded that materials could be chosen to enhance the performance of a fine grained material as an oxygen barrier. However, the performance of the cover is not only a function of the water characteristic curve of the fine-grained material but also a function of the hydraulic conductivity of the cover and the underlying coarse grained material relative to infiltration fluxes due to climate conditions (Barbour, 1990).

Bruch (1993) described a capillary break cover system as a "wick" cover. The placement of the materials was such that the upper, finer-grained layer will retain more moisture than if the coarse layer was not present. The increased degree of saturation of the upper material reduced the effective oxygen diffusion coefficient and allowed the

material to act as an oxygen barrier. Bruch studied, in detail, the evaporative fluxes from soils and stated that the application of topsoil or some other type of medium is critical for the success of an engineered cover system to limit inward oxygen transport. The analysis for capillary breaks generally assumed that the break will not be subjected to high levels of evapotranspiration, which could dry out the upper fine grained layer, negatively affect the oxygen limiting ability. Generally, a minimum of 0.3 m of soil was deemed acceptable in order to protect fine-grained layer from erosion and desiccation as well as providing a medium for vegetation growth (Swanson et al., 2003).

2.5 Chapter Summary

Many testing methods have been proposed to measure the water characteristic curve for a nonwoven geotextile. In general, the results showed that the geotextile-water characteristic curve was typical to that of a uniform coarse material such as a pea gravel. The proposed testing methods from Section 2.2 were examined and a method to measure the water characteristic curve for the nonwoven geotextile was proposed.

Measurements of the hydraulic conductivity function for the nonwoven geotextiles showed that equations used for soils were valid to approximate the hydraulic conductivity function for nonwoven geotextiles from the water characteristic curve. The equations are presented in Section 3.3 and were utilized to estimate the hydraulic conductivity function of the geotextile.

The placement of a capillary break within a soil was suggested as a means of preventing downward moisture movement and a reduction of inward oxygen transport (Stormont and Morris, 1998). Henry (1990 and 1995), Stormont and Morris (2000), and Henry and Holtz (2001) showed that a nonwoven geotextile was an effective barrier to

moisture diffusion when placed within an unsaturated soil system. The research of Nicholson et al. (1989) and Akindunni et al. (1991) showed that the placement of a fine grained material over a coarse grained material can reduce the effective oxygen diffusion coefficient by four orders of magnitude.

Therefore, when coupling the nonwoven geotextile with the fine-grained rock flour a capillary break was established. The GCB takes advantage of the moisture limiting potential of the nonwoven geotextile and the oxygen limiting ability of the saturated, fine-grained material placed on top of the geotextile and mitigated downward moisture and oxygen movement into the waste.

CHAPTER 3 THEORY

3.1 Introduction

Chapter 3 presents the theory that was used to understand and evaluate the geosynthetic capillary break. The theory included a discussion of the nature of flow processes in soils, followed by a discussion of the unsaturated behavior of porous materials. A detailed analytical model used to predict suction profiles in one-dimensional unsaturated materials was also discussed. Finally, the coupled soil-atmospheric finite element modeling software VADOSE/W was discussed. As well, a small portion of Chapter 3 was devoted to the quantification and evaluation of error in model calibration.

3.2 Flow Through a Porous Media

Flow of water in a porous media is based on Darcy's Law, named for the French engineer who studied the relationship between flow rate and hydraulic gradient. The relationship is commonly expressed as:

$$Q = -kiA \tag{3.1}$$

where: Q = flow rate (m^3/s)

k = hydraulic conductivity (m/s)

i = hydraulic gradient (unitless)

A = flow area (m^2)

This equation was originally evaluated for saturated material but can be applied to unsaturated flow as well. Fredlund and Rahardjo (1993) stated that the saturated hydraulic conductivity of a material is a constant value dependant primarily on the porosity of the material. When the material is no longer saturated, the hydraulic conductivity is no longer constant, but is a nonlinear function dependant on both the porosity of the material and the degree of saturation (Fredlund and Rahardjo, 1993). Therefore, Darcy's law can be applied to unsaturated flow providing that the unsaturated hydraulic conductivity function for the given material is known.

3.3 Unsaturated Material Functions

3.3.1 General

As stated previously, the unsaturated behaviour of a material is largely dependant on the porosity and degree of saturation. The volumetric water content of a material is a function of porosity and degree of saturation and can be expressed as follows:

$$\theta = Sn \tag{3.2}$$

where: θ = volumetric water content (unitless)

S = degree of saturation (unitless)

n = porosity (unitless)

A more detailed evaluation of the relationship between the volumetric water content and hydraulic conductivity of a porous material will be presented in the following section.

3.3.2 Water Characteristic Curve

The water characteristic curve can be defined as the relationship between the volumetric water content of a material and the suction (Fredlund and Rahardjo, 1993). The water characteristic curve can be shown to have three distinct stages (Figure 3-1):

- Pre air-entry stage: suctions are too small to overcome the capillary forces holding the water within the largest pores in the material, the material does not drain and the volumetric water content remains constant;
- Transition stage: the largest pores begin to drain, allowing air to enter the structure, pores of decreasing size are drained as the suction is increased; and
- Residual stage: characterized by a very slow decrease in volumetric water content as suctions are considerably increased.

Several closed form solutions have been developed for the water characteristic curve.

Fredlund and Xing (1994) showed a closed form equation to represent the water characteristic curve (WCC) curve for a given material.

$$\theta_i = \theta_s \left[1 - \frac{\ln(1+\frac{\psi}{h_r})}{\ln(1+\frac{10^6}{h_r})} \right] \left[\frac{1}{\left\{ \ln\left[e + (\frac{\psi}{\alpha_f})^{n_f} \right] \right\}^{m_f}} \right] \tag{3.3}$$

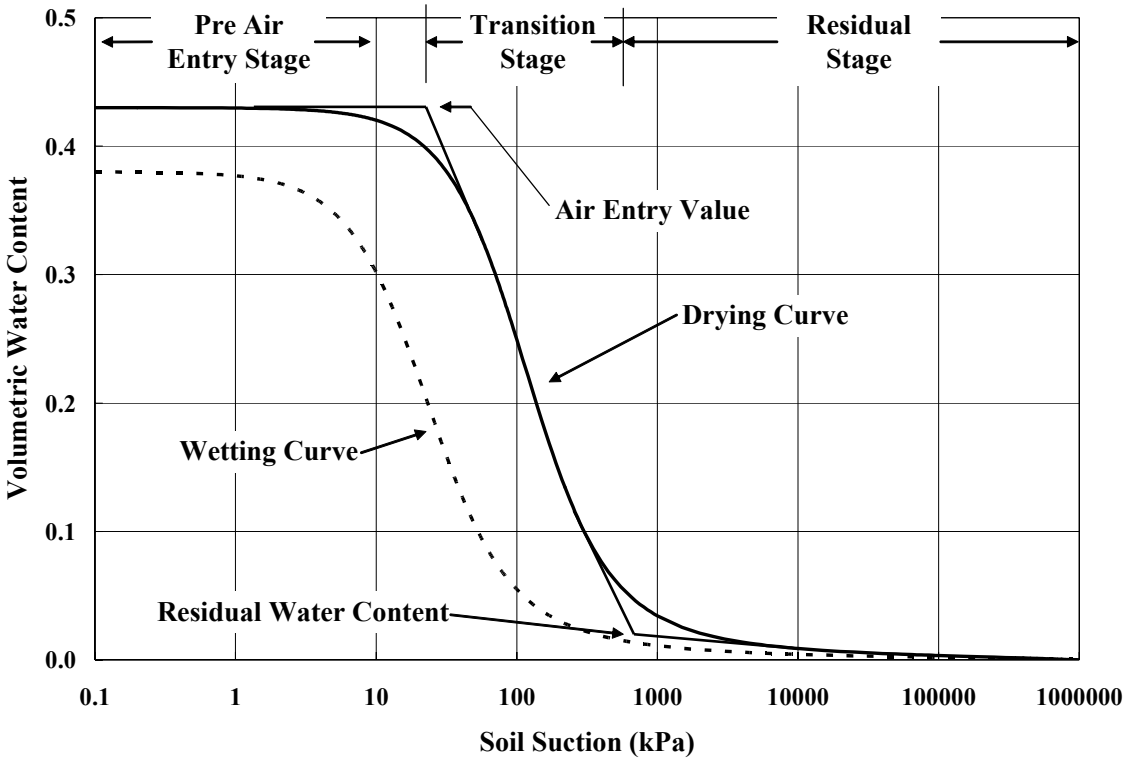

Figure 3-1. Water characteristic curve (after Fredlund and Rahardjo, 1993).

where: θ_1 = calculated volumetric water content

θ_s = saturated volumetric water content

α_f = fitting parameter corresponding to the inflection point and somewhat related to the air-entry value of the material (kPa)

n_f = fitting parameter related to the rate of desaturation of the porous material in the transition phase

m_f = fitting parameter related to the curvature of the function in the high suction range

h_r = constant used to represent the suction at the residual water content (kPa)

ψ = value for suction (kPa)

Another closed form solution used to evaluate the WCC was developed by van Genuchten (1980). The water characteristic curve is described as:

$$\theta_i = \frac{(\theta_s - \theta_r)}{\left\{1 + (\alpha\psi_i)^q\right\}^p} + \theta_r \tag{3.4}$$

where: θ_i = calculated volumetric water content

θ_s = saturated volumetric water content

θ_r = residual volumetric water content

α = fitting parameter corresponding to the inflection point on the WCC (1/kPa)

q = fitting parameter related to the rate of desaturation of the material

p = 1-1/q

ψ = value for suction (kPa)

3.3.3 Hydraulic Conductivity Functions

As the suction applied to a porous media increases, the water content tends to decrease. This decrease in water content leads to discontinuities in the water phase within the material's structure, reducing the effective porosity. This effect reduces the area available for water flow and therefore the hydraulic conductivity of the soil decreases. Figure 3-2 shows how the desaturation of the porous media affects its hydraulic conductivity.

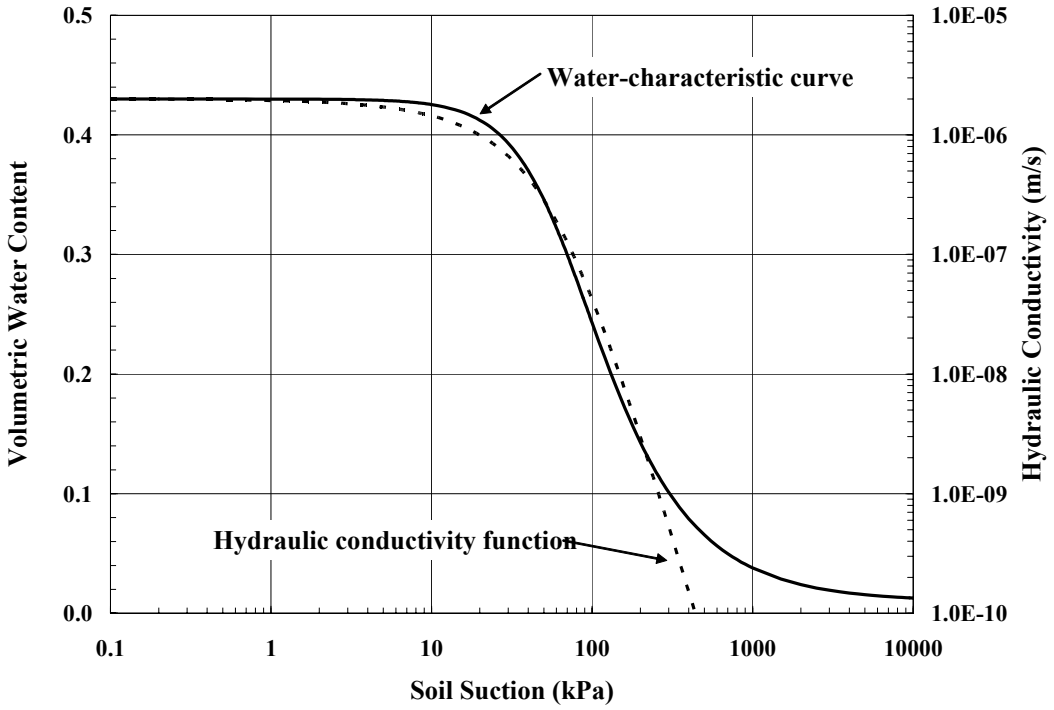

Figure 3-2. Example water characteristic curve and hydraulic conductivity function.

Fredlund et al. (1994) proposed a method for estimating the hydraulic conductivity function from the soil-water characteristic curve. The method involved integrating along the entire curve of the volumetric water content function after fitting with Fredlund and Xing (1994) parameters. The governing equation is:

$$k_w = k_s \frac{\sum_{i=j}^{N} \frac{\theta(e^y) - \theta(\psi)}{e^{yi}} \theta'(e^{yi})}{\sum_{i=1}^{N} \frac{\theta(e^y) - \theta_s}{e^{yi}} \theta'(e^{yi})} \tag{3.6}$$

where: k_w = calculated conductivity (m/s)

k_s = saturated conductivity (m/s)

θ = volumetric water content

y = a dummy variable of integration representing the log of negative pore-water pressure

i = the interval between the range of j to N

j = the least negative pore water pressure to be described (kPa)

N = the maximum negative pore water pressure to be described (kPa)

ψ = value for suction (kPa)

θ' = first derivative of Eq 3.3.

An equation to approximate the hydraulic conductivity function for a given soil from the soil-water characteristic curve was also developed by van Genuchten (1980).

$$k_i = k_s \frac{\left\{1 - \left[(\alpha\psi_i)^{(q-1)}\right]\left[1 + (\alpha\psi_i)^q\right]^{-p}\right\}^2}{\left[1 + (\alpha\psi_i)^q\right]^{p/2}} \tag{3.5}$$

where: k_i = calculated hydraulic conductivity (m/s)

k_s = saturated hydraulic conductivity

α, q, and p = fitting parameters from Eq. 3.4

ψ_i= value for suction (kPa)

Similar equations have been proposed by Childs and Collis George (1950), Gardner (1958), and Brooks and Corey (1964) to estimate hydraulic conductivity functions from water-characteristic curves.

3.4 Kisch (1959) Method of Computing Pressure Profiles

Kisch (1959) proposed the following relationship for the determination of pressure profiles in saturated or unsaturated porous media. This formulation assumed that Darcy's law is valid for flow in both saturated and unsaturated materials. In order to

correctly apply this formulation the relationship between volumetric water content and hydraulic conductivity must be know. Re-writing Darcy's law:

$$q = -k\frac{dh}{dz} \tag{3.8}$$

where: q = discharge per unit area ($m^3/s/m^2$)

k = hydraulic conductivity (m/s)

z = elevation head (m)

h = total head (m), also written as:

$$h = p + z \tag{3.9}$$

where: h = total head (m)

p = pressure head (m)

z = elevation head (m)

If the flow in the porous media is kept constant (steady state conditions), Eqs.3.8 and 3.9 can be combined to form:

$$dp = -dz\left(\frac{q}{k} + 1\right) \tag{3.10}$$

The change in pressure (dp) can then be calculated at a given steady state flux (q) by starting at a known elevation and pressure head condition (depth of phreatic surface), and moving upward in small elevation increments (dz). This procedure was initially used for obtaining the pressure profiles that would develop within a cover system which incorporated the GCB. The results of these analyses aided in the design of the column testing as part of the laboratory program. Later, this method was used in the analysis of the results from the one-dimensional column testing.

3.5 VADOSE/W Theory

3.5.1 General

The numerical model used to simulate moisture and oxygen movement through the geosynthetic capillary break was VADOSE/W (GeoStudio, 2004). VADOSE/W is a two-dimensional transient or steady state finite element model that has the ability to simulate moisture and oxygen migration in unsaturated soils. VADOSE/W also has the ability to account for precipitation, evaporation, infiltration, runoff, and actual transpiration from plants. The following theory was summarized from the VADOSE/W modeling manual (GeoStudio, 2004) with particular emphasis on model inputs.

3.5.2 Material Inputs

For each material input into the finite element model, VADOSE/W required four input functions:

- Volumetric water content function or water characteristic curve;
- Hydraulic conductivity function;
- Thermal conductivity function; and
- Volumetric specific heat function.

All functions were either input as measured curves or estimated from other known functions; therefore, not all functions were measured in the lab. However, for a higher degree of accuracy within the model, it was advantageous to have as many measured inputs as possible.

At a minimum, VADOSE/W required a measured grain size distribution for each material. From this distribution, the volumetric water content function for the material

may be estimated using the Arya and Paris (1981) method. However, the model still required an input for the saturated volumetric water content and the coefficient of volume compressibility (m_v). Once the volumetric water content function was known, or was estimated from the grain size distribution, all other required functions were estimated.

The hydraulic conductivity function for a given material required a known value for saturated conductivity, which was determined in the laboratory. VADOSE/W provided three options for estimating the function from the water characteristic curve:

- Fredlund et al. (1994);
- Green and Corey (1971); or
- van Genuchten (1980).

Differences in the horizontal and vertical conductivity for the material can also be taken into account.

Thermal conductivity and mass specific heat functions were calculated using the volumetric water content function. For the thermal conductivity function, only the volumetric water content function and a value for the thermal conductivity of the dry material were required. Similarly, the mass specific heat function was estimated from the water characteristic curve along with a measurement of dry material specific heat.

3.5.3 Boundary Conditions

The finite element modeling software VADOSE/W required user defined boundary conditions for the developed mesh. Hydraulic, gas, thermal, or climate boundary conditions may be applied to any given mesh. Hydraulic boundary conditions include head, gradient, or flux and were used to model the depth of the groundwater or

infiltration rates at the ground surface. Gas boundary conditions provided the option to apply a known gas concentration or gas flux rate to the mesh, while the thermal boundary allowed the application of a known temperature or temperature gradient.

The climate boundary condition enabled the modeler to show the effects of changing atmospheric conditions to the ground surface. To input climate data, VADOSE/W required measurements for site latitude, max/min daily temperature and relative humidity, daily precipitation, and average daily wind speed. VADOSE/W provided the option to input direct measurements of daily potential evaporation, daily net radiation, or to allow the estimation of daily radiation using the measured climate data, site latitude, time of year, and ground surface conditions.

3.5.4 Initial Conditions

When conducting a transient analysis, VADOSE/W required initial hydraulic, temperature, and concentration conditions. These conditions were specified by conducting a separate, steady state analysis or by specifying an initial water table, temperature and concentrations before the start of the transient analysis. The advantage of conducting a separate, steady state analysis was the ability to adjust initial head and flux conditions to better represent what may be encountered in the field.

3.6 Quantifying Error in Model Calibration

As part of the modeling program for this research, a VADOSE/W model was used to simulate the results from the one-dimensional column testing and to predict long-term hydraulic performance of the GCB. Anderson and Woessner (1992) recommended three error criteria to be used to quantify error in the simulated models.

The first, mean error (*ME*) was the average difference in the simulated and measured values.

$$ME = \frac{1}{n}\sum_{i=1}^{n}\left(measured - simulated\right) \tag{3.11}$$

where: *measured* = measured value

simulated = simulated or modeled value

n = number of values in series

The mean error is not recommended to evaluate error criteria alone. The calculation of the *ME* sums positive and negative error values lead to cancellation of error and a false calibration. However, the *ME* was useful in showing trends in the calibration. A positive *ME* indicated a lower simulated than observed values, while a negative *ME* indicated higher simulated than observed values (Anderson and Woessner, 1992).

A second criterion was the mean absolute error (*MAE*) which is the mean of the absolute value of the difference between simulated and measured values.

$$MAE = \frac{1}{n}\sum_{i=1}^{n}\left|\left(measured - simulated\right)\right| \tag{3.12}$$

The *MAE* provided a better indication of the error in the calibration than did *ME* alone. Positive and negative values were not allowed to cancel each other out. A lower *MAE* indicated an improved calibration (Anderson and Woessner, 1992).

Lastly, the root mean square (*RMS*) error was proposed. The *RMS* is the square root of the sum of the squared differences between simulated and measured values.

$$RMS = \left[\frac{1}{n}\sum_{i=1}^{n}\left(measured - simulated\right)^2\right]^{\frac{1}{2}} \tag{3.13}$$

The root mean square error gave the best indication as to the closeness of the simulated model (Anderson and Woessner, 1992).

3.7 Chapter Summary

The equations for the water characteristic curve and saturated hydraulic conductivity functions presented in Section 3.3 were used to estimate the hydraulic conductivity functions for the materials used to evaluate the geosynthetic break. The measured water characteristic curves were fit with van Genuchten (1980) and Fredlund and Xing (1994) parameters and utilized to develop estimates for the hydraulic conductivity functions, which were used as inputs for the analytical and numerical models.

The Kisch (1959) method for computing pressure profiles was used to examine the effect of the GCB on the pressure profiles within the engineered cover system under conditions of stead-state flow. In particular, this method was utilized to examine the pressure profiles within the one-dimensional soil columns at various fluxes.

The measured and estimated functions were used as inputs to the finite element modeling program VADOSE/W (GeoStudio, 2004). This program was utilized to simulate the results of the column testing and to predict long-term hydraulic performance of the GCB as part of an engineered cover system.

CHAPTER 4 LABORATORY PROGRAM

4.1 Introduction

A laboratory program was undertaken to determine the pertinent properties of the materials used to evaluate the geosynthetic capillary break. Once these properties were established, the methods discussed in Chapter 2 and 3 were used to evaluate the likely performance of the GCB and to design a laboratory column testing program. One-dimensional soil columns were then assembled based on these results, to simulate the use of the geosynthetic break in an engineered cover system. This chapter outlines the tests performed and the procedures used to determine the physical properties of the materials. It also describes the initial assembly and test procedure for the soil columns.

The materials testing program consisted of three phases:

- Selection of suitable materials for the geosynthetic break;
- Selection of remaining materials for engineered soil cover; and
- Determination of the basic physical properties of the selected materials.

The 1-D column testing consisted of four phases:

- Experimental design;
- Column design;
- Column construction;
- Initial conditions; and
- Boundary conditions.

4.2 Selection of Materials for Geosynthetic Break

4.2.1 General

Sections 2.3 and 2.4 have shown background as to the types of geotextiles used as moisture barriers and the criteria for the selection of the fine-grained material that may serve as oxygen barriers.

The geosynthetic capillary break was evaluated on moisture limiting and oxygen limiting criteria. Therefore, both a fine grained material to remain at, or near saturation to limit oxygen movement and a free draining geotextile to limit moisture movement were required.

4.2.2 Geotextile

Past research has shown that a single layer of nonwoven geotextile placed within a soil was effective in reducing both upward and downward moisture migration (Henry 1990 and 1995; Stormont and Morris, 2000; and Henry and Holtz 2001). The geotextile properties used in the research are summarized in Table 4-1. A geotextile with similar properties was used in this study.

The geotextile used for the GCB was manufactured by Terrafix Geosynthetics Inc. The product name was Terrafix 1200R (Figure 4-1). Terrafix 1200R was a nonwoven, polypropylene, needle-punched, continuous fiber geotextile. Table 4-2 shows other physical properties of the geotextile as provided by the manufacturer.

Table 4-1. Summary of geotextile properties evaluated as moisture limiting materials (Henry 1990, Stormont and Morris, 2000, and Henry and Holtz, 2001).

Polymer Type	Thickness (mm)	AOS (mm)	Mass per unit Area (g/m^2)	Hydraulic Conductivity (m/s)
polypropylene	2.8	0.15	500	3.00E-03
polypropylene	5.9	0.18	340	3.90E-03
polypropylene	n/a	0.15 to 0.18	339 to 543	n/a

Table 4-2. Physical properties of Terrafix 1200R (Terrafix, 2004).

Parameter	Value
Filtration Opening Size (FOS) (mm)	0.05 to 0.15
Mass per unit Area (g/m^2)	550
Hydraulic Conductivity (m/s)	1.50E-03
Grab Tensile Strength (N)	1200

Figure 4-1. Terrafix 1200R.

4.2.3 Oxygen Limiting Material

Nicholson et al. (1989) indicated that the effective diffusion coefficient can vary up to four orders of magnitude with water content and that for an increase in saturation from

75 to 95 percent, the diffusion coefficient for oxygen decreases approximately two orders of magnitude. Therefore, a material with a high degree of saturation over the anticipated range of suctions was desirable. Nicholson et al. (1989) showed that for a material to remain at a high degree of saturation in an engineered cover system the magnitude of the air-entry value (Figure 3-1) for the material must be greater than or equal to the sum of the thickness of the material and the negative pressure head where the underlying material reaches residual moisture content.

Figure 2-9 illustrated that for the underlying material for the geosynthetic capillary break (nonwoven geotextile) the residual water content was commonly reached between 1 and 4 kPa or approximately 10 to 40 cm of water. Due to constraints in the proposed manufacturing process as well as practicality of the product, the maximum thickness of the moisture retaining layer of the geosynthetic break was taken as 1.0 cm. Therefore, a material with an air-entry value no less than 4.1 kPa was required for the geosynthetic break according to the criteria proposed by Nicholson et al. (1989).

The criterion by Nicholson et al. (1989) only evaluated the effect of the desaturation of the moisture retaining layer due to downward gradients. Upward gradients or slopes may also be present within the cover system due to evaporation or ground freezing (Henry, 1990). The gradients may also cause soil suctions to become greater than the air-entry value of the material. The magnitudes of these suctions are highly dependant on the overlying growth medium type and thicknesses used in the cover system and are often difficult to quantify. Therefore, materials with higher air-entry suctions were desirable.

Rowlett (2000) measured the water characteristic curve for a fine grained silica flour for the design of a stand-pipe lysimeter. The product tested was processed silica, marketed as SIL-CO-SIL 90 by the U.S. Silica Company of Berkeley Springs, West Virginia. A processed product was desirable for use in the geosynthetic break because it could be readily obtained for manufacturing a geosynthetic product and is likely to have consistent material properties. Figure 4-2 shows the measured water-characteristic curve for the SIL-CO-SIL 90.

As can be seen from the figure, the air-entry (AEV) for the material is between 20 and 30 kPa, and is a suitable moisture retaining material for the break. However, due to the health hazards associated with crystalline silica, this product was not acceptable to be used in the manufacturing process of the GCB.

A similar product distributed by L.V. Lomas Chemicals of Brampton, Ontario was located. The product was a nepheline syenite rock flour and was distributed as Industrial Grade #75 (Figure 4-3). Comparison of specifications from the manufacturer for both grain size distributions showed that the materials possessed similar distributions (Table 4-3). Fredlund et al. (2002) showed that a materials water characteristic curve is closely related to its grain size distribution. Therefore, it was anticipated that the water characteristic curve for the rock flour would be similar to that of the silica flour.

A comparison of measured grain size distributions and the measured water characteristic for the Industrial Grade # 75 are presented in Chapter 5.

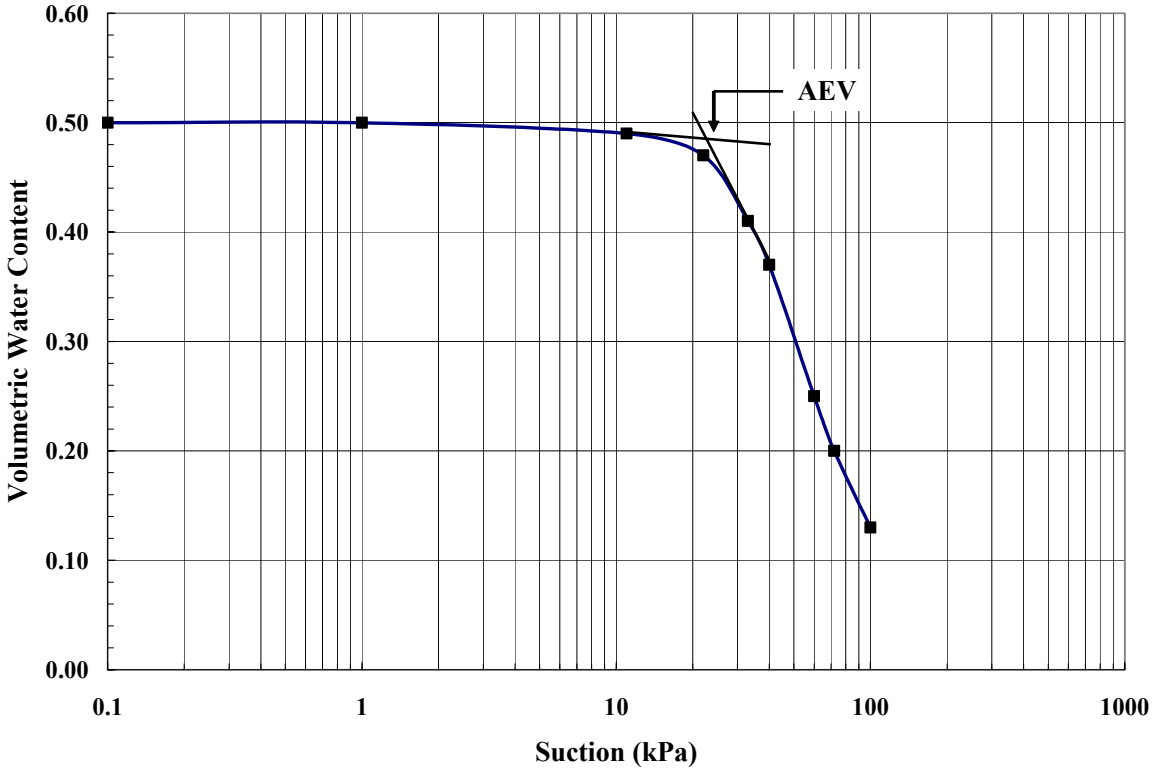

Figure 4-2. Water characteristic curve for silica flour (after Rowlett, 2000).

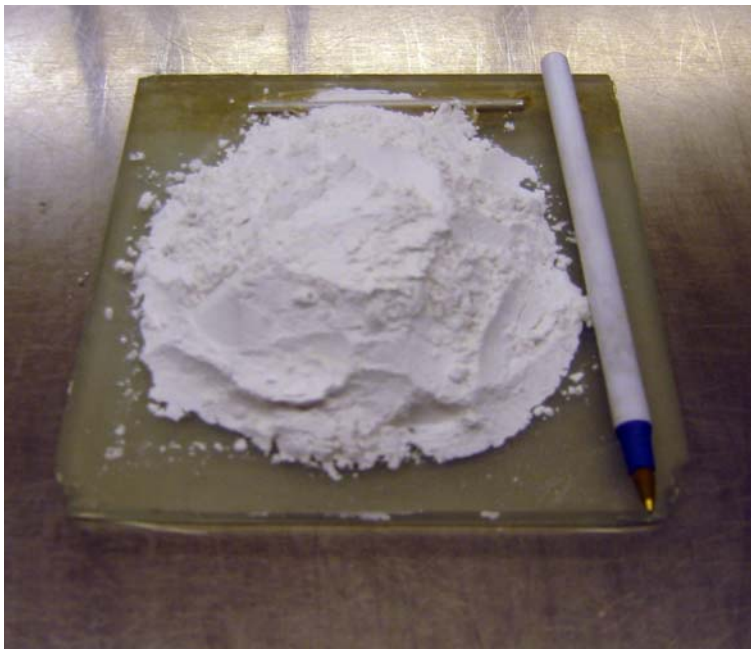

Figure 4-3. Industrial Grade #75.

Table 4-3. Manufacturer specified grain size distributions for SIL-CO-SIL 90 and Industrial Grade #75.

Grain Size (mm)	% Finer Than	
	I.G. #75	SIL-CO-SIL 90
0.300	100.0	100.0
0.150	99.9	100.0
0.106		99.9
0.075	99.5	97.5
0.053		89.0
0.045		84.0

4.3 Selection of Remaining Materials for Engineered Soil Cover

4.3.1 General

As stated in Section 2.4, the protection of the GCB from evapotranspiration is critical to success as an oxygen barrier. Therefore, a cover soil was required to be placed on top of the GCB to protect the product from evaporation, erosion, and/or to act as a growth medium for vegetation. A typical waste material was also required to be placed below the GCB. This section describes these two materials.

4.3.2 Underlying Waste

Hudson Bay Mining and Smelting (HBM&S) of Flin Flon, MB provided mine tailings to be used in this study. The tailings were dark grey in colour and were obtained from the tailings management area located at HBM&S. The tailings were approximately two months old at the time of sampling. Ten 170 L drum samples were collected and transported to the University of Saskatchewan. The samples were sealed until the start of the testing. Samples from each drum were tested in order to confirm uniformity of grain size within the samples. The resulting grain size distribution is shown in Chapter 5. The specific gravity for the tailings was measured by HBM&S to be 3.21.

4.3.3 Cover Soil

The cover soil used in the testing was spoil obtained from a commercially owned gravel pit. The pit, ASL Saskatoon's East Pit, was located approximately 15 km east of Saskatoon, SK. The soil occurred in a uniform layer in a kame and esker complex and the material was collected from a spoil pile on site. The soil was light brown in color and fine to medium grained. The measured grain size distribution is also presented in Chapter 5.

4.4 Determination of Material Properties

4.4.1 General

This portion of the laboratory program consisted of the characterization of the four selected materials:

- Geotextile
- Rock Flour
- Tailings
- Cover soil

For the three latter materials grain size distributions, saturated hydraulic conductivity, and water characteristic curve testing was performed using traditional equipment and techniques. Where necessary, all materials were tested at moisture contents and/or densities at which they were placed to in the column studies.

For the geotextile, a measurement of the water characteristic curve was performed using methods outlined in Section 4.4.4.

4.4.2 Grain Size Analysis

Grain size analysis can be performed using a variety of techniques. For materials with a large percentage of particles greater than 0.075 mm in diameter, mechanical sieving can be performed. The grain size distribution for materials with a large percentage of materials less than 0.075 mm in diameter may be determined using a hydrometer test. For the rock flour, tailings, and cover soil, mechanical sieve analysis was not required and the grain size distributions were determined using hydrometer tests.

For the geotextile, commonly a pore size distribution is performed rather than a grain size analysis in order to determine the distribution of pore sizes within the matrix of the geotextile. However, this test is difficult to perform and results may vary depending on the testing method (Elsharief and Lovell, 1997). For the purpose of this research, a pore size distribution was not deemed necessary. An estimate of the pore sizes within the geotextile can be obtained from the filtration opening size (FOS) for the tested geotextile (Table 4-3).

4.4.3 Saturated Hydraulic Conductivity Testing

Saturated hydraulic conductivity testing was performed using the constant head conductivity test. The constant head test determined the saturated conductivity of a material by measuring the flow rate through a sample while applying a constant hydraulic gradient. Darcy's law (Section 3.2) was then used to determine the saturated hydraulic conductivity. The flow rate through the sample was measured by determining the quantity of water passing through the sample over a given time period. The hydraulic gradient in the sample was determined using a manometer board. The test was

run for different gradients and the saturated hydraulic conductivity was taken as the average for each sample. The apparatus is shown in Figure 4-4. Constant head testing was performed on the cover soil, rock flour, and tailings, with the results presented in Chapter 5. The saturated hydraulic conductivity for the geotextile was taken as the value specified by the manufacturer.

4.4.4 Water Characteristic Curve Testing

The water characteristic curves for the cover soil, rock flour, and tailings were determined using the single specimen pressure plate cell (Figure 4-5) developed at the University of Saskatchewan.

The samples were formed in a consolidation ring and placed into the cells. Samples were carefully compacted with a small steel rod into the ring in order to provide a level of compaction consistent with that of the one-dimensional columns. All samples were placed inside the cell on top of a saturated 3 bar (300 kPa) ceramic disk and saturated by applying a small amount of positive pressure to the bottom of the disc using the outflow tube.

The samples were saturated, the initial weight was recorded, and suctions were slowly increased. For suctions from 0 to 10 kPa, the negative pressure head was applied by lowering the outflow tube. The suction applied to the sample was proportional to the difference in elevation between the outflow tube and the sample. Water was allowed to drain from the outlet tube until equilibrium was reached at the individual suction increments. The weight of the cell at each suction increment was recorded. The process was then repeated, lowering the elevation of the outflow tube at specified increments from 0 to 100 cm.

Figure 4-4. Constant head apparatus.

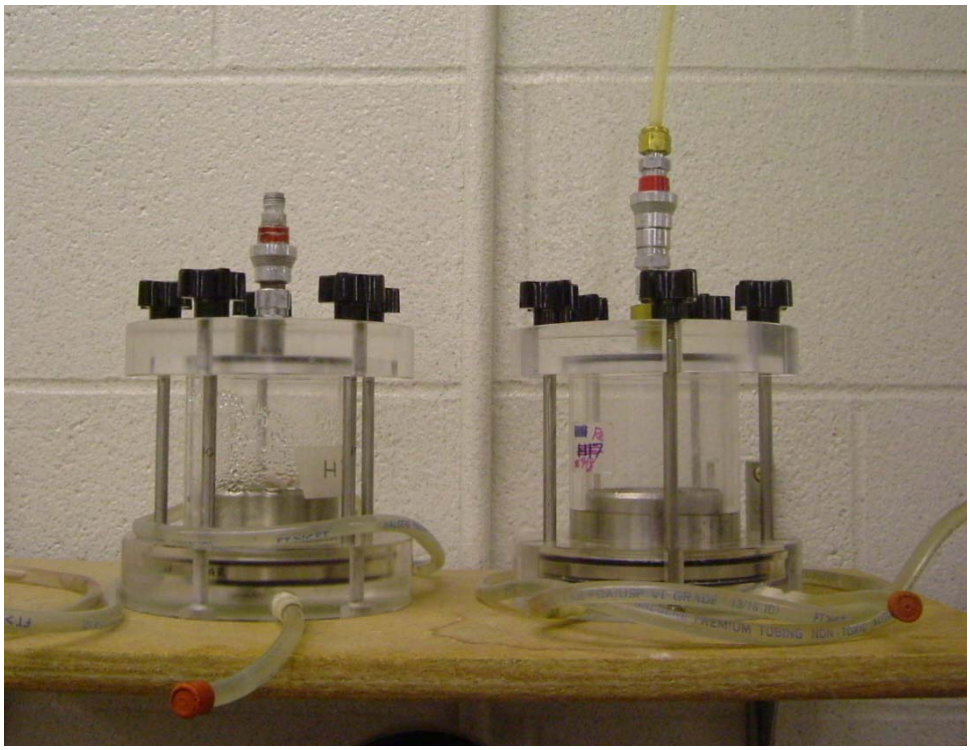

Figure 4-5. Single specimen pressure plate cells.

For suctions greater than 100 cm (10 kPa), lowering the outflow tubes became impractical. Suctions greater than 10 kPa were applied using the axis-translation technique. A known air pressure was applied to the sample while allowing the pressure at the outflow tube to remain atmospheric. The suction applied to the sample was the difference between the air pressure applied to the cell and the pressure at the outflow tube. For all cases the pressure at the outflow tube was kept at zero gauge, therefore the suction applied to the sample was taken as the measured air pressure. Similar to the lowering of the outflow tubes, the sample was allowed to come to equilibrium at each suction increment and then weighed. This process was repeated until applied air pressures approach the air-entry value of the porous disc (300 kPa).

For geotextiles, there was no generally accepted method for the measurement of the water characteristic curve (WCC). Previous researchers used the Klute (1986) procedure or controlled outflow capillary pressure cells (Knight and Kotha, 2001) to measure the geotextile-water characteristic curve (GWCC). Lafleur et al. (2000) also proposed a method for measuring the geotextiles-water characteristic curve.

Initially, the Lafleur et al. (2000) method was utilized to measure the portions of the WCC of the geotextile. This method was desirable because the WCC could be determined over the course of a few days. The test required a long narrow strip of geotextile approximately 25 x 300 cm to be cut. For the drying portion of the curve the geotextile was initially brought to saturation. The geotextile is then hung, with the bottom edge of the geotextile still submerged in water. The sample was covered by a plastic tube to reduce evaporation and the sample was allowed to come to equilibrium. The sample was then cut into small strips, to determine the volumetric water content.

The suction increment for each strip was determined by measuring the elevation above the water level.

Figure 4-6 shows the apparatus used for the hanging test. The testing method was advantageous due to the fact that the time frame to complete an entire test is only 3-5 days rather than weeks as was the case with traditional pressure plate equipment. Due to inconsistencies in the results as well as problems with the experimental procedure, the pressure plate cell was deemed a more appropriate testing apparatus.

A single specimen pressure plate cell was modified to accommodate the testing of the nonwoven geotextile. A larger ring was required for accurate measurements of changes in the mass of the geotextile due to water loss. Also, a loading ram was constructed in order to allow the application of static loading to the specimen. The procedure for the measurement of the geotextile WCC was similar to that for the other materials. The sample was placed in the cell on top of a ½ bar (50 kPa) high flow porous stone and brought to saturation. The elevation of the outflow tube was lowered in small increments of approximately 1 to 5 cm and for each increment the sample was allowed to come to equilibrium. The samples reached residual moisture contents at approximately 5 kPa; therefore axis-translation was not required.

Figure 4-6. Hanging test apparatus.

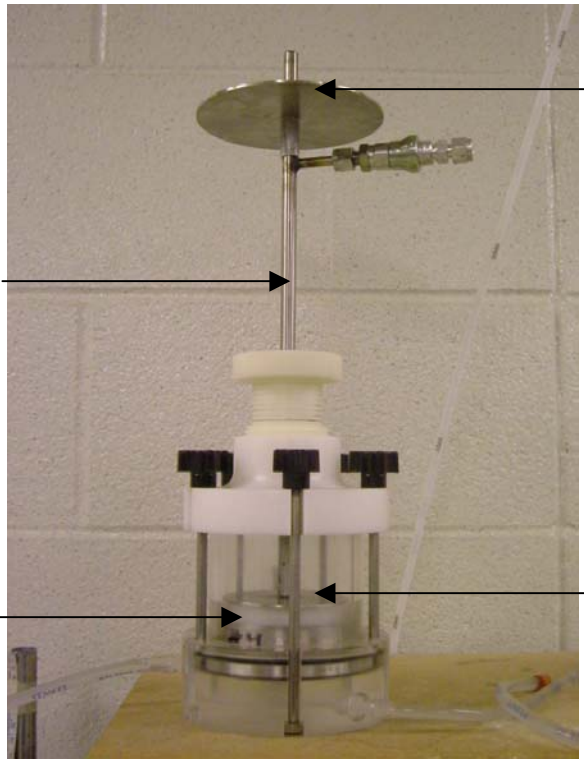

Figure 4-7. Modified pressure plate cell.

The geotextile specimens were tested under various conditions. Tests were conducted under normal loads of 0, 1, 5, 6.3, and 10 kPa in order to determine the change in the WCC of the geotextile under increasing overburden stresses within the range of stresses encountered in the cover system. Also, testing was conducted on both "new" and "washed" specimens. The washed samples were cleaned using detergent and water in an attempt to remove potentially hydrophobic lubricating oils used in the manufacturing process. These tests were performed in order to evaluate the change in the in-situ water characteristic curve of the geotextile (Stormont et al., 1997).

4.5 One-Dimensional Column Testing

The main portion of the laboratory program was the construction and monitoring of 1-D, field-scale columns. The following sections describe the columns in detail.

4.5.1 Experimental Design

The objective of the column testing was to show the geosynthetic capillary break (GCB) was effective in reducing moisture and potentially oxygen migration into the underlying waste. The column tests were devised to study the performance of the GCB under measured climate conditions and to quantify three criteria:

- Net infiltration
- Change in suction profiles
- Change in water content profiles

Four columns were constructed in pairs to compare the performance of two alternative cover soil thicknesses of 30 and 60 cm. For the specific cover thickness, one column incorporated a GCB while the other did not. The cover thicknesses were chosen based on past experience with full-scale test covers for engineered soil covers. A cover

thickness of 30 cm was generally accepted as the minimum cover thickness that could be utilized in order to allow for the development vegetation on the surface of the cover. The 30 cm cover thickness was also utilized in order to evaluate evaporative effects on the GCB which would not be realized with a thicker cover. A 30 cm cover, in most cases, would be to thin to satisfy moisture and oxygen limiting criteria. However, finite element and numerical modeling showed that this thickness of cover would perform relatively well with the inclusion of the GCB. The 60 cm cover thickness was shown through numerical and finite element modeling to perform relatively well without the inclusion of the GCB. The inclusion of the GCB for this cover thickness was evaluated to show the magnitude of improvement that could be achieved.

4.5.2 Column Design

The columns for this research were designed after those used by Bruch (1993). However, for this research, larger columns, both in height and diameter, were considered desirable in order to approximate an engineered cover system. The larger diameter of the columns allowed small changes in flux to be measured with a higher degree of accuracy. The column material used in this study was 0.457 m (18") (ID) corrugated PVC water pipe.

Table 4-4. Description of soil columns.

Name	Cover System
Column 1	60 cm of cover soil, no GCB
Column 2	60 cm of cover soil, includes GCB
Column 3	30 cm of cover soil, no GCB
Column 4	30 cm of cover soil, includes GCB

The height of the column was dependant on the thickness of the cover soil as well as the required waste thickness. For this study, cover thicknesses of 30 and 60 cm were used while the thickness of waste below the column was kept constant at 1.2 m. A freeboard of 5 cm was also included at the top of the column to prevent runoff during large precipitation events and thus to ensure one-dimensional behaviour. For the pair of columns with 60 cm of cover, the overall column height was 1.85 m and for 30 cm of cover the overall height was 1.55 m. Table 4-4 provides descriptions of the four columns.

Modifications were made to the columns in order to allow for the measurement of suction and water content profiles. For the measurement of soil suction, two 30 mm diameter tensiometer ports were drilled above and below the tailings-cover soil interface at elevations of 0.9 and 1.1 m above the base. Eight sets of 10 mm diameter holes were drilled around the circumference of each column to allow for sampling of soils for measurement of moisture content. Each set of holes was drilled at 5 cm spacing from the top of the column to an elevation of 0.5 m from the base of the column; the spacing was then increased to 10 cm for the remaining holes. The water content ports were plugged with rubber stoppers to prevent moisture from leaving or entering the columns.

A grooved PVC plate was attached to the base of each column, ensuring a watertight seal, and a drain was drilled through the plate for the measurement of moisture flux and application of the desired constant total head to be applied to the bottom as a known boundary condition. Figure 4.8 shows a schematic of a column with 30 cm of cover.

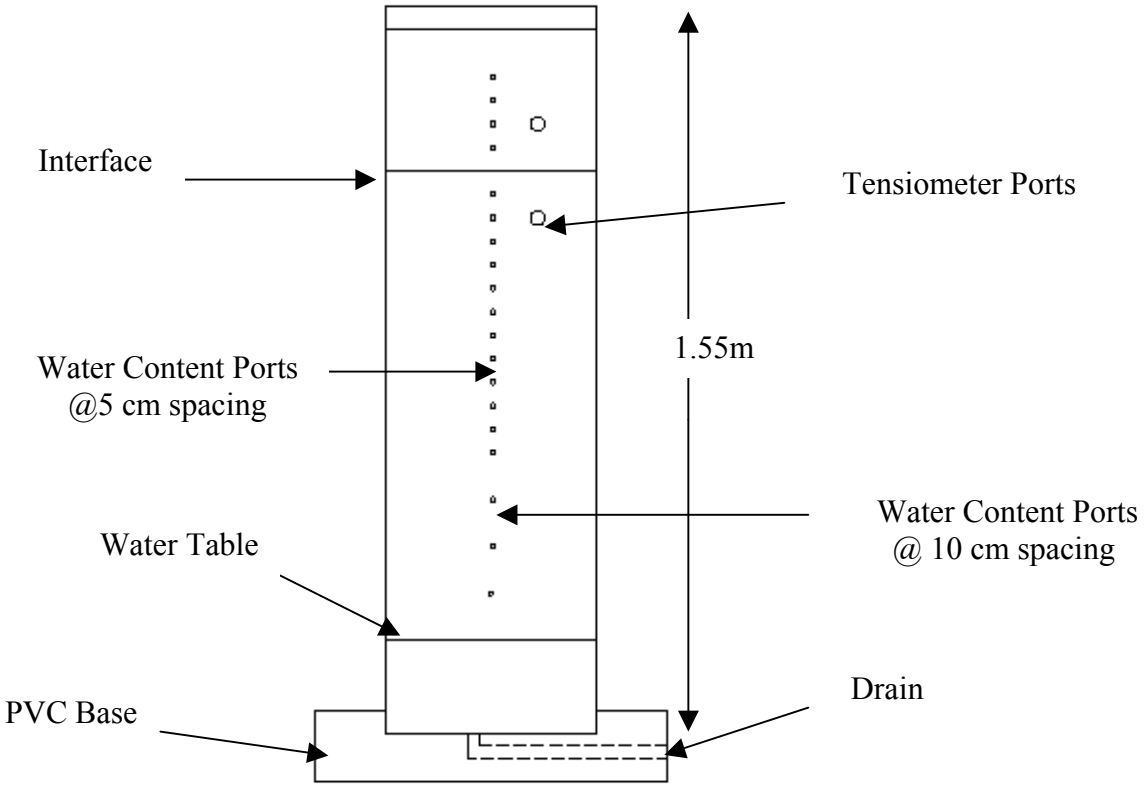

Figure 4-8. Schematic of column with 0.3 m of cover.

4.5.3 Column Assembly

All four columns were constructed identically to ensure consistency in the measured results. The tailings and cover soil were stored in 170 L drums, while the rock flour was stored in a 20 L pail until the columns were assembled. All geotextiles used in the construction were cut into 0.457 m (18") diameter discs to ensure continuous contact with the column walls.

Initially, a layer of geotextile was placed at the base of each column to act as a filter and prevent tailings from exiting through the drain. Next, a 5-7 cm layer of sand was placed on top of the geotextile to ensure that the imposed hydraulic boundary condition was applied uniformly. A second layer of geotextile was placed on top of the sand layer to serve as a separator between the sand and the overlying waste. The tailings were

placed in 20 cm lifts and compacted using a modified Marshall hammer. The tailings were compacted at in-situ moisture content to a density of approximately 1600 kg/m^3 to an elevation of 1.2 m above the base. For columns that incorporated the GCB (Columns 2 and 4), two layers of thicker geotextile (Terrafix 1200R) were placed on top of the tailings followed by a 1 cm thick layer of rock flour and finally a layer of thinner geotextile (Terrafix 600R) was placed to serve as a separator from the cover soil. Figure 4-9 shows a schematic of the geosynthetic capillary break. The final layer, the cover soil, was placed similar to the tailings. A density of approximately 1600 kg/m^3 was achieved using 15 cm, rather than 20 cm lifts. For Columns 1 and 2, the cover was compacted in four lifts to an elevation of 1.8 m, while Columns 3 and 4 were compacted in two lifts to an elevation of 1.5 m.

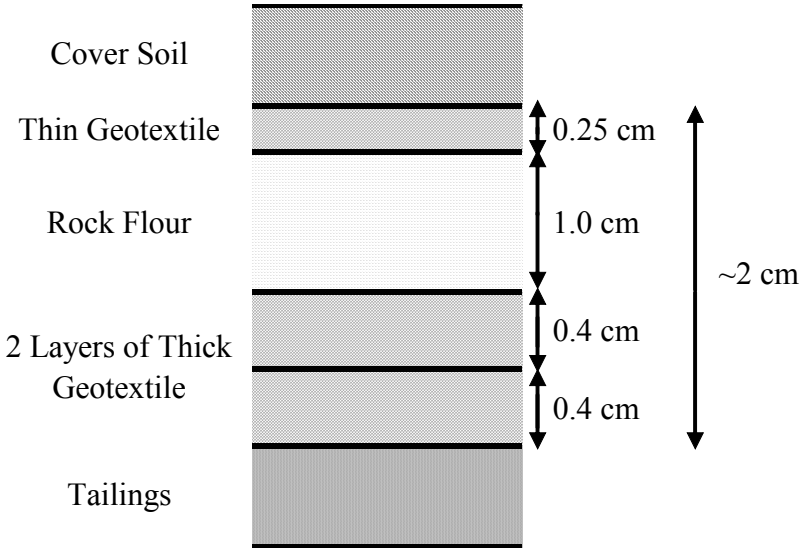

Figure 4-9. Schematic of geosynthetic capillary break.

4.5.4 Initial Conditions

The initial conditions for all columns were identical in order to ensure consistency of results. After assembly, water was allowed to flow into the drain at the base of each column to slowly raise the water table to the surface of the cover and saturate the materials. The columns were then covered and left to equilibrate until the tensiometer readings were zero for all columns. The outlet of the drainage tube was then lowered to an elevation of 20 cm above the base or 1.0 m below the cover soil-waste interface and the columns were allowed to come to equilibrium. A 160 mm diameter graduated cylinder was attached to the drainage outlet, in order to measure moisture flux into or out of the column. The water table within each column was held constant at 20 cm above the base for the remainder of the testing.

The columns were assembled in the Structures and Materials Laboratory at the University of Saskatchewan. The initial soil temperature was approximately 20^{o}C. R8 insulation was wrapped around each column to reduce vapour diffusing through the walls of the pipe and to reduce temperature gradients within the soil. Figure 4-10 shows the final column setup.

4.5.5 Boundary Conditions

The boundary condition at the base of the column was a constant water table elevation of 20 cm above the base or approximately 1.0 m below the top of the tailings. Surface flux boundary conditions consisted of precipitation (positive, downward flux) and evaporation (negative, upward flux). The potential evaporation for all columns were measured using a single evaporation pan while the precipitation was measured using a tipping-bucket rain gauge. Measurements of air temperature, relative humidity, and

wind speed were also taken using a micrometeorological station (Figure 4-11). The measured parameters from the weather station were used as the input climate data for the coupled soil-atmospheric finite element model. The model, described later, was used to simulate the performance of the 1-D column testing program.

Figure 4-10. Final experimental setup.

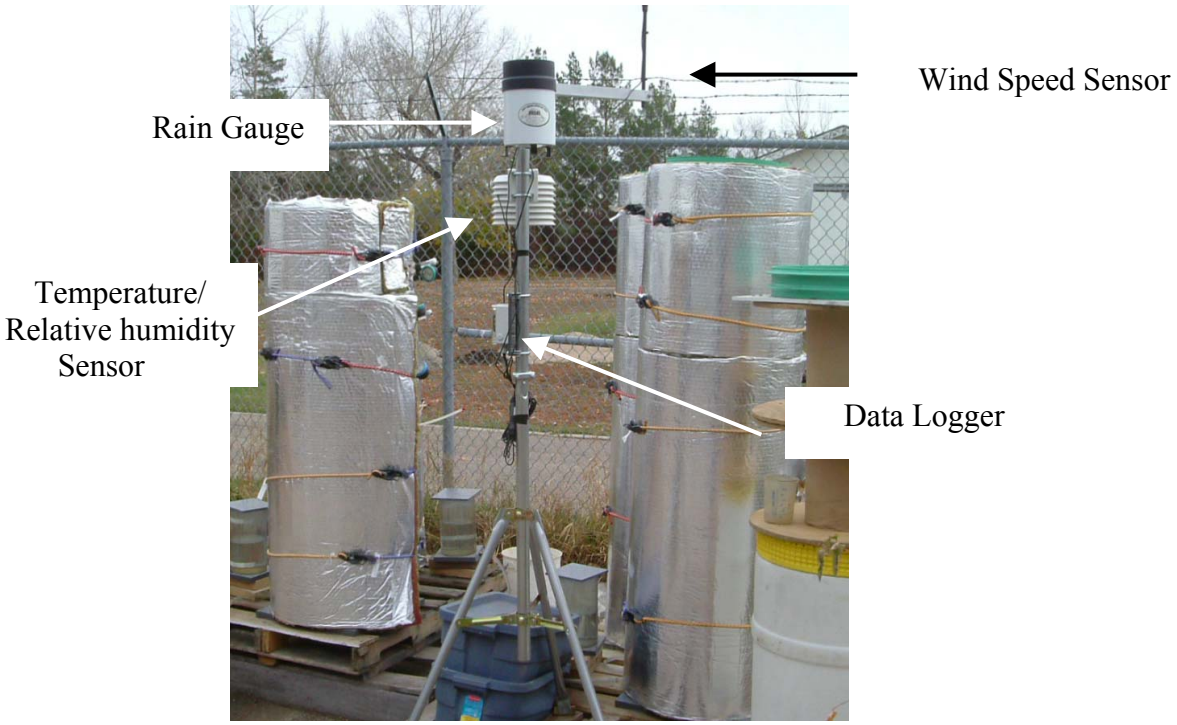

Figure 4-11. Hoskin scientific weather station.

Testing of the columns was carried out in two distinct phases with different surface boundary fluxes applied to the columns in each case. The first phase of testing was a low evaporation, high precipitation flux conducted in the Structures and Materials Lab at the University of Saskatchewan. The potential evaporation inside the lab over the 80 day period ranged from 1.0 to 2.5 mm/day with an average of 1.5 mm/day. A specific amount of precipitation was applied to the columns each day, starting with small increments and increasing as the test progressed. Table 4-5 summarizes the precipitation increments, while the measured climate data for the testing period is summarized in Appendix B.

Table 4-5. Summary of precipitation increments for low evaporation test

Start Day	End Day	Increment (mm/day)
1	12	0.33
13	25	0.67
26	38	1.33
38	57	2.00
58	62	3.50
63	80	5.00

The second surface flux boundary was a high evaporation, low precipitation condition. For this case, the columns were placed outdoors for 31 days where the average potential evaporation was 3 mm/day. Precipitation rates varied, but were significantly lower than those for the first phase of the testing. The columns were kept outdoors until inclement weather no longer allowed for further testing. Appendix B also summarizes the measured climate data for the second phases of the testing.

4.5.6 Test Procedure

After the columns achieved equilibrium and the initial conditions were identical for all columns, the covers were removed and the columns were exposed to the surface boundary flux. Each day a measurement of the amount of flux in or out of each column was taken by recording the level of water in the graduated cylinder. Water was then added to, or removed from each cylinder to return the water table elevation back to 20 cm above the base. Periodic water content and suction profiles were also recorded for each column. Tables 4-6 and 4-7 summarize the sampling dates.

The high evaporation portion of the testing was terminated after 31 days due to inclement weather, while the low evaporation portion was terminated after 80 days. No disruption to the columns was recorded over the 111 day period.

Table 4-6. Summary of suction measurements.

Column #	Elapsed Time for Measurements (days)	
	Low Evaporation Test	High Evaporation Test
1	0, 7, 14, 21, 28, 39, 46, 53, 60, 67, 74, 80	0, 3, 7, 11, 14, 21, 26, 31
2	0, 7, 14, 21, 28, 39, 46, 53, 60, 67, 74, 80	0, 3, 7, 11, 14, 21, 26, 31
3	0, 7, 14, 21, 28, 39, 46, 53, 60, 67, 74, 80	0, 3, 7, 11, 14, 21, 26, 31
4	0, 7, 14, 21, 28, 39, 46, 53, 60, 67, 74, 80	0, 3, 7, 11, 14, 21, 26, 31

Table 4-7. Summary of water content measurements.

Column #	Elapsed Time for Measurements (days)	
	Low Evaporation Test	High Evaporation Test
1	0, 14, 25, 38, 58, 80	0, 7, 14, 21, 31
2	0, 14, 25, 38, 58, 80	0, 7, 14, 21, 31
3	0, 14, 25, 38, 58, 80	0, 7, 14, 21, 31
4	0, 14, 25, 38, 58, 80	0, 7, 14, 21, 31

4.5.7 Final Conditions

At the termination of the testing, the materials within each column were removed and final measurements were taken. Shelby tubes were pushed into the cover soil and upper 50 cm of the tailings. From these samples, measurements of final density and water content were taken. For Columns 2 and 4, the individual layers of the GCB were carefully removed. For the geotextile layers, final gravimetric water content measurements were taken; while for the rock flour both final density and water contents were determined.

4.6 Chapter Summary

A material characterization program was undertaken after selection of desirable materials to construct the geosynthetic break and to design the engineered cover system. Tests included grain size, water characteristic curve, and saturated hydraulic conductivity. The GCB was evaluated based on its ability to restrict flow in an unsaturated cover system. Therefore, the saturated hydraulic conductivity and water characteristic curve for all materials were determined.

At the conclusion of the material characterization, a one-dimensional column testing program was undertaken to simulate 1-D behavior of the proposed engineered cover system. Two sets of columns were constructed; two with 30 cm of cover soil, and two with 60 cm. For each cover thickness one column incorporated the GCB, while the other did not. Two distinct climatic boundary conditions were applied to the surface of the columns in order to evaluate how the cover systems may perform under prolonged wet or dry conditions. Measurements were taken before, during, and at the completion of the testing program in order to compare the columns which incorporate the GCB with those which did not.

Chapter 5 presents the results of the material characterization and column testing program. An analysis of the 1-D column results will be presented in Chapter 6.

CHAPTER 5 PRESENTATION OF RESULTS

5.1 Introduction

Chapter 5 presents the results of the laboratory program described in Chapter 4. The data presented in this chapter shows measured grain size distributions, water characteristic curves, as well as saturated conductivity values for the materials used to evaluate the geosynthetic capillary break (GCB). Data from the one-dimensional column testing is also shown.

5.1.1 Grain Size Distributions

For the initial selection of the oxygen limiting material for the GCB, grain size distributions were performed to compare two possible materials; silica flour (SIL-CO-SIL (90)) and rock flour (Industrial Grade #75). As described in Section 4.2.3 the water characteristic curve for the silica flour had previously been measured by Rowlett (2000) and satisfied the criteria for an oxygen limiting layer as outlined by Nicholson et al. (1989). Therefore, the grain size distributions were compared to determine if the rock flour was also an acceptable oxygen-limiting layer. Figure 5-1 shows the measured curves obtained from hydrometer testing.

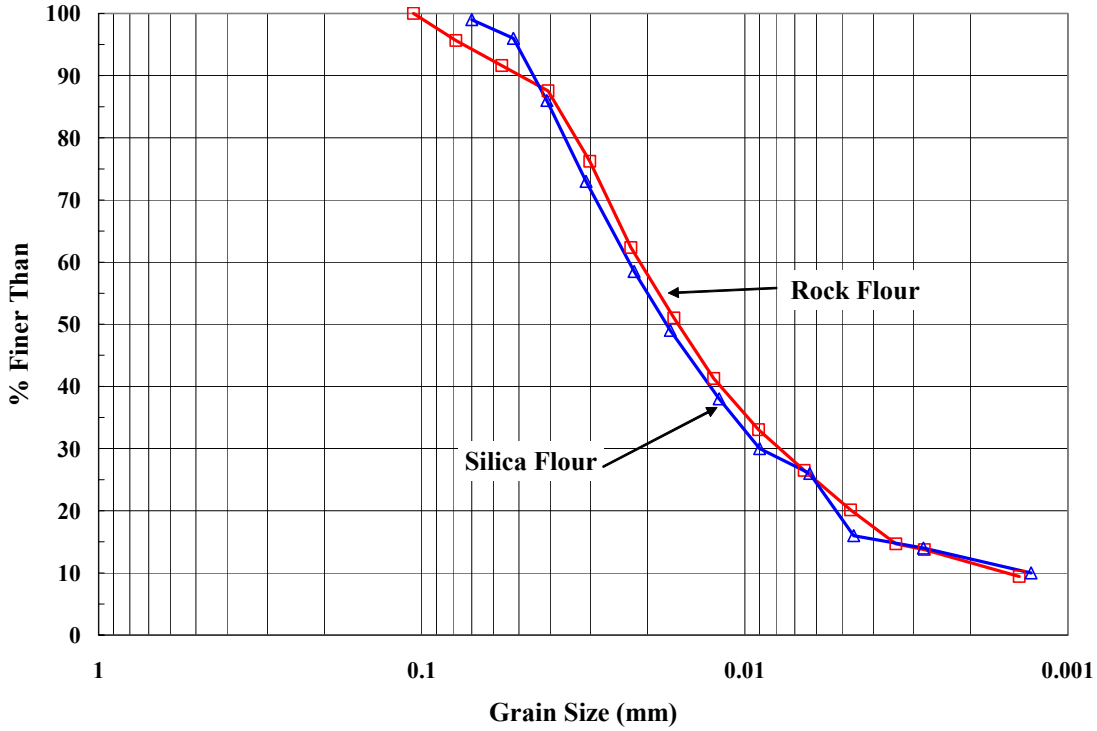

Figure 5-1. Comparisons of grain size distributions for silica and rock flour.

The results from the test show that the rock flour had a slightly finer grain size distribution than that of the silica flour. This was an indication that the AEV of the rock flour was be similar to or slightly higher than the AEV for the silica flour and will satisfy the oxygen limiting layer criteria.

Grain size curves were also determined for the cover soil and tailings used in the one-dimensional columns testing; the results are shown in Figure 5-2.

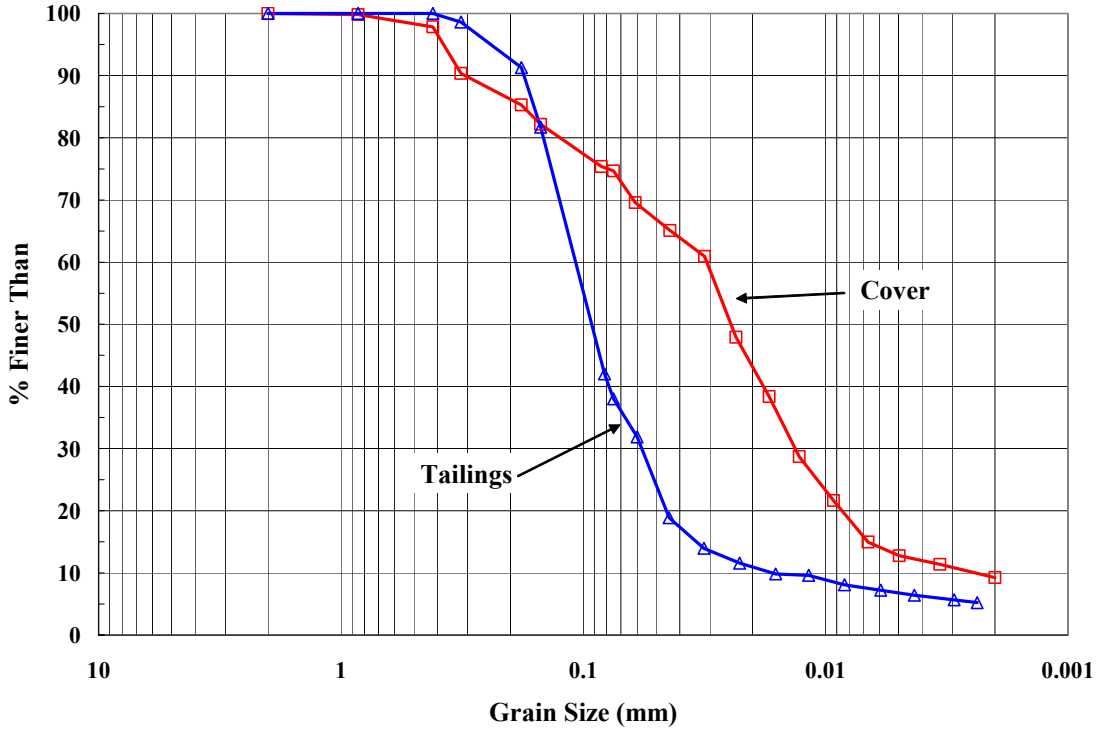

Figure 5-2. Grain size distributions for cover soil and tailings.

5.2 Saturated Hydraulic Conductivity Testing

Saturated hydraulic conductivities were measured on representative samples of the cover soil, rock flour, and tailings as described in Section 4.4.3. The constant head conductivity test was used to determine the saturated conductivity of the three materials, shown in Figure 5-3. The results are summarized in Table 5-1 along with the saturated hydraulic conductivity for the geotextile as determined by the manufacturer.

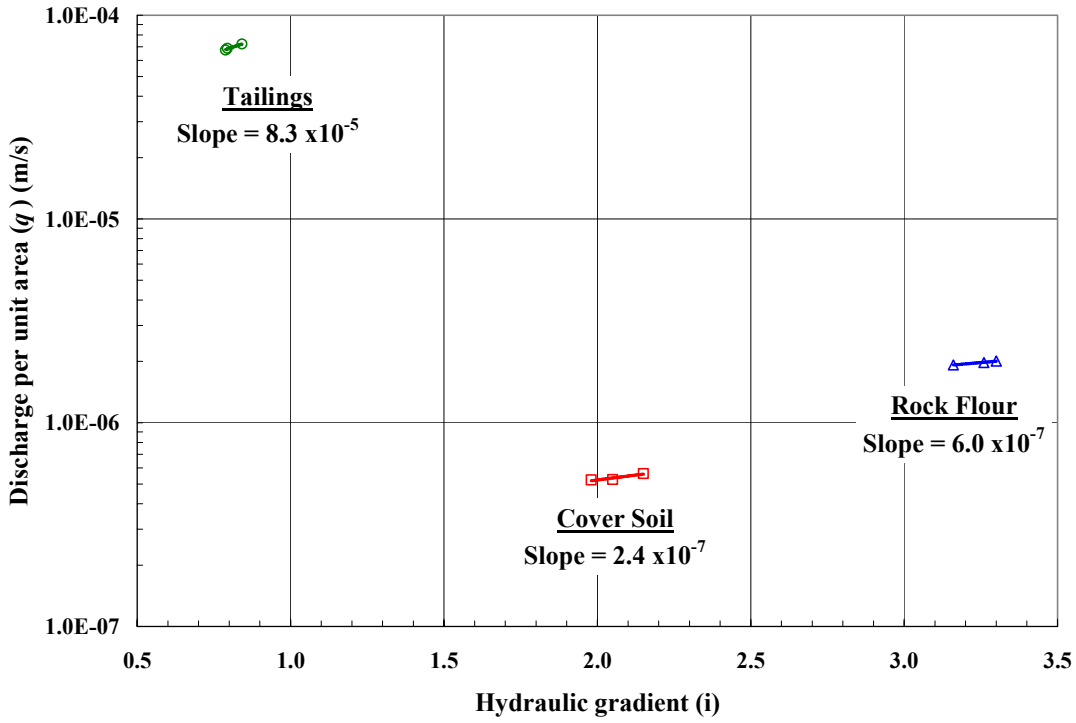

Figure 5-3. Constant head conductivity results for cover soil, rock flour and tailings.

Table 5-1. Saturated hydraulic conductivities for tested materials.

Material	Saturated Hydraulic Conductivity (m/s)
Cover Soil	2.4×10^{-7}
Rock Flour	6.0×10^{-7}
Geotextile*	1.0×10^{-3}
Tailings	8.3×10^{-5}

*specified by manufacturer (Terrafix, 2004)

Table 5-1 illustrates that the saturated hydraulic conductivity of the materials varied over a wide range of magnitudes. This conforms to expected behaviour, since the grain size distributions of the materials also showed large contrast.

5.3 Water Characteristic Curves

5.3.1 General

The water characteristic curve (WCC) for the cover soil, rock flour, and tailings were determined using the single specimen pressure plate cell as outlined in Section 4.4.4. For the geotextile, the pressure plate cell was also used to measure the WCC, however the hanging test method was also evaluated (Figure 4-6). The results of the geotextile water characteristic curve testing will be presented in Section 5.4.2. The water characteristic curves for the remaining materials will be presented in Section 5.4.3.

5.3.2 Geotextile

Two testing methods were used to measure the WCC for the geotextile. Figure 5-4 compares the measured drying curves for the two methods.

Examining Figure 5-4, when comparing the hanging test to the pressure plate, for the same material, the hanging test produces lower water contents for all initial volumetric water contents, although the measured AEV are similar. Flaws in the experimental procedure for the hanging test may account for the differences in the measured curves. During the hanging test, it is impossible to prevent at least a small amount of evaporation from occurring as well as water losses resulting from handling of the specimen. However, these effects are not a concern in the case of the pressure plate cell.

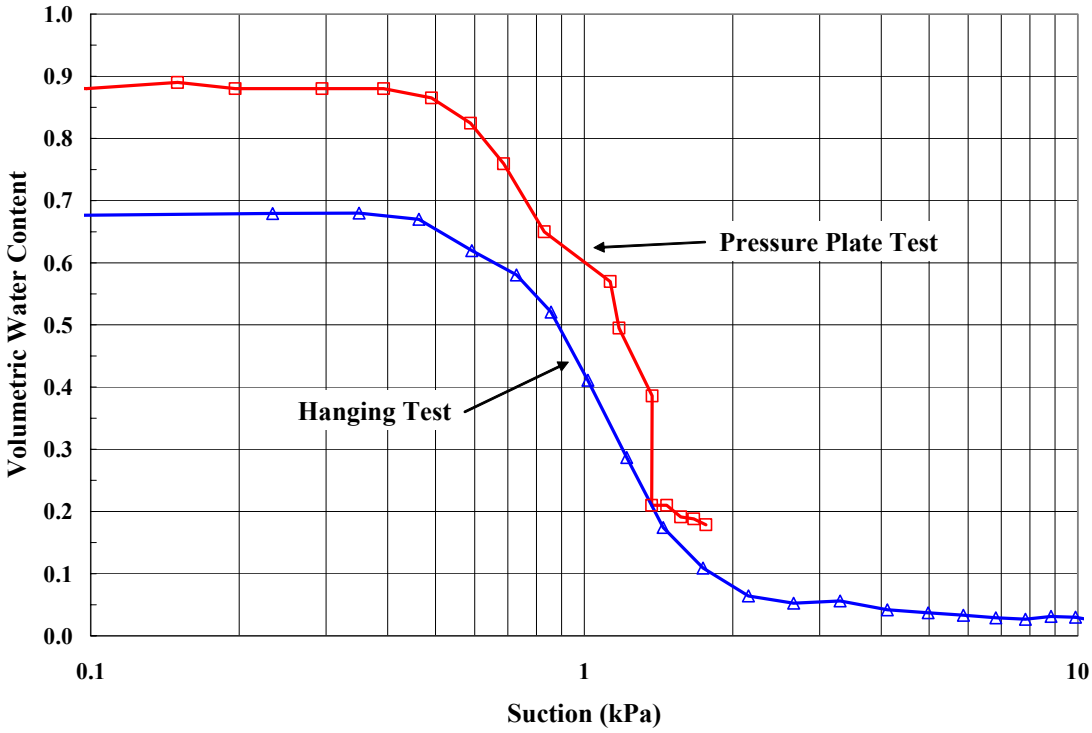

Figure 5-4. Comparison of test methods for geotextile WCC.

The geotextile was also tested using the hanging test to determine the effect of the degradation of potentially hydrophobic lubricating oils used in the manufacturing process. Two specimens of geotextile were compared; one which was washed in detergent in an attempt to remove such oils, and another which was not washed.

Figure 5-5 shows how the degradation of the oils within the geotextile over time affected the water characteristic curve. When comparing the volumetric water contents for the two specimens at the same suction, the washed specimen had a slightly higher value. This held true for points within the transition phase of the WCC; however for points within the pre-air entry and residual stage, there was no noticeable difference.

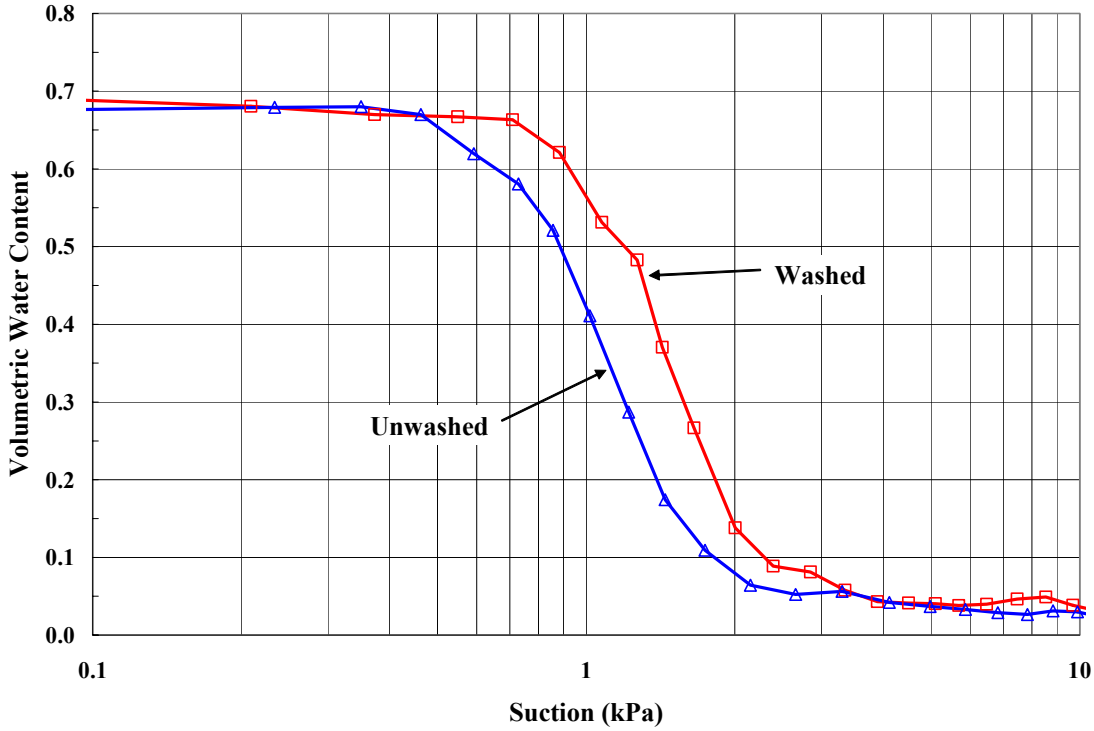

Figure 5-5. Effect of removing lubricating oils on geotextile WCC as determined using the hanging test.

Lastly, the effect of increasing overburden pressure was considered on the geotextile WCC. The pressure plate cell was utilized, and normal loads of 1, 5, 6.3, and 10 kPa were applied to the geotextile. The results are shown in Figure 5-6.

Figure 5-6 illustrates as the overburden pressure was increased, the volumetric water content increased. This effect was quite pronounced from 0 to 5 kPa, but from 5 to 10 kPa there were only small changes in the WCC for the geotextile. The porosity (saturated volumetric water content) of the specimens also reduced as the pressure is increased.

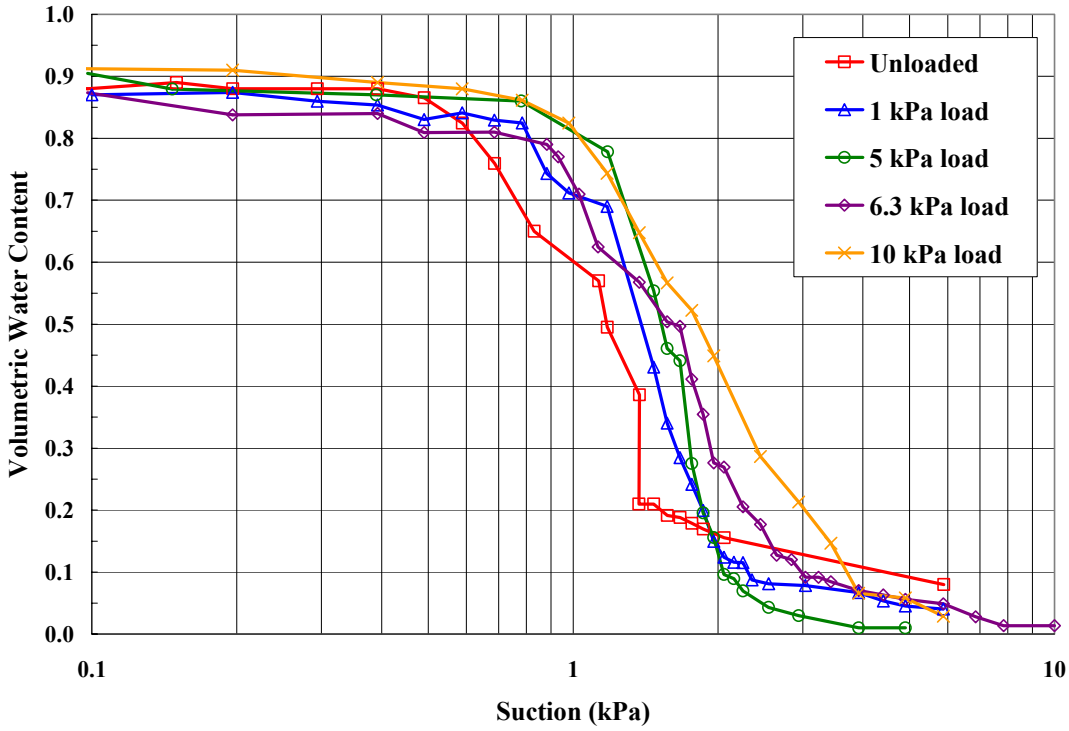

Figure 5-6. Effect of increasing overburden pressure on geotextile WCC as determined using the pressure plate cell.

5.3.3 Cover Soil, Rock Flour, and Tailings

The water characteristic curves for the cover, rock flour, and tailings were measured using the pressure plate cell and are presented in Figure 5-7. When comparing the measured curves for the geotextile (6.3 kPa load) and rock flour, it can be seen that there was a significant contrast between the two materials. For suction values between 8 and 40 kPa, the geotextile was at or near residual volumetric water content, while the rock flour was near saturation.

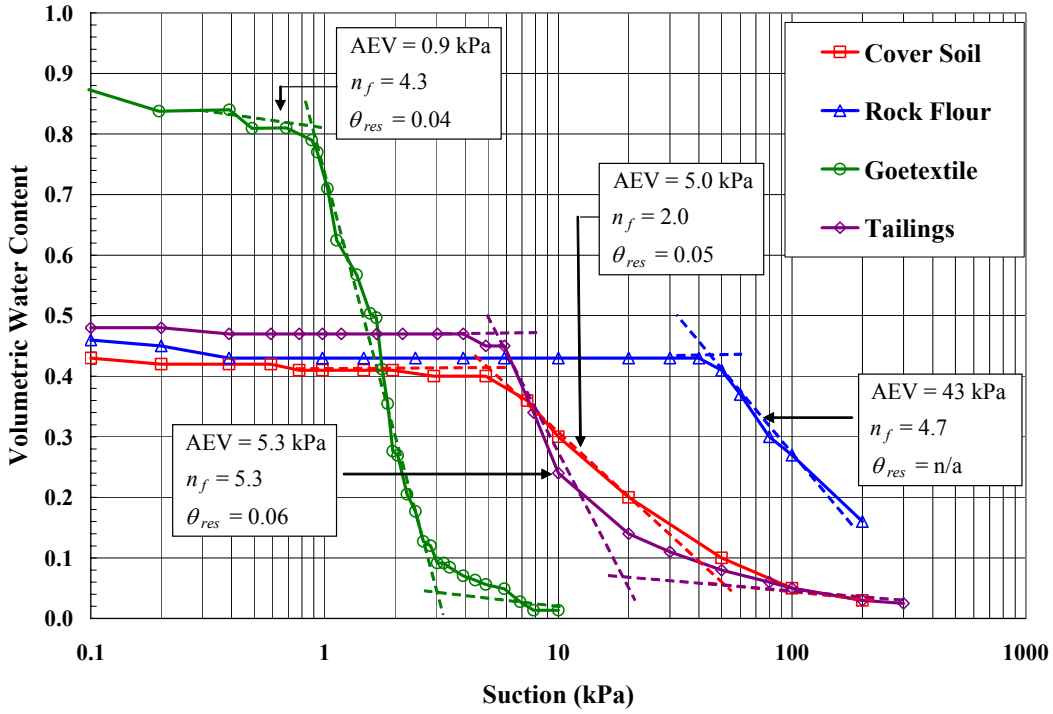

Figure 5-7. Measured water characteristic curves for materials.

5.4 One-Dimensional Column Testing

5.4.1 General

The data collected during the one-dimensional column testing is presented in the following sections. A preliminary evaluation of the data shows that the geosynthetic capillary break (GCB) was effective in reducing moisture movement across the tailings-cover soil interface and has the potential to mitigate oxygen movement.

The data collected during this testing was divided into four sections. First, the measured flux rates were presented in order to show the effect of the GCB on downward and upward moisture movement within the cover systems. Next, water content profiles were presented with an evaluation of the change in storage for the cover soil and underlying tailings within each separate column. Direct measurements of the water

content for the individual layers of the GCB could not be taken during testing; therefore soil suction measurements were taken 5 cm above and below the interface to provide an indication of the water content profile within the GCB. Lastly, at the termination of the test, Shelby tubes were pushed through the cover soil and top 50 cm of the tailings to determine the final water contents and densities. The water contents for the individual layers of the GCB were determined as well as the final density for the rock flour layer.

5.4.2 Flux Rates

Comparing the pairs of columns (Column 1 with Column 2 and Column 3 with Column 4), for identical cover thickness, the column which incorporated the GCB in both cases exhibited less fluctuation in the measured flux. This is illustrated in Figures 5-8 and 5-9 which show the cumulative daily fluxes for both the high evaporation and low evaporation phases of the testing program. Cumulative column flux refers to the cumulative total of the daily flux measurements in or out of the individual columns. The column flux is the measurement of daily flux in or out of the columns using the graduated cylinders. The cumulative surface flux refers to the cumulative total of the daily measurements for precipitation and potential evaporation. The cumulative column and surface fluxes are plotted in units of mm of water as measured over the cross sectional area of the columns.

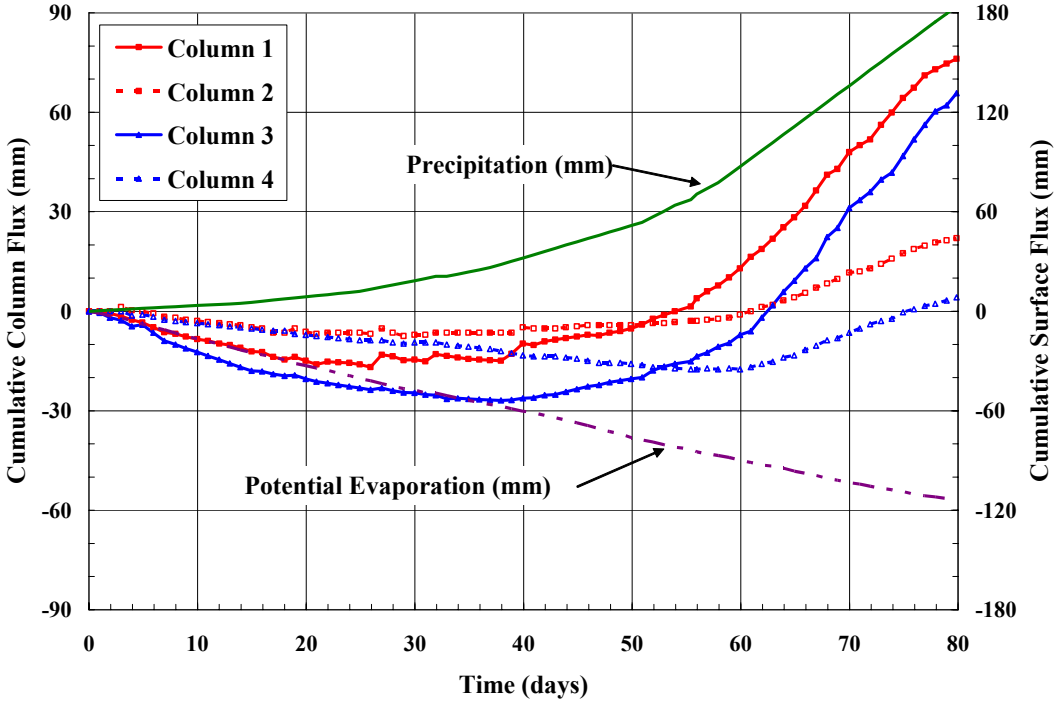

Figure 5-8. Cumulative flux measurements for low evaporation (1.5 mm/day) boundary condition.

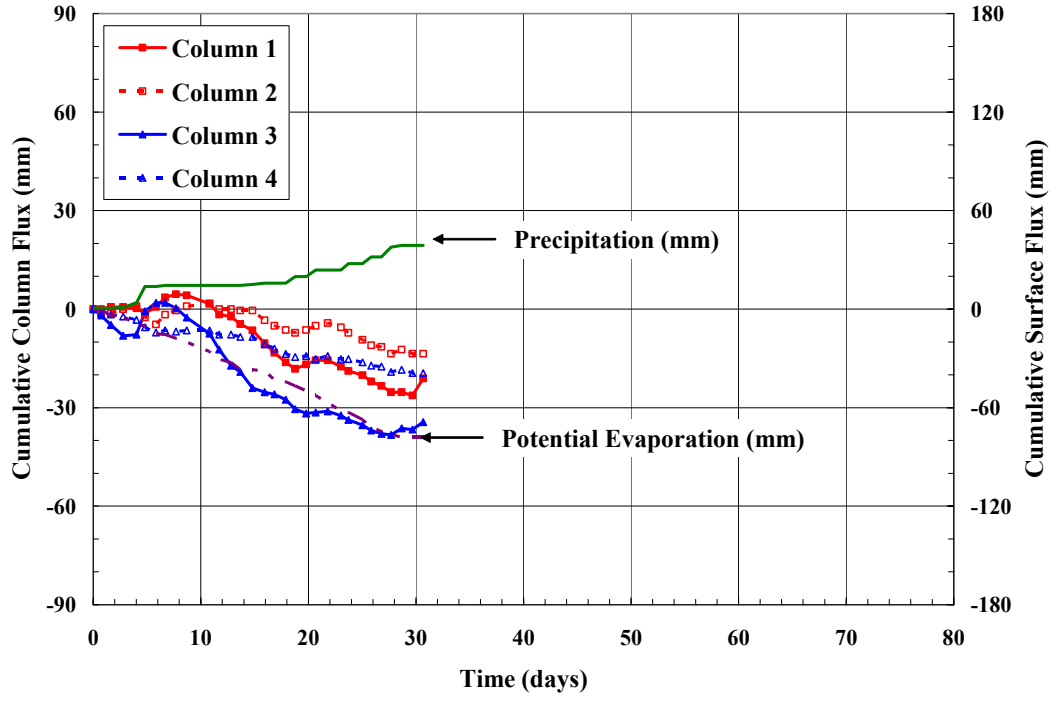

Figure 5-9. Cumulative flux measurements for high evaporation (3 mm/day) boundary condition.

For the low evaporation boundary condition, there was a high downward gradient of moisture flow. Figure 5-8 shows the effectiveness of the GCB. The curves for Columns 2 and 4 have significantly lower amplitudes and also show less fluctuation than those for Columns 1 and 3. Tables 5-2 and 5-3 also confirm the effectiveness of the GCB, by showing the maximum daily evaporation and infiltration events measured for each column. A significant reduction was noticed for columns which incorporate the GCB.

Similarly, for the high evaporative boundary conditions, high upward gradients would be anticipated. Figure 5-9 shows the flux measurements for this portion of the column testing. Again, columns which incorporate the GCB showed less amplitude and fluctuation than those which do not.

For the low evaporation boundary condition, specific values for precipitation were applied to the columns daily until a relatively constant flux was measured. It was found that all columns initially behaved similarly under low precipitation rates; relatively small daily fluxes were observed. However, as the magnitude of precipitation was increased, the measured fluxes remained relatively constant; as water was stored in the cover soil. Figure 5-10 shows a graph of the average daily measured flux rates for each column over each precipitation increment. This graph shows that for a certain value of precipitation over time, "breakthrough" occurred as water began to infiltrate into the tailings. Columns which did not incorporate the GCB experienced "breakthrough" at an earlier point in time and exhibited overall higher infiltration flux.

Table 5-2. Maximum daily flux events for low evaporation test.

	Column 1	Column 2	Reduction	Column 3	Column 4	Reduction
Max. daily infiltration event (mm)	5.0	1.9	62%	6.3	1.9	70%
Max. daily evaporation event (mm)	1.5	1.3	13%	2.4	1.3	46%

Table 5-3. Maximum daily flux events for high evaporation test.

	Column 1	Column 2	Reduction	Column 3	Column 4	Reduction
Max. daily infiltration event (mm)	5.2	3.0	42%	7.1	1.0	86%
Max. daily evaporation event (mm)	3.9	3.4	13%	4.9	2.2	55%

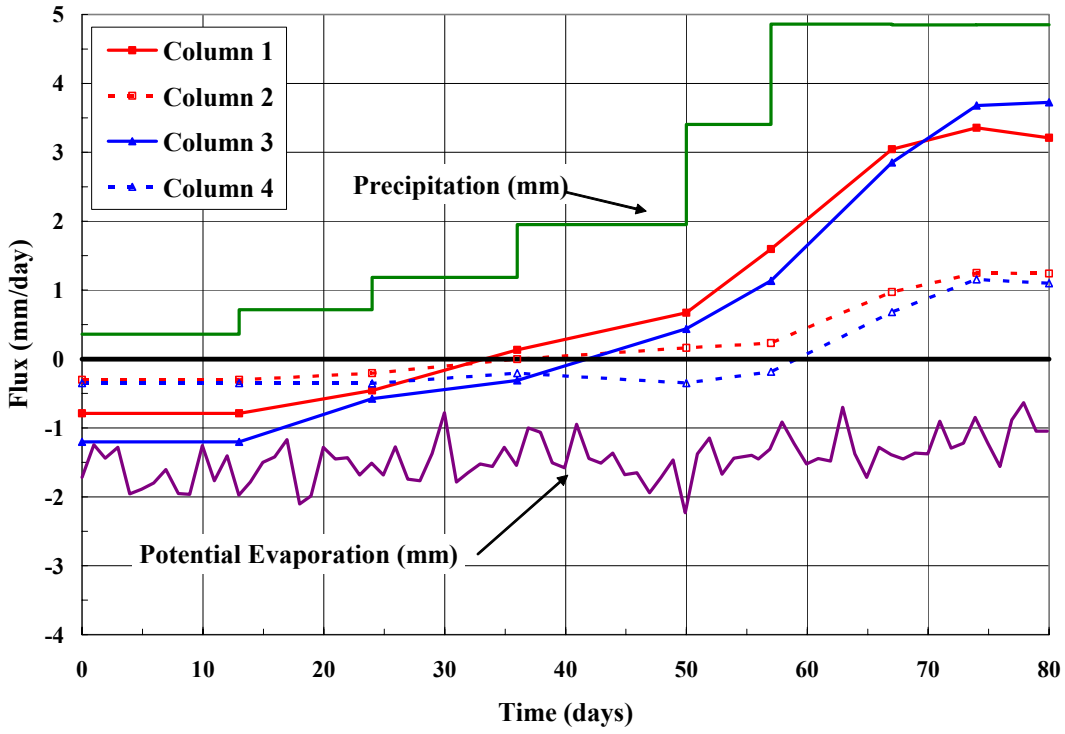

Figure 5-10. Average flux rates for each precipitation increment from low evaporation test.

5.4.3 Water Content Measurements

Throughout the course of the tests, the 10 mm holes along the perimeter of the columns were used to obtain water content profiles. Approximately 3 g of material was removed at each sampling port and the water content of the specimen was determined by oven drying. An approximately equal volume of material was placed back into the sampling port to replace the volume used for testing. Table 4-7 shows the elapsed time between each measurement. Figures 5-11 and 5-12 show the change in total volume of water within the tailings layer for both the high and low evaporation boundary conditions, while Figures 5-13 and 5-14 show the change in water volume within the cover soil for the same boundary conditions. The volume of water in the cover soil and tailings was calculated using the results of the water content profiles along with the location of the sampling port along the side of the column. The moisture content measured at the sampling port was assumed to be representative of the entire volume of material corresponding to that port. The total volume of water in the column was calculated by integrating the measured water contents and port locations along the entire length of the column.

Figures 5-11 and 5-12 illustrate that there was slightly less change in storage for the tailings within the columns which incorporate the GCB. Conversely, Figures 5-13 and 5-14 show slightly more change in storage in the cover soil for those columns which include the GCB. These effects were not as pronounced as the flux measurements due to fluctuations in individual water content measurements and soil densities at the sampling points.

5.4.4 Suction Profiles

Suction measurements were taken above and below the interface for each column. For the purpose of evaluation of the GCB, suctions at elevations immediately above and below the GCB (1.1m and 1.3m above the base) for Columns 2 and 4 were of concern. Figures 5-15 and 5-16 show that the suction below the break was kept relatively constant between 7.0 and 12.0 kPa, while the suction above the break steadily increased. The tensiometers eventually failed as a result of inclement weather and the subsequent moving of the columns, and it was therefore not possible to provide meaningful measurements during the low evaporation test.

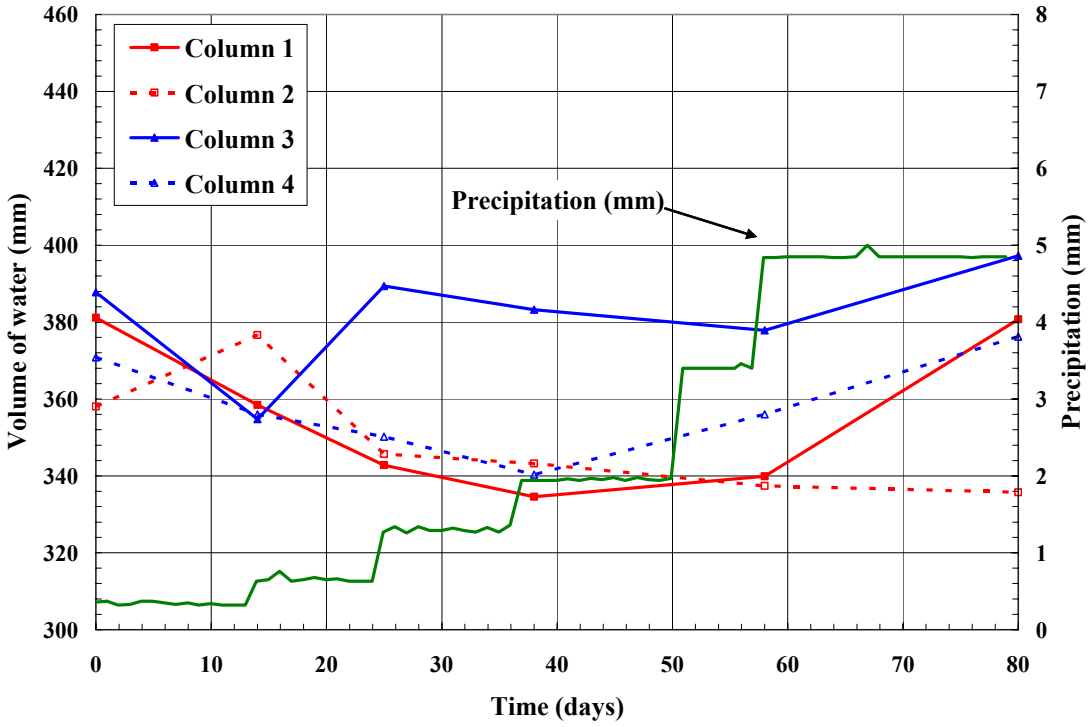

Figure 5-11. Volume of water in tailings for low evaporation (1.5 mm/day) test.

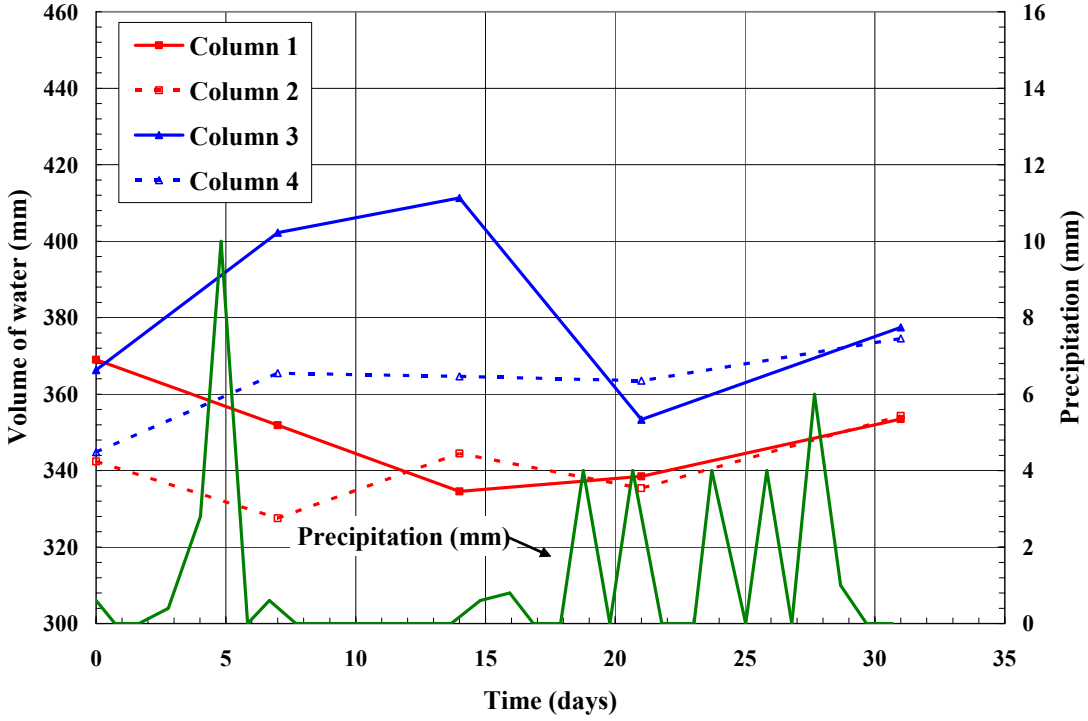

Figure 5-12. Volume of water in tailings for high evaporation (3 mm/day) test.

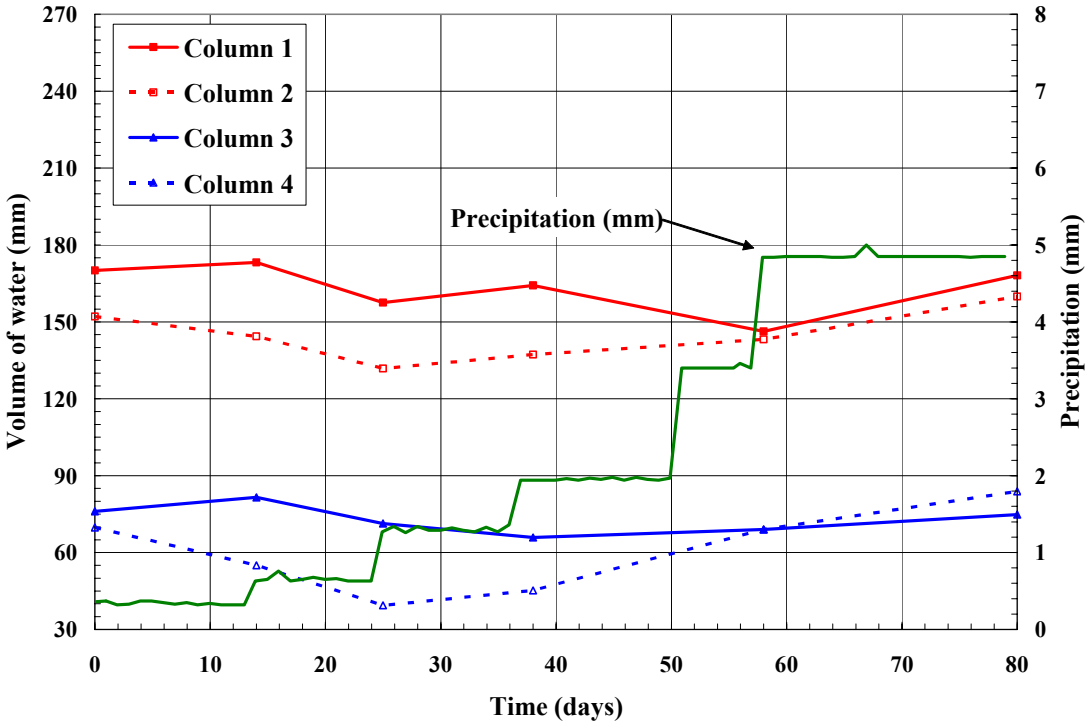

Figure 5-13. Volume of water in cover soil for low evaporation (1.5 mm/day) test.

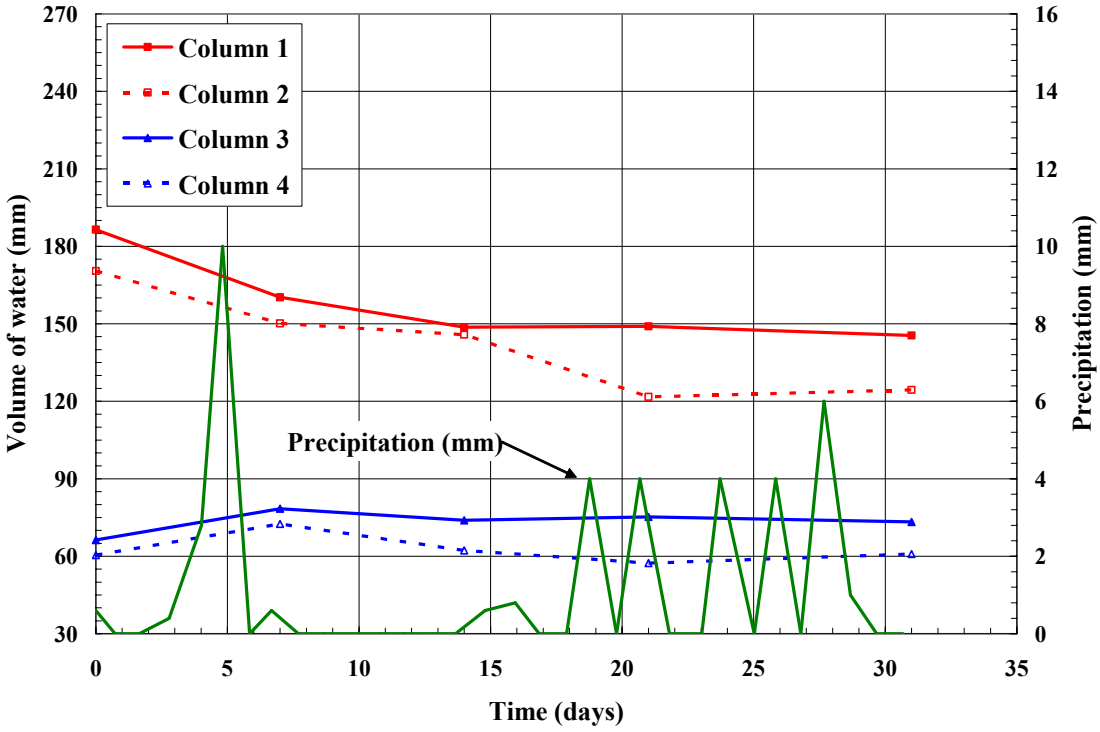

Figure 5-14. Volume of water in cover soil for high (3 mm/day) evaporation test.

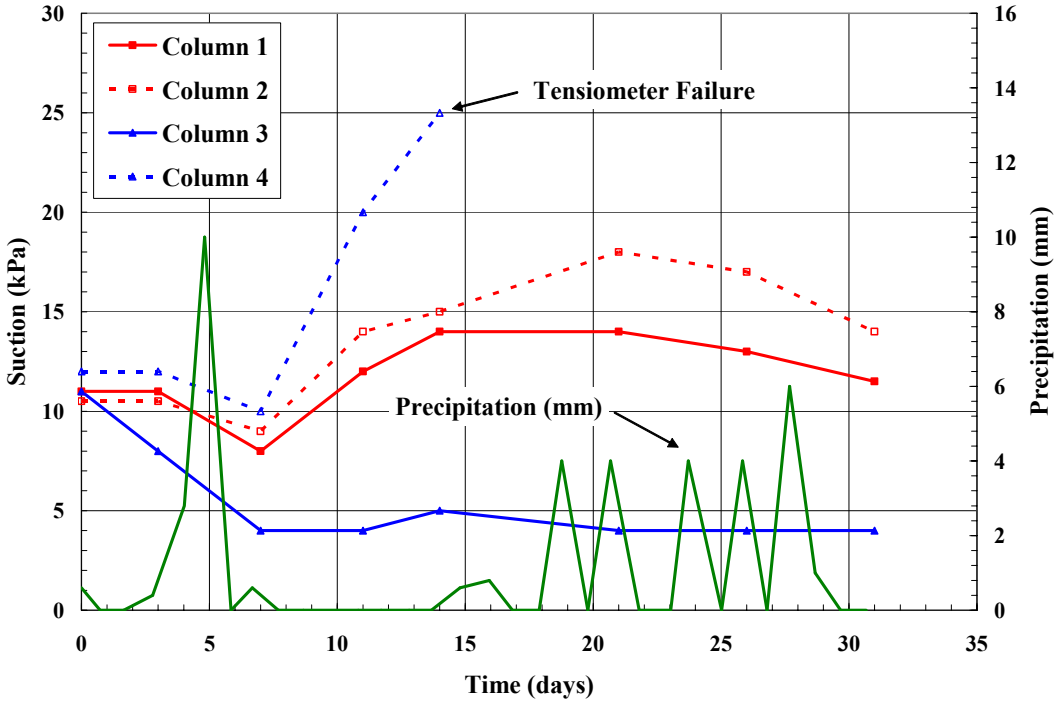

Figure 5-15. Suction measurements 5 cm above interface for high evaporation (3 mm/day) test.

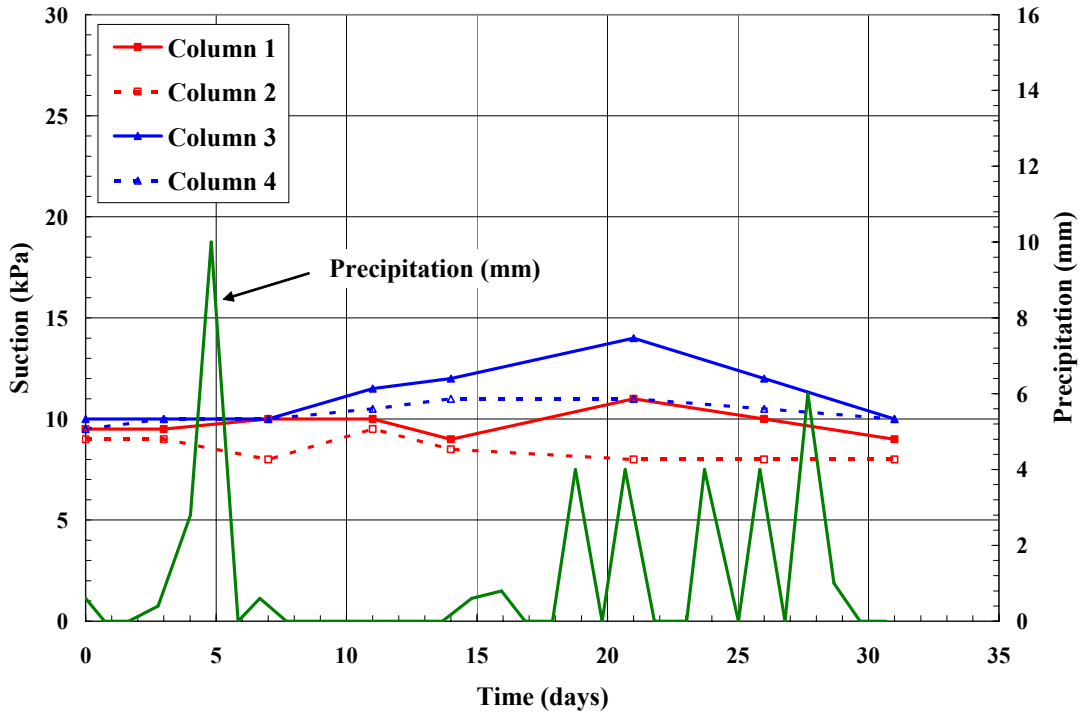

Figure 5-16. Suction measurements 5 cm below interface for high evaporation (3 mm/day) test.

5.4.5 Final Measurements

Measurements of density and water content were taken at the completion of the column testing in order to verify tests conducted throughout the testing process and allowed for final measurements of properties that could not be measured during testing.

Table 5-4 shows measurements of final densities for the cover soil and tailings for each column. The results showed that, on average, the density for both the cover soil and tailings increased slightly during the course of the tests by consolidation of the materials due to changes in effective stress. For Columns 2 and 4, Table 5-4 also shows the final density of the rock flour layer of the GCB.

Table 5-5 shows the gravimetric water contents for the individual layers of the geosynthetic capillary break. As expected, the upper layers of geotextile and the rock flour layer showed high water contents; whereas the lower geotextile layers were drier.

Figures 5-17 to 5-20 show comparisons of the water content profiles of the columns sampled from the ports located on the perimeter of the column and the moisture contents as determined from the Shelby tube samples sampled on the same day. The figure showed relatively close agreement between the two measurement techniques considering the intrusive nature of the Shelby tube sampling. The result supports the use of the moisture content measurements taken throughout the course of the testing.

Table 5-4. Final dry density measurements for column materials.

	Column 1	Column 2	Column 3	Column 4
Final Cover Dry Density (kg/m^3)	1610	1610	1620	1640
Final Rock Flour Dry Density (kg/m^3)	n/a	1660	n/a	1710
Final Tailings Dry Density (kg/m^3)	1650	1660	1610	1770

Table 5-5. Final gravimetric water content measurements of individual GCB layers.

	Column 2	Column 4
Top layer of geotextile	0.45	0.49
Rock Flour	0.25	0.26
Upper layer of bottom geotextile	0.31	0.43
Lower layer of bottom geotextile	0.18	0.20

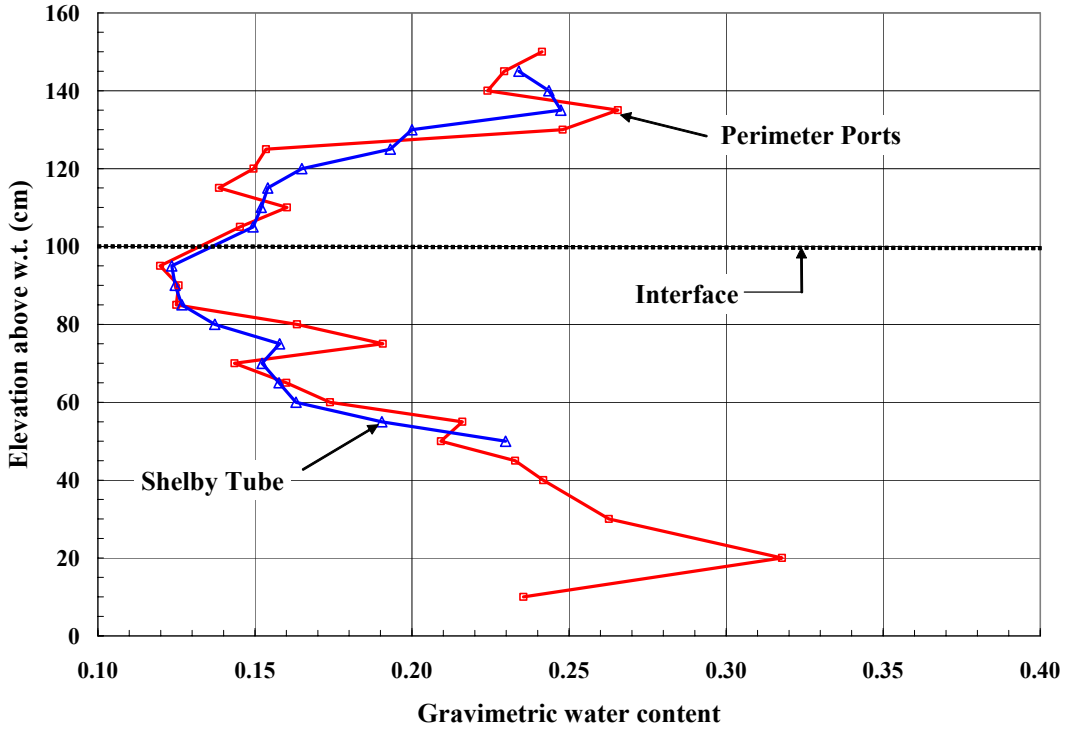

Figure 5-17. Comparison of gravimetric water content profiles for Column 1.

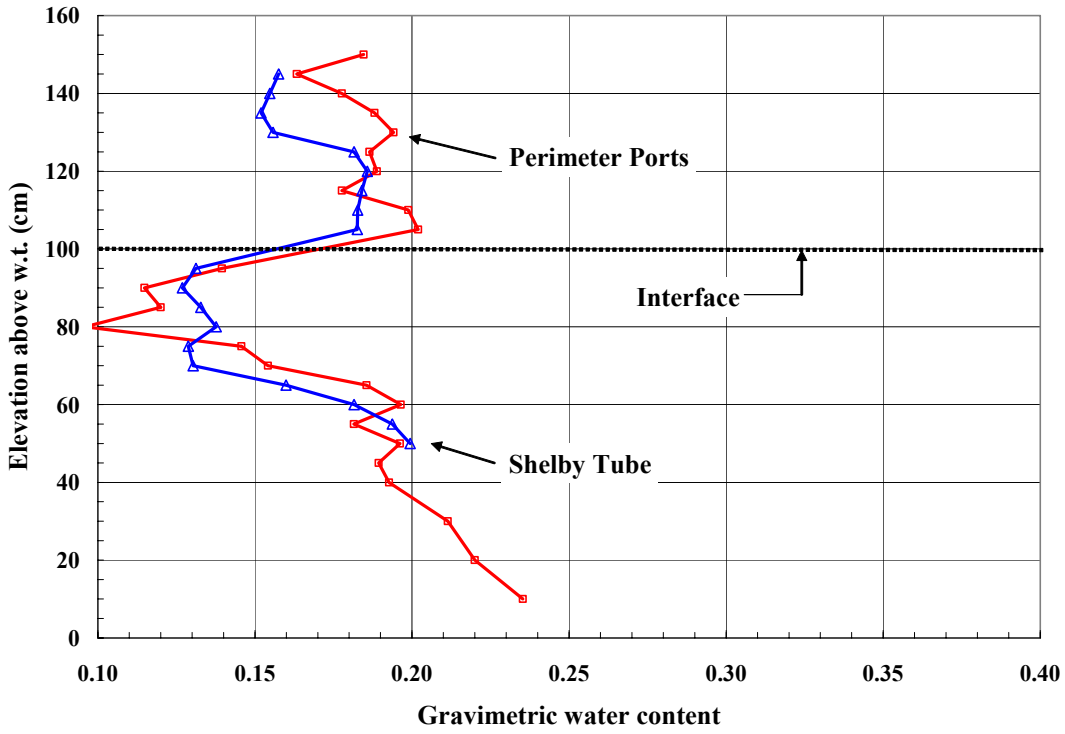

Figure 5-18. Comparison of gravimetric water content profiles for Column 2.

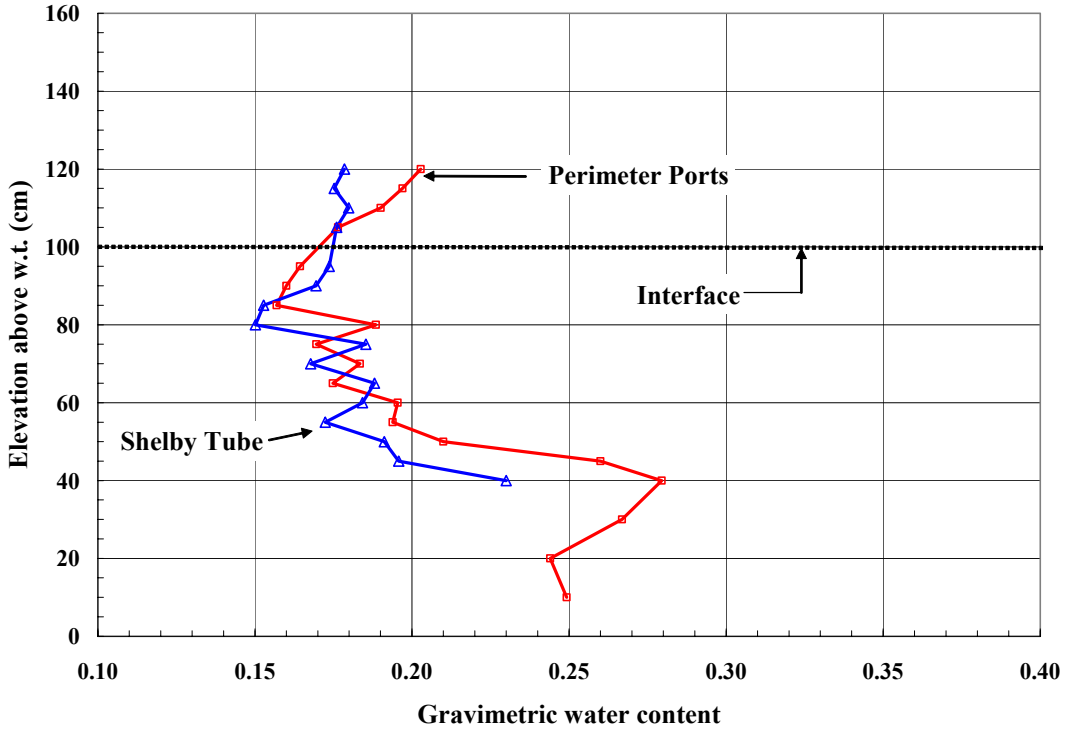

Figure 5-19. Comparison of gravimetric water content profiles for Column 3.

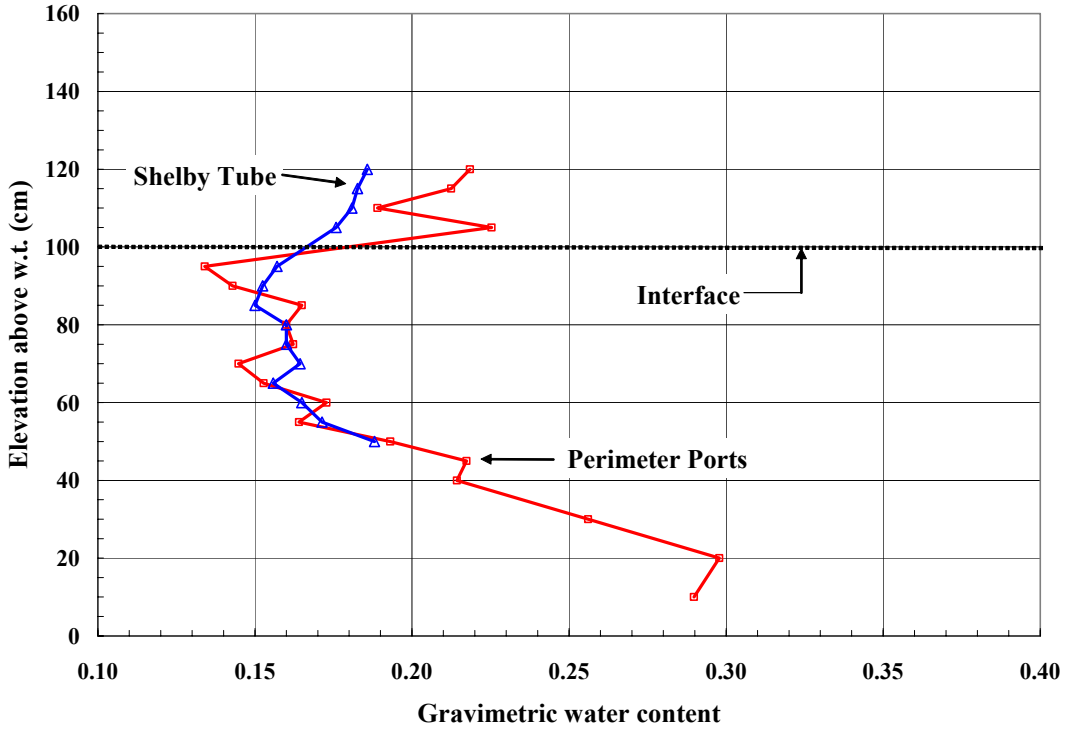

Figure 5-20. Comparison of gravimetric water content profiles for Column 4.

5.5 Chapter Summary

The material characterization program consisted of the measurement of grain size distributions and saturated hydraulic conductivities for the cover soil, tailings, and rock flour. Water characteristic curves were also measured for the three materials along with the geotextile. The results of the testing showed a sharp contrast in the unsaturated hydraulic properties for the geotextile and rock flour. Examining the water characteristic curves, the porosity of the geotextile was significantly higher (0.9 as opposed to 0.43) than that of the rock flour. Also, comparing the air-entry values the materials, the geotextile began to desaturate at approximately 0.9 kPa while the rock flour did not begin to desaturate until 40 kPa. Water characteristic curves were also measured for the cover soil and tailings which were used in the column testing. These

functions were utilized as inputs for the analytical and numerical models and were also used to estimate other pertinent functions such as the unsaturated hydraulic conductivity function. Table 5-6 shows a summary of the measured material properties.

Table 5-6. Summary of material properties measured in the laboratory.

	Cover	Rock Flour	Geotextile	Tailings
USCS classification	ML	ML	n/a	SM
Saturated hydraulic conductivity (m/s)	2.4×10^{-7}	6.0×10^{-7}	1.0×10^{-3}	8.3×10^{-5}
Porosity	0.42	0.45	0.85	0.47
Air-entry value (AEV) (kPa)	5.0	4.7	0.9	5.3
Rate of desaturation (n_f)	2.0	4.7	4.3	5.3
Residual water content (θ_{res})	0.05	n/a	0.04	0.06

One-dimensional columns were constructed in an attempt to replicate a simple, 1-D engineered cover system. The columns were subjected to two distinct boundary conditions for a total of 111 days. Throughout the course of the test, measurements of flux, water content, and soil suction were taken in order to evaluate the performance of the GCB. The initial results indicated that the GCB acted to reduce moisture migration within the cover system. The results from the column testing program will be analyzed in Chapter 6 in order to utilize finite element modeling software to predict the anticipate hydraulic performance of the GCB as part of an engineered cover system for HBM&S in Flin Flon, MB.

CHAPTER 6 `ANALYSIS AND DISCUSSION

6.1 Introduction

The laboratory program for this research was described in Chapter 4, with the results presented in Chapter 5. This chapter analyzes and interprets these results as well as provides a discussion of their significance. This chapter includes the results of a closed-form solution, analytical model (Kisch, 1959) as well as numerical modeling (GeoStudio, 2004) in order to evaluate and analyze the performance of the GCB throughout the laboratory program as well as to predict possible long-term performance of this product.

6.2 Water Characteristic Curves

The measured water characteristic curves for the materials used in the columns were presented in Chapter 5. These tests were conducted in the soils laboratory at the University of Saskatchewan under controlled conditions. The water characteristic curve (WCC) determined using the pressure plate cell may be slightly different than the observed water characteristic curve in the field due to possible nonhomogeneities in density and/or grain size within the materials. Therefore, "field" water characteristic curves were determined. The field, or in-situ, water characteristic curve was simply the water characteristic curve determined by taking actual measurements of matric suction and water content within a material after being placed in the columns. The field water characteristic curve allowed for a better understanding of the in-situ properties of the

materials and allowed for a more accurate determination of other material functions estimated from the water characteristic curve.

As described in Section 4.5.4, for the initial conditions, the columns were wetted from the bottom up, bringing all materials to saturation. The columns were then drained and allowed to come to equilibrium, at which time water content profiles were obtained. This process was repeated before the start of both the high and low evaporation test. Therefore, for the cover soil and tailings, a relationship between the volumetric water content and height above water table (suction) was developed to represent the in-situ or field water characteristic curves.

It was not possible to take in-situ water content measurements of the rock flour and geotextile layers for the GCB. Therefore, the curves measured in the lab were used as inputs for the analysis. Figures 6-1 and 6-2 show the measured data points for the field water characteristic curves as well as the measured laboratory curves for the cover soil and tailings. The field water characteristic curves in Figures 6-1 and 6-2 were approximated using Fredlund and Xing (1994) and van Genuchten (1980) closed form equations for the water characteristic curve (Eqs 3.3 and 3.4).

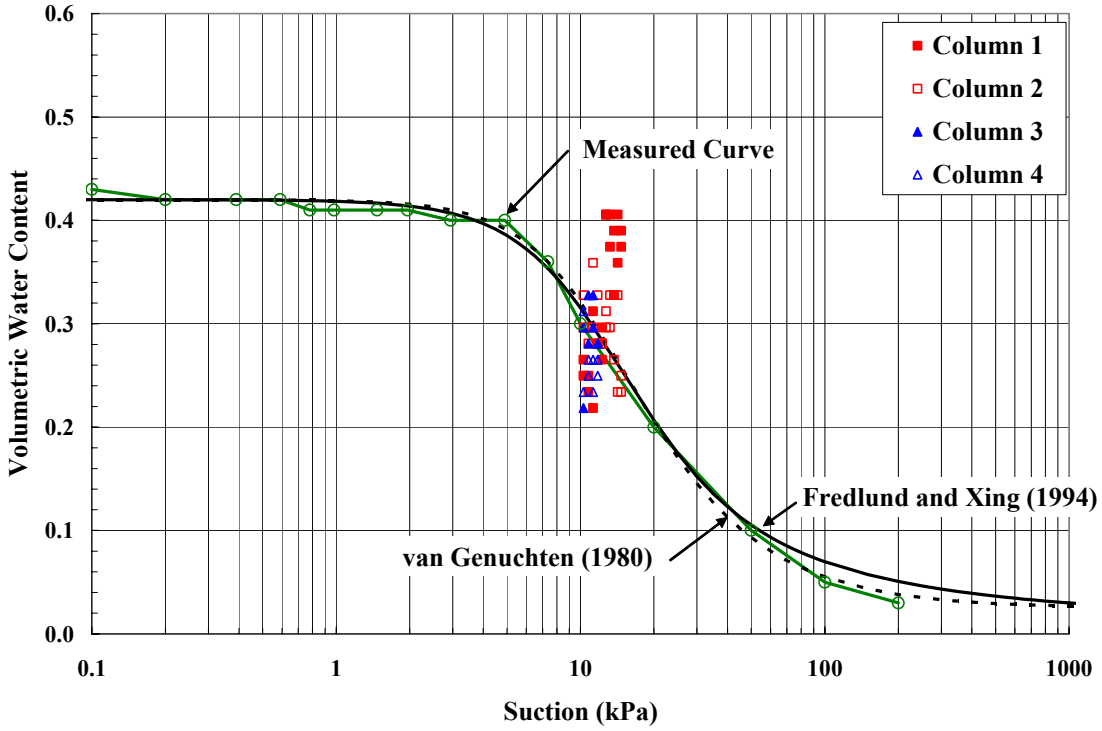

Figure 6-1. Determination of the field water characteristic curve for the cover soil.

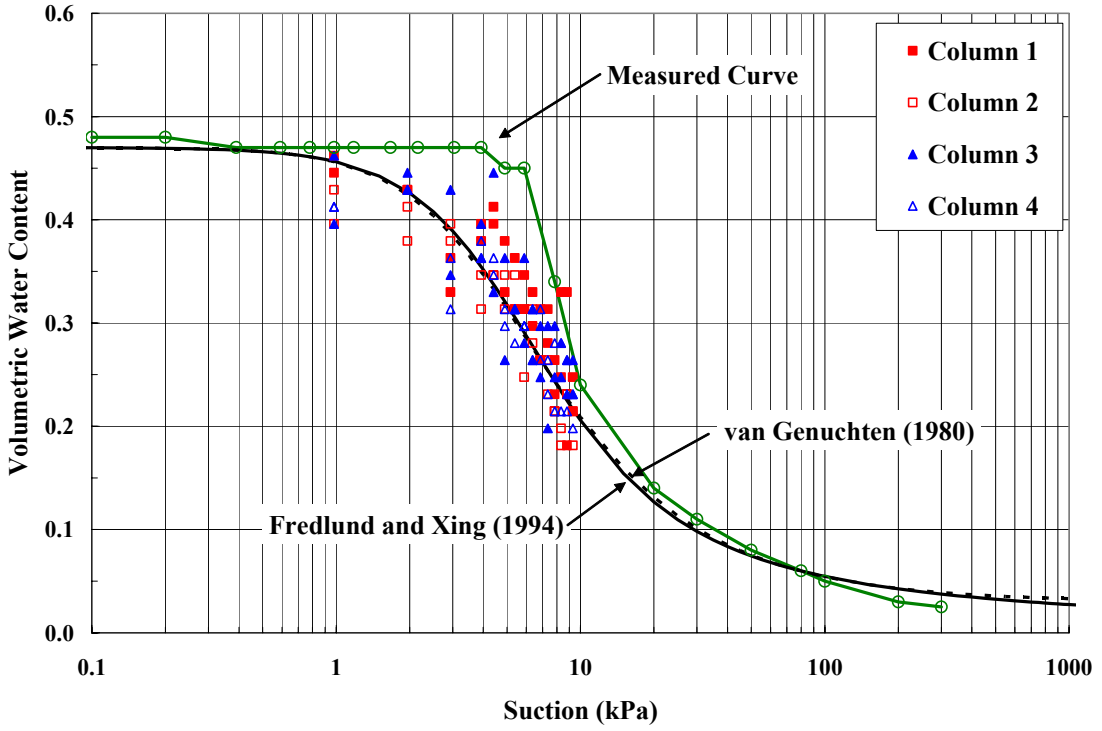

Figure 6-2. Determination of the field water characteristic curve for the tailings.

Figure 6-1 showed significant scatter for the field water characteristic curve for the cover soil. The scatter was due to small differences in placement density and/or material grain size within each sample. The measured curve for the cover soil seemed to somewhat approximate the materials behavior and was, therefore, used as the input function for the analysis. For the tailings (Figure 6-2), the measured WCC showed a more consistent trend. Compared to the measured curve, the field curve had a slightly lower air-entry value (AEV) and a softer slope in the transition phase than what was indicated in the laboratory curve.

For both the analytical and numerical analysis, closed form equations were used to express the water characteristic curves for all materials used in the column construction. Fredlund and Xing (1994) as well as van Genuchten (1980) parameters were obtained for the four water characteristic curves. The parameters for the two curve fitting methods are presented in Tables 6-1 and 6-2, while Figures 6-3 and 6-4 show the closed form water characteristic curves using Equations 3.3 and 3.4, respectively. The determination of the air-entry values (AEV), rate of desaturation (n), and residual water content (θ_r) are presented in Table 6-3.

Table 6-1. Fredlund and Xing (1994) parameters for column materials.

Material	θ_{sat}	α_f (kPa)	n_f	m_f	h_r (kPa)
Cover Soil	0.42	10.9	2.0	1.20	10^6
Rock Flour	0.44	59.5	4.7	0.58	10^6
Geotextile	0.82	1.5	4.3	1.77	10^6
Tailings	0.47	4.5	1.8	1.25	10^6

Table 6-2. van Genuchten (1980) parameters for column materials.

Material	θ_{sat}	θ_{res}	α (1/kPa)	q	p
Cover Soil	0.42	0.03	0.085	2.2	0.55
Rock Flour	0.44	0.08	0.012	2.9	0.66
Geotextile	0.82	0.02	0.690	4.2	0.76
Tailings	0.47	0.03	0.250	1.9	0.47

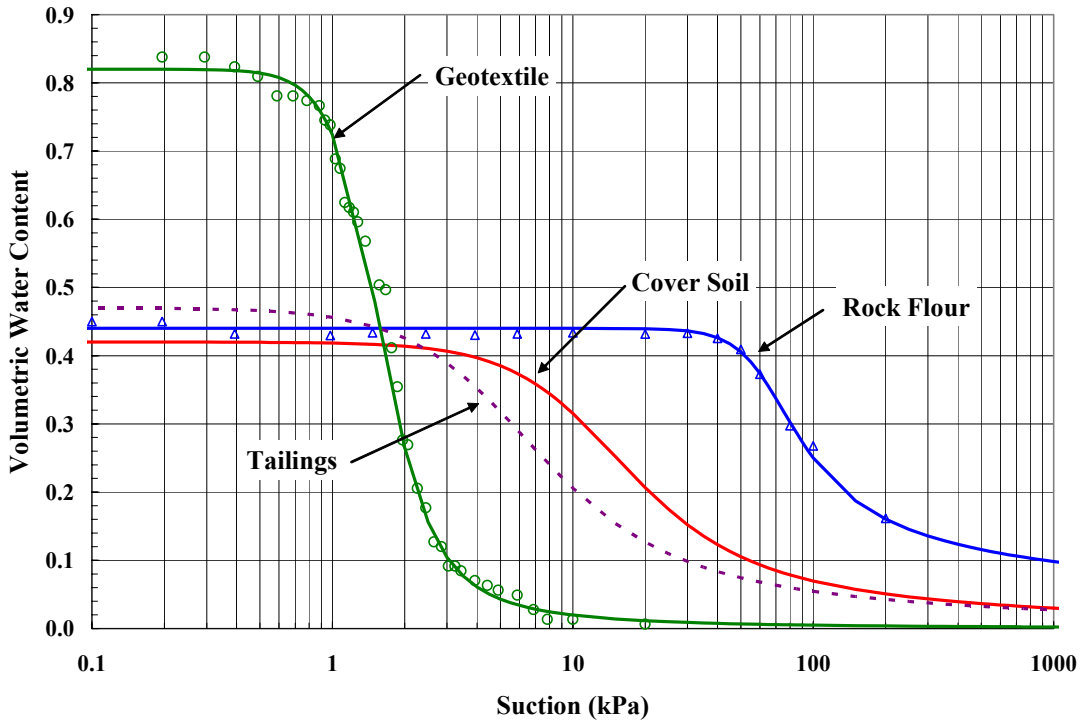

Figure 6-3. Water characteristic curves fitted with Fredlund and Xing (1994) parameters.

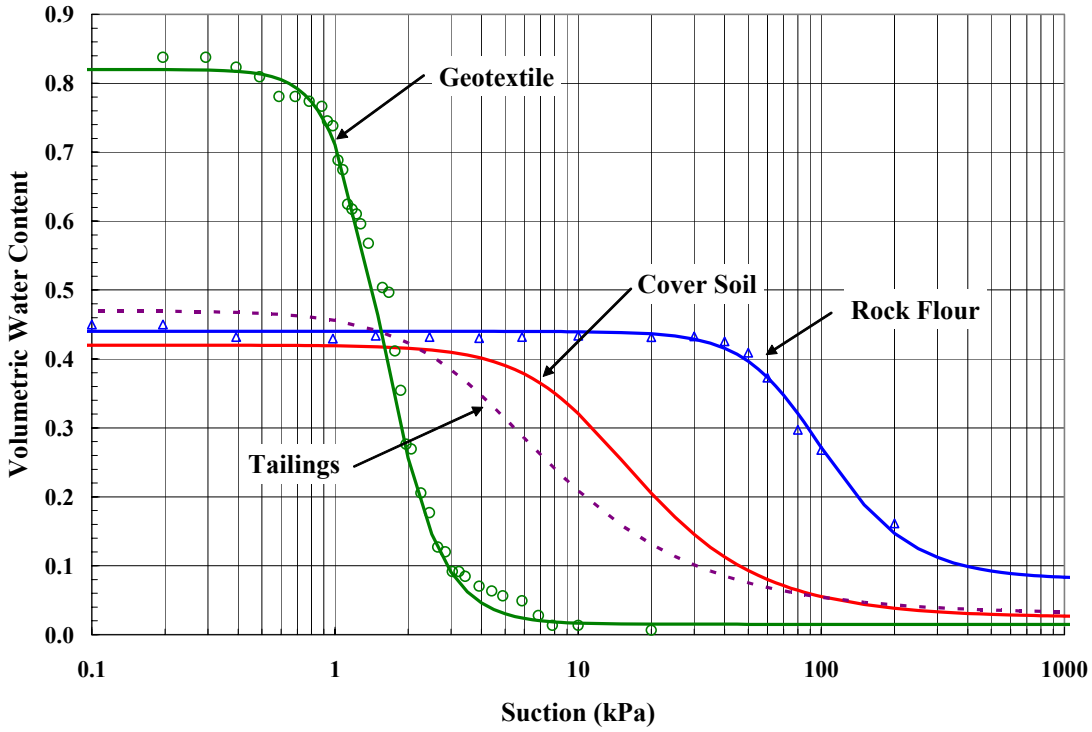

Figure 6-4. Water characteristic curves fitted with van Genuchten (1980) parameters.

6.3 Hydraulic Conductivity Functions

There have been several methods developed to predict the hydraulic conductivity function of a material from its water characteristic curve (Section 3.3.3). The Fredlund et al. (1994) and van Genuchten (1980) methods were utilized for the numerical modeling program. Saturated hydraulic conductivities for the materials were obtained (Sections 4.4.3 and 5.2) and used, along with the water characteristic curves to estimate the unsaturated hydraulic conductivity functions. Figures 6-5 and 6-6 show the estimated functions. The differences in the two estimation techniques were most noticeable past the residual range. The van Genuchten (1980) functions have been noted not to accurately approximate the hydraulic conductivity function in the residual range.

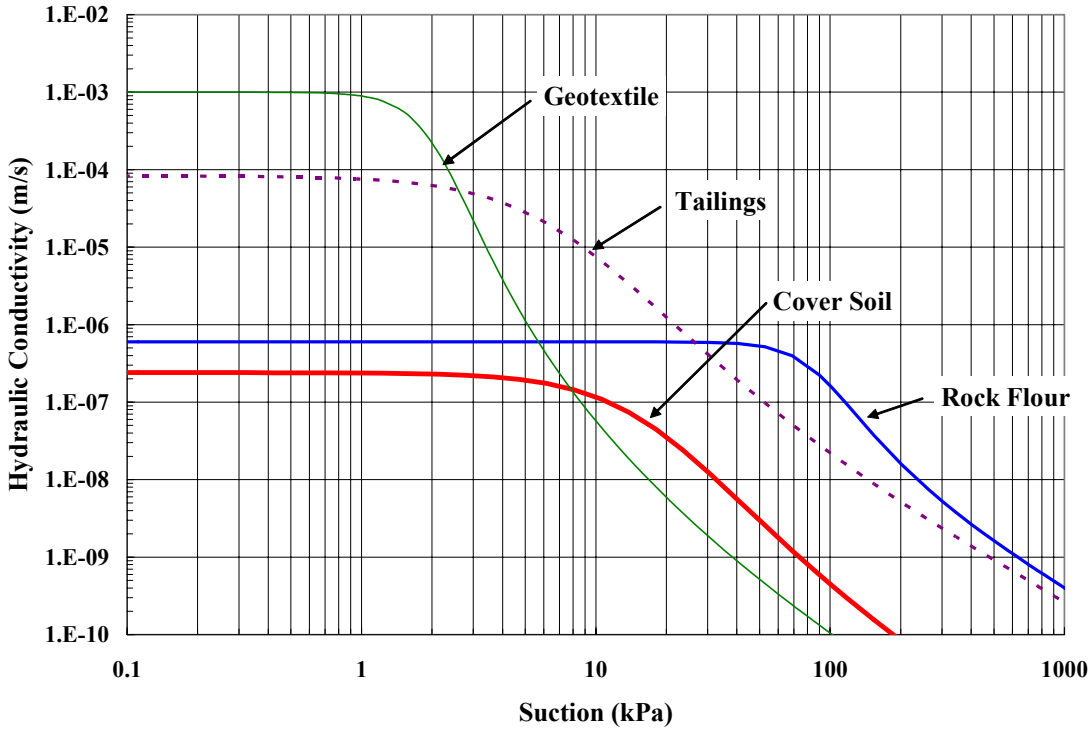

Figure 6-5. Estimated hydraulic conductivity functions from Fredlund et al. (1994).

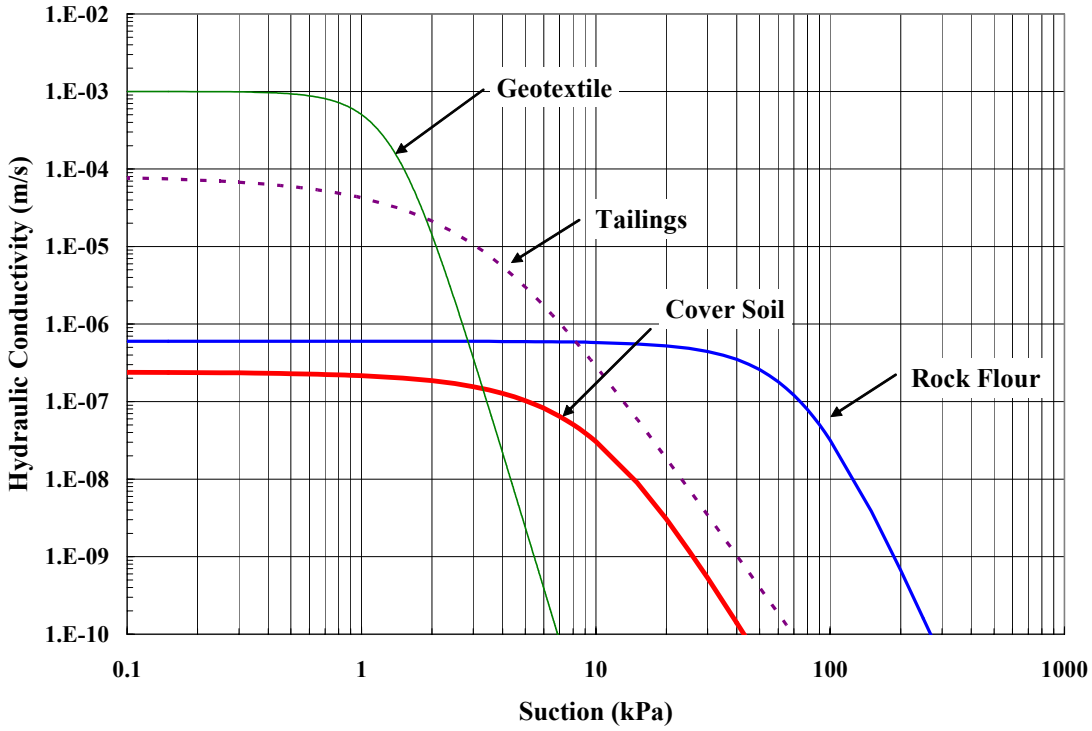

Figure 6-6. Estimated hydraulic conductivity functions from van Genuchten (1980).

6.4 Kisch (1959) Method of Computing Pressure Profiles

The Kisch (1959) method of computing steady state pressure (discussed in Section 3.4) was used to analyze the pressure profiles within the columns. This method computes pressure profiles under conditions of steady-state infiltration, but was also applicable for evaporative fluxes (Bruch, 1993). For the one-dimensional column testing, conditions of steady-state infiltration or evaporation were not likely met. However, in this case, steady state fluxes were considered extreme boundary conditions. For example, steady state infiltration was representative of a prolonged period of precipitation, whereas steady state evaporation was indicative of a prolonged period of dry weather.

A spreadsheet was developed utilizing the equations and procedures outlined in Section 3.4. For the steady state boundary conditions, the maximum daily evaporation and infiltration events from Tables 5-2 and 5-3 were used. The maximum daily infiltration and evaporation rates for the column testing were 7.1 and 4.9 mm/day respectively. Figures 6-7 and 6-8 show the computed pressure profiles along the entire length of the column, comparing columns that incorporate the GCB with those that did not.

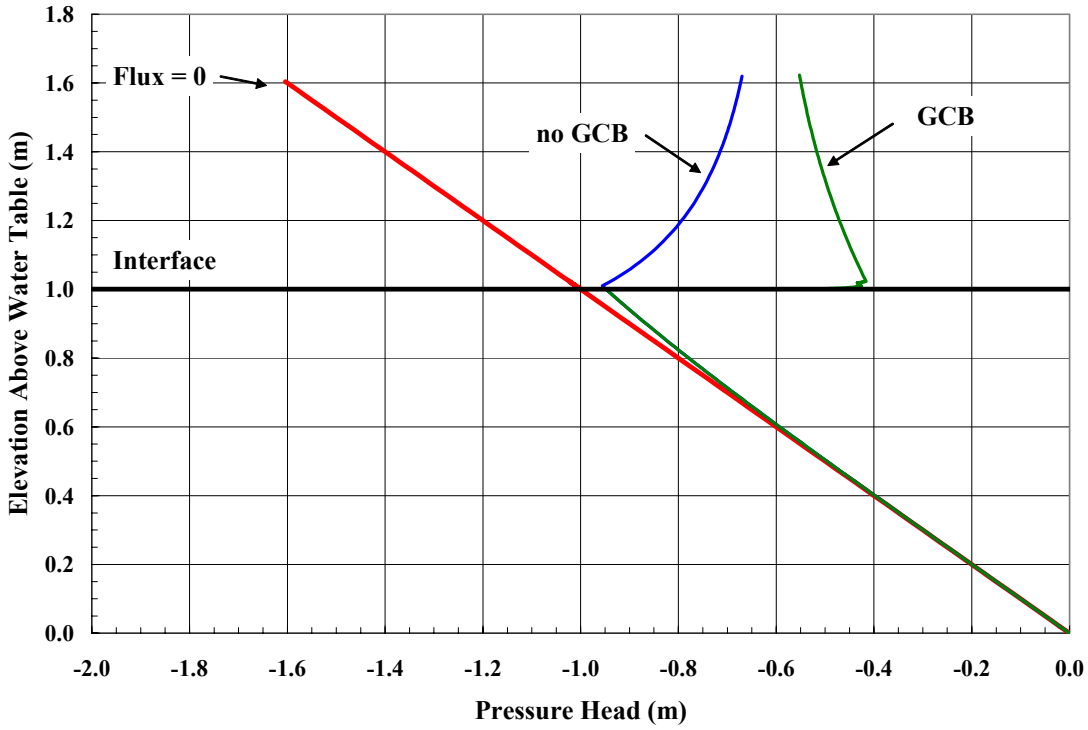

Figure 6-7. Calculated pressure profiles for 7.1 mm/day infiltration.

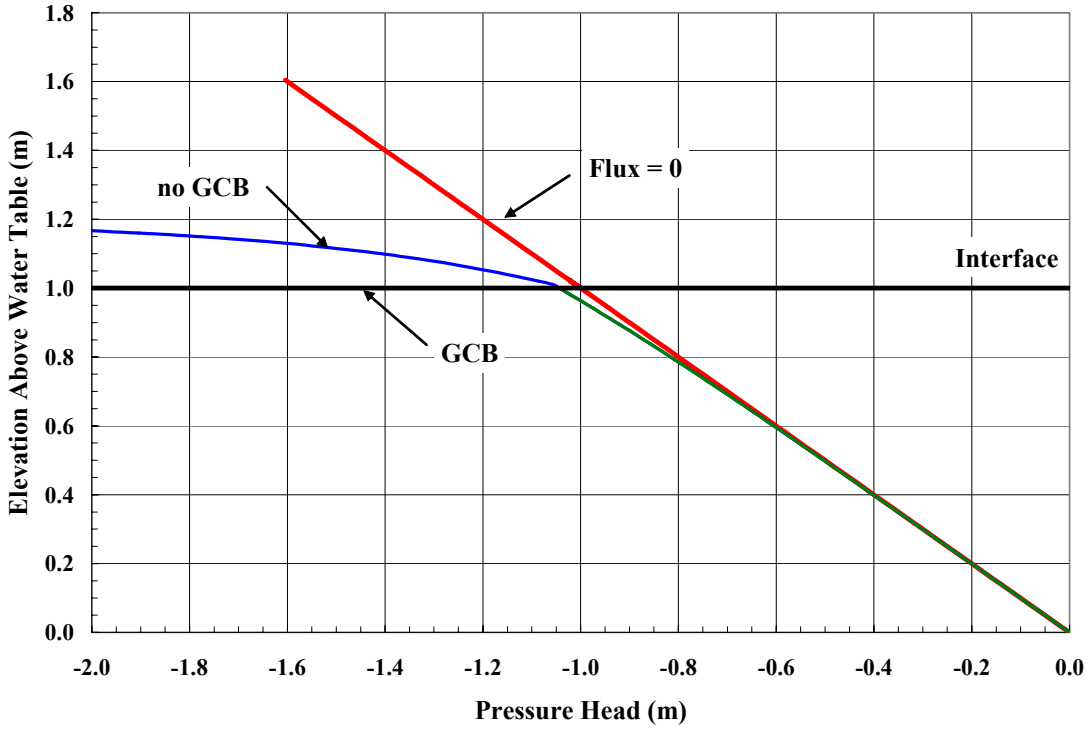

Figure 6-8. Calculated pressure profiles for 4.9 mm/day evaporation.

As is illustrated by Figure 6-7, the GCB had a significant effect on the calculated pressure profiles within the columns. For the infiltration rate of 7.1 mm/day, pressure profiles below the interface were identical; both became slightly greater than hydrostatic near the interface. Above the interface the difference was more noticeable. For the cover systems which incorporate the GCB, the calculated pressure head was greater than those without the GCB for all points in the cover soil. The increased pressure head (or reduced suction), for the same steady state flow rate, illustrated that the materials above the interface had a higher degree of saturation if the capillary break was present. This was desirable from an oxygen limiting standpoint as materials with a higher degree of saturation allow less oxygen diffusion (Nicholson et al., 1989).

For the case of steady-state evaporative fluxes (Figure 6-8), the GCB was also shown to have an effect on the pressure profile. With the inclusion of the GCB, the pressure head tended towards higher negative values above the tailings interface than was the case with no GCB. The negative pressure head was desirable from a standpoint of limiting moisture movement in that increased suctions within the lower geotextile layer will further reduce its hydraulic conductivity. Figure 6-10 shows the calculated pressure profiles immediately above the tailings interface for the evaporative case.

Figures 6-9 and 6-10 examined the same pressure profiles as Figures 6-7 and 6-8, but examined the profile in the area immediately above the tailings, comparing the pressure profiles within the GCB itself (for columns where the GCB is present).

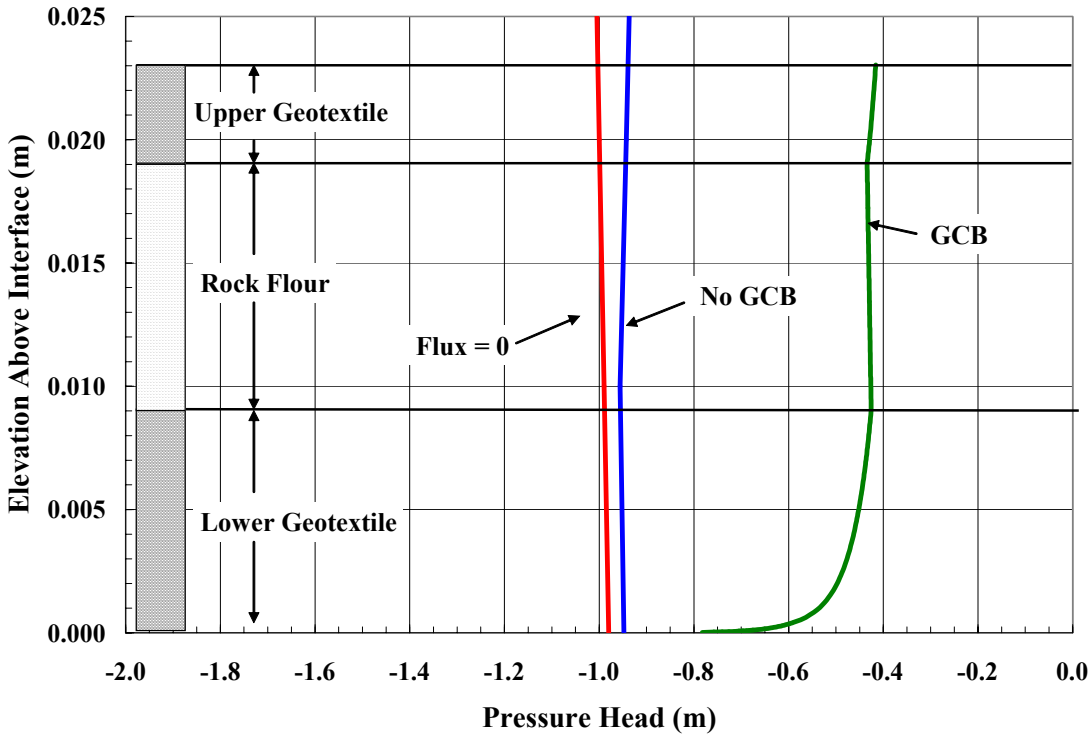

Figure 6-9. Calculated pressure profiles within GCB for 7.1 mm/day infiltration.

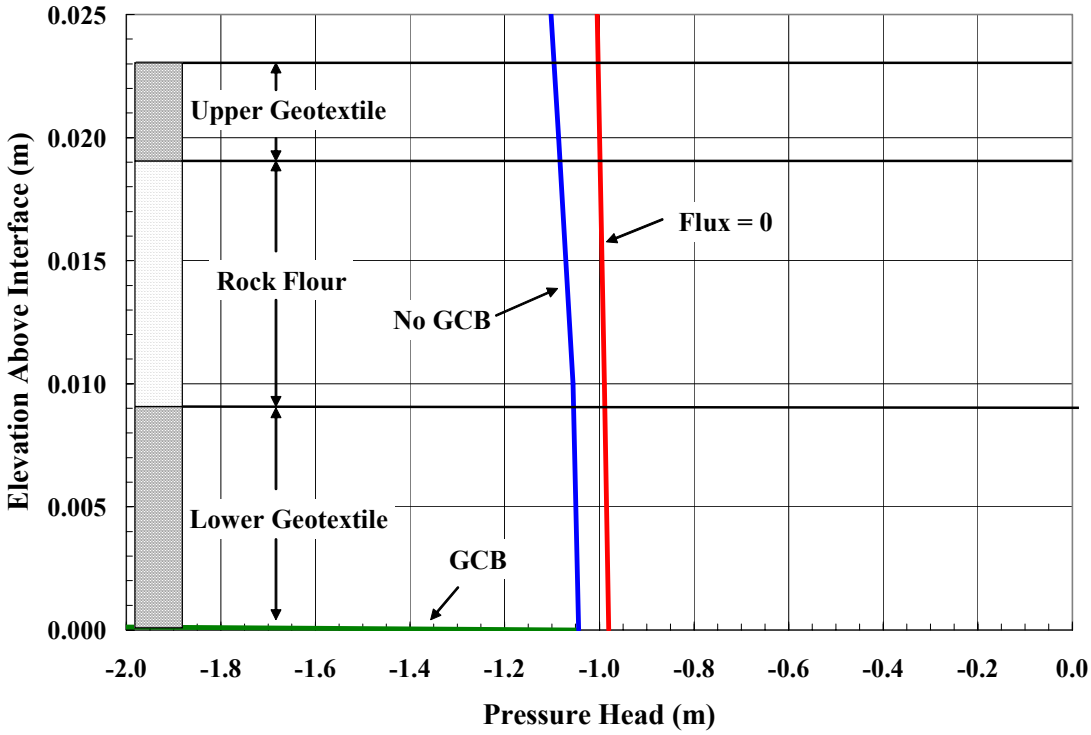

Figure 6-10. Calculated pressure profiles within GCB for 4.9 mm/day evaporation.

As can be seen from the figures, the inclusion of the GCB significantly influenced the pressure profile immediately above the interface. Comparing the zero flux case to the case with 7.1 mm/day infiltration and no GCB, the pressure profile shifted only slightly; with an increase of approximately 0.5 cm of pressure head. Comparing the inclusion of the GCB with the case with no GCB, there was an increase in pressure head of 50 cm. For the evaporative case, the inclusion of the GCB drove the pressure profile to high negative values immediately above the interface, while with no GCB the profile shifted less severely in the negative direction.

6.5 Finite Element Modeling

6.5.1 Performance Simulation

The finite element program VADOSE/W (GeoStudio, 2004) was utilized in order to simulate the performance of the one-dimensional column testing. The purpose of this modeling was to "fine tune" the hydraulic parameters for the rock flour, geotextile, and tailings in order to develop accurate inputs for a predictive model to evaluate long-term hydraulic performance of the GCB and to examine the effectiveness of the GCB as an oxygen limiting barrier. The simulated model also allowed for the opportunity to examine predicted values for parameters for which no measurements were possible in the actual column testing. These parameters included oxygen diffusion as well as the volumetric water content profiles of the rock flour and geotextile in the columns that incorporated the GCB.

The results of the column testing were previously presented in Section 5.4. The model was simulated using the cumulative flux measurements from both the high and low evaporation tests as the matching data set. Subsequently, measurements of water

content were compared to the predicted values to evaluate the accuracy of the simulation.

A "trial and error" approach was taken for the simulation process in which various parameters were modified independent of each other. The predicted cumulative flux was most sensitive to the hydraulic conductivity functions for the materials within the columns, particularly the function for the lower geotextile. Initially, Fredlund and Xing (1994) and Fredlund et al. (1994) functions (Figures 6-3 and 6-5) were input for the cover soil, rock flour, and tailings, while van Genuchten (1980) functions (Figures 6-4 and 6-6) were used for the geotextile. The van Genuchten (1980) equations were chosen for the geotextile because a better initial fit to the cumulative flux data was noted. However, the values for saturated hydraulic conductivity as well as the shape of the hydraulic conductivity functions were modified throughout the simulation process in order improve the quality of the fit. For each individual column, the changes were not identical due to the absence of homogeneity for all materials. Therefore, the final hydraulic conductivity functions varied slightly from column to column for each material. Figures 6-11 to 6-14 show the simulated behavior of the columns. The data points on the graph represent measured values from the column testing, whereas the solid and broken lines correspond to the VADOSE/W predicted values for the columns with and without the GCB, respectively.

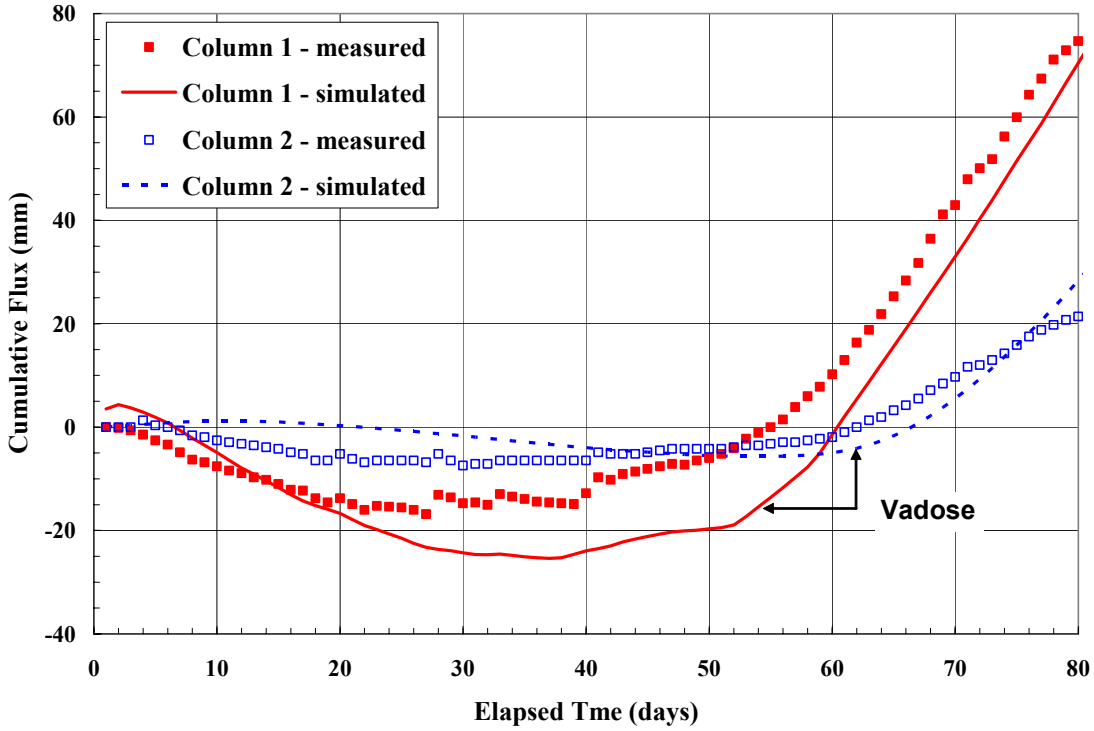

Figure 6-11. Model calibration for Columns 1 and 2 – low evaporation test.

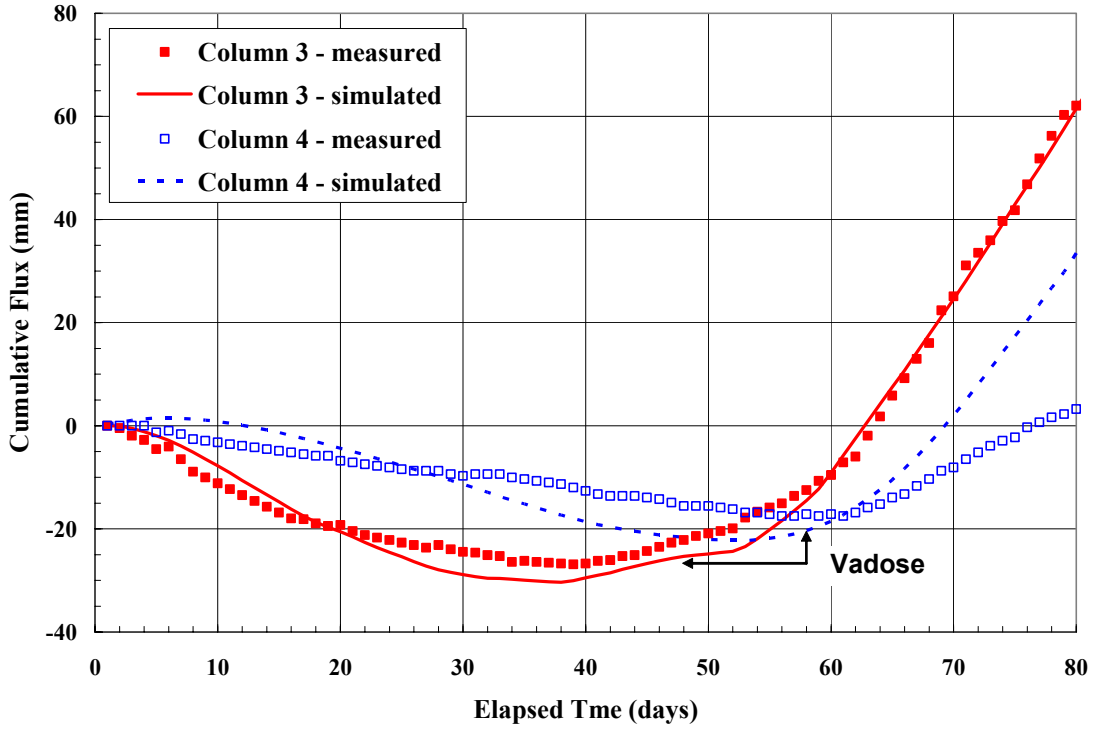

Figure 6.12. Model calibration for Columns 3 and 4 – low evaporation test.

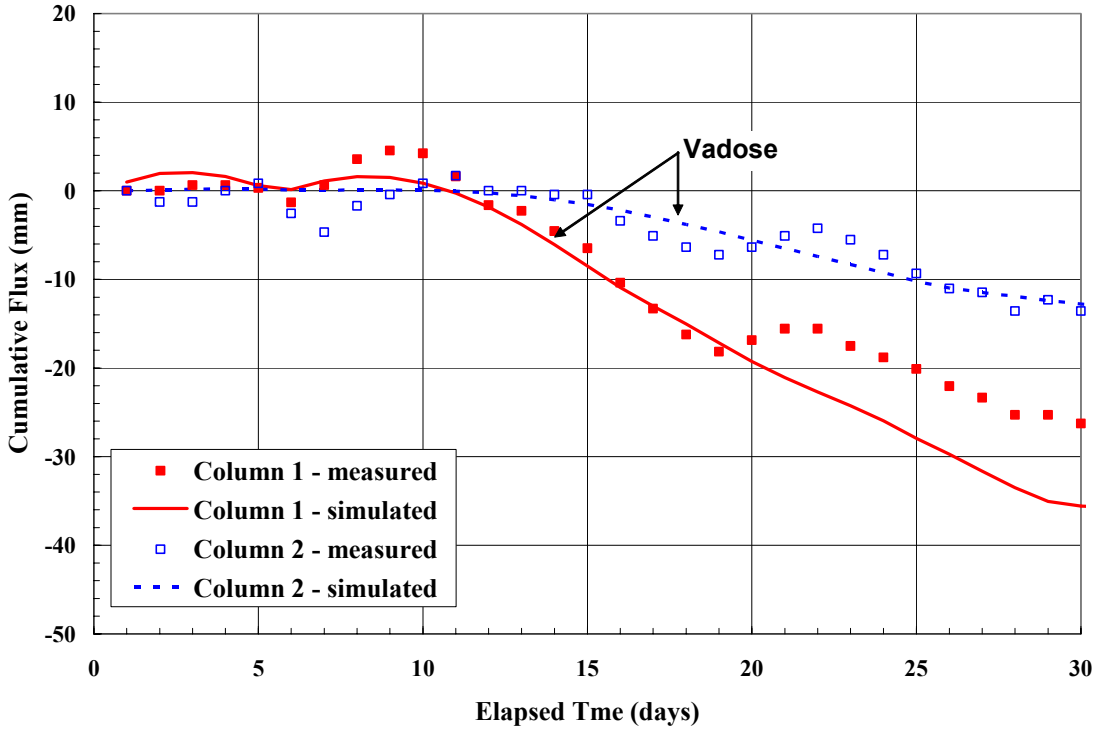

Figure 6-13. Model calibration for Columns 1 and 2 – high evaporation test.

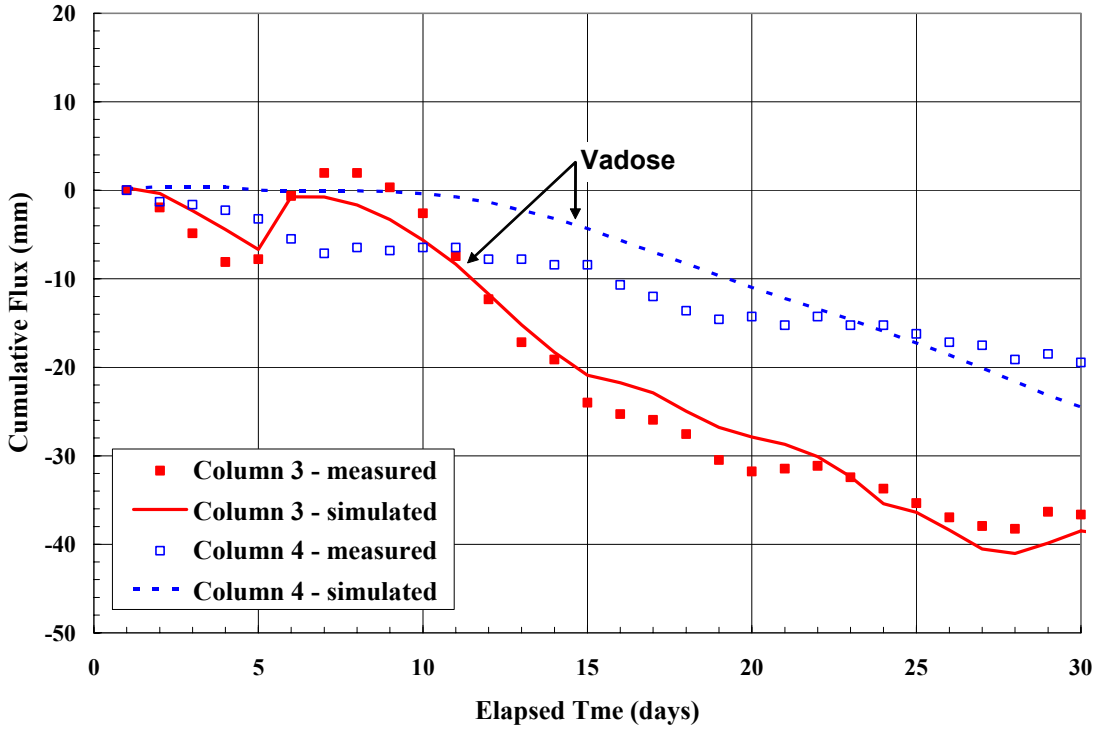

Figure 6-14. Model calibration for Columns 3 and 4 – high evaporation test.

The simulation was quantified based on the error criteria described in Section 3.6. The mean error (*ME*), mean absolute error (*MAE*), and the root mean square (*RMS*) error were used to quantify the quality of the fit to the cumulative flux data. An acceptable simulation had all error criteria below 10% of the precipitation over the course of the test. For the low evaporation test, the total precipitation was 189 mm; therefore 18.9 mm was the maximum error. Similarly, for the high evaporation test, the total precipitation was equal to 38.8 mm and the maximum error was 3.88 mm. Tables 6-3 and 6-4 summarize the calculated errors.

Table 6-3. Error calculations for low evaporation test.

Column	*ME* (mm)	Error	*MAE* (mm)	Error	*RMS* (mm)	Error
1	-7.4	3.9%	8.6	4.6%	9.6	5.1%
2	1.3	0.7%	3.4	1.8%	4.0	2.1%
3	-1.2	0.6%	2.8	1.5%	3.0	1.6%
4	2.3	1.2%	6.2	3.3%	9.3	4.9%

Table 6-4. Error calculations for high evaporation test.

Column	*ME* (mm)	Error	*MAE* (mm)	Error	*RMS* (mm)	Error
1	3.4	8.8%	4.0	**10.3%**	5.4	**13.9%**
2	0.3	0.8%	1.4	3.6%	1.7	4.4%
3	0.1	0.2%	2.3	5.9%	2.6	6.7%
4	2.4	6.2%	4.0	**10.3%**	4.4	**11.3%**

As can be seen from the previous figures and above tables, the error criteria were not satisfied in all cases. All of these cases occurred in the high evaporation portion of the testing, where total precipitation values were low. These errors may possibly be attributed to the non homogeneity of the materials within each column, and from column to column. Convergence issues within the model itself may also account for errors in

the solution. However, the performance simulation of the 1-D column testing was, in general, acceptable.

Plots of measured versus predicted data were also developed for all analyses. For a perfect simulation, the calibrated values would be equal to the measured values; a trendline drawn on the graph would have a slope equal to one, intercept of zero, and an R^2 value of 1.0. These plots were developed to further quantify the quality of the calibration and are found in Appendix D.

To further examine the accuracy of the model, volumetric water content measurements for the cover soil were compared to the predicted values. The volumetric water contents were expressed in Figures 5-13 and 5-14 as the total water volume within the cover soil with time. Figures 6-15 and 6-16 show the measured and predicted total water volumes for the cover soil. The predicted results agreed well with the values measured during the testing.

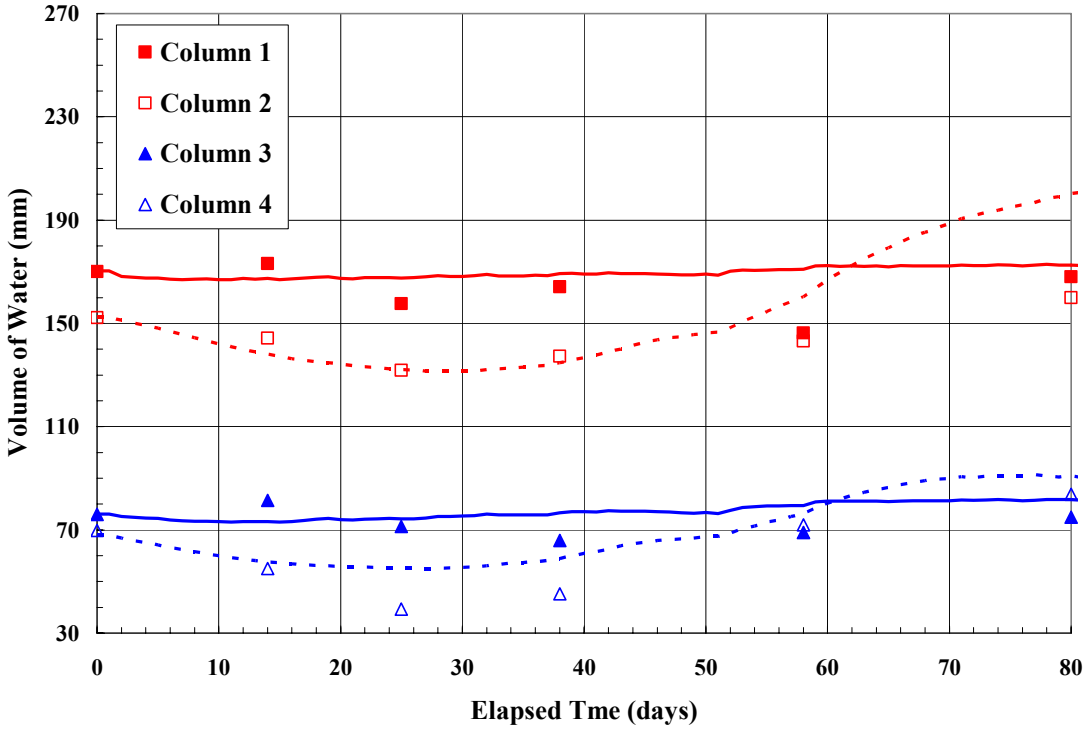

Figure 6-15. Total volume of water in cover soil for low evaporation test.

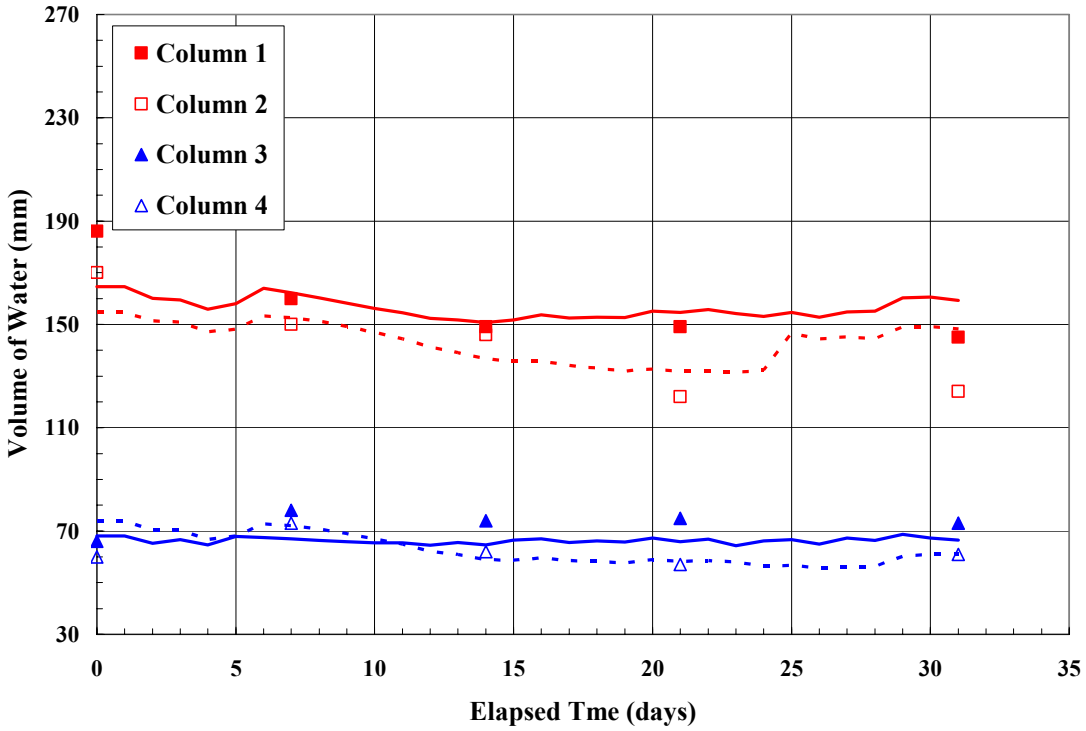

Figure 6-16. Total volume of water in cover soil for high evaporation test.

As in the previously presented figures showing cumulative flux simulation, the data points in Figures 6-15 and 6-16 correspond to measured values and the solid and broken lines correspond to the VADOSE/W simulated values. When adjusting the model to the volumetric water content measurements, it was found that the porosity (or saturated volumetric water content) of the soil was the parameter which most affected the results. As for the case for the cumulative flux calibration, slightly different values for the porosities were used for the same materials from column to column in order to reduce the error in prediction, but the differences were not significant.

Once an acceptable simulation was reached, parameters that could not be measured throughout the course of the testing; in particular, the volumetric water contents of the rock flour and the lower geotextile were examined. If the geosynthetic capillary break was effective, a sharp contrast should be predicted between the water contents of these two layers. The rock flour layer should remain near saturation, acting as an oxygen barrier while the geotextile should be near its residual moisture content, acting as a moisture barrier. Figures 6-17 and 6-18 show the simulated degrees of saturation for the two layers with time for both the high and low evaporation tests.

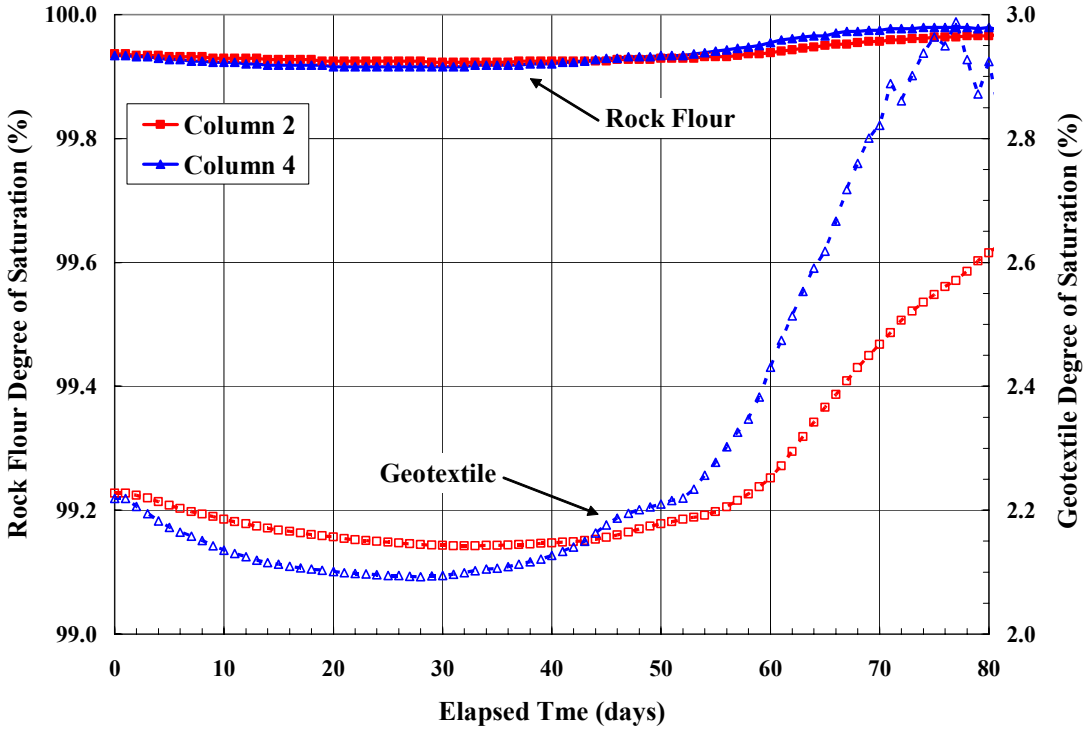

Figure 6-17. Simulated degree of saturation for GCB layers – low evaporation test.

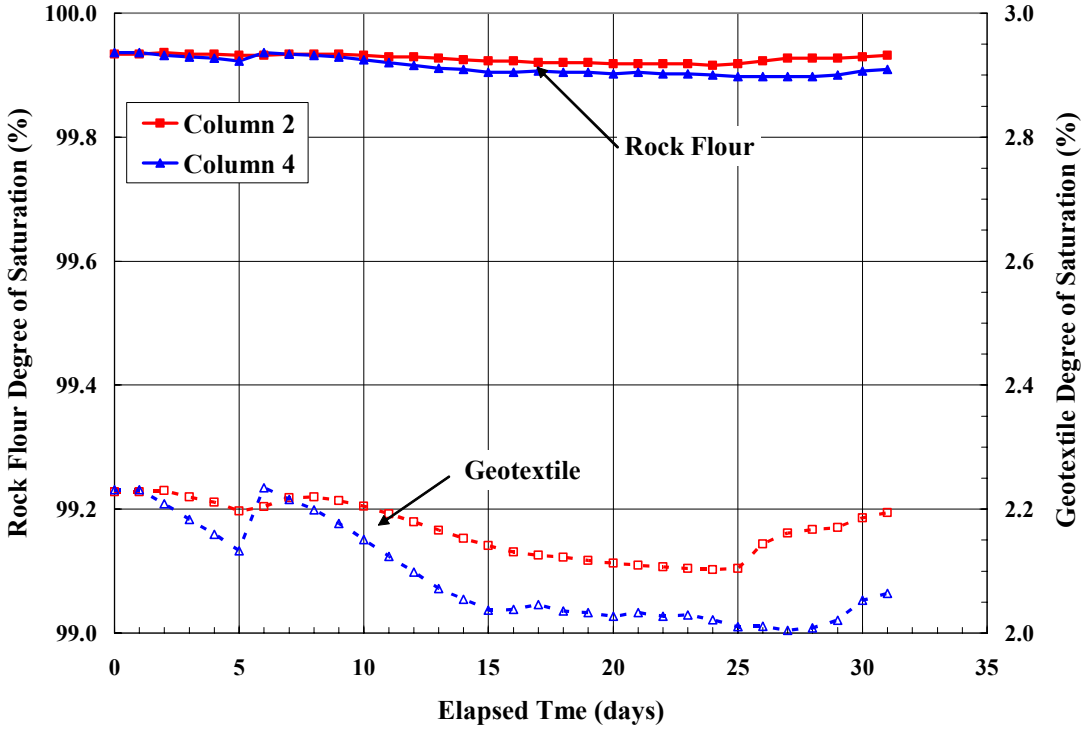

Figure 6-18. Simulated degree of saturation for GCB layers – high evaporation test.

Figures 6-17 and 6-18 showed that the capillary break was performing as desired, throughout both tests. According to the model, the rock flour should have remained near 100% saturation with very little fluctuation throughout the course of the test. The maximum change would have occurred in the low evaporation test in which the degree of saturation predicted by the model increased from 99.92 to 99.97%, which was hardly a severe change. For the geotextile, the degree of saturation, as simulated by the model, remained less than 3% over the course of the testing. However, the simulated change in degree of saturation is slightly more pronounced than for the rock flour; an almost 1% increase in the degree of saturation was predicted in the low evaporation test. The modeled results from the high evaporation test showed that the rock flour experienced almost no change in either column and the geotextile decreased only slightly (approximately 0.2%).

6.5.2 Predictive Modeling

The hydraulic functions used with the VADOSE/W simulation of the column data were combined in order to develop the eight (four volumetric water content and four hydraulic conductivity) functions inputted to the predictive modeling analysis. Figures 6-19 and 6-20 show the input functions, with dashed lines on the curves for determination of air-entry value (AEV), rate of desaturation (n_f), and residual water content (θ_{res}) (refer to Figure 4.2). Table 6-5 summarizes the material parameters.

The model was extended using historical climate data to evaluate the anticipated hydraulic performance and oxygen limiting potential of an engineered cover system incorporating the GCB at the Hudson Bay Mining Smelting tailings management area in Flin Flon, MB.

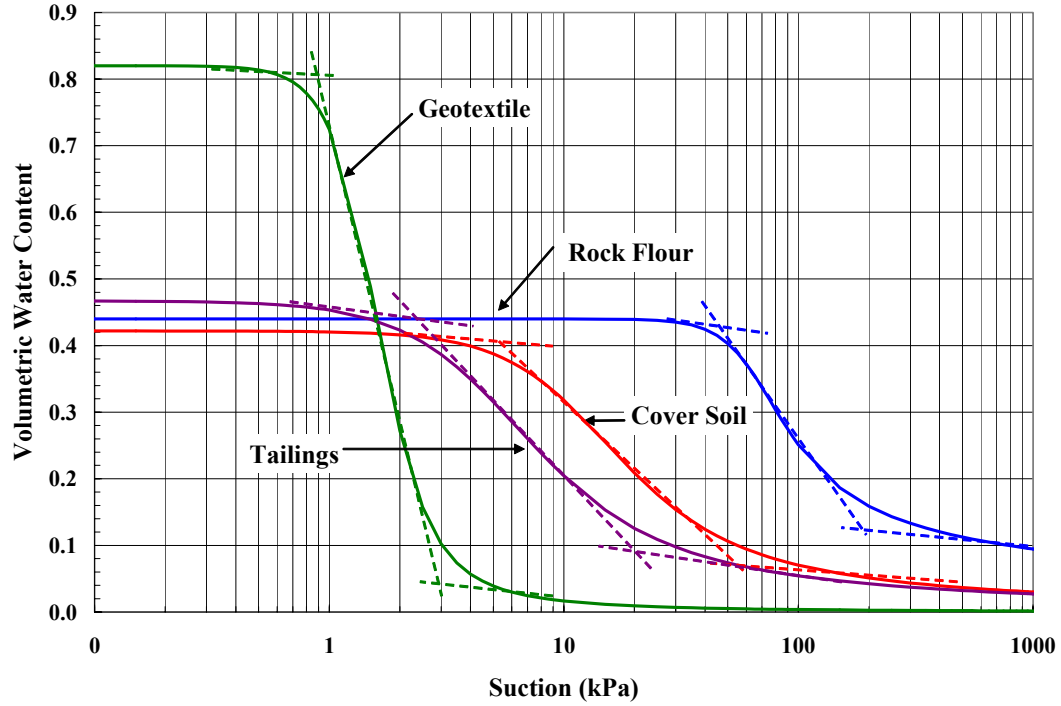

Figure 6-19. Input volumetric water content functions for predictive modeling.

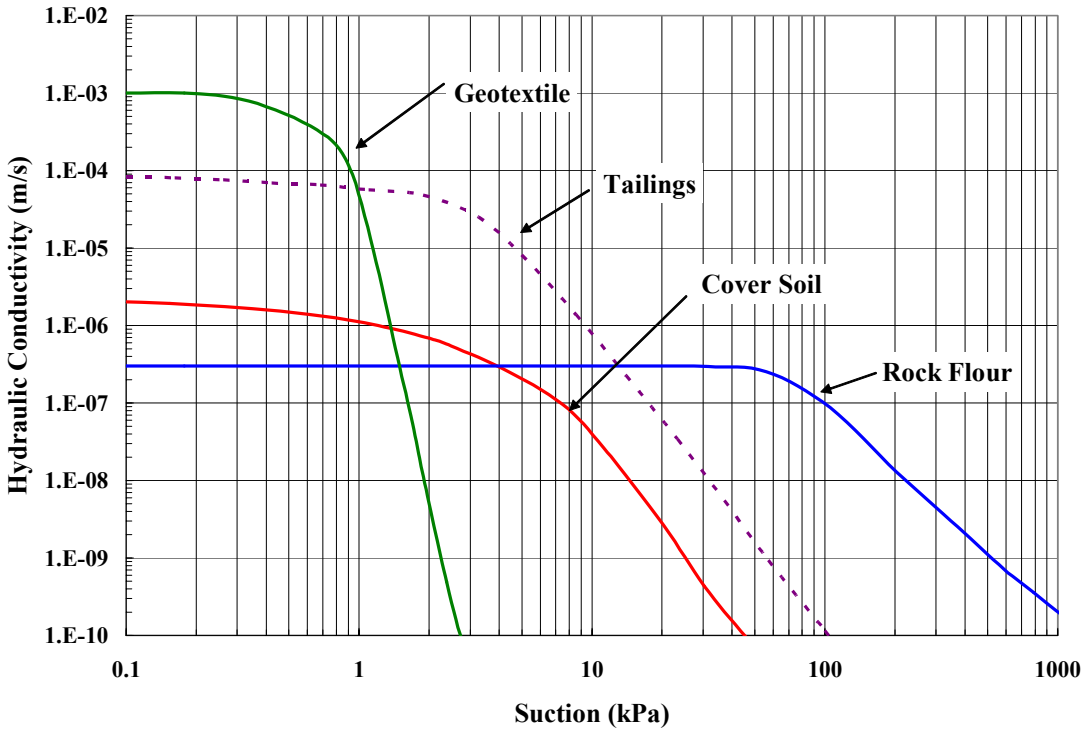

Figure 6-20. Input hydraulic conductivity functions for predictive modeling.

Table 6-5. Summary of material parameters for model inputs.

	Cover	Rock Flour	Geotextile	Tailings
Saturated hydraulic conductivity (m/s)	2.3×10^{-6}	3.0×10^{-7}	1.0×10^{-3}	8.4×10^{-5}
Porosity	0.42	0.44	0.82	0.47
Air-entry value (AEV) (kPa)	5.3	46.4	0.9	2.3
Rate of desaturation (n_f)	2.0	4.4	4.1	1.8
Residual water content (θ_{res})	0.07	0.12	0.04	0.08

The GeoStudio (2004) finite element program VADOSE/W was utilized for the predictive modeling. The intent of this section was to model how the GCB will perform hydraulically as part of a "real life" engineered soil cover system over an extended period of time. Two key parameters were examined:

- Yearly cumulative net percolation into the waste; and
- Yearly cumulative oxygen diffusion into the waste.

Cover thicknesses of 30 and 60 cm were once again evaluated and cover systems which incorporated the GCB were compared with those which did not using the above criteria. Figure 6-21 shows the finite element mesh used for the analyses,

Four years of climate data were obtained for Flin Flon, MB and were used as the data set for the predictive model (Appendix B). Flin Flon is located at a latitude of approximately 54.4^{o} N along the Saskatchewan Manitoba border. The average annual precipitation is approximately 460 mm (HBM&S, 2004) with an average annual potential evaporation of approximately 450 mm (HBM&S, 2004). Climate data was obtained from the Environment Canada website for the weather station located at the

Flin Flon airport for the years 1999 to 2003 (National Climate Archives, 2004). Table 6-6 shows the yearly precipitation and potential evaporation for the four climate years.

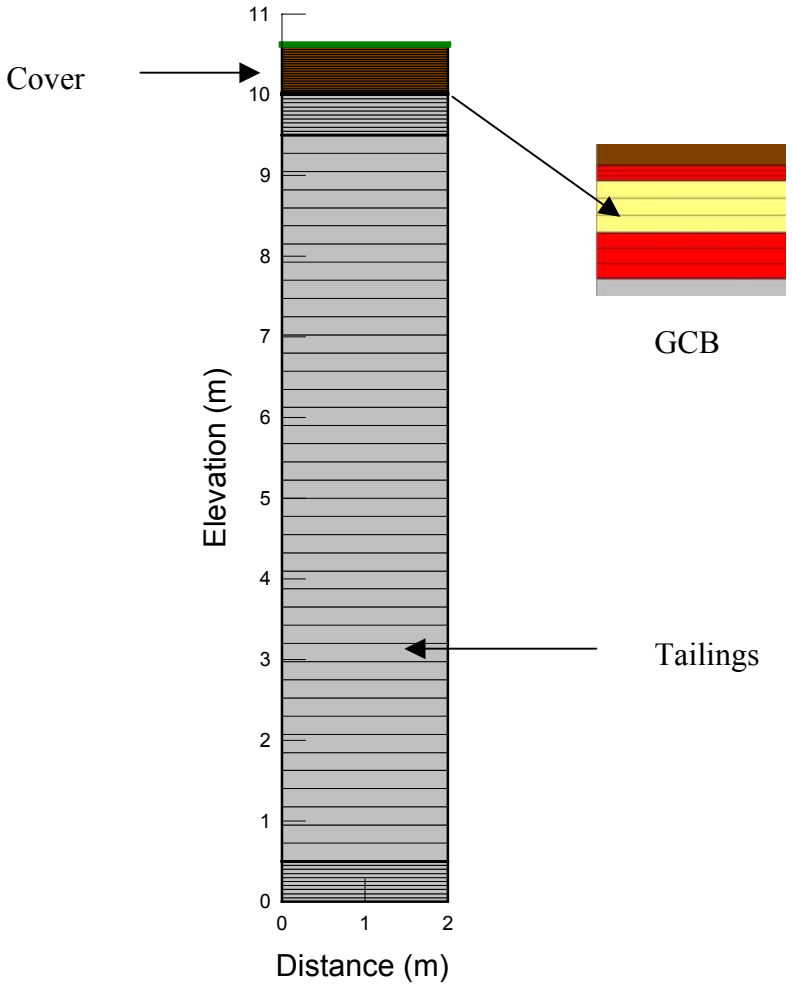

Figure 6-21. Finite element mesh used for predictive modeling.

Table 6-6. Yearly precipitation and potential evaporation (P.E.) for predictive modeling.

Year	Precipitation (mm)	P.E. (mm)
1999-00	409	480
2000-01	576	477
2001-02	408	455
2002-03	469	510
Average	449	454

Ten meters of tailings were modeled below the cover soil to ensure that the bottom boundary condition did not affect the moisture movement at the interface of the cover soil and tailings. A bottom pressure head boundary condition of -10 m was applied, corresponding to the residual suction for the tailings. The climate boundary condition was applied to the surface of the tailings.

Figures 6-19 and 6-20 show the hydraulic input functions for the predictive model. Other input functions such as the thermal conductivity and mass specific heat were estimated from the volumetric water content functions, with typical parameters assumed for dry material thermal conductivity and material specific heat.

The ground freezing option in VADOSE/W was enabled in order to reduce the hydraulic conductivity of the cover materials in months were the temperature is below zero. This significantly reduced the amounts of infiltration into the cover during the winter. For the determination of oxygen diffusion into the waste, the gas diffusion option was also enabled. At the ground surface, VADOSE/W assumed a constant atmospheric oxygen concentration of 280 g/m^2. A zero concentration node was placed 10 cm below the cover system to simulate a "worst case" scenario in which all oxygen that diffused into the tailings was consumed. For all four cases, models were simulated from December 1 of the first year to November 30 of the following year. Before the start of the 1999-2000 year, an "average" year of climate data was simulated in order to allow oxygen and temperature gradients to develop within the model which were difficult to simulate accurately in a steady-state analysis.

The results of the modeling for all cases predicted that, for the cumulative infiltration into the waste, the bulk of the annual infiltration occurred in the spring due to melting of snow. Over the summer months, evaporation prevented further deep percolation while in the fall, a small amount of percolation was predicted due to the reduction of potential evaporation later in the year. The predicted oxygen diffusion into the waste followed a similar trend. The model showed oxygen diffusing into the waste during the summer months when the input evaporation was high. Tables 6-7 and 6-8 show the comparative results of the modeling analyses.

Table 6-7. Comparative cumulative yearly flux into tailings (mm).

Year	30 cm no GCB	30 cm GCB	Reduction	60 cm no GCB	60 cm GCB	Reduction
1999-00	104	23	78%	49	10	80%
2000-01	133	15	89%	40	8	80%
2001-02	115	17	85%	51	11	78%
2002-03	65	20	69%	39	7	82%

Table 6-8. Comparative cumulative yearly oxygen diffusion into tailings (g/m^2).

Year	30 cm no GCB	30 cm GCB	Reduction	60 cm no GCB	60 cm GCB	Reduction
1999-00	10700	8200	23%	5900	4000	32%
2000-01	5290	4500	15%	6110	5600	8%
2001-02	6900	3980	42%	3300	2420	27%
2002-03	6760	5480	19%	3870	3300	15%

Table 6-7 illustrates that the GCB was effective in reducing the amount of net percolation into the underlying waste under the modeled conditions. For the two cases with the same cover thickness, the inclusion of the GCB reduced the amount of predicted percolation in the order of 75-80% for the modeled conditions. For the oxygen diffusion into the waste (Table 6-7), the modeled effect of the GCB is similar, though

not as pronounced. Under the modeled conditions, the inclusion of the GCB reduced predicted oxygen diffusion in to the tailings by an average of 25% and 20 % for 30 cm and 60 cm of cover, respectively.

6.5.3 Sensitivity Analysis

VADOSE/W was also used to perform a sensitivity analysis for the engineered cover system. The purpose of this analysis was to show how the variations in material parameters may impact the predicted values for cumulative yearly flux and oxygen diffusion. The relative effect of changes in individual parameters on the magnitude of predicted values were assessed using a single simulation for an average year of climate data. For a true sensitivity analysis, the changes in material parameters should be based on confidence limits or statistical analysis to provide a consistent comparison on the sensitivity of each variable (Bruch, 1993). However, this was not performed because it would have required several repetitive tests of the various properties of the materials involved. Instead, the soil parameters were examined over "reasonable" values to determine the effect of individual variation on predicted values. During the simulation process, it was found that the hydraulic conductivity for the materials had the largest impact on the predicted values and was also the most difficult parameter to measure. Therefore, the saturated hydraulic conductivity of each material was adjusted +/- one order of magnitude for the sensitivity analysis.

A "base case" set of predicted parameters was determined by simulating 30 cm of cover soil with the inclusion of the GCB over an average year of climate data. The simulation yielded:

- Cumulative flux → 18 mm; and

- Cumulative oxygen diffusion → 5500 g/m^2.

The results of the sensitivity analysis are shown in Figures 6-22 and 6-23. These plots are often referred to as "tornado plots", with the arrangement of the results from greatest sensitivity to least sensitive. The horizontal lines on the plots indicate the variation in the predicted parameter indicated on the plot while other values are held constant.

The results of the sensitivity analysis indicated that the variation in the saturated hydraulic conductivities of the geotextile and tailings had the greatest effect on the predicted values for flux and oxygen diffusion. The saturated hydraulic conductivities for the cover soil and rock flour had a very small effect on the yearly flux rates as compared to the other materials. However, an increased effect on the predicted oxygen diffusion within the cover system was noticed. This corresponded to the behavior noticed during the simulation of the column testing.

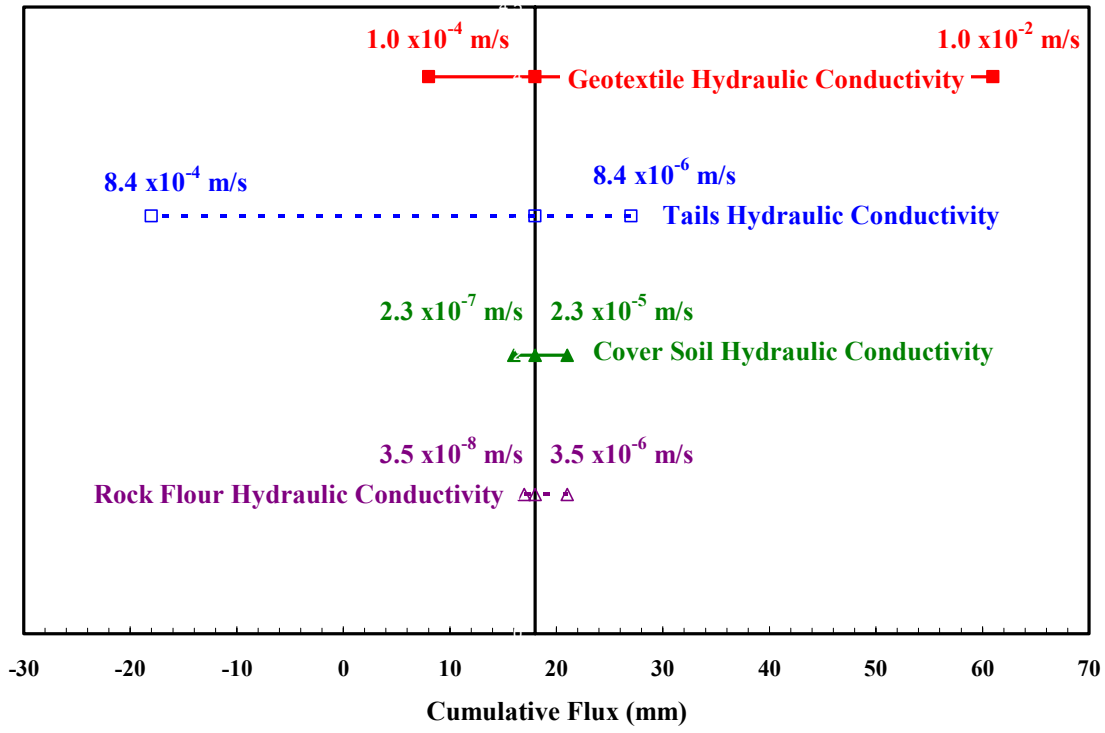

Figure 6-22. Sensitivity analysis for cumulative flux.

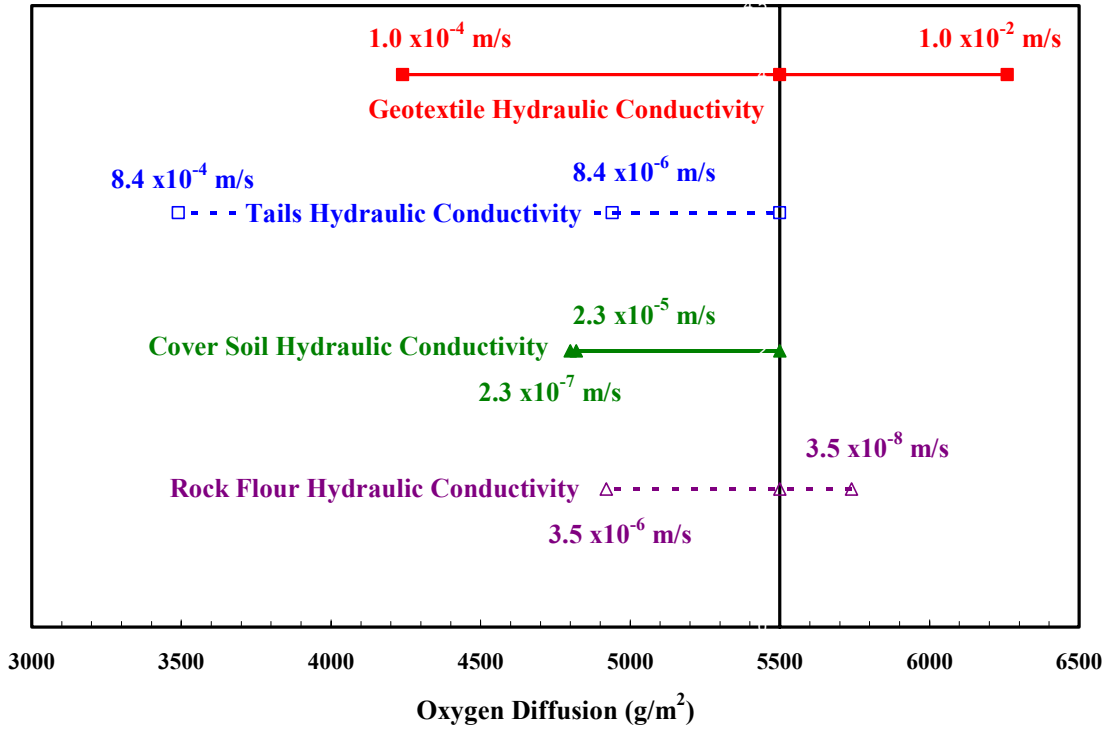

Figure 6-23. Sensitivity analysis for oxygen diffusion.

6.5.4 Limitations of Modeling Approach

VADOSE/W is a coupled soil-atmosphere model, and is a mathematical representation of moisture and heat transport within the predicted cover system. The models presented in Section 6.5.1 to 6.5.3 were constructed in order to develop an understanding of the performance of various cover systems with and without the geosynthetic capillary break. The complex hydrogeology of the problem had to be simplified into a conceptual model that could be represented in a mathematical model. The accuracy of the numerical model is thus limited by the accuracy and detail of the conceptual model as well as the convergence of the model itself.

The following limitations should be noted when interpreting the results of the model predictions for the performance of the various engineered cover systems.

- The conceptual model assumes that the materials within the cover system are homogeneous, with constant properties throughout the material. The potential influence of local heterogeneity (within a given material type) was not investigated.

- The moisture movement within the cover system is governed by the hydraulic conductivity function for the given materials. This relationship is extremely difficult to measure, and consequently, it is derived by a theoretical algorithm based on an inputted saturated hydraulic conductivity and the volumetric water content function of the material. This theoretical relationship defines the hydraulic conductivity function over several orders of magnitude, while a single

or half order of magnitude change can greatly affect the net percolation results predicted from a simulation.

- The accuracy of the predictions and simulations is also governed by the accuracy of the VADOSE/W model itself and the ability to accurately simulate the problem.

6.6 Chapter Summary

In-situ water characteristics curves for the four materials used in the laboratory program were developed. An analytical and numerical modeling program was undertaken in order to further evaluate the GCB. The results of the Kisch (1959) analytical model showed that the inclusion of the GCB as part of an engineered cover system significantly affected the predicted pressure profile within the system. For conditions of steady-state infiltration, the model showed that the GCB acted to reduce the suction immediately above the tailings surface. This is predicted to increase the degree of saturation of the overlying materials. The increase in saturation will decrease the effective oxygen diffusion coefficient in the cover system and therefore allow less oxygen to diffuse into the underlying waste. For conditions of steady-state evaporation, the model showed that the GCB acted to significantly increase the suction on the system. The model predicted that the GCB drove the suction to a large value immediately above the interface. From a moisture limiting standpoint this is advantageous due to the fact that the hydraulic conductivity of the material will decrease as suction increases and therefore reduce moisture migration within the system.

The results from the finite element modeling showed that the results from the 1-D column testing can be simulated relatively well with the VADOSE/W model. The model was utilized to predict anticipated performance of the GCB as part of an engineered cover system for a minesite in Flin Flon, MB. The predicted results showed that the GCB was effective in reducing annual percolation into the underlying waste by 70 to 90% for the conditions modeled. For the predicted yearly oxygen diffusion, the results were not as pronounced. Under the modeled conditions, the GCB reduced predicted annual oxygen diffusion 20 to 25% depending on cover thickness.

The results of the sensitivity analysis showed that the values for predicted annual percolation and oxygen diffusion were most sensitive to the predicted hydraulic conductivity functions for the geotextile and tailings.

The evaluation of the GCB as part of the cover system was limited to a 1-D analysis. The placement of the GCB on a sloped cover was not evaluated and the behavior of the cover would be significantly different considering 2-D effects.

CHAPTER 7 SUMMARY AND CONCLUSIONS

7.1 Study Objectives

The study objectives for this thesis were stated in Section 1.2. The research was undertaken to evaluate a new product, namely a geosynthetic capillary break (GCB), which could be used as part of an engineered soil cover system for waste materials. In order to achieve the objectives the research was divided into three parts:

- Determination of the pertinent material parameters for materials used to evaluate the GCB;
- One-dimensional column testing of a typical engineered soil cover system incorporating the GCB; and
- Modeling of the cover system to better understand current performance as well as predict long-term hydraulic performance of the GCB.

Chapter 2 provided an understanding of the fundamental mechanism behind the design and implementation of a capillary break as well as background on the function of engineered cover systems. Chapter 2 also provided background into the testing methods and typical results for the determination of pertinent material properties for the geosynthetic. The first two objectives of the research were achieved in Chapter 4, with the results presented in Chapter 5. The results of the materials testing as well as the column testing presented in Chapter 5 were discussed and analyzed in Chapter 6.

Chapter 6 also discussed the development and implementation of the modeling program, which was the final objective of this research.

7.2 Conclusions

7.2.1 Material Characterization

The material characterization program showed that the geotextile-rock flour combination developed a capillary break within a cover system. The unsaturated characteristics of the geotextile were similar to those that may be anticipated for a uniform pea gravel, while the rock flour exhibited behavior of a typical fine grained material. The two materials also satisfied the criteria for the selection of materials to be used as contrasting materials in a capillary break as proposed by Nicholson et al. (1989). However, in examining the data obtained from testing the geotextile, over time, or under increasing overburden stresses, the properties of the geotextile may change.

7.2.2 One-Dimensional Column Testing

The data collected for both the high and low evaporation surface flux boundaries demonstrated that the geosynthetic capillary break (GCB) improved the performance of the engineered cover systems. The measured data showed that the two columns which incorporated the GCB exhibited less moisture fluctuation during severe events (Tables 5-2 and 5-3), and also less cumulative moisture movement (Figures 5-8 and 5-9) compared with those without the GCB. Calculations of the total volume of water stored within the cover soil and tailings for each column with time also show that the GCB improved cover performance. For the columns with the GCB (Columns 2 and 4) the volume of water within the tailings changed slightly less than for the other columns (Figures 5-11 and 5-12). Figures 5-13 and 5-14 show the change of volume of water

within the cover soil with time. For these figures, the cover systems with the GCB exhibited more fluctuation than those without. This indicated that the GCB acted to store more water within the cover soil during infiltration; such water may be released by evapotranspiration during dry periods.

The results of the suction measurements provided an indication of the degree of saturation of the components of the GCB. Measurements of the suctions above and below the GCB over time showed that the soil suction in the cover system was high enough to desaturate the lower geotextile. However, the measured suctions were not high enough to desaturate, the rock flour layer. This layer, remaining near saturation, was potentially acting as the oxygen barrier in the system. It was not possible to take a direct measurement of oxygen diffusion during the column testing.

VADOSE/W (GeoStudio, 2004) allowed for the estimation of oxygen diffusion; therefore the numerical model was used to evaluate the GCB as an oxygen barrier.

7.2.3 Kisch (1959) Analytical Modeling

The results of the analytical modeling showed that the inclusion of the GCB had a significant effect on the pressure profiles which are developed in the cover soil. For the case of an infiltration event, the pressure head in the soil was less negative than for the case without the GCB. If the negative pressure head within the soil was reduced, the water content of the soil will be allowed to increase. An increase in the water content of the cover soil due to the inclusion of the GCB led to a reduction in the air phase within the soil and a reduction in oxygen movement from the base case.

For an evaporative flux, the pressure profile was also dramatically affected. For the case without the GCB, the pressure head in the cover soil tended to a large negative

value at a height of approximately 20 cm above the interface. For the case with the GCB, the pressure head tended to a high negative value immediately above the interface, within the lower geotextile layer. The reduced pressure profile within the cover soil caused reduced moisture content. The reduction in moisture content decreased the continuous water phase within the soil and reduced moisture movement across the interface.

7.2.4 Finite Element Modeling

The finite element software VADOSE/W (GeoStudio, 2004) was utilized for three purposes. The first was to develop a model to simulate performance of the one-dimensional column testing; the second was to utilize the simulated model to predict the long-term hydraulic performance of the GCB as part of an engineered soil cover system; and the third was to conduct a sensitivity analysis to determine the material parameters which had the greatest effect on net percolation and oxygen diffusion into the tailings.

The results of the model calibration concluded that the GCB acted to reduce moisture movement within the one-dimensional columns. The simulated results showed that the fluxes and water contents within the columns can be predicted using the FEM program by making small adjustments to the input functions for the specific materials.

The predictive modeling program showed that the geosynthetic break mitigates net percolation into the tailings. A reduction of approximately 80% is predicted for a cover system with a GCB relative to a system without for the systems evaluated. Also, the predictive model provided an estimate of oxygen flux into the underlying waste. For the modeled scenarios, the results suggest a reduction of 20 to 25% of cumulative yearly oxygen diffusion by inclusion of the GCB. From the results it can be concluded that the

geosynthetic capillary break acts to reduce both net percolation and, to a lesser extent, oxygen diffusion into the tailings for the cover scenarios examined.

Lastly, the sensitivity analysis showed the material parameters which had the greatest affect on the values for net percolation and oxygen diffusion. Figures 6-22 and 6-23 showed that a one order of magnitude change in saturated hydraulic conductivity for the geotextile has the greatest impact on these values. This is expected, as the geotextile provides the capillary break in the cover system and the movement of moisture in the system should be governed by its hydraulic conductivity function. The geotextile acted to reduce moisture movement in the system and net percolation is reduced; at the same time the reduced moisture into the tailings was stored in the rock flour layer as well as the cover soil, acting as a barrier to oxygen diffusion.

7.3 Future Research

The primary objective of this research was a preliminary evaluation for the geosynthetic capillary break. This research only looked at the basic unsaturated characteristics of the materials involved and used numerical simulations to predict long-term hydraulic performance of the product. Also, the GCB as part of an engineered cover system was evaluated under controlled conditions in the laboratory. Some areas where additional research is required are summarized below.

The unsaturated characteristics of geotextiles are a relatively new concept and therefore, not a great deal of research has been performed. The measurement of the water characteristic curve for the geotextile is only the first step in understanding its behavior. More research should be done to get a sense of the magnitude of change in the

shape of the geotextile-water characteristic curve as the geotextile remains in the soil of long periods of time under overburden stress.

The sensitivity analysis showed that the hydraulic conductivity function for the geotextile was the most sensitive parameter to change when examining net percolation and oxygen diffusion. For this research this function was estimated from the volumetric water content function and adjusted in the model calibration section. Due to the importance of this function to the performance of the GCB, it would be beneficial to examine the hydraulic conductivity function for the geotextile in greater detail.

Also, the effectiveness of the geosynthetic capillary break was only evaluated as part of a one-dimensional system which only takes into account how the GCB may perform on a relatively flat surface. Additional research is needed to evaluate the two-dimensional performance of the GCB in order to evaluate how the break may perform on waste rock side slopes or other sloped surfaces.

The effect of physical, biological, and chemical processes throughout the life of the cover systems was not evaluated. Significant changes in hydraulic material properties due to volume change and other factors will affect the long-term performance of the GCB. Further research should be undertaken to evaluate these effects.

Lastly, for this research the GCB was examined with one type of mine waste and one type of cover soil. It is important to evaluate the performance of the break under various physical properties of waste and cover soil to evaluate its performance from site to site.

This product is not intended to be applicable for all sites and for all projects. It is hoped that this particular product will provide engineers with another “tool” in order to continue to improve the performance of cover systems.

REFERENCES

Akindunni, F.F., Gillham, R.W., and Nicholson, R.V. 1991. Numerical simulations to investigate moisture-retention characteristics in the design of oxygen-limiting covers for reactive mine tailings. Canadian Geotechnical Journal, Vol. 28, pp. 446-451.

Anderson, M.P., and Woessner, W.W., Applied Groundwater Modeling: Simulation of Flow and Advective Transport. © 1992. Academic Press, Sand Diego.

Arya, L.M., and Paris, J.F. 1981. A physicoemperical model to predict the soil moisture characteristic from particle-size distribution and bulk density data. Soil Science of America Journal, Vol. 45, pp. 1023-1030.

Barbour, S.L. 1990. Reduction of acid generation in mine tailings through the use of moisture-retaining cover layers as oxygen barriers: Discussion. Canadian Geotechnical Journal, Vol. 27, pp. 398-401.

Brooks, R.H., and Corey, J.C. 1964. Hydraulic properties of porous media. CSU Hydrology Paper No. 3.

Bruch, P.C. 1993. A laboratory study of evaporative fluxes in homogeneous and layered soils. M. Sc. Thesis, University of Saskatchewan, Saskatoon, Sask., Canada.

Childs, E.C., and Collis-George, N. 1950. The permeability of porous materials. Proceedings of the Royal Society of London. Series A, Vol. 201, pp. 392-405.

Dierickx, W., 1996. Determination of water penetration resistance of geotextiles. In: Bhatia, S.K., Suits, L.D., Recent Developments in Geotextile Filters and Prefabricated

Drainage Geocomposites, ASTM STP 1281. American Society for Testing Materials, pp. 65-74.

Elsharief, A.M., and Lovell, C.W. 1997. A probabilistic retention criteria for nonwoven geotextiles. Geotextiles and Geomembranes, Vol. 14, pp. 601-617.

Feasby, D.G., Blanchette, M., and Tremblay, M. 1991. The mine environment neutral drainage (MEND) program. Second International Conference on the Abatement of Acidic Drainage, Montreal, PQ, Vol. 1, pp. 1-26.

Fredlund, D.G. 2000. The 1999 R.M. Hardy Lecture: The implementation of unsaturated soil mechanics into to geotechnical engineering. Canadian Geotechnical Journal, Vol. 37, pp. 963-986.

Fredlund, D.G., Rahardjo, H. Soil Mechanics for Unsaturated Soils. © 1993. John Wiley and Sons Inc., New York, NY.

Fredlund, D.G., and Xing, A. 1994. Equations for the soil-water characteristic curve. Canadian Geotechnical Journal, Vol. 31, pp.521-532.

Fredlund, D.G., Xing, A., and Huang, S. 1994. Predicting the permeability function for unsaturated soil using the soil-water characteristic curve. Canadian Geotechnical Journal, Vol. 31, pp. 533-546.

Fredlund, M.D., Wilson, G.W., Fredlund, D.G. 2002. Use of the grain-size distribution for estimation of the soil-water characteristic curve. Canadian Geotechnical Journal, Vol. 39, pp. 1103-1117.

Freeze, R.A., and Cherry, J.A., Groundwater. © 1979. Prentice Hall, Englewood Cliffs, NJ.

GeoStudio 2004. Version 6.13. GEO-SLOPE International, Ltd. © 1991-2005.

Gardner, W.R. 1958. Some steady state solutions of the unsaturated moisture flow equation with application to evaporation from a water table. Soil Science, Vol. 85, No. 4, pp. 228-232.

Goode, D.J. 1986. Selection of soils for wick effect covers. In, Geotechnical and Geohydrological Aspects of Waste Management, Proceedings of the 8th Annual Symposium. Fort Collins, Co.

Green, R.E. and Corey, J.C. 1971. Calculation of hydraulic conductivity: A further evaluation of some predictive methods. Soil Science Society of America Proceedings, Vol. 35, pp. 3-8.

HBM&S. (2004). Conversations with Riley Little of HBM&S regarding input functions for modeling.

Henry, K.S. 1990. Geotextiles as capillary barriers. Geotechnical Fabrics Report, Vol. 8, No. 2, pp. 30-36.

Henry, K.S. 1995., The Use of Geosynthetic Capillary Barriers to Reduce Moisture Migration in Soils. Geosynthetics International, Vol. 2, No. 5. pp. 883-888.

Henry, K.S., Holtz, R.D., 2001. Geocomposite capillary barrier to reduce frost heave in soils. Canadian Geotechnical Journal, Vol. 38, pp. 678-694.

Iryo, T., Rowe, R.K. 2003. On the hydraulic behavior of unsaturated nonwoven geotextiles. Geotextiles and Geomembranes, Vol. 21, pp. 381-404.

Kisch, M. 1959. The theory of seepage from clay-blanketed reservoirs. Geotechnique, 9:9-21.

Klute, A. 1986. Water retention: laboratory methods. In: Page, A.L., Miller, R.H., Keeney, D.R., Methods of Soil Analysis, Part 1, Agronomy Monograph No. 9. 2nd

Edition. American Society of Agronomy-Soil Science of America, Madison, WI, USA, p. 687-734.

Knight, M.A., Kotha, S.M. 2001. Measurement of geotextile-water characteristic curves using a controlled outflow capillary pressure cell. Geosynthetics International 8 (3), 271-282.

Lafleur, J., Lebeau, M., Faure, Y., Savard, Y., Kehila, Y. 2000. Influence of matric suction on the drainage performance of polyester geotextiles. The 53rd Annual Conference of Canadian Geotechnical Society, Montreal, Canada, 15-18 October 2000, Vol. 2, pp. 1115-1122.

Lorentz, S.A., DurnFord, D.S., and Corey, A. 1993. Liquid retention measurement on porous media using a controlled outflow cell. Proceedings of American Society of Agronomy-Crop Science Society of America-Soil Science Society of America 1991 Annual Meeting, Denver, Colorado, USA.

National Climate Archive – Environment Canada. Internet source. http://www.climate.weatheroffice.ec.gc.ca. accessed: June, 2004.

Nicholson, R.V., Gillham, R.W., Cherry, J.A., and Reardon, E.J. 1989. Reduction pf acid generation in mine tailings through the use of moisture-retaining cover layers as oxygen barriers. Canadian Geotechnical Journal. Vol 26, pp. 1-8.

Nicholson, R.V., Akindunni, F.F., Sydor, R.C., and Gillham, R.W. 1991. Saturated tailings covers above the water table: The physics and criteria for design. Second International Conference on the Abatement of Acidic Drainage, Montreal, PQ, Vol. 1, pp. 443-485.

O'Kane, M., Wilson, G.W., Barbour, S.L., 1998. Instrumentation and monitoring of an engineered soil cover system for mine waste rock. Canadian Geotechnical Journal, Vol. 35, pp. 828-846.

Richardson, G.N. 1997. Fundamental mistakes in slope design. Geotechnical Fabrics Report, Vol. 15, No. 2. pp. 15-17.

Rowlett, D.K. 2000. Development of a stand-pipe lysimeter for unsaturated waste rock. M.Sc. Thesis, University of Saskatchewan, Saskatoon, Sask., Canada.

Stormont, J.C., Henry K.S., Evans T.M., 1997. Water Retention Functions of Four Nonwoven Polypropylene Geotextiles. Geosynthetics International, Vol. 2, No. 6. pp. 661-672.

Stormont, J.C., Morris, C.E., 1998. Method to estimate water storage capacity of capillary barriers. Journal of Geotechnical and Geoenvironmental Engineering. Vol. 124, No. 4. pp. 297-302.

Stormont, J.C., Morris, C.E., 2000. Characterization of unsaturated nonwoven geotextiles. In: Shackelford, C.D., Houston, S.L., Chang, N.Y. (Eds.), Advances in Unsaturated Geotechnics. ASCE, Reston, VA, USA, pp. 153-164.

Swanson, D.A., Barbour, S.L., Wilson, G.W., O'Kane M., 2003. Soil-atmosphere modeling of an engineered soil cover for acid generating mine waste in a humid, alpine environment. Canadian Geotechnical Journal, Vol. 40, pp. 276-292.

Terrafix Geosynthetics Inc. Internet source. http://www.terrafixgeo.com, accessed: March, 2004.

van Genuchten, M.Th., 1980. A closed form equation for predicting the hydraulic conductivity of unsaturated soils. Soil Science Society of America Journal, Vol. 44, pp. 92-898.

Yanful, E.K., 191. Engineered soil covers for reactive tailings management: Theoretical concepts and laboratory development. Second International Conference on the Abandonment of Acidic Drainage, Montreal, Vol. 1, pp. 461-485.

APPENDIX A:
GRAIN SIZE AND WATER CHARACTERISTIC CURVE TESTING

Table A-1. Summary of grain size distribution testing.

Cover Soil		Rock Flour		Tailings	
Diameter (mm)	% Finer	Diameter (mm)	% Finer	Diameter (mm)	% Finer
2.000	100.0	2.000	100.0	2.000	100.0
0.850	99.8	0.850	100.0	0.850	100.0
0.417	97.8	0.417	100.0	0.417	100.0
0.320	90.3	0.320	100.0	0.320	98.6
0.180	85.3	0.180	100.0	0.180	91.3
0.150	82.2	0.106	100.0	0.150	81.7
0.084	75.4	0.078	95.7	0.082	42.0
0.075	74.7	0.056	91.6	0.075	38.0
0.061	69.6	0.041	87.6	0.060	31.9
0.044	65.1	0.030	76.2	0.044	18.9
0.032	60.9	0.023	62.4	0.032	14.0
0.023	47.9	0.017	51.0	0.023	11.6
0.017	38.4	0.012	41.3	0.016	9.8
0.013	28.7	0.0091	33.0	0.012	9.6
0.0093	21.7	0.0065	26.5	0.0083	8.1
0.0067	15.0	0.0047	20.1	0.0059	7.2
0.0050	12.8	0.0034	14.7	0.0043	6.4
0.0034	11.4	0.0028	13.8	0.0029	5.7
0.0020	9.3	0.0014	9.4	0.0024	5.2

Table A-2. Water characteristic curve for cover soil.

Suction (kPa)	Volumetric Water Content
0.10	0.43
0.20	0.42
0.39	0.42
0.59	0.42
0.78	0.41
0.98	0.41
1.47	0.41
1.96	0.41
2.94	0.40
4.90	0.40
7.35	0.36
10.0	0.30
20.0	0.20
50.0	0.10
100.0	0.05
200.0	0.03

Table A-3. Water characteristic curve for rock flour.

Suction (kPa)	Volumetric Water Content
0.10	0.46
0.20	0.45
0.39	0.43
0.98	0.43
1.47	0.43
2.45	0.43
3.92	0.43
5.88	0.43
10.0	0.43
20.0	0.43
30.0	0.43
40.0	0.43
50.0	0.41
60.0	0.37
80.0	0.30
100.0	0.27
200.0	0.16

Table A-4. Water characteristic curve for tailings.

Suction (kPa)	Volumetric Water Content
0.10	0.48
0.20	0.48
0.39	0.47
0.59	0.47
0.78	0.47
0.98	0.47
1.18	0.47
1.67	0.47
2.16	0.47
3.04	0.47
3.92	0.47
4.90	0.45
5.88	0.45
7.84	0.34
10.0	0.24
20.0	0.14
30.0	0.11
50.0	0.08
80.0	0.06
100.0	0.05
200.0	0.03
300.0	0.03

Table A-5. Water characteristic curves for geotextile – test method comparison.

Hanging Test		Pressure Plate Cell	
Suction (kPa)	Volumetric Water Content	Suction (kPa)	Volumetric Water Content
0.09	0.68	0.05	0.89
0.23	0.68	0.10	0.88
0.35	0.68	0.15	0.89
0.46	0.67	0.20	0.88
0.59	0.62	0.29	0.88
0.73	0.58	0.39	0.88
0.86	0.52	0.49	0.87
1.02	0.41	0.59	0.82
1.22	0.29	0.69	0.76
1.45	0.17	0.83	0.65
1.74	0.11	1.13	0.57
2.15	0.06	1.18	0.49
2.66	0.05	1.37	0.39
3.30	0.06	1.37	0.21
4.11	0.04	1.47	0.21
4.98	0.04	1.57	0.19
5.86	0.03	1.67	0.19
6.83	0.03	1.77	0.18
7.84	0.03	1.86	0.17
8.83	0.03	2.06	0.16
9.90	0.03	5.89	0.08
11.1	0.02		
12.2	0.02		
13.5	0.02		

Table A-6. Water characteristic curves for geotextile – effect of removing lubricating oils.

Unwashed		Washed	
Suction (kPa)	Volumetric Water Content	Suction (kPa)	Volumetric Water Content
0.09	0.68	0.07	0.69
0.23	0.68	0.21	0.68
0.35	0.68	0.37	0.67
0.46	0.67	0.55	0.67
0.59	0.62	0.71	0.66
0.73	0.58	0.88	0.62
0.86	0.52	1.08	0.53
1.02	0.41	1.27	0.48
1.22	0.29	1.43	0.37
1.45	0.17	1.65	0.27
1.74	0.11	2.00	0.14
2.15	0.06	2.39	0.09
2.66	0.05	2.85	0.08
3.30	0.06	3.35	0.06
4.11	0.04	3.89	0.04
4.98	0.04	4.50	0.04
5.86	0.03	5.10	0.04
6.83	0.03	5.69	0.04
7.84	0.03	6.48	0.04
8.83	0.03	7.48	0.05
9.90	0.03	8.54	0.05
11.1	0.02	9.69	0.04
12.2	0.02	10.9	0.03
13.5	0.02		

Table A-7. Geotextile water characteristic curves – effect of increasing overburden stress.

1 kPa		5kPa		6.3 kPa		10 kPa	
Suction (kPa)	Volumetric Water Content	Suction (kPa)	Volumetric Water Content	Suction (kPa)	Volumetric Water Content	Suction (kPa)	Volumetric Water Content
0.10	0.87	0.10	0.90	0.10	0.87	0.10	0.92
0.20	0.87	0.15	0.88	0.20	0.84	0.20	0.91
0.29	0.86	0.39	0.87	0.39	0.84	0.39	0.89
0.39	0.85	0.78	0.86	0.49	0.81	0.59	0.88
0.49	0.83	1.18	0.78	0.69	0.81	0.78	0.86
0.59	0.84	1.47	0.55	0.88	0.79	0.98	0.82
0.69	0.83	1.57	0.46	0.93	0.77	1.18	0.74
0.78	0.82	1.67	0.44	1.03	0.71	1.37	0.65
0.88	0.74	1.76	0.28	1.13	0.62	1.57	0.57
0.98	0.71	1.86	0.20	1.37	0.57	1.76	0.52
1.18	0.69	1.96	0.16	1.57	0.50	1.96	0.45
1.47	0.43	2.06	0.10	1.67	0.50	2.45	0.29
1.57	0.34	2.16	0.09	1.76	0.41	2.94	0.21
1.67	0.28	2.25	0.07	1.86	0.35	3.43	0.15
1.76	0.24	2.55	0.04	1.96	0.28	3.92	0.07
1.86	0.20	2.94	0.03	2.06	0.27	4.90	0.06
1.96	0.15	3.92	0.01	2.25	0.21	5.88	0.03
2.06	0.12	4.90	0.01	2.45	0.18		
2.16	0.12			2.65	0.13		
2.25	0.12			2.84	0.12		
2.35	0.09			3.04	0.09		
2.55	0.08			3.23	0.09		
3.04	0.08			3.43	0.08		
3.92	0.07			3.92	0.07		
4.41	0.05			4.41	0.06		
4.90	0.05			4.90	0.06		
5.88	0.04			5.88	0.05		
				6.86	0.03		
				7.84	0.01		
				10.0	0.01		

APPENDIX B:
CLIMATIC DATA

APPENDIX C:
COLUMN TESTING DATA

APPENDIX D:
ERROR PLOTS FOR COLUMN CALIBRATION

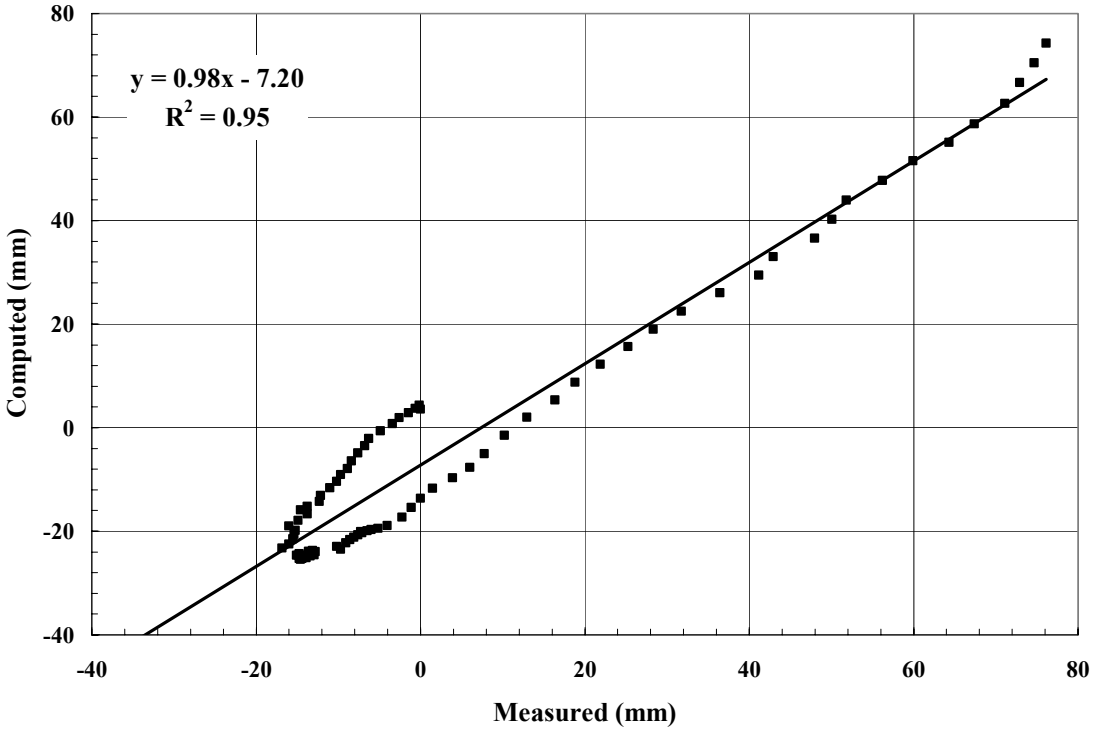

Figure D-1. Error plot for Column 1 – low evaporation test.

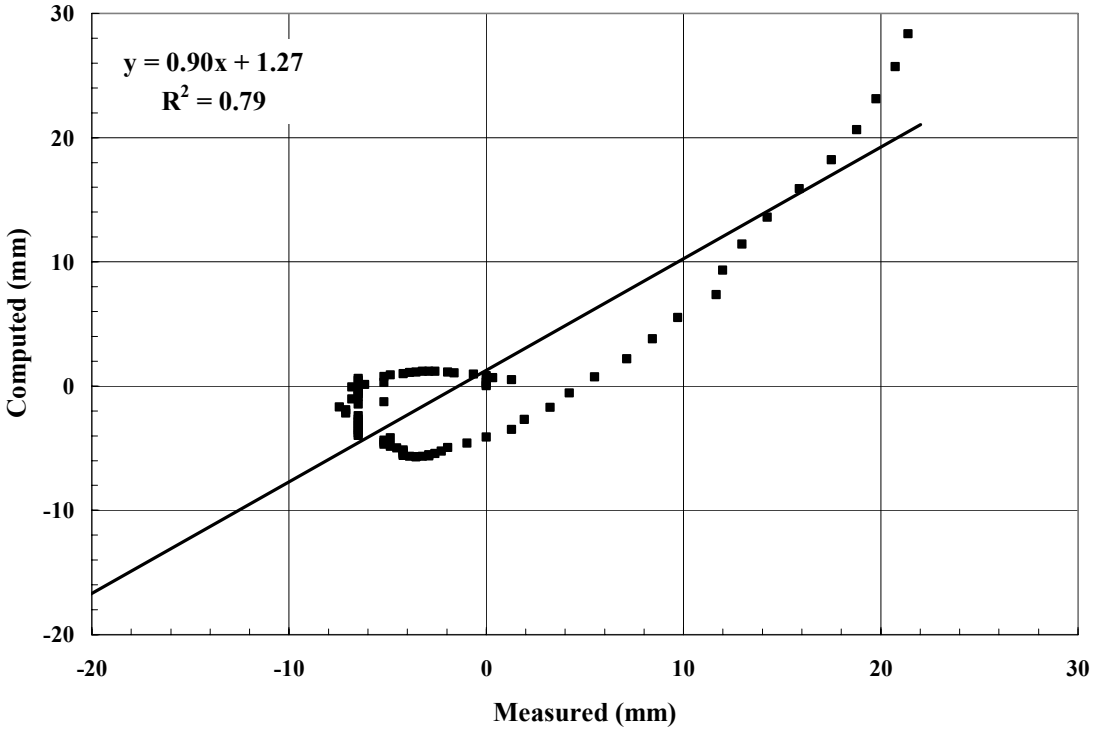

Figure D-2. Error plot for Column 2 – low evaporation test.

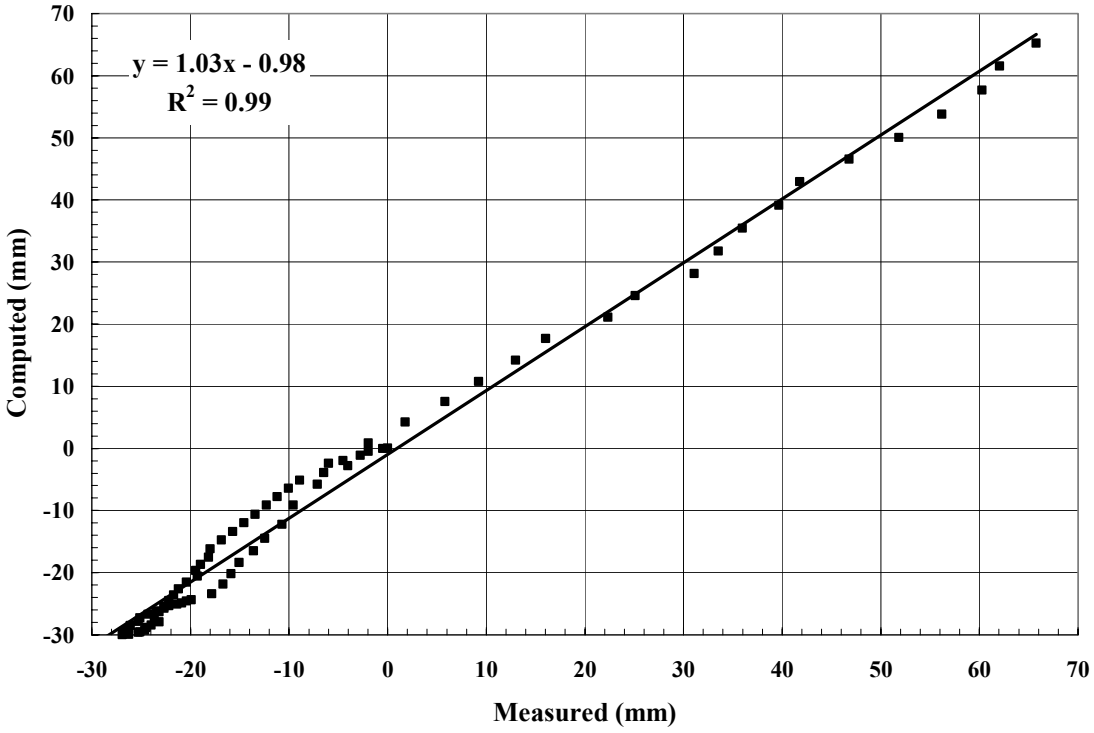

Figure D-3. Error plot for Column 3 – low evaporation test.

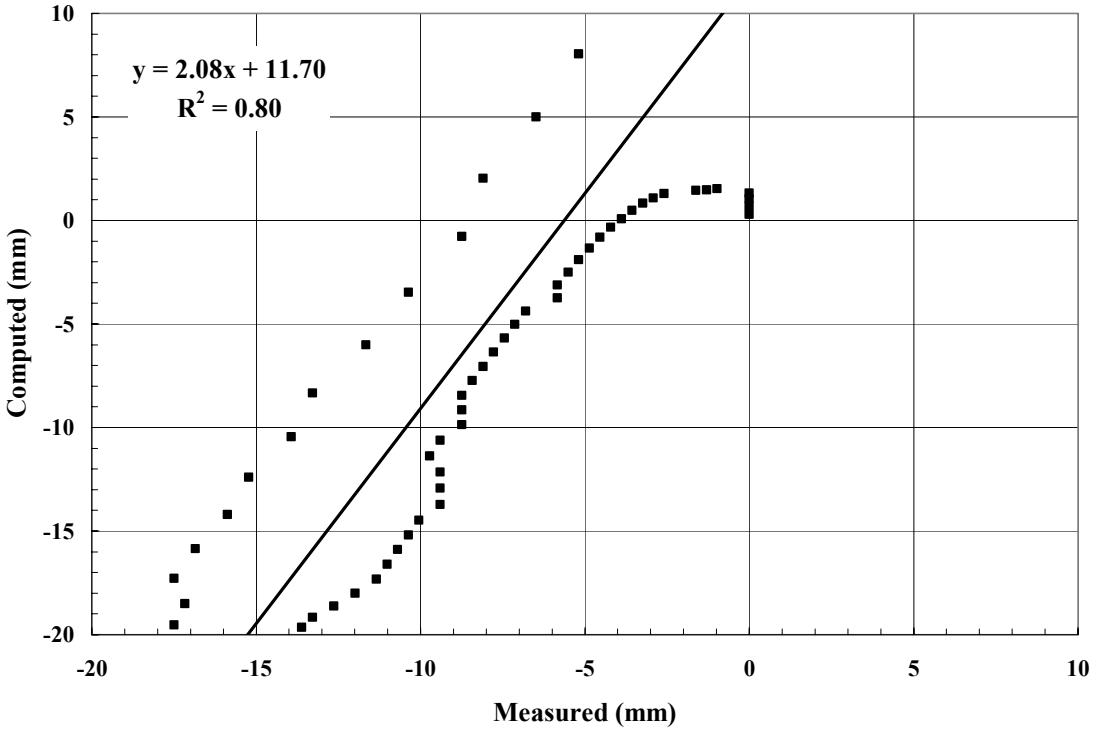

Figure D-4. Error plot for Column 4 – low evaporation test.

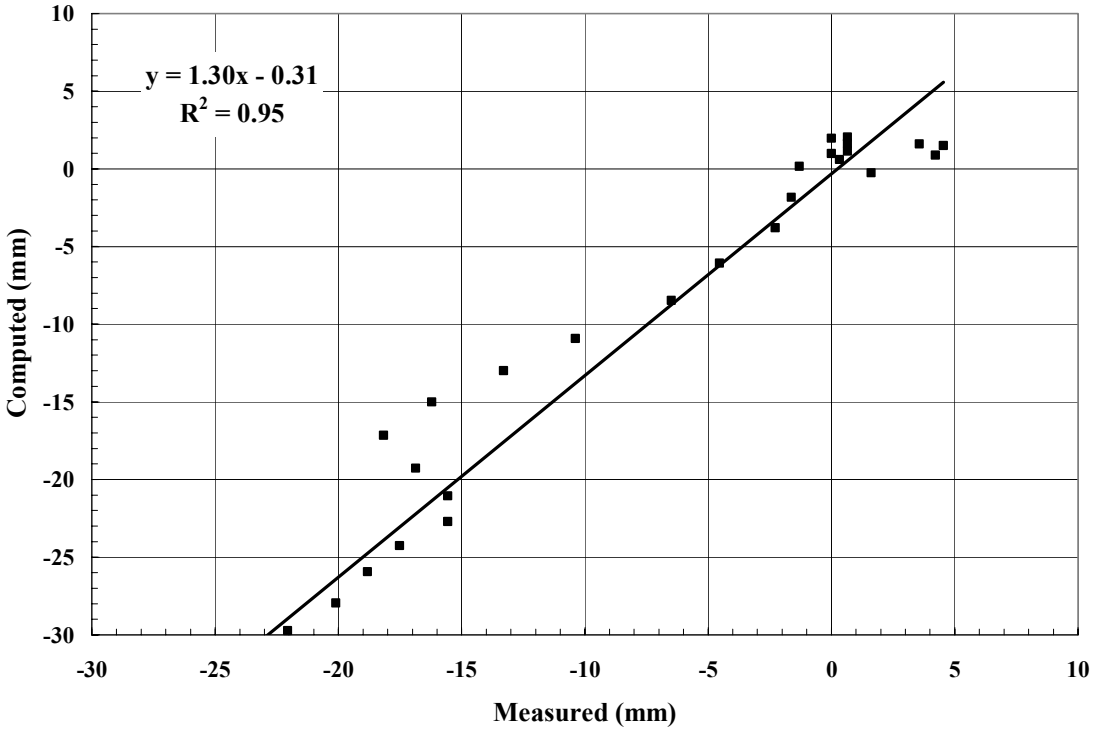

Figure D-5. Error plot for Column 1 – high evaporation test.

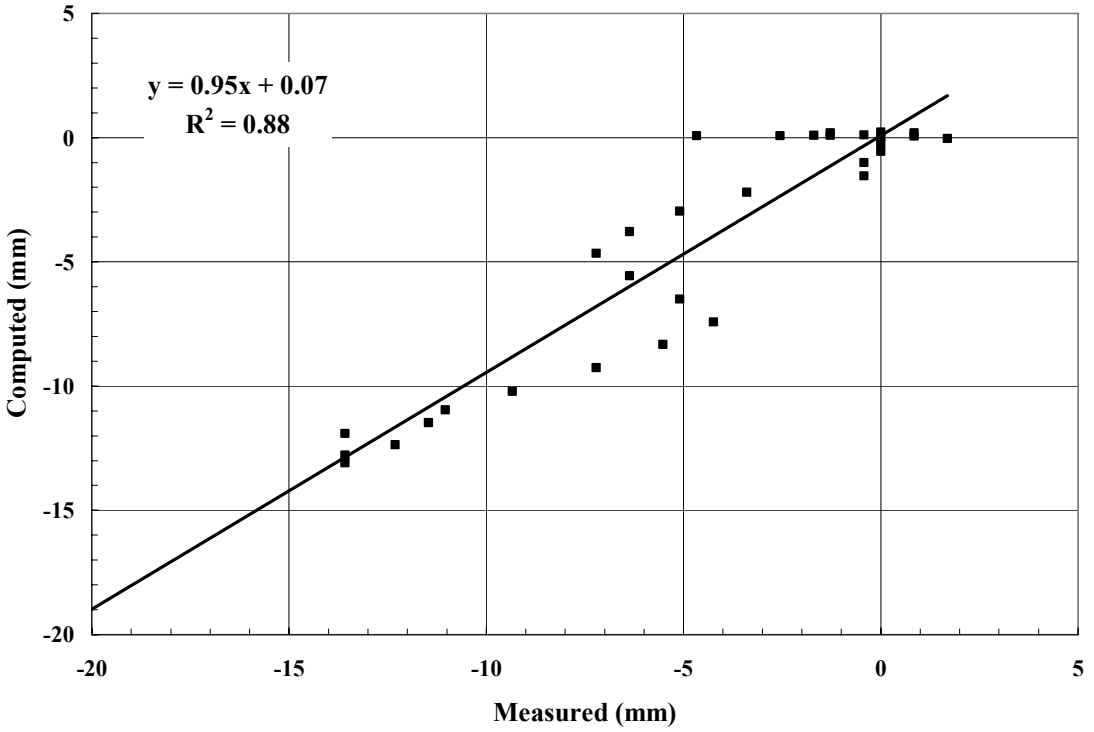

Figure D-6. Error plot for Column 2 – high evaporation test.

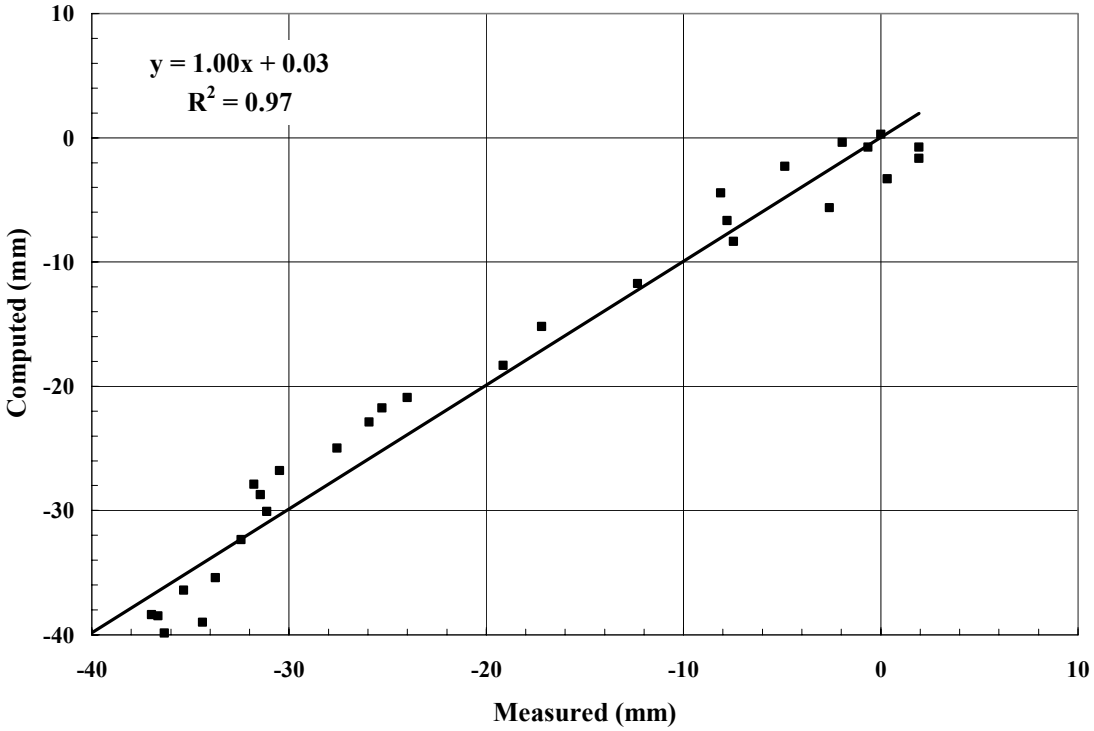

Figure D-7. Error plot for Column 3 – high evaporation test.

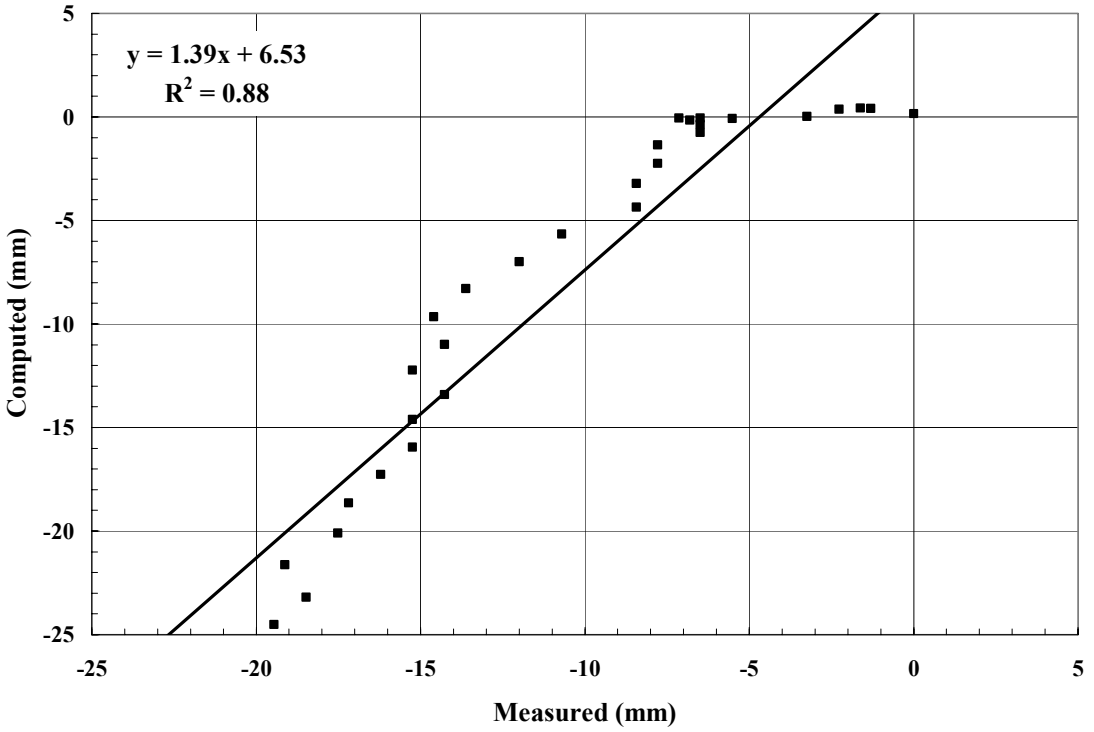

Figure D-8. Error plot for Column 4 – high evaporation test.

Table B-1. Input climate for low evaporation test.

Date	Day	Temp (°C)		RH (%)		Wind	Precip	Precip Period		P.E.
		Max	Min	Max	Min	(m/s)	(mm)	Start	End	(mm/day)
21-Nov-04	1	22.9	22.5	19.3	11.8	0.0	0.0	0.0	24.0	2.0
22-Nov-04	2	23.6	16.4	22.3	10.8	0.0	0.4	11.0	12.0	1.7
23-Nov-04	3	23.2	21.7	13.8	10.8	0.0	0.4	11.0	12.0	1.2
24-Nov-04	4	22.9	21.0	13.8	10.3	0.0	0.3	11.0	12.0	1.4
25-Nov-04	5	23.2	21.3	18.3	13.8	0.0	0.3	11.0	12.0	1.3
26-Nov-04	6	23.2	19.8	15.8	11.8	0.0	0.4	11.0	12.0	2.0
27-Nov-04	7	21.7	19.0	16.8	12.3	0.0	0.4	11.0	12.0	1.9
28-Nov-04	8	21.3	18.3	15.3	10.8	0.0	0.4	11.0	12.0	1.8
29-Nov-04	9	21.7	19.8	19.3	12.3	0.0	0.3	11.0	12.0	1.6
30-Nov-04	10	21.7	18.7	18.8	9.8	0.0	0.4	11.0	12.0	2.0
1-Dec-04	11	21.3	17.9	15.8	9.8	0.0	0.3	11.0	12.0	2.0
2-Dec-04	12	21.3	18.3	24.3	13.8	0.0	0.3	11.0	12.0	1.3
3-Dec-04	13	21.0	19.4	24.3	19.3	0.0	0.3	11.0	12.0	1.8
4-Dec-04	14	20.2	18.7	22.3	7.3	0.0	0.3	11.0	12.0	1.4
5-Dec-04	15	20.2	17.1	11.8	8.8	0.0	0.3	11.0	12.0	2.0
6-Dec-04	16	21.0	17.5	13.8	7.8	0.0	0.6	11.0	12.0	1.8
7-Dec-04	17	21.0	17.1	11.8	6.8	0.0	0.7	11.0	12.0	1.5
8-Dec-04	18	20.6	16.8	10.8	6.8	0.0	0.8	11.0	12.0	1.4
9-Dec-04	19	20.6	17.9	11.3	7.3	0.0	0.6	11.0	12.0	1.2
10-Dec-04	20	20.6	17.9	15.8	9.8	0.0	0.7	11.0	12.0	2.1
11-Dec-04	21	20.2	19.0	21.8	15.8	0.0	0.7	11.0	12.0	2.0
12-Dec-04	22	20.6	18.7	17.3	12.3	0.0	0.6	11.0	12.0	1.3
13-Dec-04	23	20.6	17.9	16.3	9.8	0.0	0.7	11.0	12.0	1.5
14-Dec-04	24	21.0	18.7	17.8	12.8	0.0	0.6	11.0	12.0	1.4
15-Dec-04	25	20.6	19.4	21.8	17.3	0.0	0.6	11.0	12.0	1.7
16-Dec-04	26	20.6	18.3	18.8	10.8	0.0	0.6	11.0	12.0	1.5
17-Dec-04	27	21.0	20.2	20.8	14.8	0.0	1.3	11.0	12.0	1.7
18-Dec-04	28	21.3	18.7	15.3	7.8	0.0	1.3	11.0	12.0	1.3
19-Dec-04	29	20.6	18.3	24.8	10.8	0.0	1.3	11.0	12.0	1.7
20-Dec-04	30	20.2	18.3	21.8	7.8	0.0	1.3	11.0	12.0	1.8
21-Dec-04	31	20.2	17.5	12.3	6.8	0.0	1.3	11.0	12.0	1.4
22-Dec-04	32	19.8	16.4	10.8	5.3	0.0	1.3	11.0	12.0	0.8
23-Dec-04	33	21.0	14.5	10.3	5.8	0.0	1.3	11.0	12.0	1.8
30-Dec-04	34	19.8	17.1	11.3	5.8	0.0	1.3	11.0	12.0	1.5
31-Dec-04	35	19.8	17.5	10.8	5.8	0.0	1.3	11.0	12.0	1.6
1-Jan-05	36	19.8	16.8	9.8	5.8	0.0	1.3	11.0	12.0	1.3
2-Jan-05	37	19.8	15.6	9.3	5.3	0.0	1.4	11.0	12.0	1.5
3-Jan-05	38	20.2	14.9	9.3	5.3	0.0	1.9	11.0	12.0	1.0
4-Jan-05	39	20.6	14.9	9.8	3.8	0.0	1.9	11.0	12.0	1.1
5-Jan-05	40	20.6	16.4	10.8	5.3	0.0	1.9	11.0	12.0	1.5
6-Jan-05	41	20.2	18.3	11.3	6.3	0.0	1.9	11.0	12.0	1.6
7-Jan-05	42	20.2	18.7	10.8	7.3	0.0	2.0	11.0	12.0	0.9
8-Jan-05	43	20.2	18.3	9.3	6.8	0.0	1.9	11.0	12.0	1.4
9-Jan-05	44	19.8	17.9	8.3	4.8	0.0	2.0	11.0	12.0	1.5
10-Jan-05	45	20.2	16.0	7.8	5.8	0.0	2.0	11.0	12.0	1.4
11-Jan-05	46	20.6	15.6	8.3	5.3	0.0	2.0	11.0	12.0	1.7
12-Jan-05	47	18.3	15.6	7.8	5.3	0.0	1.9	11.0	12.0	1.7

13-Jan-05	48	20.6	15.2	6.8	3.8	0.0	2.0	11.0	12.0	1.9
14-Jan-05	49	19.0	15.6	6.8	3.8	0.0	2.0	11.0	12.0	1.7
15-Jan-05	50	17.1	15.6	5.8	5.3	0.0	1.9	11.0	12.0	1.5
16-Jan-05	51	17.1	15.6	6.3	4.8	0.0	2.0	11.0	12.0	2.2
17-Jan-05	52	19.8	15.2	12.3	5.3	0.0	3.4	11.0	12.0	1.4
18-Jan-05	53	19.8	16.8	17.3	8.3	0.0	3.4	11.0	12.0	1.1
19-Jan-05	54	19.4	16.4	10.8	8.3	0.0	3.4	11.0	12.0	1.7
20-Jan-05	55	19.4	17.5	9.3	7.3	0.0	3.4	11.0	12.0	1.4
21-Jan-05	56	17.9	16.0	9.8	5.8	0.0	3.4	11.0	12.0	1.4
22-Jan-05	57	19.4	15.2	9.8	5.3	0.0	3.5	11.0	12.0	1.5
23-Jan-05	58	18.7	17.1	20.3	8.8	0.0	3.4	11.0	12.0	1.3
24-Jan-05	59	19.0	17.9	24.3	18.3	0.0	4.8	11.0	12.0	0.9
25-Jan-05	60	18.7	17.1	24.8	11.3	0.0	4.8	11.0	12.0	1.2
26-Jan-05	61	19.0	16.8	12.8	9.8	0.0	4.8	11.0	12.0	1.5
27-Jan-05	62	19.8	17.1	17.3	10.3	0.0	4.8	11.0	12.0	1.4
28-Jan-05	63	19.4	17.9	17.3	9.8	0.0	4.8	11.0	12.0	1.5
29-Jan-05	64	19.0	17.1	18.3	11.8	0.0	4.8	11.0	12.0	1.4
30-Jan-05	65	19.0	17.9	19.3	12.8	0.0	4.8	11.0	12.0	1.7
31-Jan-05	66	19.0	17.9	20.3	12.8	0.0	4.9	11.0	12.0	1.3
1-Feb-05	67	19.8	18.3	21.8	16.3	0.0	5.0	11.0	12.0	1.4
2-Feb-05	68	19.8	18.3	25.3	17.3	0.0	4.8	11.0	12.0	1.5
3-Feb-05	69	19.4	17.9	23.8	15.3	0.0	4.8	11.0	12.0	1.4
4-Feb-05	70	18.7	17.9	16.3	9.3	0.0	4.8	11.0	12.0	1.4
5-Feb-05	71	18.3	17.5	9.8	7.8	0.0	4.8	11.0	12.0	0.9
6-Feb-05	72	18.7	17.1	8.8	5.8	0.0	4.8	11.0	12.0	1.3
7-Feb-05	73	19.4	16.0	7.8	6.3	0.0	4.9	11.0	12.0	1.2
8-Feb-05	74	19.0	16.4	9.8	7.3	0.0	4.9	11.0	12.0	0.8
9-Feb-05	75	18.7	17.1	13.8	9.3	0.0	4.8	11.0	12.0	1.2
10-Feb-05	76	19.8	17.5	15.3	12.3	0.0	4.8	11.0	12.0	1.6
11-Feb-05	77	19.4	18.3	16.8	13.8	0.0	4.8	11.0	12.0	0.9
12-Feb-05	78	18.7	17.9	18.3	12.3	0.0	4.8	11.0	12.0	0.6
13-Feb-05	79	19.4	16.4	25.3	12.3	0.0	4.8	11.0	12.0	1.0
14-Feb-05	80	19.4	15.2	18.3	9.3	0.0	4.9	11.0	12.0	1.0
15-Feb-05	81	20.2	14.9	13.8	7.8	0.0	4.9	11.0	12.0	1.2
							189			**118**

Table B-2. Input climate for high evaporation test.

Date	Day	Temp (°C)		RH (%)		Wind	Precip	Precip Period		P.E.
		Max	Min	Max	Min	(m/s)	(mm)	St.	End	(mm/day)
15-Sep-04	1	21.3	5.4	93.3	39.3	0.0	0.6	17.0	18.0	2.2
16-Sep-04	2	20.2	5.8	99.3	40.3	0.0	0.0	0.0	24.0	4.4
17-Sep-04	3	21.7	7.8	93.8	36.8	0.0	0.0	0.0	24.0	3.8
18-Sep-04	4	20.6	10.6	93.8	52.8	0.0	0.4	5.0	7.0	5.3
19-Sep-04	5	15.2	7.8	97.8	62.3	0.0	2.8	8.0	24.0	1.4
20-Sep-04	6	11.0	5.0	96.3	48.8	0.0	10.0	0.0	7.0	4.9
21-Sep-04	7	17.1	1.2	89.3	33.8	0.0	0.0	0.0	24.0	2.6
22-Sep-04	8	16.4	8.2	90.8	48.3	0.0	0.6	16.0	17.0	2.3
23-Sep-04	9	21.3	4.2	96.8	32.3	0.0	0.0	0.0	24.0	2.4
24-Sep-04	10	22.9	7.4	88.8	22.8	0.0	0.0	0.0	24.0	2.8
25-Sep-04	11	23.2	8.6	84.8	31.8	0.0	0.0	0.0	24.0	2.8
26-Sep-04	12	18.7	5.8	81.8	23.8	0.0	0.0	0.0	24.0	4.6
27-Sep-04	13	19.0	0.7	89.3	29.8	0.0	0.0	0.0	24.0	2.0
28-Sep-04	14	24.4	8.2	78.3	35.8	0.0	0.0	0.0	24.0	4.3
29-Sep-04	15	16.4	4.2	88.8	22.3	0.0	0.0	0.0	24.0	2.0
30-Sep-04	16	12.9	-1.5	92.8	52.3	0.0	0.6	21.0	24.0	2.8
1-Oct-04	17	8.4	-5.0	82.0	30.0	0.0	0.8	15.0	17.0	5.5
2-Oct-04	18	19.3	-2.0	77.0	34.0	0.0	0.0	0.0	24.0	1.2
3-Oct-04	19	6.5	-2.1	73.0	41.0	0.0	0.0	0.0	24.0	2.4
4-Oct-04	20	22.2	-2.7	79.0	27.0	0.0	4.0	11.0	13.0	3.1
5-Oct-04	21	22.9	1.1	82.0	26.0	0.0	0.0	0.0	24.0	2.7
6-Oct-04	22	24.3	7.2	70.0	29.0	0.0	4.0	11.5	12.5	4.3
7-Oct-04	23	15.8	5.3	86.0	49.0	0.0	0.0	0.0	24.0	5.5
8-Oct-04	24	19.0	-0.8	82.0	25.0	0.0	0.0	0.0	24.0	3.6
9-Oct-04	25	26.3	7.8	67.0	24.0	0.0	4.0	10.5	11.5	4.4
10-Oct-04	26	18.2	3.1	87.0	29.0	0.0	0.0	0.0	24.0	4.3
11-Oct-04	27	18.1	3.6	74.0	29.0	0.0	4.0	13.0	14.0	3.1
12-Oct-04	28	12.2	0.4	92.0	41.0	0.0	0.0	0.0	24.0	1.7
13-Oct-04	29	10.4	-4.7	95.0	50.0	0.0	6.0	10.0	11.5	1.8
14-Oct-04	30	13.3	0.3	87.0	50.0	0.0	1.0	7.0	11.0	1.5
15-Oct-04	31	4.2	-1.0	96.0	63.0	0.0	0.0	0.0	24.0	1.5
							39			**97**

Table B-3. Flin Flon climate 1999-00.

Date	Day	Temp (°C)		RH (%)		Wind	Precip	Precip Period		P.E.
		Max	Min	Max	Min	(m/s)	(mm)	Start	End	(mm/day)
1-Dec-99	1	1.0	-4.5	78.0	59.0	15.3	8.1	0.0	24.0	0.0
2-Dec-99	2	-0.5	-13.5	95.0	79.0	5.3	0.0	0.0	24.0	0.0
3-Dec-99	3	-9.0	-10.5	90.0	85.0	13.2	10.0	0.0	24.0	0.0
4-Dec-99	4	-11.5	-17.0	88.0	72.0	7.7	0.0	0.0	24.0	0.0
5-Dec-99	5	-2.0	-22.0	91.0	83.0	12.6	0.0	0.0	24.0	0.0
6-Dec-99	6	-1.5	-7.5	100.0	77.0	8.0	0.0	0.0	24.0	0.0
7-Dec-99	7	-2.5	-14.0	96.0	85.0	5.8	0.2	0.0	24.0	0.0
8-Dec-99	8	-9.0	-13.0	93.0	75.0	9.0	0.0	0.0	24.0	0.0
9-Dec-99	9	-10.0	-19.5	91.0	68.0	5.1	0.0	0.0	24.0	0.0
10-Dec-99	10	-2.0	-15.5	93.0	83.0	15.5	0.6	0.0	24.0	0.0
11-Dec-99	11	-3.0	-8.5	95.0	86.0	5.0	0.2	0.0	24.0	0.0
12-Dec-99	12	-7.0	-11.0	98.0	86.0	4.3	0.4	0.0	24.0	0.0
13-Dec-99	13	-2.0	-8.5	96.0	91.0	13.0	3.0	0.0	24.0	0.0
14-Dec-99	14	-11.5	-21.5	87.0	51.0	11.3	0.0	0.0	24.0	0.0
15-Dec-99	15	-24.0	-30.5	67.0	57.0	6.4	0.0	0.0	24.0	0.0
16-Dec-99	16	-16.5	-33.0	67.0	58.0	6.6	0.6	0.0	24.0	0.0
17-Dec-99	17	-13.0	-21.0	79.0	72.0	9.5	0.4	0.0	24.0	0.0
18-Dec-99	18	-11.5	-22.5	89.0	72.0	8.7	7.2	0.0	24.0	0.0
19-Dec-99	19	-14.5	-28.5	80.0	55.0	25.1	1.4	0.0	24.0	0.0
20-Dec-99	20	-26.0	-32.5	64.0	56.0	7.3	0.0	0.0	24.0	0.0
21-Dec-99	21	-23.5	-31.5	66.0	59.0	5.8	0.0	0.0	24.0	0.0
22-Dec-99	22	-9.5	-31.0	75.0	63.0	4.3	0.0	0.0	24.0	0.0
23-Dec-99	23	-5.5	-16.5	92.0	88.0	6.1	0.0	0.0	24.0	0.0
24-Dec-99	24	6.5	-9.5	96.0	78.0	10.8	0.0	0.0	24.0	0.0
25-Dec-99	25	6.0	-11.5	60.0	50.0	31.2	0.0	0.0	24.0	0.0
26-Dec-99	26	-14.0	-19.5	84.0	67.0	6.5	3.6	0.0	24.0	0.0
27-Dec-99	27	4.5	-25.0	97.0	82.0	12.8	0.2	0.0	24.0	0.0
28-Dec-99	28	-5.0	-7.5	98.0	90.0	7.0	7.2	0.0	24.0	0.0
29-Dec-99	29	-11.0	-18.5	91.0	61.0	9.0	0.8	0.0	24.0	0.0
30-Dec-99	30	-16.5	-22.0	80.0	47.0	4.5	1.8	0.0	24.0	0.0
31-Dec-99	31	-19.0	-24.0	77.0	62.0	9.3	0.0	0.0	24.0	0.0
1-Jan-00	32	-29.5	-38.0	70.0	64.0	0.7	0.0	0.0	24.0	0.0
2-Jan-00	33	-21.0	-38.5	86.0	60.0	7.9	0.0	0.0	24.0	0.0
3-Jan-00	34	-20.0	-26.5	71.0	63.0	10.1	0.0	0.0	24.0	0.0
4-Jan-00	35	-23.5	-35.0	70.0	64.0	0.5	0.0	0.0	24.0	0.0
5-Jan-00	36	-21.0	-30.5	70.0	63.0	3.5	0.0	0.0	24.0	0.0
6-Jan-00	37	-17.0	-24.5	76.0	67.0	3.3	0.0	0.0	24.0	0.0
7-Jan-00	38	-12.0	-27.0	91.0	74.0	6.9	2.4	0.0	24.0	0.0
8-Jan-00	39	-12.5	-20.5	92.0	72.0	3.2	1.4	0.0	24.0	0.0
9-Jan-00	40	-6.5	-15.5	94.0	88.0	5.6	2.4	0.0	24.0	0.0
10-Jan-00	41	-19.0	-23.0	70.0	59.0	19.9	0.6	0.0	24.0	0.0
11-Jan-00	42	-24.5	-31.5	66.0	54.0	3.8	0.0	0.0	24.0	0.0
12-Jan-00	43	-23.5	-39.5	71.0	59.0	0.9	0.0	0.0	24.0	0.0
13-Jan-00	44	-22.5	-36.0	71.0	58.0	1.5	0.2	0.0	24.0	0.0
14-Jan-00	45	-21.0	-26.5	73.0	60.0	9.3	0.4	0.0	24.0	0.0
15-Jan-00	46	-26.0	-33.0	69.0	57.0	5.5	0.0	0.0	24.0	0.0
16-Jan-00	47	-17.0	-39.0	71.0	61.0	5.2	2.6	0.0	24.0	0.0

17-Jan-00	48	-16.0	-22.0	77.0	68.0	12.2	0.8	0.0	24.0	0.0
18-Jan-00	49	-24.5	-27.5	68.0	57.0	11.8	0.0	0.0	24.0	0.0
19-Jan-00	50	-26.5	-39.5	69.0	63.0	0.0	0.0	0.0	24.0	0.0
20-Jan-00	51	-24.5	-39.0	79.0	54.0	1.6	0.0	0.0	24.0	0.0
21-Jan-00	52	-20.0	-34.0	70.0	65.0	10.3	2.0	0.0	24.0	0.0
22-Jan-00	53	-17.5	-24.0	72.0	62.0	12.8	0.6	0.0	24.0	0.0
23-Jan-00	54	-9.0	-28.5	89.0	70.0	13.7	0.2	0.0	24.0	0.0
24-Jan-00	55	-9.5	-16.5	79.0	69.0	15.8	0.0	0.0	24.0	0.0
25-Jan-00	56	-5.5	-27.5	83.0	68.0	12.2	0.0	0.0	24.0	0.0
26-Jan-00	57	-8.0	-22.5	91.0	69.0	2.9	0.0	0.0	24.0	0.0
27-Jan-00	58	-7.0	-24.0	91.0	71.0	1.5	0.0	0.0	24.0	0.0
28-Jan-00	59	-5.0	-8.5	95.0	73.0	17.3	0.0	0.0	24.0	0.0
29-Jan-00	60	-5.5	-17.5	94.0	67.0	5.8	0.0	0.0	24.0	0.0
30-Jan-00	61	1.0	-11.0	76.0	56.0	18.2	0.0	0.0	24.0	0.0
31-Jan-00	62	-7.5	-10.5	100.0	95.0	3.1	0.0	0.0	24.0	0.0
1-Feb-00	63	-6.0	-13.5	98.0	86.0	9.8	0.0	0.0	24.0	0.0
2-Feb-00	64	-5.0	-9.5	98.0	75.0	14.9	0.6	0.0	24.0	0.0
3-Feb-00	65	-6.5	-12.5	82.0	55.0	17.8	0.0	0.0	24.0	0.0
4-Feb-00	66	-1.5	-13.0	86.0	57.0	10.5	0.0	0.0	24.0	0.0
5-Feb-00	67	-8.0	-21.5	95.0	68.0	10.1	0.0	0.0	24.0	0.0
6-Feb-00	68	-7.0	-12.5	80.0	58.0	14.5	0.0	0.0	24.0	0.0
7-Feb-00	69	-1.5	-21.0	87.0	48.0	9.8	0.0	0.0	24.0	0.0
8-Feb-00	70	-1.0	-15.5	72.0	34.0	17.8	0.0	0.0	24.0	0.0
9-Feb-00	71	-17.5	-27.0	62.0	35.0	11.5	0.0	0.0	24.0	0.0
10-Feb-00	72	-15.5	-24.5	55.0	32.0	13.8	0.0	0.0	24.0	0.0
11-Feb-00	73	-10.5	-22.5	64.0	33.0	14.7	0.0	0.0	24.0	0.0
12-Feb-00	74	-20.0	-27.0	67.0	37.0	6.8	0.0	0.0	24.0	0.0
13-Feb-00	75	-14.5	-36.0	67.0	53.0	10.4	0.0	0.0	24.0	0.0
14-Feb-00	76	-9.0	-17.5	78.0	41.0	14.8	0.0	0.0	24.0	0.0
15-Feb-00	77	-19.0	-28.0	64.0	40.0	9.8	0.0	0.0	24.0	0.0
16-Feb-00	78	-18.5	-34.5	69.0	42.0	6.7	0.0	0.0	24.0	0.0
17-Feb-00	79	-9.0	-31.5	75.0	55.0	4.8	0.0	0.0	24.0	0.0
18-Feb-00	80	-10.0	-26.5	73.0	57.0	1.6	0.0	0.0	24.0	0.0
19-Feb-00	81	-6.5	-24.5	87.0	74.0	4.0	0.2	0.0	24.0	0.0
20-Feb-00	82	0.5	-12.5	92.0	57.0	4.4	0.0	0.0	24.0	0.0
21-Feb-00	83	-2.0	-17.5	96.0	61.0	3.1	0.0	0.0	24.0	0.0
22-Feb-00	84	7.5	-15.5	95.0	49.0	6.3	0.0	0.0	24.0	0.0
23-Feb-00	85	5.0	-12.0	98.0	56.0	6.6	0.0	0.0	24.0	0.0
24-Feb-00	86	6.0	-0.5	74.0	50.0	10.5	0.6	0.0	24.0	0.0
25-Feb-00	87	2.0	0.5	100.0	95.0	8.4	0.6	0.0	24.0	0.0
26-Feb-00	88	4.5	-4.0	96.0	47.0	11.2	0.0	0.0	24.0	0.0
27-Feb-00	89	4.5	-12.5	94.0	48.0	5.2	0.0	0.0	24.0	0.0
28-Feb-00	90	1.0	-11.0	98.0	69.0	5.7	7.4	0.0	24.0	0.0
29-Feb-00	91	0.5	-2.5	95.0	63.0	18.2	0.0	0.0	24.0	0.0
1-Mar-00	92	-1.0	-18.5	90.0	63.0	6.5	0.0	0.0	24.0	0.0
2-Mar-00	93	5.5	-10.5	97.0	60.0	4.9	0.0	0.0	24.0	0.0
3-Mar-00	94	9.0	0.0	78.0	42.0	11.1	0.0	0.0	24.0	0.0
4-Mar-00	95	10.0	-3.0	93.0	44.0	3.4	0.0	0.0	24.0	0.0
5-Mar-00	96	8.0	-3.5	96.0	40.0	6.4	0.0	0.0	24.0	0.0
6-Mar-00	97	6.5	-4.5	90.0	35.0	4.1	0.0	0.0	24.0	0.0
7-Mar-00	98	0.0	-10.5	98.0	83.0	18.5	7.2	0.0	24.0	0.0

8-Mar-00	99	-12.0	-25.5	86.0	46.0	14.1	0.0	0.0	24.0	0.0
9-Mar-00	100	-10.0	-30.0	69.0	39.0	7.3	0.0	0.0	24.0	0.0
10-Mar-00	101	-8.0	-13.5	77.0	57.0	12.2	0.2	0.0	24.0	0.0
11-Mar-00	102	-8.5	-28.5	69.0	27.0	10.0	0.0	0.0	24.0	0.0
12-Mar-00	103	-6.5	-21.0	57.0	24.0	12.6	0.0	0.0	24.0	0.0
13-Mar-00	104	-9.5	-19.5	54.0	25.0	14.2	0.0	0.0	24.0	0.0
14-Mar-00	105	-13.5	-28.0	71.0	35.0	9.9	0.0	0.0	24.0	0.0
15-Mar-00	106	-13.0	-29.0	66.0	34.0	6.1	0.0	0.0	24.0	0.0
16-Mar-00	107	-11.5	-29.5	66.0	31.0	6.5	0.0	0.0	24.0	0.0
17-Mar-00	108	-0.5	-15.5	90.0	61.0	11.9	5.6	0.0	24.0	0.0
18-Mar-00	109	4.0	-8.5	84.0	51.0	11.4	0.0	0.0	24.0	0.0
19-Mar-00	110	7.5	-9.5	90.0	48.0	10.8	0.0	0.0	24.0	0.0
20-Mar-00	111	2.0	-1.0	92.0	74.0	17.5	0.4	0.0	24.0	0.0
21-Mar-00	112	6.0	-4.0	89.0	55.0	12.3	0.0	0.0	24.0	0.0
22-Mar-00	113	9.0	1.5	88.0	33.0	12.8	0.0	0.0	24.0	0.0
23-Mar-00	114	11.5	-1.0	71.0	42.0	10.9	0.0	0.0	24.0	0.0
24-Mar-00	115	5.0	1.0	96.0	61.0	15.1	0.6	0.0	24.0	0.0
25-Mar-00	116	10.5	-1.0	78.0	32.0	14.7	0.0	0.0	24.0	0.1
26-Mar-00	117	3.5	-2.5	63.0	42.0	20.2	0.0	0.0	24.0	0.7
27-Mar-00	118	-0.5	-10.0	77.0	50.0	11.5	0.0	0.0	24.0	0.3
28-Mar-00	119	4.5	-8.5	88.0	42.0	10.4	0.0	0.0	24.0	0.3
29-Mar-00	120	10.5	-4.0	88.0	43.0	5.0	0.0	0.0	24.0	0.3
30-Mar-00	121	10.5	-0.5	90.0	49.0	10.1	0.2	0.0	24.0	0.3
31-Mar-00	122	4.5	0.5	97.0	74.0	8.8	0.6	0.0	24.0	0.3
1-Apr-00	123	8.5	-5.5	97.0	39.0	5.3	0.0	0.0	24.0	0.2
2-Apr-00	124	4.0	-2.0	86.0	43.0	13.1	0.0	0.0	24.0	0.4
3-Apr-00	125	4.0	-5.5	73.0	30.0	10.9	0.0	0.0	24.0	0.4
4-Apr-00	126	3.5	-5.0	90.0	56.0	9.4	0.0	0.0	24.0	0.3
5-Apr-00	127	0.5	-7.0	94.0	50.0	17.8	0.0	0.0	24.0	0.4
6-Apr-00	128	-4.0	-16.0	71.0	30.0	7.0	0.0	0.0	24.0	0.2
7-Apr-00	129	-3.0	-13.0	91.0	46.0	7.8	0.0	0.0	24.0	0.2
8-Apr-00	130	-2.5	-8.5	88.0	37.0	8.3	0.8	0.0	24.0	0.0
9-Apr-00	131	-2.0	-16.5	78.0	27.0	4.7	0.0	0.0	24.0	0.0
10-Apr-00	132	1.0	-15.5	82.0	25.0	5.8	0.0	0.0	24.0	0.0
11-Apr-00	133	0.0	-11.5	63.0	29.0	6.8	0.0	0.0	24.0	0.0
12-Apr-00	134	5.0	-11.0	84.0	24.0	6.8	0.8	0.0	24.0	0.1
13-Apr-00	135	-7.0	-14.0	81.0	51.0	20.1	0.0	0.0	24.0	0.0
14-Apr-00	136	-3.5	-18.5	65.0	26.0	6.1	0.0	0.0	24.0	0.0
15-Apr-00	137	3.0	-16.0	79.0	23.0	5.0	0.0	0.0	24.0	0.1
16-Apr-00	138	5.5	-5.5	71.0	51.0	4.7	0.6	0.0	24.0	0.1
17-Apr-00	139	5.5	-1.0	93.0	72.0	7.1	1.8	0.0	24.0	0.3
18-Apr-00	140	4.0	-3.0	85.0	51.0	12.3	0.0	0.0	24.0	0.3
19-Apr-00	141	14.0	-2.0	73.0	30.0	11.2	0.0	0.0	24.0	0.6
20-Apr-00	142	21.0	4.0	58.0	21.0	9.6	0.0	0.0	24.0	0.8
21-Apr-00	143	16.0	2.0	62.0	23.0	8.5	0.0	0.0	24.0	0.7
22-Apr-00	144	14.0	-3.0	89.0	36.0	8.0	0.0	0.0	24.0	0.5
23-Apr-00	145	18.5	2.5	84.0	37.0	11.3	0.2	0.0	24.0	0.7
24-Apr-00	146	14.5	4.5	92.0	72.0	5.6	0.6	0.0	24.0	0.4
25-Apr-00	147	8.5	3.5	97.0	74.0	5.0	4.8	0.0	24.0	0.4
26-Apr-00	148	14.5	-2.5	99.0	29.0	5.0	0.0	0.0	24.0	0.4
27-Apr-00	149	9.5	3.0	89.0	53.0	14.0	0.0	0.0	24.0	0.6

28-Apr-00	150	9.5	-2.5	96.0	58.0	10.5	0.0	0.0	24.0	0.4
29-Apr-00	151	16.5	1.5	84.0	42.0	8.1	1.2	0.0	24.0	0.6
30-Apr-00	152	14.5	5.5	89.0	43.0	19.0	0.0	0.0	24.0	0.8
1-May-00	153	11.0	1.0	96.0	61.0	10.8	0.2	0.0	24.0	0.5
2-May-00	154	21.0	3.0	98.0	24.0	6.8	0.0	0.0	24.0	0.6
3-May-00	155	21.0	2.5	88.0	18.0	4.4	0.0	0.0	24.0	0.5
4-May-00	156	11.5	7.5	98.0	65.0	9.3	15.0	0.0	24.0	0.6
5-May-00	157	21.0	2.5	100.0	17.0	10.4	0.0	0.0	24.0	0.7
6-May-00	158	18.5	1.0	96.0	34.0	5.6	0.4	0.0	24.0	0.5
7-May-00	159	11.0	5.5	95.0	73.0	15.1	2.8	0.0	24.0	0.6
8-May-00	160	3.5	0.5	99.0	88.0	14.1	8.4	0.0	24.0	0.4
9-May-00	161	4.0	-0.5	97.0	90.0	13.0	2.0	0.0	24.0	0.4
10-May-00	162	5.5	0.5	92.0	70.0	14.8	0.6	0.0	24.0	0.5
11-May-00	163	3.5	-1.0	82.0	57.0	16.4	0.0	0.0	24.0	0.6
12-May-00	164	6.0	0.0	79.0	57.0	14.9	0.0	0.0	24.0	0.6
13-May-00	165	12.5	-2.0	81.0	29.0	6.3	0.0	0.0	24.0	0.6
14-May-00	166	10.0	-1.0	90.0	39.0	8.9	0.0	0.0	24.0	0.6
15-May-00	167	9.0	-2.0	81.0	38.0	7.0	1.0	0.0	24.0	0.5
16-May-00	168	9.5	4.0	89.0	49.0	17.5	0.2	0.0	24.0	0.8
17-May-00	169	8.0	0.0	61.0	41.0	9.3	0.0	0.0	24.0	0.7
18-May-00	170	7.5	-2.5	95.0	51.0	6.8	2.8	0.0	24.0	0.4
19-May-00	171	15.0	4.5	94.0	55.0	5.8	0.0	0.0	24.0	0.6
20-May-00	172	20.5	3.5	98.0	43.0	7.6	9.0	0.0	24.0	0.6
21-May-00	173	16.0	3.5	95.0	53.0	12.3	0.4	0.0	24.0	0.7
22-May-00	174	18.5	3.0	100.0	43.0	5.8	1.0	0.0	24.0	0.6
23-May-00	175	10.5	6.0	96.0	75.0	9.3	3.0	0.0	24.0	0.6
24-May-00	176	15.0	2.5	87.0	38.0	12.1	0.0	0.0	24.0	0.8
25-May-00	177	17.0	3.0	87.0	37.0	9.5	1.4	0.0	24.0	0.7
26-May-00	178	18.5	6.5	94.0	49.0	12.3	2.2	0.0	24.0	0.8
27-May-00	179	14.0	10.5	96.0	65.0	14.3	7.2	0.0	24.0	0.8
28-May-00	180	13.0	5.0	99.0	86.0	9.1	13.4	0.0	24.0	0.5
29-May-00	181	12.5	7.5	84.0	44.0	21.7	0.2	0.0	24.0	1.1
30-May-00	182	6.0	0.5	89.0	48.0	20.1	0.6	0.0	24.0	0.8
31-May-00	183	15.5	3.5	76.0	27.0	13.3	0.0	0.0	24.0	0.9
1-Jun-00	184	19.5	1.0	98.0	22.0	7.0	0.0	0.0	24.0	3.5
2-Jun-00	185	13.5	5.0	82.0	40.0	9.0	0.0	0.0	24.0	3.7
3-Jun-00	186	19.5	2.0	93.0	25.0	5.6	0.0	0.0	24.0	3.3
4-Jun-00	187	23.0	5.0	94.0	33.0	9.7	1.6	0.0	24.0	4.1
5-Jun-00	188	13.5	7.0	99.0	50.0	13.0	0.0	0.0	24.0	3.8
6-Jun-00	189	10.5	2.5	79.0	44.0	11.3	0.8	0.0	24.0	3.7
7-Jun-00	190	7.0	5.5	96.0	85.0	12.3	6.8	0.0	24.0	2.8
8-Jun-00	191	14.0	5.0	97.0	51.0	6.1	0.0	0.0	24.0	3.1
9-Jun-00	192	13.0	6.0	64.0	42.0	12.3	0.0	0.0	24.0	4.7
10-Jun-00	193	11.0	7.0	68.0	43.0	17.2	0.0	0.0	24.0	5.5
11-Jun-00	194	9.5	6.5	67.0	57.0	16.7	10.2	0.0	24.0	4.8
12-Jun-00	195	15.5	5.0	98.0	72.0	11.0	4.8	0.0	24.0	3.1
13-Jun-00	196	12.0	8.5	99.0	82.0	9.3	0.4	0.0	24.0	3.0
14-Jun-00	197	15.5	6.5	97.0	64.0	4.5	0.0	0.0	24.0	2.9
15-Jun-00	198	10.0	4.5	94.0	66.0	17.3	0.0	0.0	24.0	3.6
16-Jun-00	199	15.5	4.5	87.0	34.0	15.3	0.0	0.0	24.0	4.8
17-Jun-00	200	21.0	4.0	79.0	24.0	7.8	0.0	0.0	24.0	4.1

18-Jun-00	201	23.5	6.5	87.0	25.0	10.0	0.0	0.0	24.0	4.7
19-Jun-00	202	23.5	8.5	84.0	43.0	8.7	0.0	0.0	24.0	4.2
20-Jun-00	203	15.5	12.0	85.0	76.0	11.1	4.0	0.0	24.0	3.9
21-Jun-00	204	18.0	12.0	94.0	75.0	10.9	5.4	0.0	24.0	3.7
22-Jun-00	205	23.0	10.0	99.0	40.0	6.8	4.2	0.0	24.0	3.8
23-Jun-00	206	22.5	9.0	91.0	30.0	11.8	0.0	0.0	24.0	5.0
24-Jun-00	207	19.5	10.0	86.0	43.0	13.1	0.0	0.0	24.0	4.9
25-Jun-00	208	18.5	7.0	88.0	47.0	7.8	3.6	0.0	24.0	3.7
26-Jun-00	209	17.0	9.0	93.0	47.0	17.6	0.0	0.0	24.0	5.0
27-Jun-00	210	21.5	9.0	72.0	42.0	14.0	0.4	0.0	24.0	5.4
28-Jun-00	211	27.0	7.0	90.0	26.0	10.0	0.4	0.0	24.0	4.8
29-Jun-00	212	26.5	11.0	93.0	33.0	7.0	0.2	0.0	24.0	4.2
30-Jun-00	213	26.5	15.0	88.0	47.0	10.5	7.0	0.0	24.0	4.9
1-Jul-00	214	17.5	9.0	95.0	49.0	9.4	1.8	0.0	24.0	3.7
2-Jul-00	215	21.0	8.0	84.0	39.0	6.8	0.0	0.0	24.0	3.7
3-Jul-00	216	23.5	9.0	95.0	36.0	7.3	0.0	0.0	24.0	3.8
4-Jul-00	217	20.5	12.5	82.0	49.0	12.0	3.2	0.0	24.0	4.6
5-Jul-00	218	21.0	14.0	89.0	66.0	13.0	0.0	0.0	24.0	4.2
6-Jul-00	219	23.5	15.0	87.0	65.0	9.7	6.0	0.0	24.0	4.0
7-Jul-00	220	23.5	16.5	95.0	53.0	16.1	3.6	0.0	24.0	5.0
8-Jul-00	221	21.5	15.0	91.0	73.0	10.2	10.4	0.0	24.0	3.7
9-Jul-00	222	22.5	14.5	94.0	59.0	7.8	0.0	0.0	24.0	3.7
10-Jul-00	223	21.0	13.5	88.0	58.0	8.3	0.0	0.0	24.0	3.8
11-Jul-00	224	21.0	14.5	94.0	81.0	12.3	18.8	0.0	24.0	3.5
12-Jul-00	225	23.5	14.0	93.0	61.0	10.8	1.0	0.0	24.0	4.0
13-Jul-00	226	27.5	15.5	91.0	42.0	7.2	0.6	0.0	24.0	4.1
14-Jul-00	227	28.0	14.0	97.0	47.0	11.0	0.0	0.0	24.0	4.4
15-Jul-00	228	27.5	14.0	80.0	42.0	14.6	3.6	0.0	24.0	5.5
16-Jul-00	229	11.5	6.0	94.0	66.0	23.4	1.2	0.0	24.0	3.9
17-Jul-00	230	17.5	5.0	94.0	35.0	4.1	0.0	0.0	24.0	2.9
18-Jul-00	231	15.5	9.5	89.0	60.0	7.9	2.0	0.0	24.0	3.3
19-Jul-00	232	20.5	7.5	89.0	35.0	9.9	0.0	0.0	24.0	4.0
20-Jul-00	233	22.5	9.0	88.0	33.0	6.2	0.0	0.0	24.0	3.5
21-Jul-00	234	24.0	10.0	90.0	31.0	9.8	8.4	0.0	24.0	4.3
22-Jul-00	235	26.5	14.5	94.0	46.0	8.0	2.4	0.0	24.0	3.9
23-Jul-00	236	28.0	13.5	96.0	37.0	4.9	4.2	0.0	24.0	3.5
24-Jul-00	237	28.0	14.5	97.0	44.0	4.3	0.0	0.0	24.0	3.3
25-Jul-00	238	27.5	15.5	77.0	37.0	5.5	0.0	0.0	24.0	3.9
26-Jul-00	239	27.5	17.5	81.0	48.0	6.9	1.8	0.0	24.0	4.1
27-Jul-00	240	29.5	16.5	93.0	51.0	10.3	0.0	0.0	24.0	4.2
28-Jul-00	241	30.5	20.5	83.0	49.0	11.3	0.0	0.0	24.0	5.0
29-Jul-00	242	33.0	21.0	85.0	41.0	10.1	2.8	0.0	24.0	5.1
30-Jul-00	243	28.5	18.0	70.0	27.0	13.8	0.0	0.0	24.0	6.4
31-Jul-00	244	25.5	16.5	66.0	39.0	9.8	0.0	0.0	24.0	5.0
1-Aug-00	245	25.5	14.0	86.0	30.0	6.7	0.0	0.0	24.0	3.6
2-Aug-00	246	25.5	13.0	94.0	38.0	9.2	0.0	0.0	24.0	3.6
3-Aug-00	247	19.5	15.5	90.0	64.0	8.6	3.4	0.0	24.0	3.2
4-Aug-00	248	23.0	15.5	96.0	60.0	9.9	0.0	0.0	24.0	3.2
5-Aug-00	249	24.5	14.5	97.0	45.0	7.7	0.0	0.0	24.0	3.2
6-Aug-00	250	25.5	13.0	88.0	38.0	6.9	0.0	0.0	24.0	3.3
7-Aug-00	251	24.5	14.0	77.0	40.0	12.2	0.0	0.0	24.0	4.3

8-Aug-00	252	20.0	16.5	93.0	72.0	9.1	6.2	0.0	24.0	3.0
9-Aug-00	253	21.0	14.0	87.0	56.0	15.3	0.0	0.0	24.0	3.9
10-Aug-00	254	25.5	10.0	95.0	44.0	9.2	0.0	0.0	24.0	3.1
11-Aug-00	255	23.5	17.5	79.0	67.0	9.5	0.4	0.0	24.0	3.4
12-Aug-00	256	21.0	13.5	92.0	50.0	17.7	3.0	0.0	24.0	4.1
13-Aug-00	257	23.5	11.5	87.0	37.0	8.4	0.0	0.0	24.0	3.2
14-Aug-00	258	17.0	12.0	91.0	64.0	12.8	4.4	0.0	24.0	3.1
15-Aug-00	259	21.0	11.5	79.0	42.0	12.6	0.0	0.0	24.0	3.8
16-Aug-00	260	21.5	12.0	83.0	50.0	9.9	2.2	0.0	24.0	3.2
17-Aug-00	261	15.5	9.5	87.0	53.0	11.3	0.2	0.0	24.0	3.0
18-Aug-00	262	19.5	9.0	76.0	52.0	14.1	0.0	0.0	24.0	3.6
19-Aug-00	263	22.5	11.5	87.0	53.0	17.3	0.0	0.0	24.0	3.8
20-Aug-00	264	20.0	14.0	94.0	73.0	5.6	5.4	0.0	24.0	2.3
21-Aug-00	265	23.0	12.0	99.0	34.0	13.0	0.2	0.0	24.0	3.4
22-Aug-00	266	23.5	11.5	82.0	38.0	10.6	0.0	0.0	24.0	3.4
23-Aug-00	267	29.5	11.0	88.0	29.0	8.0	0.0	0.0	24.0	3.1
24-Aug-00	268	27.5	15.0	75.0	36.0	8.8	0.2	0.0	24.0	3.5
25-Aug-00	269	22.5	10.0	83.0	37.0	7.4	1.0	0.0	24.0	2.8
26-Aug-00	270	24.5	13.5	90.0	56.0	14.5	1.4	0.0	24.0	3.3
27-Aug-00	271	23.0	14.0	84.0	32.0	17.2	0.0	0.0	24.0	4.6
28-Aug-00	272	14.5	10.5	73.0	50.0	17.2	0.0	0.0	24.0	4.0
29-Aug-00	273	14.0	8.0	71.0	44.0	14.7	0.0	0.0	24.0	3.6
30-Aug-00	274	14.0	4.5	89.0	43.0	8.2	0.0	0.0	24.0	2.2
31-Aug-00	275	16.5	3.5	91.0	32.0	6.8	0.0	0.0	24.0	2.1
1-Sep-00	276	16.5	4.5	89.0	41.0	7.6	0.0	0.0	24.0	1.9
2-Sep-00	277	18.0	8.0	86.0	37.0	14.5	0.0	0.0	24.0	3.0
3-Sep-00	278	15.0	8.0	73.0	43.0	13.0	0.0	0.0	24.0	3.0
4-Sep-00	279	16.5	10.5	72.0	49.0	13.8	0.0	0.0	24.0	3.1
5-Sep-00	280	18.0	12.5	96.0	66.0	7.8	1.8	0.0	24.0	1.9
6-Sep-00	281	19.5	12.5	95.0	55.0	11.2	6.2	0.0	24.0	2.2
7-Sep-00	282	17.5	10.5	88.0	47.0	14.4	0.0	0.0	24.0	2.7
8-Sep-00	283	23.5	9.5	87.0	38.0	13.4	0.0	0.0	24.0	2.8
9-Sep-00	284	21.0	14.0	75.0	49.0	9.2	1.4	0.0	24.0	2.6
10-Sep-00	285	14.0	10.0	92.0	56.0	23.5	8.8	0.0	24.0	3.1
11-Sep-00	286	12.0	6.0	78.0	49.0	16.7	0.0	0.0	24.0	2.7
12-Sep-00	287	12.0	2.5	89.0	62.0	7.7	0.0	0.0	24.0	1.4
13-Sep-00	288	15.0	7.0	93.0	52.0	12.8	0.6	0.0	24.0	2.0
14-Sep-00	289	17.0	4.0	89.0	44.0	7.8	0.2	0.0	24.0	1.6
15-Sep-00	290	24.5	11.0	70.0	37.0	14.8	0.0	0.0	24.0	3.4
16-Sep-00	291	19.0	9.5	69.0	26.0	13.6	0.0	0.0	24.0	3.2
17-Sep-00	292	9.0	7.5	95.0	68.0	9.5	7.8	0.0	24.0	1.6
18-Sep-00	293	10.5	7.0	100.0	95.0	7.4	17.4	0.0	24.0	1.1
19-Sep-00	294	9.0	6.5	97.0	88.0	17.0	4.0	0.0	24.0	1.3
20-Sep-00	295	10.0	5.0	91.0	66.0	12.8	0.8	0.0	24.0	1.6
21-Sep-00	296	7.0	3.0	89.0	55.0	13.1	0.8	0.0	24.0	1.7
22-Sep-00	297	4.0	-0.5	92.0	57.0	9.9	0.2	0.0	24.0	1.3
23-Sep-00	298	8.0	-1.5	79.0	39.0	19.2	0.0	0.0	24.0	2.2
24-Sep-00	299	11.5	2.5	93.0	50.0	9.8	1.2	0.0	24.0	1.4
25-Sep-00	300	8.0	2.0	93.0	75.0	9.0	1.6	0.0	24.0	1.1
26-Sep-00	301	4.0	-3.0	71.0	40.0	12.6	0.0	0.0	24.0	1.7
27-Sep-00	302	7.5	-3.0	76.0	52.0	9.2	0.0	0.0	24.0	1.2

28-Sep-00	303	16.0	1.0	98.0	56.0	6.2	0.0	0.0	24.0	0.9
29-Sep-00	304	12.0	2.0	100.0	66.0	7.6	0.0	0.0	24.0	0.9
30-Sep-00	305	10.5	2.0	99.0	94.0	8.0	7.8	0.0	24.0	0.7
1-Oct-00	306	10.0	4.0	86.0	35.0	18.0	0.0	0.0	24.0	2.7
2-Oct-00	307	3.5	-0.5	68.0	49.0	20.8	0.4	0.0	24.0	2.4
3-Oct-00	308	3.5	-1.5	94.0	52.0	18.3	1.4	0.0	24.0	1.3
4-Oct-00	309	1.0	-2.5	89.0	46.0	18.2	0.6	0.0	24.0	0.7
5-Oct-00	310	0.0	-5.0	67.0	59.0	14.0	0.0	0.0	24.0	0.0
6-Oct-00	311	3.5	-2.0	64.0	46.0	12.1	0.0	0.0	24.0	1.0
7-Oct-00	312	7.5	-4.5	81.0	36.0	15.7	0.0	0.0	24.0	1.9
8-Oct-00	313	13.0	1.5	59.0	29.0	17.8	0.0	0.0	24.0	3.3
9-Oct-00	314	16.0	0.0	75.0	35.0	6.1	0.0	0.0	24.0	1.2
10-Oct-00	315	16.5	1.5	79.0	35.0	7.8	0.0	0.0	24.0	1.4
11-Oct-00	316	16.0	-0.5	99.0	46.0	8.7	0.0	0.0	24.0	0.9
12-Oct-00	317	8.0	-1.5	90.0	51.0	6.2	0.0	0.0	24.0	0.9
13-Oct-00	318	10.5	-0.5	90.0	52.0	9.3	0.0	0.0	24.0	1.0
14-Oct-00	319	4.5	-2.5	99.0	70.0	8.8	0.0	0.0	24.0	0.7
15-Oct-00	320	7.0	1.5	84.0	70.0	11.3	0.0	0.0	24.0	1.2
16-Oct-00	321	13.0	-1.5	98.0	61.0	5.0	0.0	0.0	24.0	0.5
17-Oct-00	322	13.5	4.5	82.0	33.0	12.9	0.0	0.0	24.0	1.9
18-Oct-00	323	12.0	-2.0	96.0	37.0	9.2	0.0	0.0	24.0	1.0
19-Oct-00	324	13.0	2.0	80.0	38.0	17.6	0.0	0.0	24.0	2.1
20-Oct-00	325	2.0	0.0	92.0	64.0	11.5	0.0	0.0	24.0	1.2
21-Oct-00	326	9.0	1.0	74.0	62.0	19.9	0.6	0.0	24.0	2.0
22-Oct-00	327	10.5	4.5	83.0	46.0	16.5	0.0	0.0	24.0	2.1
23-Oct-00	328	14.5	4.5	64.0	49.0	13.3	0.0	0.0	24.0	2.1
24-Oct-00	329	14.5	2.5	97.0	42.0	5.1	0.4	0.0	24.0	0.7
25-Oct-00	330	9.5	4.5	88.0	70.0	9.6	0.0	0.0	24.0	1.0
26-Oct-00	331	2.5	-3.0	93.0	56.0	13.0	0.0	0.0	24.0	0.9
27-Oct-00	332	4.0	-4.0	91.0	67.0	14.9	0.0	0.0	24.0	0.8
28-Oct-00	333	4.5	1.0	86.0	76.0	14.7	0.6	0.0	24.0	1.0
29-Oct-00	334	7.0	4.0	100.0	98.0	5.9	1.4	0.0	24.0	0.5
30-Oct-00	335	7.5	6.0	100.0	97.0	4.1	0.0	0.0	24.0	0.6
31-Oct-00	336	2.5	1.0	94.0	80.0	9.0	0.0	0.0	24.0	0.7
1-Nov-00	337	1.0	-1.0	99.0	93.0	6.0	0.0	0.0	24.0	0.4
2-Nov-00	338	2.0	-1.0	93.0	77.0	18.9	0.0	0.0	24.0	0.8
3-Nov-00	339	3.5	-1.5	78.0	55.0	11.3	0.4	0.0	24.0	0.6
4-Nov-00	340	5.5	-4.0	95.0	73.0	10.0	3.6	0.0	24.0	0.0
5-Nov-00	341	0.0	-6.5	94.0	82.0	24.1	2.0	0.0	24.0	0.0
6-Nov-00	342	-8.5	-13.5	90.0	74.0	18.4	0.4	0.0	24.0	0.0
7-Nov-00	343	-9.5	-13.0	89.0	78.0	20.0	7.0	0.0	24.0	0.0
8-Nov-00	344	-7.0	-11.0	90.0	86.0	22.9	7.0	0.0	24.0	0.0
9-Nov-00	345	-8.5	-10.5	88.0	85.0	17.7	0.6	0.0	24.0	0.0
10-Nov-00	346	-10.0	-18.0	86.0	68.0	3.3	0.2	0.0	24.0	0.0
11-Nov-00	347	-7.0	-16.5	90.0	83.0	12.5	0.0	0.0	24.0	0.0
12-Nov-00	348	-5.5	-11.5	89.0	72.0	17.3	0.0	0.0	24.0	0.0
13-Nov-00	349	-4.5	-13.0	88.0	71.0	7.3	0.0	0.0	24.0	0.0
14-Nov-00	350	-2.0	-15.0	99.0	84.0	9.7	1.0	0.0	24.0	0.0
15-Nov-00	351	-5.5	-7.5	86.0	77.0	19.6	0.2	0.0	24.0	0.0
16-Nov-00	352	-7.0	-11.0	95.0	78.0	7.8	0.2	0.0	24.0	0.0
17-Nov-00	353	-6.5	-9.5	88.0	72.0	12.2	0.2	0.0	24.0	0.0

18-Nov-00	354	-11.0	-14.5	87.0	78.0	14.3	3.0	0.0	24.0	0.0
19-Nov-00	355	-11.0	-16.5	83.0	72.0	5.8	0.0	0.0	24.0	0.0
20-Nov-00	356	-8.0	-19.5	95.0	83.0	6.9	0.0	0.0	24.0	0.0
21-Nov-00	357	-10.5	-18.5	91.0	80.0	9.0	0.4	0.0	24.0	0.0
22-Nov-00	358	-4.5	-14.5	96.0	89.0	7.2	0.0	0.0	24.0	0.0
23-Nov-00	359	-1.0	-7.0	100.0	92.0	7.7	0.0	0.0	24.0	0.0
24-Nov-00	360	1.0	-11.0	95.0	83.0	7.4	0.0	0.0	24.0	0.0
25-Nov-00	361	2.0	-6.5	90.0	64.0	12.0	0.0	0.0	24.0	0.0
26-Nov-00	362	2.5	-5.0	94.0	74.0	9.9	0.0	0.0	24.0	0.0
27-Nov-00	363	-3.5	-10.5	85.0	70.0	9.5	0.0	0.0	24.0	0.0
28-Nov-00	364	-6.0	-18.5	89.0	72.0	5.0	0.0	0.0	24.0	0.0
29-Nov-00	365	-7.0	-17.0	92.0	79.0	7.0	0.8	0.0	24.0	0.0
30-Nov-00	366	-13.0	-25.5	76.0	67.0	1.4	0.0	0.0	24.0	0.0

Table B-4. Flin Flon climate 2000-01.

Date	Day	Temp (°C)		RH (%)		Wind	Precip	Precip Period		P.E.
		Max	Min	Max	Min	(m/s)	(mm)	Start	End	(mm/day)
1-Dec-00	1	-9.5	-24.5	88.0	64.0	6.9	8.0	0.0	24.0	0.0
2-Dec-00	2	-5.0	-11.5	89.0	79.0	14.3	0.8	0.0	24.0	0.0
3-Dec-00	3	-2.0	-12.0	94.0	78.0	16.0	2.6	0.0	24.0	0.0
4-Dec-00	4	-20.0	-23.5	61.0	51.0	17.5	0.0	0.0	24.0	0.0
5-Dec-00	5	-20.5	-30.5	70.0	63.0	5.4	1.0	0.0	24.0	0.0
6-Dec-00	6	-19.0	-27.0	71.0	67.0	8.0	4.2	0.0	24.0	0.0
7-Dec-00	7	-22.0	-29.0	69.0	62.0	4.5	0.2	0.0	24.0	0.0
8-Dec-00	8	-21.0	-33.0	68.0	62.0	6.7	0.0	0.0	24.0	0.0
9-Dec-00	9	-26.0	-36.0	92.0	53.0	11.8	0.8	0.0	24.0	0.0
10-Dec-00	10	-22.5	-32.0	62.0	39.0	17.8	0.0	0.0	24.0	0.0
11-Dec-00	11	-23.5	-26.5	66.0	57.0	9.2	0.0	0.0	24.0	0.0
12-Dec-00	12	-24.5	-30.0	65.0	60.0	3.5	0.0	0.0	24.0	0.0
13-Dec-00	13	-24.5	-30.5	63.0	59.0	4.3	0.0	0.0	24.0	0.0
14-Dec-00	14	-26.5	-37.0	70.0	60.0	0.8	0.0	0.0	24.0	0.0
15-Dec-00	15	-26.0	-37.5	67.0	62.0	4.6	0.4	0.0	24.0	0.0
16-Dec-00	16	-27.0	-31.5	65.0	54.0	5.7	0.0	0.0	24.0	0.0
17-Dec-00	17	-21.5	-35.5	64.0	61.0	4.8	0.8	0.0	24.0	0.0
18-Dec-00	18	-21.5	-27.0	70.0	57.0	6.5	0.0	0.0	24.0	0.0
19-Dec-00	19	-20.5	-33.5	67.0	63.0	12.2	4.2	0.0	24.0	0.0
20-Dec-00	20	-25.0	-30.5	64.0	59.0	12.0	0.0	0.0	24.0	0.0
21-Dec-00	21	-21.0	-35.0	67.0	64.0	8.6	1.0	0.0	24.0	0.0
22-Dec-00	22	-21.0	-24.5	67.0	59.0	10.8	0.0	0.0	24.0	0.0
23-Dec-00	23	-24.0	-31.0	66.0	61.0	2.8	0.0	0.0	24.0	0.0
24-Dec-00	24	-19.5	-33.5	66.0	60.0	9.8	0.8	0.0	24.0	0.0
25-Dec-00	25	-20.0	-24.5	63.0	57.0	10.8	0.0	0.0	24.0	0.0
26-Dec-00	26	-22.5	-30.5	69.0	60.0	4.1	0.0	0.0	24.0	0.0
27-Dec-00	27	-17.5	-24.0	69.0	62.0	9.5	2.6	0.0	24.0	0.0
28-Dec-00	28	-16.5	-18.5	74.0	64.0	6.3	0.8	0.0	24.0	0.0
29-Dec-00	29	-17.5	-20.5	67.0	62.0	7.5	0.2	0.0	24.0	0.0
30-Dec-00	30	-15.5	-18.0	72.0	69.0	7.1	0.0	0.0	24.0	0.0
31-Dec-00	31	-13.0	-22.5	72.0	70.0	10.4	0.0	0.0	24.0	0.0
1-Jan-01	32	-4.5	-19.0	90.0	78.0	11.3	0.0	0.0	24.0	0.0
2-Jan-01	33	-5.5	-10.0	97.0	92.0	4.8	0.0	0.0	24.0	0.0
3-Jan-01	34	-4.0	-8.5	96.0	91.0	4.5	0.8	0.0	24.0	0.0
4-Jan-01	35	3.0	-9.0	91.0	58.0	22.3	0.0	0.0	24.0	0.0
5-Jan-01	36	-11.5	-21.0	78.0	67.0	7.8	7.0	0.0	24.0	0.0
6-Jan-01	37	-12.5	-15.0	85.0	79.0	7.0	0.4	0.0	24.0	0.0
7-Jan-01	38	-12.5	-15.5	84.0	72.0	6.0	0.2	0.0	24.0	0.0
8-Jan-01	39	-6.5	-18.5	87.0	75.0	8.3	0.0	0.0	24.0	0.0
9-Jan-01	40	-1.5	-17.0	91.0	71.0	7.0	0.0	0.0	24.0	0.0
10-Jan-01	41	-5.0	-16.5	95.0	85.0	2.5	0.0	0.0	24.0	0.0
11-Jan-01	42	-6.5	-19.0	94.0	83.0	0.8	0.0	0.0	24.0	0.0
12-Jan-01	43	-7.5	-18.5	98.0	85.0	11.5	0.0	0.0	24.0	0.0
13-Jan-01	44	-16.0	-24.5	73.0	60.0	3.0	0.0	0.0	24.0	0.0
14-Jan-01	45	-13.5	-27.0	74.0	67.0	3.3	0.2	0.0	24.0	0.0
15-Jan-01	46	-13.5	-21.5	90.0	69.0	9.3	0.4	0.0	24.0	0.0
16-Jan-01	47	-6.5	-29.5	86.0	64.0	11.2	0.0	0.0	24.0	0.0

17-Jan-01	48	-3.0	-14.0	90.0	71.0	16.3	0.2	0.0	24.0	0.0
18-Jan-01	49	-8.5	-28.5	73.0	61.0	4.8	0.0	0.0	24.0	0.0
19-Jan-01	50	-4.5	-24.0	94.0	80.0	14.4	0.0	0.0	24.0	0.0
20-Jan-01	51	-4.5	-7.0	94.0	89.0	10.1	0.0	0.0	24.0	0.0
21-Jan-01	52	-7.5	-13.0	94.0	91.0	5.3	0.0	0.0	24.0	0.0
22-Jan-01	53	-2.5	-11.0	92.0	65.0	13.9	0.0	0.0	24.0	0.0
23-Jan-01	54	-7.5	-17.0	77.0	49.0	14.1	0.0	0.0	24.0	0.0
24-Jan-01	55	-4.5	-28.0	74.0	58.0	14.1	0.0	0.0	24.0	0.0
25-Jan-01	56	-3.5	-11.5	87.0	74.0	16.9	0.0	0.0	24.0	0.0
26-Jan-01	57	-4.0	-16.0	83.0	79.0	11.4	0.0	0.0	24.0	0.0
27-Jan-01	58	-9.5	-16.5	90.0	76.0	7.9	0.0	0.0	24.0	0.0
28-Jan-01	59	1.5	-20.0	92.0	57.0	10.1	0.0	0.0	24.0	0.0
29-Jan-01	60	-4.0	-14.0	94.0	85.0	8.1	3.6	0.0	24.0	0.0
30-Jan-01	61	-17.0	-19.0	87.0	67.0	11.8	3.2	0.0	24.0	0.0
31-Jan-01	62	-21.0	-25.5	66.0	56.0	15.9	0.0	0.0	24.0	0.0
1-Feb-01	63	-15.0	-36.0	68.0	61.0	9.5	3.0	0.0	24.0	0.0
2-Feb-01	64	-3.5	-19.5	98.0	76.0	9.4	0.0	0.0	24.0	0.0
3-Feb-01	65	-6.0	-10.0	95.0	87.0	5.3	1.2	0.0	24.0	0.0
4-Feb-01	66	0.0	-9.5	94.0	87.0	10.2	1.8	0.0	24.0	0.0
5-Feb-01	67	-12.0	-15.0	85.0	73.0	12.2	0.0	0.0	24.0	0.0
6-Feb-01	68	-15.5	-23.5	71.0	62.0	5.6	1.4	0.0	24.0	0.0
7-Feb-01	69	-18.0	-26.5	70.0	62.0	2.4	0.6	0.0	24.0	0.0
8-Feb-01	70	-18.5	-33.5	72.0	58.0	4.7	0.0	0.0	24.0	0.0
9-Feb-01	71	-24.0	-35.5	65.0	55.0	5.7	0.0	0.0	24.0	0.0
10-Feb-01	72	-20.5	-39.5	66.0	52.0	4.2	0.0	0.0	24.0	0.0
11-Feb-01	73	-16.5	-33.5	70.0	56.0	2.1	0.0	0.0	24.0	0.0
12-Feb-01	74	-16.0	-29.0	74.0	65.0	1.7	1.4	0.0	24.0	0.0
13-Feb-01	75	-17.0	-28.5	69.0	55.0	6.9	0.0	0.0	24.0	0.0
14-Feb-01	76	-13.0	-29.0	86.0	64.0	10.5	3.2	0.0	24.0	0.0
15-Feb-01	77	-17.5	-20.5	73.0	52.0	21.3	0.0	0.0	24.0	0.0
16-Feb-01	78	-18.5	-27.0	65.0	53.0	14.4	0.0	0.0	24.0	0.0
17-Feb-01	79	-8.0	-21.0	67.0	51.0	17.9	0.0	0.0	24.0	0.0
18-Feb-01	80	-11.0	-16.0	83.0	47.0	13.0	1.2	0.0	24.0	0.0
19-Feb-01	81	-15.0	-22.5	66.0	53.0	19.0	0.8	0.0	24.0	0.0
20-Feb-01	82	-21.0	-31.5	55.0	35.0	14.2	0.0	0.0	24.0	0.0
21-Feb-01	83	-12.0	-32.5	63.0	43.0	7.0	0.0	0.0	24.0	0.0
22-Feb-01	84	-16.5	-19.5	58.0	47.0	15.1	0.2	0.0	24.0	0.0
23-Feb-01	85	-14.0	-31.5	66.0	46.0	6.0	0.4	0.0	24.0	0.0
24-Feb-01	86	-12.5	-19.0	72.0	52.0	10.3	0.0	0.0	24.0	0.0
25-Feb-01	87	-18.0	-25.5	65.0	44.0	12.4	0.0	0.0	24.0	0.0
26-Feb-01	88	-17.5	-28.0	61.0	40.0	14.3	0.0	0.0	24.0	0.0
27-Feb-01	89	-10.0	-29.0	63.0	50.0	10.9	0.0	0.0	24.0	0.0
28-Feb-01	90	0.5	-19.5	79.0	57.0	6.9	0.0	0.0	24.0	0.0
1-Mar-01	91	4.0	-15.5	95.0	73.0	5.9	2.2	0.0	24.0	0.0
2-Mar-01	92	4.5	-8.0	95.0	67.0	9.2	0.0	0.0	24.0	0.0
3-Mar-01	93	-4.0	-12.5	83.0	45.0	12.1	0.0	0.0	24.0	0.0
4-Mar-01	94	-3.0	-21.0	73.0	42.0	5.8	0.0	0.0	24.0	0.0
5-Mar-01	95	0.0	-19.5	82.0	43.0	6.2	0.2	0.0	24.0	0.0
6-Mar-01	96	-1.0	-6.0	90.0	67.0	9.7	0.0	0.0	24.0	0.0
7-Mar-01	97	1.5	-4.0	88.0	57.0	8.0	0.0	0.0	24.0	0.0
8-Mar-01	98	3.5	-15.5	93.0	59.0	8.4	0.0	0.0	24.0	0.0

9-Mar-01	99	2.5	-5.5	84.0	50.0	14.4	0.0	0.0	24.0	0.0
10-Mar-01	100	-8.5	-23.0	68.0	32.0	7.5	0.2	0.0	24.0	0.0
11-Mar-01	101	0.0	-13.0	90.0	83.0	12.1	1.4	0.0	24.0	0.0
12-Mar-01	102	1.0	-6.5	95.0	70.0	4.7	0.8	0.0	24.0	0.0
13-Mar-01	103	5.0	-2.5	96.0	59.0	8.1	0.8	0.0	24.0	0.0
14-Mar-01	104	-1.5	-9.5	75.0	61.0	10.1	4.0	0.0	24.0	0.0
15-Mar-01	105	0.5	-6.0	94.0	77.0	3.9	12.2	0.0	24.0	0.0
16-Mar-01	106	-1.0	-6.5	91.0	81.0	7.8	0.0	0.0	24.0	0.0
17-Mar-01	107	4.0	-7.0	93.0	70.0	6.7	0.0	0.0	24.0	0.0
18-Mar-01	108	3.5	-3.5	92.0	63.0	13.2	0.0	0.0	24.0	0.0
19-Mar-01	109	1.0	-6.0	85.0	71.0	13.2	8.6	0.0	24.0	0.0
20-Mar-01	110	-11.0	-16.5	81.0	47.0	26.2	0.0	0.0	24.0	0.0
21-Mar-01	111	-12.0	-23.5	61.0	40.0	14.2	0.0	0.0	24.0	0.0
22-Mar-01	112	-14.5	-23.0	56.0	37.0	16.5	0.0	0.0	24.0	0.0
23-Mar-01	113	-14.5	-24.0	53.0	47.0	23.2	0.0	0.0	24.0	0.0
24-Mar-01	114	-8.5	-19.0	66.0	46.0	17.3	0.0	0.0	24.0	0.0
25-Mar-01	115	-6.0	-26.0	68.0	28.0	3.1	0.0	0.0	24.0	0.0
26-Mar-01	116	-1.0	-23.0	65.0	40.0	7.5	0.0	0.0	24.0	0.0
27-Mar-01	117	-5.0	-13.5	75.0	62.0	7.9	0.0	0.0	24.0	0.0
28-Mar-01	118	-2.0	-8.0	82.0	62.0	9.4	0.2	0.0	24.0	0.0
29-Mar-01	119	0.0	-6.0	94.0	84.0	8.2	2.0	0.0	24.0	0.0
30-Mar-01	120	5.5	-10.0	96.0	51.0	6.8	0.0	0.0	24.0	0.0
31-Mar-01	121	2.5	-7.5	87.0	54.0	12.6	0.0	0.0	24.0	0.0
1-Apr-01	122	3.5	-6.0	96.0	72.0	8.0	0.0	0.0	24.0	0.0
2-Apr-01	123	5.0	-3.5	95.0	73.0	5.8	0.4	0.0	24.0	0.0
3-Apr-01	124	7.0	-4.0	91.0	51.0	5.2	0.0	0.0	24.0	0.0
4-Apr-01	125	7.5	-8.0	92.0	40.0	6.3	2.0	0.0	24.0	0.0
5-Apr-01	126	4.5	0.0	96.0	69.0	7.6	0.4	0.0	24.0	0.0
6-Apr-01	127	11.5	-3.0	91.0	34.0	3.0	0.0	0.0	24.0	0.0
7-Apr-01	128	12.0	-3.0	85.0	29.0	5.8	0.0	0.0	24.0	0.0
8-Apr-01	129	7.0	-5.0	87.0	41.0	8.1	0.0	0.0	24.0	0.0
9-Apr-01	130	8.0	-6.5	89.0	47.0	6.0	0.0	0.0	24.0	0.0
10-Apr-01	131	8.5	-1.5	88.0	54.0	4.7	0.0	0.0	24.0	0.0
11-Apr-01	132	6.0	0.0	95.0	75.0	6.8	5.0	0.0	24.0	0.0
12-Apr-01	133	-1.0	-5.5	90.0	74.0	12.8	3.2	0.0	24.0	0.0
13-Apr-01	134	-1.0	-6.5	90.0	70.0	8.0	0.8	0.0	24.0	0.0
14-Apr-01	135	-2.5	-13.5	79.0	34.0	16.9	0.0	0.0	24.0	0.0
15-Apr-01	136	-1.0	-12.5	60.0	32.0	18.3	0.0	0.0	24.0	0.0
16-Apr-01	137	6.0	-14.5	80.0	19.0	7.3	0.0	0.0	24.0	0.0
17-Apr-01	138	8.5	-8.5	73.0	25.0	7.9	0.0	0.0	24.0	0.0
18-Apr-01	139	13.0	-1.5	65.0	36.0	7.0	0.0	0.0	24.0	0.1
19-Apr-01	140	12.0	-2.5	86.0	39.0	3.3	0.0	0.0	24.0	1.4
20-Apr-01	141	5.0	-9.5	83.0	62.0	19.1	12.4	0.0	24.0	0.0
21-Apr-01	142	-0.5	-18.0	84.0	42.0	7.9	0.0	0.0	24.0	0.0
22-Apr-01	143	9.5	-12.5	81.0	25.0	10.1	0.0	0.0	24.0	0.0
23-Apr-01	144	11.5	-4.0	84.0	27.0	8.8	0.0	0.0	24.0	1.4
24-Apr-01	145	16.5	-1.0	76.0	31.0	7.2	0.0	0.0	24.0	2.1
25-Apr-01	146	15.0	-3.5	56.0	23.0	18.8	0.0	0.0	24.0	3.8
26-Apr-01	147	13.0	-0.5	80.0	34.0	10.5	0.0	0.0	24.0	2.4
27-Apr-01	148	19.0	0.5	75.0	26.0	8.8	0.0	0.0	24.0	2.5
28-Apr-01	149	20.5	4.5	68.0	43.0	9.0	0.0	0.0	24.0	2.6

29-Apr-01	150	22.0	5.5	91.0	37.0	9.7	0.4	0.0	24.0	2.6
30-Apr-01	151	20.0	-1.0	91.0	28.0	6.2	0.0	0.0	24.0	2.0
1-May-01	152	18.0	-2.0	90.0	30.0	10.1	0.0	0.0	24.0	2.4
2-May-01	153	11.0	0.5	82.0	47.0	19.2	0.0	0.0	24.0	0.7
3-May-01	154	15.5	-3.0	92.0	31.0	6.8	0.0	0.0	24.0	0.5
4-May-01	155	19.5	3.0	76.0	21.0	13.1	0.0	0.0	24.0	0.9
5-May-01	156	19.5	5.5	59.0	32.0	11.2	0.0	0.0	24.0	0.9
6-May-01	157	10.5	7.0	86.0	77.0	6.6	0.0	0.0	24.0	0.5
7-May-01	158	7.0	2.0	88.0	57.0	21.9	6.0	0.0	24.0	0.7
8-May-01	159	12.0	-0.5	67.0	32.0	19.2	0.0	0.0	24.0	0.9
9-May-01	160	9.5	-1.5	71.0	44.0	9.8	0.0	0.0	24.0	0.6
10-May-01	161	12.0	1.5	83.0	40.0	7.4	2.2	0.0	24.0	0.6
11-May-01	162	15.5	-0.5	94.0	32.0	7.0	0.4	0.0	24.0	0.5
12-May-01	163	20.0	0.5	92.0	29.0	5.7	0.0	0.0	24.0	0.5
13-May-01	164	19.5	8.0	69.0	34.0	14.0	5.6	0.0	24.0	1.0
14-May-01	165	21.5	6.5	97.0	33.0	8.7	0.0	0.0	24.0	0.7
15-May-01	166	11.0	8.5	93.0	82.0	10.4	9.8	0.0	24.0	0.5
16-May-01	167	10.5	4.0	91.0	70.0	16.0	6.0	0.0	24.0	0.6
17-May-01	168	19.5	7.5	69.0	24.0	18.8	0.0	0.0	24.0	1.2
18-May-01	169	19.5	4.5	91.0	22.0	9.4	0.0	0.0	24.0	0.8
19-May-01	170	17.5	5.5	69.0	30.0	9.9	6.0	0.0	24.0	0.8
20-May-01	171	8.5	6.0	90.0	84.0	18.3	10.8	0.0	24.0	0.6
21-May-01	172	10.0	3.0	71.0	44.0	20.7	0.0	0.0	24.0	1.0
22-May-01	173	13.0	1.5	75.0	41.0	16.6	0.0	0.0	24.0	0.9
23-May-01	174	18.5	2.0	87.0	36.0	6.9	0.0	0.0	24.0	0.6
24-May-01	175	17.5	4.0	89.0	47.0	7.1	0.0	0.0	24.0	0.6
25-May-01	176	21.0	6.0	97.0	30.0	7.9	0.0	0.0	24.0	0.7
26-May-01	177	20.5	5.0	99.0	38.0	4.0	0.2	0.0	24.0	0.6
27-May-01	178	20.5	12.0	92.0	63.0	14.5	0.0	0.0	24.0	0.8
28-May-01	179	19.0	7.5	79.0	29.0	12.5	0.0	0.0	24.0	1.0
29-May-01	180	20.0	8.5	65.0	35.0	16.8	0.0	0.0	24.0	1.2
30-May-01	181	19.0	10.5	76.0	38.0	17.1	0.8	0.0	24.0	1.1
31-May-01	182	12.5	5.5	87.0	56.0	15.6	0.0	0.0	24.0	0.8
1-Jun-01	183	13.5	6.0	89.0	66.0	13.3	0.0	0.0	24.0	0.7
2-Jun-01	184	18.0	4.0	89.0	24.0	8.7	0.0	0.0	24.0	3.8
3-Jun-01	185	19.5	4.5	74.0	27.0	8.3	0.0	0.0	24.0	4.0
4-Jun-01	186	22.0	5.5	88.0	26.0	5.6	0.0	0.0	24.0	3.5
5-Jun-01	187	23.5	6.0	82.0	23.0	7.7	0.0	0.0	24.0	4.0
6-Jun-01	188	25.0	7.5	88.0	25.0	7.7	0.0	0.0	24.0	4.1
7-Jun-01	189	20.5	12.5	84.0	57.0	5.5	0.6	0.0	24.0	3.5
8-Jun-01	190	22.5	9.5	97.0	51.0	7.5	0.4	0.0	24.0	3.5
9-Jun-01	191	24.5	9.0	94.0	40.0	6.0	0.0	0.0	24.0	3.5
10-Jun-01	192	16.0	12.0	92.0	78.0	11.3	19.8	0.0	24.0	3.4
11-Jun-01	193	11.5	9.0	94.0	84.0	14.0	8.0	0.0	24.0	3.1
12-Jun-01	194	18.5	3.5	96.0	43.0	8.3	0.0	0.0	24.0	3.3
13-Jun-01	195	22.0	6.5	94.0	28.0	7.1	0.0	0.0	24.0	3.7
14-Jun-01	196	21.0	9.5	93.0	47.0	6.5	1.8	0.0	24.0	3.5
15-Jun-01	197	13.0	9.5	80.0	49.0	22.8	0.0	0.0	24.0	5.7
16-Jun-01	198	14.5	5.0	69.0	39.0	15.1	0.0	0.0	24.0	4.9
17-Jun-01	199	16.5	3.5	82.0	35.0	4.4	0.0	0.0	24.0	3.0
18-Jun-01	200	18.5	4.5	74.0	44.0	11.5	1.0	0.0	24.0	4.2

19-Jun-01	201	17.5	7.0	85.0	36.0	10.0	0.0	0.0	24.0	4.1
20-Jun-01	202	22.5	4.5	91.0	34.0	6.4	0.0	0.0	24.0	3.5
21-Jun-01	203	28.0	11.5	75.0	27.0	15.7	0.0	0.0	24.0	6.5
22-Jun-01	204	26.0	14.5	79.0	42.0	11.0	0.4	0.0	24.0	5.1
23-Jun-01	205	22.0	14.5	71.0	52.0	11.8	1.2	0.0	24.0	5.1
24-Jun-01	206	15.5	10.0	85.0	59.0	11.5	2.4	0.0	24.0	4.0
25-Jun-01	207	18.5	10.5	93.0	79.0	5.0	28.0	0.0	24.0	2.9
26-Jun-01	208	15.5	9.0	89.0	58.0	17.4	0.0	0.0	24.0	4.4
27-Jun-01	209	21.0	11.0	84.0	38.0	9.6	0.0	0.0	24.0	4.4
28-Jun-01	210	22.0	11.0	91.0	46.0	12.0	6.0	0.0	24.0	4.4
29-Jun-01	211	14.0	8.5	96.0	77.0	19.7	4.4	0.0	24.0	3.5
30-Jun-01	212	16.5	5.0	93.0	38.0	13.2	0.6	0.0	24.0	4.1
1-Jul-01	213	18.0	5.0	89.0	39.0	11.5	0.0	0.0	24.0	4.0
2-Jul-01	214	22.0	10.0	86.0	46.0	13.7	1.6	0.0	24.0	4.5
3-Jul-01	215	18.5	7.5	95.0	33.0	18.0	0.0	0.0	24.0	5.0
4-Jul-01	216	22.0	9.0	76.0	37.0	8.8	0.0	0.0	24.0	4.1
5-Jul-01	217	23.5	13.5	78.0	45.0	17.5	3.0	0.0	24.0	5.7
6-Jul-01	218	26.5	14.5	83.0	30.0	21.1	0.0	0.0	24.0	7.2
7-Jul-01	219	26.0	15.5	59.0	35.0	20.6	0.0	0.0	24.0	7.9
8-Jul-01	220	26.5	14.5	76.0	25.0	16.9	0.0	0.0	24.0	6.8
9-Jul-01	221	23.0	14.5	60.0	42.0	18.8	0.0	0.0	24.0	6.8
10-Jul-01	222	25.5	10.0	94.0	34.0	4.3	0.0	0.0	24.0	3.2
11-Jul-01	223	26.5	12.5	83.0	39.0	9.2	0.0	0.0	24.0	4.3
12-Jul-01	224	26.5	16.5	76.0	39.0	12.8	6.0	0.0	24.0	5.4
13-Jul-01	225	26.5	14.0	94.0	34.0	8.6	0.0	0.0	24.0	4.2
14-Jul-01	226	24.5	15.0	91.0	60.0	10.6	4.6	0.0	24.0	3.9
15-Jul-01	227	26.5	16.0	91.0	60.0	8.6	2.0	0.0	24.0	3.7
16-Jul-01	228	29.5	17.0	93.0	51.0	7.0	0.0	0.0	24.0	3.8
17-Jul-01	229	24.5	19.0	90.0	73.0	6.5	2.6	0.0	24.0	3.5
18-Jul-01	230	26.5	17.5	93.0	58.0	9.3	22.0	0.0	24.0	3.9
19-Jul-01	231	29.5	16.5	100.0	25.0	10.7	0.2	0.0	24.0	4.7
20-Jul-01	232	29.5	17.0	80.0	33.0	11.5	0.0	0.0	24.0	5.2
21-Jul-01	233	30.0	16.0	91.0	33.0	13.5	0.6	0.0	24.0	5.2
22-Jul-01	234	19.5	15.5	93.0	71.0	17.2	0.8	0.0	24.0	4.0
23-Jul-01	235	22.5	12.0	83.0	46.0	16.9	0.0	0.0	24.0	5.0
24-Jul-01	236	24.0	12.0	91.0	45.0	7.1	0.0	0.0	24.0	3.4
25-Jul-01	237	21.0	13.5	77.0	47.0	15.3	0.4	0.0	24.0	4.9
26-Jul-01	238	17.0	12.0	97.0	78.0	13.3	19.4	0.0	24.0	3.0
27-Jul-01	239	23.5	14.5	97.0	52.0	9.9	0.0	0.0	24.0	3.6
28-Jul-01	240	26.0	12.5	98.0	58.0	5.5	0.0	0.0	24.0	2.9
29-Jul-01	241	25.0	17.0	96.0	41.0	14.8	35.8	0.0	24.0	4.7
30-Jul-01	242	22.0	15.5	88.0	62.0	24.3	1.6	0.0	24.0	5.1
31-Jul-01	243	27.0	15.0	87.0	40.0	9.1	0.0	0.0	24.0	4.0
1-Aug-01	244	26.5	16.5	87.0	39.0	6.2	0.0	0.0	24.0	3.6
2-Aug-01	245	28.5	14.0	96.0	39.0	9.3	0.0	0.0	24.0	3.5
3-Aug-01	246	32.0	16.5	89.0	29.0	8.1	0.0	0.0	24.0	3.8
4-Aug-01	247	29.5	20.0	87.0	55.0	8.0	1.0	0.0	24.0	3.5
5-Aug-01	248	27.5	19.5	90.0	45.0	9.8	0.6	0.0	24.0	3.8
6-Aug-01	249	29.0	13.5	84.0	35.0	6.9	0.0	0.0	24.0	3.3
7-Aug-01	250	26.5	16.0	76.0	37.0	9.4	0.6	0.0	24.0	3.9
8-Aug-01	251	22.0	14.5	90.0	58.0	15.2	2.0	0.0	24.0	3.7

9-Aug-01	252	19.5	10.0	82.0	44.0	15.6	0.0	0.0	24.0	3.9
10-Aug-01	253	24.0	13.0	88.0	47.0	13.8	0.6	0.0	24.0	3.8
11-Aug-01	254	17.0	11.0	74.0	41.0	15.8	0.0	0.0	24.0	4.2
12-Aug-01	255	21.5	9.5	86.0	36.0	10.6	0.0	0.0	24.0	3.3
13-Aug-01	256	26.0	8.5	94.0	30.0	9.2	2.0	0.0	24.0	3.0
14-Aug-01	257	22.0	14.0	97.0	61.0	7.1	10.8	0.0	24.0	2.5
15-Aug-01	258	21.5	13.0	97.0	49.0	8.5	0.0	0.0	24.0	2.7
16-Aug-01	259	27.0	12.0	87.0	48.0	10.2	0.4	0.0	24.0	3.1
17-Aug-01	260	21.0	12.0	88.0	50.0	9.9	0.0	0.0	24.0	2.9
18-Aug-01	261	23.0	12.0	91.0	47.0	12.0	0.0	0.0	24.0	3.1
19-Aug-01	262	25.0	13.0	95.0	45.0	12.2	0.0	0.0	24.0	3.2
20-Aug-01	263	24.5	15.5	75.0	33.0	12.4	26.8	0.0	24.0	4.1
21-Aug-01	264	23.0	14.0	97.0	39.0	10.1	0.0	0.0	24.0	3.0
22-Aug-01	265	22.0	10.0	92.0	48.0	8.1	0.0	0.0	24.0	2.5
23-Aug-01	266	23.0	15.0	85.0	64.0	16.7	6.4	0.0	24.0	3.4
24-Aug-01	267	26.5	17.0	96.0	39.0	10.7	0.0	0.0	24.0	3.3
25-Aug-01	268	23.5	12.5	73.0	30.0	17.4	0.0	0.0	24.0	4.8
26-Aug-01	269	23.0	14.0	65.0	34.0	14.5	0.0	0.0	24.0	4.5
27-Aug-01	270	23.5	10.5	80.0	38.0	6.4	0.0	0.0	24.0	2.5
28-Aug-01	271	23.5	13.5	85.0	58.0	7.0	1.2	0.0	24.0	2.4
29-Aug-01	272	17.5	14.0	97.0	87.0	12.9	29.8	0.0	24.0	2.1
30-Aug-01	273	17.5	8.0	98.0	65.0	9.9	1.0	0.0	24.0	1.9
31-Aug-01	274	20.0	8.5	100.0	47.0	9.1	0.0	0.0	24.0	2.1
1-Sep-01	275	22.5	13.5	88.0	58.0	12.4	0.8	0.0	24.0	2.7
2-Sep-01	276	16.0	13.0	97.0	87.0	12.6	45.2	0.0	24.0	1.8
3-Sep-01	277	21.0	11.0	88.0	49.0	9.4	0.0	0.0	24.0	2.2
4-Sep-01	278	22.0	11.5	95.0	31.0	11.3	0.0	0.0	24.0	2.5
5-Sep-01	279	19.0	10.0	91.0	52.0	10.0	0.8	0.0	24.0	2.0
6-Sep-01	280	20.5	9.5	92.0	33.0	10.1	0.0	0.0	24.0	2.3
7-Sep-01	281	18.0	10.0	79.0	52.0	6.0	0.0	0.0	24.0	1.8
8-Sep-01	282	16.5	10.5	89.0	63.0	10.8	11.6	0.0	24.0	2.0
9-Sep-01	283	15.0	10.0	97.0	61.0	9.6	0.0	0.0	24.0	1.7
10-Sep-01	284	12.5	8.0	100.0	83.0	8.5	8.2	0.0	24.0	1.3
11-Sep-01	285	9.5	6.0	94.0	67.0	8.6	0.0	0.0	24.0	1.5
12-Sep-01	286	12.5	5.0	91.0	52.0	5.9	0.0	0.0	24.0	1.4
13-Sep-01	287	15.0	2.5	100.0	46.0	7.0	0.0	0.0	24.0	1.3
14-Sep-01	288	20.5	9.0	78.0	45.0	15.8	0.0	0.0	24.0	2.7
15-Sep-01	289	24.0	10.0	92.0	44.0	10.3	0.0	0.0	24.0	2.0
16-Sep-01	290	16.5	11.0	87.0	60.0	14.0	0.0	0.0	24.0	2.1
17-Sep-01	291	15.5	3.0	98.0	41.0	8.5	0.0	0.0	24.0	1.4
18-Sep-01	292	19.0	7.0	88.0	52.0	8.7	0.0	0.0	24.0	1.5
19-Sep-01	293	16.5	11.5	97.0	78.0	12.4	19.2	0.0	24.0	1.5
20-Sep-01	294	14.5	9.5	97.0	94.0	10.6	14.4	0.0	24.0	1.1
21-Sep-01	295	10.5	6.5	94.0	57.0	15.2	0.0	0.0	24.0	1.7
22-Sep-01	296	8.0	-0.5	81.0	43.0	9.4	0.0	0.0	24.0	1.4
23-Sep-01	297	12.0	0.0	83.0	43.0	17.2	0.0	0.0	24.0	2.0
24-Sep-01	298	18.0	7.0	74.0	49.0	13.8	0.0	0.0	24.0	2.2
25-Sep-01	299	21.5	6.5	93.0	46.0	6.0	0.0	0.0	24.0	1.2
26-Sep-01	300	21.0	8.5	97.0	48.0	11.7	0.0	0.0	24.0	1.6
27-Sep-01	301	21.5	11.5	76.0	49.0	11.8	0.0	0.0	24.0	2.1
28-Sep-01	302	19.5	8.5	98.0	60.0	6.5	0.0	0.0	24.0	1.1

29-Sep-01	303	15.5	10.0	87.0	53.0	12.6	0.0	0.0	24.0	1.8
30-Sep-01	304	19.5	4.0	98.0	20.0	13.8	0.0	0.0	24.0	1.9
1-Oct-01	305	15.5	8.0	58.0	39.0	11.8	0.0	0.0	24.0	2.4
2-Oct-01	306	14.5	6.0	79.0	44.0	5.5	0.2	0.0	24.0	1.5
3-Oct-01	307	8.0	4.5	95.0	70.0	16.2	12.2	0.0	24.0	1.6
4-Oct-01	308	2.0	-0.5	82.0	65.0	21.1	0.8	0.0	24.0	1.7
5-Oct-01	309	3.5	-1.5	85.0	45.0	9.1	0.6	0.0	24.0	0.6
6-Oct-01	310	7.0	-3.0	94.0	54.0	9.6	0.0	0.0	24.0	0.5
7-Oct-01	311	12.0	2.5	85.0	47.0	11.4	0.0	0.0	24.0	1.6
8-Oct-01	312	16.5	5.5	82.0	45.0	6.2	0.0	0.0	24.0	1.3
9-Oct-01	313	16.5	5.0	81.0	42.0	6.1	0.4	0.0	24.0	1.3
10-Oct-01	314	12.5	4.5	89.0	47.0	6.0	0.4	0.0	24.0	1.1
11-Oct-01	315	13.0	1.5	86.0	46.0	7.0	0.0	0.0	24.0	1.1
12-Oct-01	316	8.5	4.0	94.0	71.0	10.0	0.0	0.0	24.0	1.1
13-Oct-01	317	12.5	0.0	99.0	42.0	1.6	0.0	0.0	24.0	0.5
14-Oct-01	318	7.5	4.5	90.0	59.0	11.5	0.6	0.0	24.0	1.4
15-Oct-01	319	6.0	0.5	82.0	46.0	17.3	0.0	0.0	24.0	1.8
16-Oct-01	320	6.5	-2.5	92.0	50.0	10.6	0.0	0.0	24.0	1.0
17-Oct-01	321	8.0	3.5	78.0	58.0	21.7	2.4	0.0	24.0	2.4
18-Oct-01	322	6.0	0.0	65.0	41.0	20.5	0.0	0.0	24.0	2.7
19-Oct-01	323	1.5	-1.0	77.0	60.0	17.3	0.0	0.0	24.0	1.7
20-Oct-01	324	1.0	-2.5	84.0	64.0	16.6	0.2	0.0	24.0	0.7
21-Oct-01	325	1.0	-3.0	75.0	46.0	11.9	0.0	0.0	24.0	0.8
22-Oct-01	326	-0.5	-7.0	86.0	46.0	8.2	0.0	0.0	24.0	0.7
23-Oct-01	327	-3.0	-7.5	84.0	67.0	13.1	0.2	0.0	24.0	0.1
24-Oct-01	328	-0.5	-4.0	91.0	77.0	13.7	0.0	0.0	24.0	0.0
25-Oct-01	329	1.0	-4.0	90.0	56.0	8.3	0.0	0.0	24.0	0.2
26-Oct-01	330	2.0	-8.0	92.0	50.0	8.4	0.0	0.0	24.0	0.6
27-Oct-01	331	4.0	-0.5	71.0	59.0	14.6	0.4	0.0	24.0	1.0
28-Oct-01	332	3.5	0.5	79.0	43.0	15.2	0.0	0.0	24.0	1.6
29-Oct-01	333	7.0	-7.0	77.0	43.0	7.2	0.4	0.0	24.0	0.3
30-Oct-01	334	7.5	0.0	86.0	51.0	11.5	0.0	0.0	24.0	0.8
31-Oct-01	335	3.0	-4.0	93.0	78.0	4.3	13.2	0.0	24.0	0.0
1-Nov-01	336	1.5	0.0	94.0	91.0	7.7	10.0	0.0	24.0	0.0
2-Nov-01	337	4.0	-1.5	91.0	82.0	7.2	0.0	0.0	24.0	0.0
3-Nov-01	338	7.5	-0.5	77.0	46.0	11.8	0.0	0.0	24.0	0.0
4-Nov-01	339	6.5	-4.0	87.0	53.0	7.4	0.0	0.0	24.0	0.0
5-Nov-01	340	8.5	-2.5	85.0	55.0	10.0	0.0	0.0	24.0	0.0
6-Nov-01	341	2.0	-3.5	76.0	51.0	5.8	0.0	0.0	24.0	0.0
7-Nov-01	342	4.0	-4.5	85.0	55.0	8.3	0.0	0.0	24.0	0.0
8-Nov-01	343	5.0	-1.5	89.0	59.0	10.6	0.0	0.0	24.0	0.0
9-Nov-01	344	0.5	-1.5	93.0	81.0	4.5	4.2	0.0	24.0	0.0
10-Nov-01	345	2.5	-0.5	94.0	88.0	9.6	0.0	0.0	24.0	0.0
11-Nov-01	346	1.0	-3.0	76.0	69.0	11.5	0.0	0.0	24.0	0.0
12-Nov-01	347	0.5	-1.5	93.0	88.0	11.3	0.0	0.0	24.0	0.0
13-Nov-01	348	0.5	-1.5	94.0	89.0	9.5	0.0	0.0	24.0	0.0
14-Nov-01	349	0.0	-2.5	97.0	94.0	6.3	0.2	0.0	24.0	0.0
15-Nov-01	350	-0.5	-3.5	94.0	84.0	11.0	0.0	0.0	24.0	0.0
16-Nov-01	351	3.5	-5.0	94.0	86.0	13.9	0.0	0.0	24.0	0.0
17-Nov-01	352	2.0	0.0	99.0	85.0	8.0	0.0	0.0	24.0	0.0
18-Nov-01	353	-0.5	-1.0	74.0	54.0	14.0	0.0	0.0	24.0	0.0

19-Nov-01	354	0.5	-8.5	89.0	68.0	8.1	0.0	0.0	24.0	0.0
20-Nov-01	355	-2.0	-4.0	84.0	73.0	12.3	0.0	0.0	24.0	0.0
21-Nov-01	356	-5.5	-6.5	91.0	80.0	12.8	0.0	0.0	24.0	0.0
22-Nov-01	357	-4.5	-6.5	93.0	90.0	7.4	0.8	0.0	24.0	0.0
23-Nov-01	358	-1.5	-5.5	96.0	90.0	0.6	0.2	0.0	24.0	0.0
24-Nov-01	359	-1.5	-11.5	94.0	79.0	15.3	2.0	0.0	24.0	0.0
25-Nov-01	360	-13.0	-15.5	82.0	76.0	20.2	0.2	0.0	24.0	0.0
26-Nov-01	361	-13.5	-23.0	72.0	66.0	10.5	0.6	0.0	24.0	0.0
27-Nov-01	362	-12.0	-15.5	75.0	67.0	9.3	0.6	0.0	24.0	0.0
28-Nov-01	363	-9.5	-13.5	83.0	69.0	11.1	1.0	0.0	24.0	0.0
29-Nov-01	364	-8.5	-11.0	86.0	83.0	8.7	0.6	0.0	24.0	0.0
30-Nov-01	365	-8.0	-10.0	87.0	81.0	10.3	0.4	0.0	24.0	0.0

Table B-5. Flin Flon climate 2001-02.

Date	Day	Temp (°C)		RH (%)		Wind	Precip	Precip Period		P.E.
		Max	Min	Max	Min	(m/s)	(mm)	Start	End	(mm/day)
1-Dec-01	1	-11.5	-17.0	83.0	65.0	4.6	2.1	0.0	24.0	0.0
2-Dec-01	2	-7.5	-19.5	89.0	79.0	9.9	3.2	0.0	24.0	0.0
3-Dec-01	3	-6.0	-9.0	88.0	82.0	4.3	1.8	0.0	24.0	0.0
4-Dec-01	4	-9.5	-17.0	79.0	67.0	11.6	0.0	0.0	24.0	0.0
5-Dec-01	5	-13.5	-25.5	75.0	65.0	2.8	0.0	0.0	24.0	0.0
6-Dec-01	6	-11.0	-21.5	78.0	70.0	4.7	0.0	0.0	24.0	0.0
7-Dec-01	7	-9.5	-18.0	82.0	64.0	14.2	0.2	0.0	24.0	0.0
8-Dec-01	8	-3.0	-21.0	81.0	69.0	13.6	0.0	0.0	24.0	0.0
9-Dec-01	9	-1.0	-10.5	90.0	68.0	12.2	0.2	0.0	24.0	0.0
10-Dec-01	10	-19.5	-21.5	64.0	58.0	12.0	0.2	0.0	24.0	0.0
11-Dec-01	11	-20.0	-28.0	64.0	59.0	6.8	2.6	0.0	24.0	0.0
12-Dec-01	12	-17.5	-22.0	69.0	58.0	4.7	0.0	0.0	24.0	0.0
13-Dec-01	13	-11.5	-23.0	74.0	68.0	7.9	0.0	0.0	24.0	0.0
14-Dec-01	14	-3.0	-14.0	84.0	79.0	15.8	0.6	0.0	24.0	0.0
15-Dec-01	15	-2.0	-7.5	85.0	70.0	16.5	0.0	0.0	24.0	0.0
16-Dec-01	16	-3.5	-17.5	91.0	59.0	6.3	0.2	0.0	24.0	0.0
17-Dec-01	17	-3.0	-7.0	90.0	79.0	7.4	0.0	0.0	24.0	0.0
18-Dec-01	18	-9.5	-16.0	70.0	51.0	10.0	0.0	0.0	24.0	0.0
19-Dec-01	19	-11.5	-22.5	69.0	53.0	4.6	0.0	0.0	24.0	0.0
20-Dec-01	20	-13.5	-26.0	74.0	62.0	4.4	0.2	0.0	24.0	0.0
21-Dec-01	21	-13.0	-18.5	76.0	69.0	2.9	0.2	0.0	24.0	0.0
22-Dec-01	22	-10.0	-26.0	79.0	64.0	4.1	0.0	0.0	24.0	0.0
23-Dec-01	23	-9.5	-19.0	81.0	77.0	9.6	0.2	0.0	24.0	0.0
24-Dec-01	24	-11.0	-22.5	75.0	62.0	1.0	0.0	0.0	24.0	0.0
25-Dec-01	25	-8.0	-24.0	76.0	69.0	3.3	0.0	0.0	24.0	0.0
26-Dec-01	26	-4.0	-15.0	86.0	80.0	18.5	0.0	0.0	24.0	0.0
27-Dec-01	27	-12.5	-14.5	72.0	66.0	21.8	0.2	0.0	24.0	0.0
28-Dec-01	28	-8.5	-17.0	75.0	69.0	21.2	0.4	0.0	24.0	0.0
29-Dec-01	29	-15.5	-21.5	72.0	61.0	13.2	0.0	0.0	24.0	0.0
30-Dec-01	30	-15.0	-20.5	70.0	59.0	7.6	0.0	0.0	24.0	0.0
31-Dec-01	31	-13.0	-18.5	75.0	66.0	11.7	0.0	0.0	24.0	0.0
1-Jan-02	32	-13.5	-16.5	78.0	69.0	10.5	0.0	0.0	24.0	0.0
2-Jan-02	33	-16.0	-24.0	69.0	62.0	3.1	0.0	0.0	24.0	0.0
3-Jan-02	34	-9.0	-21.5	71.0	66.0	3.6	0.0	0.0	24.0	0.0
4-Jan-02	35	-6.0	-16.0	83.0	72.0	10.0	0.0	0.0	24.0	0.0
5-Jan-02	36	-14.0	-16.5	72.0	59.0	14.4	0.0	0.0	24.0	0.0
6-Jan-02	37	-3.5	-22.0	80.0	70.0	10.7	0.0	0.0	24.0	0.0
7-Jan-02	38	1.5	-11.5	87.0	71.0	5.8	0.0	0.0	24.0	0.0
8-Jan-02	39	5.0	-8.0	81.0	69.0	9.0	0.4	0.0	24.0	0.0
9-Jan-02	40	1.0	-2.0	89.0	72.0	14.5	0.0	0.0	24.0	0.0
10-Jan-02	41	-2.0	-7.5	84.0	71.0	6.4	0.0	0.0	24.0	0.0
11-Jan-02	42	3.0	-10.5	78.0	53.0	14.1	0.0	0.0	24.0	0.0
12-Jan-02	43	-4.5	-8.5	72.0	61.0	9.6	0.0	0.0	24.0	0.0
13-Jan-02	44	-6.5	-9.0	84.0	80.0	7.5	4.4	0.0	24.0	0.0
14-Jan-02	45	-12.0	-14.5	75.0	70.0	12.5	0.4	0.0	24.0	0.0
15-Jan-02	46	-10.5	-14.0	78.0	71.0	6.7	0.2	0.0	24.0	0.0
16-Jan-02	47	-13.0	-21.5	76.0	65.0	10.1	0.2	0.0	24.0	0.0

17-Jan-02	48	-22.5	-29.0	59.0	54.0	8.0	0.0	0.0	24.0	0.0
18-Jan-02	49	-16.5	-29.0	68.0	60.0	8.8	0.4	0.0	24.0	0.0
19-Jan-02	50	-24.5	-33.5	62.0	53.0	5.5	0.0	0.0	24.0	0.0
20-Jan-02	51	-30.5	-36.5	59.0	52.0	8.3	0.0	0.0	24.0	0.0
21-Jan-02	52	-28.5	-38.5	58.0	52.0	8.0	0.4	0.0	24.0	0.0
22-Jan-02	53	-26.0	-32.0	56.0	54.0	9.0	1.2	0.0	24.0	0.0
23-Jan-02	54	-27.0	-39.0	60.0	54.0	2.9	0.0	0.0	24.0	0.0
24-Jan-02	55	-24.0	-37.5	59.0	51.0	2.2	0.0	0.0	24.0	0.0
25-Jan-02	56	-23.5	-35.5	60.0	49.0	8.8	0.0	0.0	24.0	0.0
26-Jan-02	57	-24.0	-33.0	59.0	50.0	6.9	0.0	0.0	24.0	0.0
27-Jan-02	58	-27.0	-35.5	59.0	48.0	5.2	0.0	0.0	24.0	0.0
28-Jan-02	59	-26.0	-41.5	65.0	48.0	2.1	0.0	0.0	24.0	0.0
29-Jan-02	60	-21.0	-37.5	59.0	48.0	1.8	0.0	0.0	24.0	0.0
30-Jan-02	61	-21.5	-36.5	59.0	52.0	1.7	0.0	0.0	24.0	0.0
31-Jan-02	62	-19.0	-33.0	60.0	54.0	3.2	0.0	0.0	24.0	0.0
1-Feb-02	63	-16.0	-32.5	83.0	54.0	4.3	1.6	0.0	24.0	0.0
2-Feb-02	64	-16.5	-23.5	63.0	53.0	8.5	0.0	0.0	24.0	0.0
3-Feb-02	65	-11.5	-32.0	64.0	55.0	7.2	0.2	0.0	24.0	0.0
4-Feb-02	66	-6.0	-16.5	74.0	52.0	15.1	0.4	0.0	24.0	0.0
5-Feb-02	67	-10.0	-18.5	68.0	59.0	9.1	5.4	0.0	24.0	0.0
6-Feb-02	68	-16.5	-20.0	69.0	61.0	9.0	4.2	0.0	24.0	0.0
7-Feb-02	69	-15.5	-28.0	65.0	60.0	1.3	0.0	0.0	24.0	0.0
8-Feb-02	70	-9.5	-23.0	75.0	64.0	4.3	5.4	0.0	24.0	0.0
9-Feb-02	71	-6.5	-21.0	73.0	66.0	9.5	0.0	0.0	24.0	0.0
10-Feb-02	72	-10.5	-27.5	72.0	59.0	9.9	6.0	0.0	24.0	0.0
11-Feb-02	73	-6.5	-12.5	74.0	60.0	16.0	0.6	0.0	24.0	0.0
12-Feb-02	74	-10.0	-25.5	68.0	57.0	6.1	0.4	0.0	24.0	0.0
13-Feb-02	75	0.5	-19.5	84.0	72.0	6.5	1.4	0.0	24.0	0.0
14-Feb-02	76	-4.0	-9.0	83.0	73.0	8.7	1.0	0.0	24.0	0.0
15-Feb-02	77	0.0	-12.0	84.0	72.0	8.0	3.4	0.0	24.0	0.0
16-Feb-02	78	-3.5	-9.5	91.0	73.0	8.0	0.0	0.0	24.0	0.0
17-Feb-02	79	6.5	-11.5	95.0	56.0	13.0	0.0	0.0	24.0	0.0
18-Feb-02	80	-6.5	-12.0	67.0	39.0	12.4	0.0	0.0	24.0	0.0
19-Feb-02	81	-8.0	-22.5	74.0	53.0	7.0	0.0	0.0	24.0	0.0
20-Feb-02	82	-2.0	-14.5	69.0	52.0	8.0	0.0	0.0	24.0	0.0
21-Feb-02	83	2.5	-11.5	86.0	32.0	13.4	0.0	0.0	24.0	0.0
22-Feb-02	84	1.5	-10.5	81.0	38.0	3.6	0.0	0.0	24.0	0.0
23-Feb-02	85	-12.5	-16.5	81.0	61.0	20.0	0.2	0.0	24.0	0.0
24-Feb-02	86	-13.0	-19.0	69.0	62.0	10.5	1.4	0.0	24.0	0.0
25-Feb-02	87	-11.0	-20.0	71.0	35.0	11.5	0.0	0.0	24.0	0.0
26-Feb-02	88	-8.5	-27.5	71.0	47.0	10.1	0.4	0.0	24.0	0.0
27-Feb-02	89	-13.0	-20.0	78.0	36.0	14.0	0.0	0.0	24.0	0.0
28-Feb-02	90	-16.0	-28.5	60.0	28.0	13.8	0.0	0.0	24.0	0.0
1-Mar-02	91	-19.0	-24.5	53.0	44.0	14.8	0.2	0.0	24.0	0.0
2-Mar-02	92	-16.5	-39.0	67.0	36.0	6.8	0.0	0.0	24.0	0.0
3-Mar-02	93	-10.5	-30.0	89.0	46.0	10.0	2.2	0.0	24.0	0.0
4-Mar-02	94	-12.0	-17.0	80.0	45.0	17.0	0.0	0.0	24.0	0.0
5-Mar-02	95	-18.0	-29.5	63.0	39.0	13.5	0.0	0.0	24.0	0.0
6-Mar-02	96	-19.0	-28.5	57.0	39.0	12.3	0.0	0.0	24.0	0.0
7-Mar-02	97	-15.5	-37.5	64.0	31.0	2.6	0.0	0.0	24.0	0.0
8-Mar-02	98	-12.0	-29.5	63.0	40.0	3.4	0.0	0.0	24.0	0.0

9-Mar-02	99	-9.5	-32.0	64.0	32.0	7.9	0.0	0.0	24.0	0.0
10-Mar-02	100	-10.5	-30.0	66.0	36.0	2.2	0.2	0.0	24.0	0.0
11-Mar-02	101	-10.5	-27.0	70.0	37.0	3.4	0.0	0.0	24.0	0.0
12-Mar-02	102	-8.0	-18.5	72.0	49.0	9.1	0.4	0.0	24.0	0.0
13-Mar-02	103	-10.5	-24.5	74.0	41.0	6.7	0.0	0.0	24.0	0.0
14-Mar-02	104	-8.5	-31.0	67.0	32.0	4.5	0.0	0.0	24.0	0.0
15-Mar-02	105	-7.5	-27.0	83.0	65.0	4.4	2.0	0.0	24.0	0.0
16-Mar-02	106	-9.0	-23.0	77.0	50.0	4.0	0.2	0.0	24.0	0.0
17-Mar-02	107	-11.5	-28.5	71.0	42.0	7.0	0.0	0.0	24.0	0.0
18-Mar-02	108	-12.5	-24.0	62.0	39.0	6.8	0.0	0.0	24.0	0.0
19-Mar-02	109	-13.0	-32.5	66.0	39.0	5.5	0.0	0.0	24.0	0.0
20-Mar-02	110	-13.5	-33.5	64.0	36.0	11.8	0.0	0.0	24.0	0.0
21-Mar-02	111	-4.0	-18.5	50.0	28.0	17.2	0.0	0.0	24.0	0.0
22-Mar-02	112	-0.5	-12.0	69.0	48.0	17.3	0.0	0.0	24.0	0.0
23-Mar-02	113	-7.5	-14.5	71.0	34.0	15.0	0.0	0.0	24.0	0.0
24-Mar-02	114	-8.5	-26.5	68.0	31.0	8.7	0.0	0.0	24.0	0.0
25-Mar-02	115	-2.5	-18.5	57.0	49.0	12.5	0.0	0.0	24.0	0.0
26-Mar-02	116	-3.0	-8.5	76.0	70.0	7.5	0.0	0.0	24.0	0.0
27-Mar-02	117	1.5	-9.0	93.0	62.0	9.3	0.4	0.0	24.0	0.0
28-Mar-02	118	0.5	-3.5	94.0	71.0	10.9	0.0	0.0	24.0	0.0
29-Mar-02	119	-3.5	-7.5	83.0	71.0	24.7	3.8	0.0	24.0	0.0
30-Mar-02	120	-11.5	-17.0	75.0	58.0	23.4	2.2	0.0	24.0	0.0
31-Mar-02	121	-4.0	-16.0	86.0	47.0	10.8	0.0	0.0	24.0	0.0
1-Apr-02	122	-6.0	-18.5	86.0	62.0	11.4	0.2	0.0	24.0	0.0
2-Apr-02	123	-4.5	-16.0	80.0	45.0	15.5	0.0	0.0	24.0	0.0
3-Apr-02	124	-4.0	-20.5	77.0	37.0	4.5	0.2	0.0	24.0	0.0
4-Apr-02	125	-3.5	-13.0	88.0	56.0	3.8	0.0	0.0	24.0	0.0
5-Apr-02	126	-3.5	-19.0	88.0	26.0	6.4	0.0	0.0	24.0	0.0
6-Apr-02	127	-7.0	-13.0	85.0	45.0	14.1	4.6	0.0	24.0	0.0
7-Apr-02	128	-1.5	-18.0	90.0	36.0	5.4	0.0	0.0	24.0	0.0
8-Apr-02	129	-0.5	-17.5	84.0	41.0	5.4	0.2	0.0	24.0	0.0
9-Apr-02	130	-1.0	-17.0	94.0	24.0	8.5	0.0	0.0	24.0	0.0
10-Apr-02	131	2.0	-22.5	70.0	47.0	9.7	0.0	0.0	24.0	0.0
11-Apr-02	132	10.0	0.0	88.0	53.0	15.5	0.0	0.0	24.0	0.0
12-Apr-02	133	10.0	0.0	74.0	32.0	9.0	0.0	0.0	24.0	0.0
13-Apr-02	134	12.0	-0.5	77.0	47.0	9.0	0.0	0.0	24.0	0.0
14-Apr-02	135	6.0	-2.0	89.0	61.0	13.3	7.8	0.0	24.0	0.0
15-Apr-02	136	-2.0	-5.5	91.0	87.0	16.0	0.2	0.0	24.0	0.0
16-Apr-02	137	-2.0	-7.0	93.0	81.0	9.9	7.2	0.0	24.0	0.0
17-Apr-02	138	-1.5	-5.0	90.0	76.0	17.7	3.4	0.0	24.0	0.0
18-Apr-02	139	-1.5	-7.0	85.0	56.0	14.2	0.0	0.0	24.0	0.0
19-Apr-02	140	1.5	-10.0	90.0	46.0	4.6	0.0	0.0	24.0	0.0
20-Apr-02	141	6.0	-13.5	88.0	42.0	8.0	0.0	0.0	24.0	0.0
21-Apr-02	142	10.0	-5.0	85.0	41.0	11.2	0.0	0.0	24.0	0.2
22-Apr-02	143	12.5	-0.5	86.0	40.0	10.2	1.8	0.0	24.0	1.7
23-Apr-02	144	1.5	-5.5	97.0	86.0	16.3	14.4	0.0	24.0	0.0
24-Apr-02	145	-8.0	-11.5	83.0	72.0	23.3	2.4	0.0	24.0	0.0
25-Apr-02	146	-2.0	-12.0	65.0	36.0	19.8	0.0	0.0	24.0	0.0
26-Apr-02	147	4.0	-16.0	87.0	31.0	7.1	0.0	0.0	24.0	0.0
27-Apr-02	148	4.5	-11.5	98.0	31.0	3.9	0.0	0.0	24.0	0.0
28-Apr-02	149	6.5	-2.0	94.0	48.0	8.0	2.8	0.0	24.0	0.4

29-Apr-02	150	7.5	-1.0	80.0	30.0	13.9	0.0	0.0	24.0	2.0
30-Apr-02	151	3.0	-1.0	88.0	36.0	17.1	0.2	0.0	24.0	1.7
1-May-02	152	2.5	-6.5	79.0	45.0	15.0	0.0	0.0	24.0	2.0
2-May-02	153	5.0	-8.5	88.0	48.0	10.9	0.0	0.0	24.0	0.4
3-May-02	154	2.5	-8.5	96.0	70.0	9.3	10.2	0.0	24.0	0.0
4-May-02	155	-1.5	-11.0	72.0	43.0	18.3	0.0	0.0	24.0	0.0
5-May-02	156	2.5	-11.0	71.0	46.0	8.5	0.0	0.0	24.0	0.0
6-May-02	157	3.5	-9.0	91.0	43.0	5.7	0.0	0.0	24.0	0.0
7-May-02	158	7.5	-7.5	69.0	29.0	8.3	0.0	0.0	24.0	0.5
8-May-02	159	11.0	-7.5	89.0	23.0	6.0	0.0	0.0	24.0	0.4
9-May-02	160	11.0	-4.0	74.0	21.0	5.4	0.0	0.0	24.0	0.5
10-May-02	161	11.0	-4.5	66.0	23.0	4.2	0.0	0.0	24.0	0.5
11-May-02	162	17.5	0.0	54.0	28.0	6.5	0.0	0.0	24.0	0.6
12-May-02	163	12.0	3.0	63.0	38.0	12.1	0.0	0.0	24.0	0.8
13-May-02	164	14.0	-1.5	95.0	36.0	5.6	0.4	0.0	24.0	0.5
14-May-02	165	15.0	3.0	80.0	44.0	14.1	0.0	0.0	24.0	0.8
15-May-02	166	5.5	-5.0	78.0	43.0	14.2	0.0	0.0	24.0	0.6
16-May-02	167	9.5	-6.5	86.0	30.0	5.0	0.0	0.0	24.0	0.4
17-May-02	168	12.0	-5.5	85.0	25.0	3.8	0.0	0.0	24.0	0.4
18-May-02	169	14.5	-3.0	77.0	24.0	4.6	0.0	0.0	24.0	0.5
19-May-02	170	14.0	-1.0	64.0	26.0	7.6	0.0	0.0	24.0	0.6
20-May-02	171	19.0	2.0	69.0	27.0	8.4	0.0	0.0	24.0	0.7
21-May-02	172	11.0	4.0	72.0	54.0	13.8	0.0	0.0	24.0	0.8
22-May-02	173	7.5	-0.5	62.0	30.0	18.4	0.0	0.0	24.0	0.9
23-May-02	174	8.0	-3.0	65.0	22.0	17.9	0.0	0.0	24.0	0.9
24-May-02	175	12.5	-4.5	85.0	29.0	5.6	0.0	0.0	24.0	0.5
25-May-02	176	14.5	1.0	75.0	38.0	6.0	2.0	0.0	24.0	0.6
26-May-02	177	19.0	5.0	88.0	26.0	16.0	0.0	0.0	24.0	1.0
27-May-02	178	26.5	5.5	68.0	16.0	11.0	0.0	0.0	24.0	1.0
28-May-02	179	18.5	5.5	76.0	44.0	13.5	0.0	0.0	24.0	0.9
29-May-02	180	18.5	5.0	71.0	38.0	12.6	9.8	0.0	24.0	0.9
30-May-02	181	23.5	6.0	99.0	34.0	12.8	0.4	0.0	24.0	0.9
31-May-02	182	20.0	9.0	72.0	38.0	14.6	3.6	0.0	24.0	1.0
1-Jun-02	183	14.5	5.0	86.0	50.0	5.0	0.2	0.0	24.0	0.6
2-Jun-02	184	19.0	4.0	76.0	38.0	5.1	0.0	0.0	24.0	3.1
3-Jun-02	185	21.0	4.5	90.0	39.0	6.8	0.6	0.0	24.0	3.3
4-Jun-02	186	21.0	9.0	80.0	34.0	8.5	4.2	0.0	24.0	4.1
5-Jun-02	187	22.0	11.5	90.0	44.0	8.6	0.0	0.0	24.0	3.9
6-Jun-02	188	19.5	11.0	83.0	56.0	19.5	4.2	0.0	24.0	5.1
7-Jun-02	189	12.5	9.0	90.0	78.0	9.8	2.6	0.0	24.0	3.1
8-Jun-02	190	21.5	6.5	97.0	39.0	4.7	0.0	0.0	24.0	3.1
9-Jun-02	191	20.5	8.5	70.0	32.0	8.5	0.0	0.0	24.0	4.3
10-Jun-02	192	21.5	8.5	59.0	26.0	15.1	0.0	0.0	24.0	6.2
11-Jun-02	193	15.0	12.0	59.0	45.0	18.1	0.0	0.0	24.0	6.3
12-Jun-02	194	22.5	9.0	77.0	43.0	7.9	0.0	0.0	24.0	4.0
13-Jun-02	195	26.0	8.5	84.0	27.0	10.8	0.0	0.0	24.0	4.8
14-Jun-02	196	22.5	7.0	92.0	24.0	8.3	0.0	0.0	24.0	4.1
15-Jun-02	197	21.5	8.0	67.0	24.0	5.2	0.0	0.0	24.0	3.8
16-Jun-02	198	20.0	7.5	76.0	36.0	6.1	0.0	0.0	24.0	3.7
17-Jun-02	199	23.5	12.0	66.0	41.0	10.8	8.6	0.0	24.0	5.0
18-Jun-02	200	12.5	7.0	96.0	77.0	14.8	0.0	0.0	24.0	3.2

19-Jun-02	201	10.0	7.5	85.0	72.0	9.2	2.2	0.0	24.0	3.1
20-Jun-02	202	20.5	4.5	97.0	37.0	7.6	0.0	0.0	24.0	3.4
21-Jun-02	203	27.5	9.5	69.0	28.0	20.7	0.0	0.0	24.0	7.5
22-Jun-02	204	25.0	12.5	76.0	41.0	14.2	0.0	0.0	24.0	5.6
23-Jun-02	205	27.5	14.0	78.0	37.0	7.9	0.0	0.0	24.0	4.6
24-Jun-02	206	26.5	15.0	91.0	50.0	6.5	0.0	0.0	24.0	3.9
25-Jun-02	207	30.0	14.0	91.0	28.0	9.5	0.0	0.0	24.0	4.9
26-Jun-02	208	33.0	14.5	82.0	28.0	8.6	0.0	0.0	24.0	5.0
27-Jun-02	209	31.0	16.0	88.0	34.0	6.8	0.0	0.0	24.0	4.4
28-Jun-02	210	34.0	20.5	78.0	42.0	9.6	0.6	0.0	24.0	5.4
29-Jun-02	211	30.0	21.0	71.0	32.0	12.3	1.4	0.0	24.0	6.5
30-Jun-02	212	19.0	15.5	93.0	83.0	28.0	0.0	0.0	24.0	4.6
1-Jul-02	213	25.5	12.0	75.0	24.0	24.5	0.0	0.0	24.0	8.4
2-Jul-02	214	17.0	12.5	87.0	55.0	20.0	3.2	0.0	24.0	5.0
3-Jul-02	215	21.5	8.5	92.0	40.0	9.6	0.0	0.0	24.0	3.8
4-Jul-02	216	16.5	10.5	92.0	66.0	17.8	7.2	0.0	24.0	3.9
5-Jul-02	217	27.5	14.0	92.0	54.0	15.8	0.0	0.0	24.0	4.8
6-Jul-02	218	25.5	11.5	70.0	36.0	19.2	0.0	0.0	24.0	6.5
7-Jul-02	219	27.0	12.0	90.0	27.0	7.9	0.0	0.0	24.0	4.2
8-Jul-02	220	26.0	9.5	78.0	30.0	5.2	0.0	0.0	24.0	3.5
9-Jul-02	221	27.0	12.0	91.0	30.0	9.8	0.0	0.0	24.0	4.4
10-Jul-02	222	28.0	11.0	89.0	32.0	13.5	0.0	0.0	24.0	5.1
11-Jul-02	223	30.5	19.0	67.0	35.0	14.7	0.0	0.0	24.0	6.6
12-Jul-02	224	32.5	19.0	74.0	43.0	10.3	0.0	0.0	24.0	5.2
13-Jul-02	225	32.5	18.0	93.0	31.0	10.9	0.0	0.0	24.0	5.1
14-Jul-02	226	27.5	18.5	68.0	54.0	13.4	0.0	0.0	24.0	5.4
15-Jul-02	227	29.5	20.0	79.0	19.0	20.8	0.0	0.0	24.0	8.5
16-Jul-02	228	23.0	16.5	55.0	40.0	19.8	0.0	0.0	24.0	7.4
17-Jul-02	229	23.5	9.5	89.0	46.0	7.2	0.4	0.0	24.0	3.4
18-Jul-02	230	18.0	15.5	95.0	84.0	10.6	2.2	0.0	24.0	3.2
19-Jul-02	231	21.0	14.5	79.0	72.0	6.0	0.4	0.0	24.0	3.2
20-Jul-02	232	19.0	15.0	90.0	74.0	7.9	7.4	0.0	24.0	3.2
21-Jul-02	233	14.0	11.5	96.0	88.0	13.9	1.0	0.0	24.0	2.8
22-Jul-02	234	24.5	11.0	90.0	35.0	13.8	0.0	0.0	24.0	4.6
23-Jul-02	235	26.5	10.5	92.0	34.0	10.8	0.0	0.0	24.0	4.2
24-Jul-02	236	23.5	18.0	61.0	46.0	10.9	0.0	0.0	24.0	5.1
25-Jul-02	237	28.5	13.0	94.0	37.0	7.1	0.0	0.0	24.0	3.6
26-Jul-02	238	31.5	16.5	83.0	41.0	6.9	0.4	0.0	24.0	3.9
27-Jul-02	239	22.0	18.0	90.0	70.0	7.5	1.0	0.0	24.0	3.4
28-Jul-02	240	25.5	12.5	91.0	43.0	10.8	2.6	0.0	24.0	3.9
29-Jul-02	241	22.5	14.0	87.0	43.0	12.4	6.2	0.0	24.0	4.3
30-Jul-02	242	22.5	11.0	86.0	32.0	22.5	0.0	0.0	24.0	6.1
31-Jul-02	243	18.5	12.0	70.0	60.0	16.3	0.4	0.0	24.0	4.6
1-Aug-02	244	14.0	10.5	90.0	57.0	25.2	0.0	0.0	24.0	4.7
2-Aug-02	245	15.5	8.0	76.0	47.0	20.5	0.0	0.0	24.0	4.5
3-Aug-02	246	17.0	8.0	70.0	49.0	19.1	0.0	0.0	24.0	4.5
4-Aug-02	247	18.5	8.5	72.0	47.0	12.8	0.0	0.0	24.0	3.7
5-Aug-02	248	20.0	10.5	83.0	49.0	8.6	0.0	0.0	24.0	3.0
6-Aug-02	249	19.0	14.0	89.0	69.0	10.8	1.6	0.0	24.0	3.0
7-Aug-02	250	25.5	16.0	96.0	64.0	6.8	0.0	0.0	24.0	2.7
8-Aug-02	251	20.0	16.5	96.0	85.0	1.8	0.4	0.0	24.0	2.3

9-Aug-02	252	26.0	14.0	99.0	40.0	5.5	0.0	0.0	24.0	2.7
10-Aug-02	253	25.5	13.0	94.0	49.0	6.5	0.0	0.0	24.0	2.7
11-Aug-02	254	18.0	11.5	93.0	67.0	5.0	5.0	0.0	24.0	2.3
12-Aug-02	255	21.0	12.0	80.0	46.0	21.4	0.0	0.0	24.0	4.7
13-Aug-02	256	21.0	10.0	81.0	42.0	8.7	0.0	0.0	24.0	3.0
14-Aug-02	257	21.5	12.0	87.0	43.0	8.3	0.0	0.0	24.0	3.0
15-Aug-02	258	17.0	12.0	89.0	66.0	8.4	2.2	0.0	24.0	2.5
16-Aug-02	259	13.5	10.5	93.0	75.0	12.5	15.6	0.0	24.0	2.5
17-Aug-02	260	16.0	9.0	94.0	60.0	15.8	2.8	0.0	24.0	2.8
18-Aug-02	261	13.0	7.5	92.0	74.0	5.9	0.4	0.0	24.0	1.9
19-Aug-02	262	21.5	7.0	94.0	45.0	18.2	0.8	0.0	24.0	3.4
20-Aug-02	263	18.5	7.5	84.0	39.0	12.8	0.0	0.0	24.0	3.1
21-Aug-02	264	19.0	7.5	91.0	51.0	5.1	0.8	0.0	24.0	2.1
22-Aug-02	265	29.0	14.5	72.0	39.0	15.9	0.4	0.0	24.0	4.6
23-Aug-02	266	26.0	13.0	91.0	37.0	8.8	0.0	0.0	24.0	3.0
24-Aug-02	267	32.5	14.5	80.0	32.0	12.0	0.0	0.0	24.0	4.0
25-Aug-02	268	24.0	13.5	62.0	43.0	8.6	0.0	0.0	24.0	3.3
26-Aug-02	269	23.0	11.5	86.0	47.0	9.0	0.0	0.0	24.0	2.7
27-Aug-02	270	25.5	10.0	94.0	47.0	5.9	0.0	0.0	24.0	2.1
28-Aug-02	271	28.5	13.0	92.0	44.0	3.6	0.0	0.0	24.0	2.0
29-Aug-02	272	29.5	15.5	88.0	38.0	9.2	0.0	0.0	24.0	3.0
30-Aug-02	273	27.0	18.0	87.0	55.0	10.4	53.8	0.0	24.0	3.0
31-Aug-02	274	22.0	17.0	95.0	75.0	8.3	3.8	0.0	24.0	2.2
1-Sep-02	275	21.5	10.5	90.0	52.0	6.4	24.6	0.0	24.0	2.1
2-Sep-02	276	16.0	11.5	95.0	77.0	18.9	28.8	0.0	24.0	2.2
3-Sep-02	277	15.0	9.0	86.0	61.0	8.7	3.2	0.0	24.0	1.9
4-Sep-02	278	12.5	8.0	95.0	81.0	13.4	1.8	0.0	24.0	1.7
5-Sep-02	279	19.0	11.0	95.0	59.0	3.1	0.0	0.0	24.0	1.5
6-Sep-02	280	13.5	11.5	97.0	84.0	1.7	1.6	0.0	24.0	1.4
7-Sep-02	281	16.0	11.5	97.0	82.0	2.8	2.4	0.0	24.0	1.4
8-Sep-02	282	18.0	12.0	98.0	55.0	7.6	0.2	0.0	24.0	1.8
9-Sep-02	283	22.0	10.5	94.0	38.0	8.5	0.0	0.0	24.0	2.0
10-Sep-02	284	23.5	8.0	96.0	32.0	7.1	0.0	0.0	24.0	1.8
11-Sep-02	285	26.0	12.0	75.0	38.0	8.6	0.0	0.0	24.0	2.3
12-Sep-02	286	20.5	9.5	78.0	37.0	6.5	0.0	0.0	24.0	1.9
13-Sep-02	287	12.5	8.5	95.0	71.0	12.4	9.4	0.0	24.0	1.7
14-Sep-02	288	17.5	6.5	94.0	42.0	9.5	0.0	0.0	24.0	1.8
15-Sep-02	289	22.0	10.5	69.0	46.0	15.8	0.4	0.0	24.0	3.0
16-Sep-02	290	13.0	8.5	97.0	81.0	8.4	0.0	0.0	24.0	1.3
17-Sep-02	291	13.5	10.5	94.0	83.0	5.4	0.0	0.0	24.0	1.3
18-Sep-02	292	17.5	10.5	98.0	44.0	3.5	0.0	0.0	24.0	1.3
19-Sep-02	293	18.0	7.0	87.0	49.0	10.7	6.8	0.0	24.0	1.7
20-Sep-02	294	12.0	8.0	96.0	83.0	10.2	12.4	0.0	24.0	1.3
21-Sep-02	295	9.0	5.5	89.0	57.0	22.5	0.6	0.0	24.0	2.2
22-Sep-02	296	8.5	2.5	90.0	48.0	14.9	0.4	0.0	24.0	1.8
23-Sep-02	297	9.0	2.0	62.0	49.0	14.3	0.2	0.0	24.0	2.1
24-Sep-02	298	4.0	-0.5	83.0	48.0	15.9	0.0	0.0	24.0	1.8
25-Sep-02	299	3.0	-1.5	70.0	42.0	12.5	0.0	0.0	24.0	1.7
26-Sep-02	300	5.0	-0.5	73.0	48.0	13.7	0.0	0.0	24.0	1.7
27-Sep-02	301	6.0	-2.0	91.0	46.0	8.6	0.0	0.0	24.0	1.1
28-Sep-02	302	12.5	-2.5	69.0	40.0	18.3	0.0	0.0	24.0	2.2

29-Sep-02	303	15.5	10.5	66.0	55.0	14.1	0.4	0.0	24.0	2.5
30-Sep-02	304	8.0	5.0	80.0	61.0	18.8	0.0	0.0	24.0	2.1
1-Oct-02	305	4.5	-2.5	81.0	56.0	12.7	0.0	0.0	24.0	1.3
2-Oct-02	306	12.5	-0.5	81.0	44.0	21.0	0.0	0.0	24.0	2.5
3-Oct-02	307	10.0	6.5	81.0	59.0	21.0	1.4	0.0	24.0	2.7
4-Oct-02	308	4.0	0.0	73.0	47.0	14.5	0.0	0.0	24.0	2.0
5-Oct-02	309	2.0	-2.0	95.0	57.0	5.3	0.2	0.0	24.0	0.6
6-Oct-02	310	5.5	-6.5	98.0	43.0	5.3	0.0	0.0	24.0	0.7
7-Oct-02	311	2.5	-4.5	100.0	80.0	7.7	5.2	0.0	24.0	0.1
8-Oct-02	312	6.5	-1.0	100.0	59.0	11.9	0.0	0.0	24.0	0.4
9-Oct-02	313	13.0	4.0	86.0	57.0	11.4	0.0	0.0	24.0	1.4
10-Oct-02	314	10.0	0.5	96.0	66.0	4.5	0.6	0.0	24.0	0.7
11-Oct-02	315	4.5	0.5	99.0	90.0	11.7	7.8	0.0	24.0	0.7
12-Oct-02	316	-1.5	-5.0	85.0	60.0	13.4	0.4	0.0	24.0	0.0
13-Oct-02	317	-0.5	-9.5	93.0	59.0	13.0	1.0	0.0	24.0	0.0
14-Oct-02	318	-0.5	-2.5	88.0	64.0	17.8	0.0	0.0	24.0	0.0
15-Oct-02	319	-4.5	-7.5	78.0	60.0	9.8	0.0	0.0	24.0	0.0
16-Oct-02	320	-3.5	-10.5	92.0	62.0	12.2	0.0	0.0	24.0	0.0
17-Oct-02	321	-2.0	-11.5	94.0	71.0	5.2	0.0	0.0	24.0	0.0
18-Oct-02	322	-3.0	-9.0	93.0	71.0	7.3	0.2	0.0	24.0	0.0
19-Oct-02	323	-3.5	-8.0	90.0	67.0	10.4	1.6	0.0	24.0	0.0
20-Oct-02	324	-1.0	-10.5	93.0	74.0	2.6	0.2	0.0	24.0	0.0
21-Oct-02	325	2.0	-6.5	92.0	58.0	3.0	0.0	0.0	24.0	0.0
22-Oct-02	326	0.0	-3.5	78.0	62.0	4.9	0.0	0.0	24.0	0.0
23-Oct-02	327	3.0	-8.5	93.0	46.0	12.5	0.0	0.0	24.0	0.0
24-Oct-02	328	0.5	-4.5	80.0	66.0	10.6	0.0	0.0	24.0	0.0
25-Oct-02	329	-0.5	-3.5	94.0	79.0	11.1	1.4	0.0	24.0	0.0
26-Oct-02	330	-1.5	-5.5	96.0	62.0	8.8	0.0	0.0	24.0	0.0
27-Oct-02	331	-2.5	-10.0	92.0	60.0	4.1	0.2	0.0	24.0	0.0
28-Oct-02	332	-5.5	-12.0	90.0	72.0	8.5	0.6	0.0	24.0	0.0
29-Oct-02	333	-2.0	-8.5	81.0	49.0	12.0	0.0	0.0	24.0	0.0
30-Oct-02	334	-2.0	-10.5	87.0	55.0	9.5	0.0	0.0	24.0	0.0
31-Oct-02	335	-2.5	-13.5	93.0	69.0	5.0	0.0	0.0	24.0	0.0
1-Nov-02	336	-2.0	-4.5	81.0	61.0	12.5	0.0	0.0	24.0	0.0
2-Nov-02	337	-4.0	-5.5	82.0	78.0	3.8	0.5	0.0	24.0	0.0
3-Nov-02	338	-1.5	-8.0	95.0	73.0	5.6	0.0	0.0	24.0	0.0
4-Nov-02	339	-1.5	-2.5	90.0	83.0	8.0	0.4	0.0	24.0	0.0
5-Nov-02	340	1.0	-7.0	91.0	49.0	16.8	0.2	0.0	24.0	0.0
6-Nov-02	341	-7.5	-17.0	71.0	44.0	12.3	3.8	0.0	24.0	0.0
7-Nov-02	342	-9.5	-13.0	86.0	67.0	12.3	0.4	0.0	24.0	0.0
8-Nov-02	343	-10.5	-18.0	81.0	70.0	5.5	0.0	0.0	24.0	0.0
9-Nov-02	344	-8.5	-17.5	91.0	70.0	8.4	0.8	0.0	24.0	0.0
10-Nov-02	345	-8.0	-14.0	89.0	72.0	4.2	0.0	0.0	24.0	0.0
11-Nov-02	346	-9.5	-15.0	84.0	74.0	10.5	0.2	0.0	24.0	0.0
12-Nov-02	347	-9.5	-14.5	81.0	72.0	12.1	0.0	0.0	24.0	0.0
13-Nov-02	348	-9.0	-12.5	81.0	70.0	10.5	0.8	0.0	24.0	0.0
14-Nov-02	349	-8.5	-13.0	88.0	67.0	5.7	0.0	0.0	24.0	0.0
15-Nov-02	350	-7.0	-23.0	78.0	65.0	7.2	0.0	0.0	24.0	0.0
16-Nov-02	351	-4.0	-8.5	96.0	86.0	10.5	0.2	0.0	24.0	0.0
17-Nov-02	352	-1.0	-5.0	96.0	91.0	14.1	0.0	0.0	24.0	0.0
18-Nov-02	353	1.0	-7.0	98.0	82.0	4.0	0.0	0.0	24.0	0.0

19-Nov-02	354	1.0	-5.5	89.0	69.0	5.7	0.0	0.0	24.0	0.0
20-Nov-02	355	-2.5	-6.0	95.0	91.0	3.3	2.8	0.0	24.0	0.0
21-Nov-02	356	-2.0	-4.0	93.0	84.0	4.7	0.0	0.0	24.0	0.0
22-Nov-02	357	0.5	-4.0	94.0	80.0	15.9	1.2	0.0	24.0	0.0
23-Nov-02	358	-10.0	-13.5	79.0	70.0	25.8	0.2	0.0	24.0	0.0
24-Nov-02	359	-12.0	-23.0	85.0	68.0	10.5	1.0	0.0	24.0	0.0
25-Nov-02	360	-9.5	-14.0	87.0	71.0	8.1	0.0	0.0	24.0	0.0
26-Nov-02	361	-7.0	-15.0	90.0	77.0	12.0	0.0	0.0	24.0	0.0
27-Nov-02	362	-5.5	-15.0	90.0	83.0	5.1	0.2	0.0	24.0	0.0
28-Nov-02	363	9.0	-9.0	94.0	45.0	20.6	1.2	0.0	24.0	0.0
29-Nov-02	364	-11.0	-12.5	80.0	58.0	26.1	0.0	0.0	24.0	0.0
30-Nov-02	365	-9.0	-13.5	84.0	73.0	6.9	0.0	0.0	24.0	0.0

Table B-6. Flin Flon climate 2002-03

Date	Day	Temp (°C)		RH (%)		Wind	Precip	Precip Period		P.E.
		Max	Min	Max	Min	(m/s)	(mm)	Start	End	(mm/day)
1-Dec-02	1	-15.5	-18.5	73.0	61.0	9.3	6.0	0.0	24.0	0.0
2-Dec-02	2	-19.0	-26.0	69.0	64.0	5.5	0.0	0.0	24.0	0.0
3-Dec-02	3	-15.5	-25.0	68.0	59.0	7.0	0.0	0.0	24.0	0.0
4-Dec-02	4	-11.5	-20.0	85.0	65.0	9.8	0.8	0.0	24.0	0.0
5-Dec-02	5	-7.0	-14.5	87.0	81.0	8.7	0.0	0.0	24.0	0.0
6-Dec-02	6	-6.5	-10.5	88.0	51.0	16.3	0.4	0.0	24.0	0.0
7-Dec-02	7	-15.0	-18.0	63.0	49.0	12.3	0.0	0.0	24.0	0.0
8-Dec-02	8	-3.0	-23.5	87.0	65.0	14.3	0.2	0.0	24.0	0.0
9-Dec-02	9	-2.0	-8.5	95.0	86.0	11.7	0.2	0.0	24.0	0.0
10-Dec-02	10	-4.0	-8.5	96.0	91.0	6.2	1.0	0.0	24.0	0.0
11-Dec-02	11	-4.0	-8.0	95.0	87.0	8.8	4.8	0.0	24.0	0.0
12-Dec-02	12	-10.0	-14.0	85.0	81.0	8.0	0.0	0.0	24.0	0.0
13-Dec-02	13	-7.0	-12.0	95.0	89.0	7.2	0.0	0.0	24.0	0.0
14-Dec-02	14	-6.0	-8.5	93.0	90.0	4.3	0.0	0.0	24.0	0.0
15-Dec-02	15	-1.5	-8.0	93.0	89.0	20.5	0.4	0.0	24.0	0.0
16-Dec-02	16	-1.5	-4.0	91.0	86.0	22.1	0.0	0.0	24.0	0.0
17-Dec-02	17	-4.0	-4.5	84.0	75.0	16.8	0.0	0.0	24.0	0.0
18-Dec-02	18	-4.0	-5.5	94.0	87.0	6.9	1.4	0.0	24.0	0.0
19-Dec-02	19	-4.0	-6.0	91.0	86.0	23.3	0.0	0.0	24.0	0.0
20-Dec-02	20	-4.0	-5.5	86.0	79.0	24.4	1.6	0.0	24.0	0.0
21-Dec-02	21	-6.5	-7.5	83.0	80.0	20.2	0.8	0.0	24.0	0.0
22-Dec-02	22	-9.0	-15.0	86.0	71.0	12.6	0.0	0.0	24.0	0.0
23-Dec-02	23	-15.0	-22.0	81.0	70.0	5.0	0.0	0.0	24.0	0.0
24-Dec-02	24	-9.5	-22.0	86.0	76.0	9.8	0.0	0.0	24.0	0.0
25-Dec-02	25	-6.5	-19.5	88.0	70.0	5.5	0.0	0.0	24.0	0.0
26-Dec-02	26	-6.0	-18.5	89.0	74.0	7.1	1.6	0.0	24.0	0.0
27-Dec-02	27	-4.5	-10.0	92.0	78.0	13.3	1.0	0.0	24.0	0.0
28-Dec-02	28	-10.5	-15.5	89.0	78.0	6.5	0.2	0.0	24.0	0.0
29-Dec-02	29	-12.0	-16.5	88.0	84.0	9.1	11.8	0.0	24.0	0.0
30-Dec-02	30	-13.0	-17.5	85.0	77.0	16.4	1.6	0.0	24.0	0.0
31-Dec-02	31	-15.0	-28.5	73.0	64.0	4.8	0.0	0.0	24.0	0.0
1-Jan-03	32	-10.5	-21.0	87.0	72.0	9.1	0.0	0.0	24.0	0.0
2-Jan-03	33	-9.5	-18.5	96.0	85.0	6.6	0.0	0.0	24.0	0.0
3-Jan-03	34	-10.0	-17.0	92.0	89.0	2.0	0.2	0.0	24.0	0.0
4-Jan-03	35	-9.5	-17.5	94.0	85.0	0.3	0.0	0.0	24.0	0.0
5-Jan-03	36	-9.0	-18.0	88.0	85.0	5.9	0.0	0.0	24.0	0.0
6-Jan-03	37	4.5	-12.0	90.0	80.0	12.5	0.0	0.0	24.0	0.0
7-Jan-03	38	7.0	-1.5	93.0	66.0	10.1	0.0	0.0	24.0	0.0
8-Jan-03	39	7.0	-5.5	91.0	47.0	27.3	1.6	0.0	24.0	0.0
9-Jan-03	40	-11.5	-17.5	73.0	49.0	23.5	0.0	0.0	24.0	0.0
10-Jan-03	41	-22.0	-28.0	61.0	55.0	16.8	0.0	0.0	24.0	0.0
11-Jan-03	42	-22.5	-29.0	63.0	54.0	6.7	0.4	0.0	24.0	0.0
12-Jan-03	43	-22.5	-28.5	62.0	51.0	13.9	0.0	0.0	24.0	0.0
13-Jan-03	44	-19.5	-28.0	62.0	53.0	12.5	0.0	0.0	24.0	0.0
14-Jan-03	45	-13.0	-22.5	53.0	37.0	9.5	0.0	0.0	24.0	0.0
15-Jan-03	46	-12.0	-24.0	55.0	27.0	9.8	0.0	0.0	24.0	0.0
16-Jan-03	47	-10.0	-24.0	61.0	33.0	4.6	0.0	0.0	24.0	0.0

17-Jan-03	48	-8.0	-19.0	88.0	56.0	27.1	0.0	0.0	24.0	0.0
18-Jan-03	49	-13.5	-22.0	71.0	62.0	11.3	0.0	0.0	24.0	0.0
19-Jan-03	50	-13.5	-23.5	64.0	48.0	16.8	0.0	0.0	24.0	0.0
20-Jan-03	51	-19.5	-26.5	63.0	50.0	22.2	0.2	0.0	24.0	0.0
21-Jan-03	52	-23.0	-26.0	66.0	47.0	8.8	0.0	0.0	24.0	0.0
22-Jan-03	53	-26.0	-36.0	65.0	54.0	8.1	0.0	0.0	24.0	0.0
23-Jan-03	54	-25.5	-34.0	68.0	56.0	2.8	1.0	0.0	24.0	0.0
24-Jan-03	55	-21.5	-31.5	64.0	40.0	10.8	0.2	0.0	24.0	0.0
25-Jan-03	56	-22.5	-29.5	60.0	47.0	24.2	0.0	0.0	24.0	0.0
26-Jan-03	57	-18.0	-34.0	65.0	46.0	7.9	3.4	0.0	24.0	0.0
27-Jan-03	58	-15.0	-21.5	71.0	57.0	17.0	0.0	0.0	24.0	0.0
28-Jan-03	59	-20.0	-31.0	63.0	45.0	8.2	0.0	0.0	24.0	0.0
29-Jan-03	60	-15.0	-29.5	67.0	62.0	9.9	0.4	0.0	24.0	0.0
30-Jan-03	61	-13.0	-18.0	67.0	52.0	2.9	0.0	0.0	24.0	0.0
31-Jan-03	62	-16.0	-23.0	71.0	58.0	10.5	0.0	0.0	24.0	0.0
1-Feb-03	63	-14.5	-21.5	73.0	61.0	9.5	4.2	0.0	24.0	0.0
2-Feb-03	64	-14.0	-26.0	74.0	65.0	5.5	0.0	0.0	24.0	0.0
3-Feb-03	65	-18.0	-29.0	70.0	56.0	5.7	0.0	0.0	24.0	0.0
4-Feb-03	66	-16.5	-35.5	70.0	60.0	1.7	0.0	0.0	24.0	0.0
5-Feb-03	67	-17.5	-27.5	69.0	54.0	7.1	0.0	0.0	24.0	0.0
6-Feb-03	68	-6.5	-33.5	80.0	60.0	13.4	0.0	0.0	24.0	0.0
7-Feb-03	69	-6.5	-17.5	89.0	45.0	23.8	1.6	0.0	24.0	0.0
8-Feb-03	70	-18.0	-26.0	59.0	41.0	18.0	0.0	0.0	24.0	0.0
9-Feb-03	71	-22.0	-26.0	54.0	39.0	21.2	0.0	0.0	24.0	0.0
10-Feb-03	72	-14.5	-33.0	64.0	51.0	13.5	0.2	0.0	24.0	0.0
11-Feb-03	73	-20.0	-28.5	48.0	40.0	19.4	0.0	0.0	24.0	0.0
12-Feb-03	74	-17.0	-26.5	62.0	42.0	12.0	0.0	0.0	24.0	0.0
13-Feb-03	75	-15.0	-30.5	64.0	37.0	9.6	0.0	0.0	24.0	0.0
14-Feb-03	76	-20.0	-31.5	61.0	31.0	7.8	0.0	0.0	24.0	0.0
15-Feb-03	77	-17.0	-32.0	68.0	44.0	9.6	1.2	0.0	24.0	0.0
16-Feb-03	78	-12.5	-20.0	81.0	68.0	5.9	0.6	0.0	24.0	0.0
17-Feb-03	79	-13.5	-21.0	86.0	64.0	11.6	0.0	0.0	24.0	0.0
18-Feb-03	80	-12.5	-22.0	71.0	53.0	2.8	0.0	0.0	24.0	0.0
19-Feb-03	81	-19.0	-21.0	66.0	55.0	16.2	0.4	0.0	24.0	0.0
20-Feb-03	82	-23.0	-31.5	62.0	39.0	10.8	0.0	0.0	24.0	0.0
21-Feb-03	83	-21.0	-38.5	67.0	42.0	8.4	0.0	0.0	24.0	0.0
22-Feb-03	84	-21.0	-36.0	63.0	41.0	7.3	0.0	0.0	24.0	0.0
23-Feb-03	85	-25.0	-37.0	63.0	40.0	8.5	0.0	0.0	24.0	0.0
24-Feb-03	86	-18.5	-38.0	63.0	39.0	6.0	0.0	0.0	24.0	0.0
25-Feb-03	87	-14.5	-35.5	62.0	38.0	4.1	0.0	0.0	24.0	0.0
26-Feb-03	88	-8.0	-19.0	67.0	52.0	10.4	0.2	0.0	24.0	0.0
27-Feb-03	89	-14.5	-26.5	68.0	50.0	5.2	1.6	0.0	24.0	0.0
28-Feb-03	90	-19.0	-22.0	69.0	59.0	17.2	1.4	0.0	24.0	0.0
1-Mar-03	91	-24.0	-35.0	61.0	42.0	15.7	0.0	0.0	24.0	0.0
2-Mar-03	92	-19.0	-40.5	68.0	41.0	5.2	0.2	0.0	24.0	0.0
3-Mar-03	93	-18.5	-27.5	64.0	43.0	15.0	0.0	0.0	24.0	0.0
4-Mar-03	94	-19.0	-29.5	62.0	39.0	16.2	0.0	0.0	24.0	0.0
5-Mar-03	95	-16.0	-34.0	70.0	45.0	9.7	0.0	0.0	24.0	0.0
6-Mar-03	96	-22.0	-32.0	54.0	32.0	18.4	0.0	0.0	24.0	0.0
7-Mar-03	97	-22.0	-34.0	59.0	39.0	18.2	0.0	0.0	24.0	0.0
8-Mar-03	98	-19.0	-28.5	54.0	45.0	23.5	0.4	0.0	24.0	0.0

9-Mar-03	99	-13.0	-22.5	62.0	44.0	18.2	0.0	0.0	24.0	0.0
10-Mar-03	100	-12.5	-25.0	69.0	43.0	9.2	1.4	0.0	24.0	0.0
11-Mar-03	101	-16.5	-23.0	67.0	44.0	14.8	0.0	0.0	24.0	0.0
12-Mar-03	102	-11.0	-34.5	65.0	32.0	8.5	0.0	0.0	24.0	0.0
13-Mar-03	103	-10.0	-24.5	71.0	47.0	14.8	0.4	0.0	24.0	0.0
14-Mar-03	104	-6.5	-14.5	85.0	72.0	9.8	0.2	0.0	24.0	0.0
15-Mar-03	105	-1.0	-8.5	90.0	79.0	6.5	0.0	0.0	24.0	0.0
16-Mar-03	106	-4.0	-8.5	89.0	67.0	9.5	0.0	0.0	24.0	0.0
17-Mar-03	107	-3.5	-9.5	85.0	76.0	13.0	0.0	0.0	24.0	0.0
18-Mar-03	108	9.0	-11.0	90.0	35.0	10.3	0.0	0.0	24.0	0.0
19-Mar-03	109	7.5	-5.5	83.0	44.0	5.2	0.0	0.0	24.0	0.0
20-Mar-03	110	12.0	-8.5	90.0	27.0	2.5	0.0	0.0	24.0	0.0
21-Mar-03	111	9.0	-8.0	90.0	41.0	7.2	0.0	0.0	24.0	0.0
22-Mar-03	112	12.0	-3.5	96.0	34.0	7.4	0.0	0.0	24.0	0.0
23-Mar-03	113	9.0	-2.5	94.0	53.0	9.8	1.0	0.0	24.0	0.0
24-Mar-03	114	0.0	-2.5	93.0	71.0	23.8	0.0	0.0	24.0	0.0
25-Mar-03	115	2.0	-6.0	88.0	53.0	5.9	0.0	0.0	24.0	0.0
26-Mar-03	116	3.0	-4.5	93.0	65.0	8.2	0.0	0.0	24.0	0.0
27-Mar-03	117	-2.0	-9.5	98.0	74.0	7.2	4.2	0.0	24.0	0.0
28-Mar-03	118	-5.0	-16.5	83.0	60.0	16.0	0.0	0.0	24.0	0.0
29-Mar-03	119	-7.5	-14.0	87.0	73.0	12.2	2.6	0.0	24.0	0.0
30-Mar-03	120	-3.5	-20.0	84.0	57.0	16.0	2.6	0.0	24.0	0.0
31-Mar-03	121	-1.0	-6.0	95.0	54.0	18.5	0.0	0.0	24.0	0.0
1-Apr-03	122	-7.0	-20.5	85.0	50.0	13.1	0.0	0.0	24.0	0.0
2-Apr-03	123	-6.0	-24.0	65.0	28.0	9.4	0.0	0.0	24.0	0.0
3-Apr-03	124	-7.0	-19.5	58.0	26.0	16.2	0.0	0.0	24.0	0.0
4-Apr-03	125	-4.5	-16.5	44.0	19.0	11.7	0.0	0.0	24.0	0.0
5-Apr-03	126	-4.0	-20.0	59.0	23.0	11.1	0.0	0.0	24.0	0.0
6-Apr-03	127	-1.0	-18.0	52.0	25.0	9.7	1.0	0.0	24.0	0.0
7-Apr-03	128	1.5	-4.5	95.0	56.0	5.9	0.0	0.0	24.0	0.0
8-Apr-03	129	12.0	-6.0	87.0	41.0	10.6	0.0	0.0	24.0	0.0
9-Apr-03	130	14.5	-3.5	96.0	45.0	8.5	0.0	0.0	24.0	0.0
10-Apr-03	131	9.0	3.0	71.0	42.0	28.9	0.0	0.0	24.0	1.3
11-Apr-03	132	5.5	-4.5	89.0	54.0	8.0	0.8	0.0	24.0	0.8
12-Apr-03	133	2.0	-1.0	99.0	92.0	14.6	4.2	0.0	24.0	0.9
13-Apr-03	134	3.5	0.5	99.0	91.0	11.8	0.0	0.0	24.0	1.2
14-Apr-03	135	7.0	-1.5	90.0	41.0	10.5	0.0	0.0	24.0	1.7
15-Apr-03	136	6.0	-5.0	82.0	39.0	9.9	0.0	0.0	24.0	1.7
16-Apr-03	137	2.0	-7.0	61.0	34.0	15.3	0.2	0.0	24.0	0.9
17-Apr-03	138	7.5	-2.5	85.0	64.0	8.2	0.0	0.0	24.0	1.2
18-Apr-03	139	17.0	-4.0	99.0	36.0	8.5	0.0	0.0	24.0	1.7
19-Apr-03	140	17.0	-1.5	97.0	41.0	7.8	3.4	0.0	24.0	1.6
20-Apr-03	141	14.0	-1.5	100.0	34.0	8.8	0.0	0.0	24.0	1.7
21-Apr-03	142	15.5	-3.0	100.0	30.0	7.9	0.0	0.0	24.0	1.7
22-Apr-03	143	20.5	-0.5	85.0	32.0	7.8	0.0	0.0	24.0	2.0
23-Apr-03	144	15.5	5.0	76.0	52.0	3.1	0.2	0.0	24.0	1.7
24-Apr-03	145	13.0	2.0	82.0	49.0	14.7	0.0	0.0	24.0	2.5
25-Apr-03	146	5.5	0.5	92.0	59.0	14.7	9.6	0.0	24.0	2.0
26-Apr-03	147	9.5	0.0	95.0	36.0	16.4	0.0	0.0	24.0	2.5
27-Apr-03	148	9.0	-3.0	81.0	32.0	14.1	0.0	0.0	24.0	2.4
28-Apr-03	149	5.0	-6.0	70.0	33.0	15.5	0.0	0.0	24.0	2.4

29-Apr-03	150	12.5	-7.5	86.0	17.0	11.8	0.0	0.0	24.0	2.3
30-Apr-03	151	7.0	-3.0	82.0	28.0	14.2	0.0	0.0	24.0	2.5
1-May-03	152	9.0	-7.5	80.0	18.0	6.8	0.0	0.0	24.0	1.8
2-May-03	153	13.5	-0.5	63.0	34.0	11.6	0.6	0.0	24.0	0.6
3-May-03	154	16.0	3.5	67.0	46.0	8.1	0.4	0.0	24.0	0.6
4-May-03	155	20.0	2.5	100.0	44.0	7.9	2.2	0.0	24.0	0.5
5-May-03	156	19.0	2.0	89.0	49.0	14.8	0.0	0.0	24.0	0.7
6-May-03	157	20.0	3.0	81.0	22.0	11.0	0.0	0.0	24.0	0.8
7-May-03	158	13.5	4.0	97.0	51.0	10.5	4.8	0.0	24.0	0.6
8-May-03	159	12.0	3.5	100.0	71.0	7.8	5.2	0.0	24.0	0.4
9-May-03	160	4.5	0.0	87.0	64.0	21.5	0.0	0.0	24.0	0.6
10-May-03	161	11.5	-3.0	87.0	27.0	12.5	0.0	0.0	24.0	0.6
11-May-03	162	18.0	-3.0	94.0	16.0	13.0	0.0	0.0	24.0	0.8
12-May-03	163	22.5	2.5	50.0	17.0	14.8	0.0	0.0	24.0	1.1
13-May-03	164	24.0	2.5	82.0	21.0	7.2	0.0	0.0	24.0	0.7
14-May-03	165	24.0	3.5	94.0	27.0	9.2	0.0	0.0	24.0	0.7
15-May-03	166	22.0	9.0	64.0	30.0	14.8	0.6	0.0	24.0	1.1
16-May-03	167	17.0	9.5	94.0	61.0	14.3	7.6	0.0	24.0	0.7
17-May-03	168	16.5	5.0	79.0	25.0	25.2	0.2	0.0	24.0	1.3
18-May-03	169	7.0	1.0	73.0	35.0	24.5	0.0	0.0	24.0	1.0
19-May-03	170	10.5	0.0	64.0	27.0	20.0	0.0	0.0	24.0	1.0
20-May-03	171	14.0	1.0	87.0	39.0	7.7	0.0	0.0	24.0	0.6
21-May-03	172	20.0	0.0	100.0	21.0	13.0	0.0	0.0	24.0	0.8
22-May-03	173	21.5	2.5	95.0	25.0	12.8	0.0	0.0	24.0	0.8
23-May-03	174	21.5	8.0	76.0	40.0	8.3	0.8	0.0	24.0	0.8
24-May-03	175	16.5	7.5	99.0	63.0	8.8	0.0	0.0	24.0	0.6
25-May-03	176	22.0	9.0	95.0	47.0	11.5	0.0	0.0	24.0	0.8
26-May-03	177	26.5	11.0	81.0	37.0	12.7	1.6	0.0	24.0	1.0
27-May-03	178	23.5	13.0	97.0	27.0	18.0	1.8	0.0	24.0	1.2
28-May-03	179	24.5	8.5	62.0	26.0	10.4	0.0	0.0	24.0	1.0
29-May-03	180	15.0	10.5	80.0	47.0	19.2	0.0	0.0	24.0	1.1
30-May-03	181	15.5	4.0	78.0	29.0	9.7	0.0	0.0	24.0	0.8
31-May-03	182	23.0	4.0	83.0	34.0	10.6	0.0	0.0	24.0	0.8
1-Jun-03	183	24.5	8.0	100.0	30.0	5.8	0.0	0.0	24.0	0.7
2-Jun-03	184	24.0	10.0	92.0	32.0	8.3	0.0	0.0	24.0	4.0
3-Jun-03	185	20.0	12.0	91.0	59.0	10.1	0.8	0.0	24.0	3.8
4-Jun-03	186	18.0	11.0	97.0	75.0	9.0	11.8	0.0	24.0	3.1
5-Jun-03	187	15.5	12.5	98.0	93.0	4.8	24.0	0.0	24.0	2.8
6-Jun-03	188	15.0	7.0	92.0	48.0	15.4	7.2	0.0	24.0	4.2
7-Jun-03	189	16.0	7.0	81.0	49.0	7.0	0.0	0.0	24.0	3.4
8-Jun-03	190	15.5	7.5	90.0	42.0	8.1	3.4	0.0	24.0	3.6
9-Jun-03	191	19.5	8.0	97.0	33.0	7.8	0.0	0.0	24.0	3.7
10-Jun-03	192	22.5	10.5	63.0	29.0	6.4	0.2	0.0	24.0	4.2
11-Jun-03	193	22.5	8.5	86.0	33.0	9.2	0.0	0.0	24.0	4.3
12-Jun-03	194	23.0	12.0	84.0	46.0	7.8	1.6	0.0	24.0	4.0
13-Jun-03	195	23.5	10.5	87.0	45.0	9.8	0.0	0.0	24.0	4.2
14-Jun-03	196	26.5	16.5	92.0	46.0	16.4	19.2	0.0	24.0	5.6
15-Jun-03	197	24.5	14.0	93.0	37.0	10.3	0.0	0.0	24.0	4.6
16-Jun-03	198	26.0	11.5	86.0	26.0	12.9	0.0	0.0	24.0	5.5
17-Jun-03	199	23.0	13.0	72.0	34.0	18.5	0.0	0.0	24.0	6.8
18-Jun-03	200	25.0	9.0	79.0	30.0	8.5	0.0	0.0	24.0	4.5

19-Jun-03	201	30.5	16.0	65.0	35.0	15.9	0.2	0.0	24.0	7.1
20-Jun-03	202	20.5	17.0	94.0	83.0	10.6	21.6	0.0	24.0	3.7
21-Jun-03	203	17.0	11.0	100.0	93.0	12.0	8.6	0.0	24.0	2.8
22-Jun-03	204	21.0	13.5	93.0	43.0	25.1	0.0	0.0	24.0	6.5
23-Jun-03	205	17.5	11.0	77.0	48.0	19.1	0.6	0.0	24.0	5.7
24-Jun-03	206	19.0	6.0	87.0	42.0	10.8	0.0	0.0	24.0	4.0
25-Jun-03	207	21.0	8.0	92.0	38.0	4.2	0.6	0.0	24.0	3.2
26-Jun-03	208	23.5	7.0	96.0	34.0	8.8	0.0	0.0	24.0	3.9
27-Jun-03	209	21.5	10.0	93.0	50.0	9.4	19.0	0.0	24.0	3.8
28-Jun-03	210	23.0	13.0	89.0	41.0	12.3	0.0	0.0	24.0	4.8
29-Jun-03	211	22.5	12.0	89.0	44.0	7.3	0.4	0.0	24.0	3.9
30-Jun-03	212	16.5	11.5	84.0	52.0	10.2	2.8	0.0	24.0	4.1
1-Jul-03	213	16.0	11.0	95.0	67.0	13.1	7.2	0.0	24.0	3.7
2-Jul-03	214	22.0	14.5	94.0	73.0	5.9	18.8	0.0	24.0	3.2
3-Jul-03	215	22.0	13.0	95.0	43.0	19.2	0.0	0.0	24.0	5.3
4-Jul-03	216	20.5	11.5	86.0	58.0	11.3	5.4	0.0	24.0	3.9
5-Jul-03	217	15.0	11.0	89.0	73.0	10.4	0.4	0.0	24.0	3.3
6-Jul-03	218	14.0	8.5	90.0	71.0	21.1	0.0	0.0	24.0	3.9
7-Jul-03	219	18.0	10.5	86.0	49.0	10.7	0.4	0.0	24.0	3.9
8-Jul-03	220	21.5	7.0	97.0	42.0	7.5	0.0	0.0	24.0	3.3
9-Jul-03	221	22.0	13.5	87.0	52.0	10.9	21.4	0.0	24.0	4.1
10-Jul-03	222	22.0	15.0	98.0	63.0	13.2	4.6	0.0	24.0	3.9
11-Jul-03	223	26.5	14.0	95.0	39.0	8.6	0.0	0.0	24.0	4.0
12-Jul-03	224	30.0	14.0	86.0	38.0	14.8	2.0	0.0	24.0	5.4
13-Jul-03	225	24.0	15.5	99.0	36.0	14.3	0.0	0.0	24.0	4.9
14-Jul-03	226	22.5	11.0	81.0	37.0	8.3	0.0	0.0	24.0	4.0
15-Jul-03	227	27.5	14.0	79.0	33.0	17.4	0.0	0.0	24.0	6.2
16-Jul-03	228	21.0	10.0	90.0	36.0	8.9	0.0	0.0	24.0	3.8
17-Jul-03	229	24.0	13.5	76.0	43.0	16.5	0.0	0.0	24.0	5.6
18-Jul-03	230	27.0	16.0	82.0	32.0	13.2	0.0	0.0	24.0	5.5
19-Jul-03	231	23.0	14.5	83.0	49.0	11.7	0.0	0.0	24.0	4.4
20-Jul-03	232	21.0	13.5	93.0	58.0	11.7	0.0	0.0	24.0	3.8
21-Jul-03	233	25.0	10.5	89.0	35.0	3.8	0.0	0.0	24.0	3.1
22-Jul-03	234	26.5	12.0	97.0	36.0	10.8	3.0	0.0	24.0	4.1
23-Jul-03	235	28.5	17.0	92.0	45.0	8.9	0.0	0.0	24.0	4.1
24-Jul-03	236	29.5	14.0	82.0	28.0	8.1	0.0	0.0	24.0	4.3
25-Jul-03	237	25.0	15.0	79.0	45.0	6.3	0.0	0.0	24.0	3.7
26-Jul-03	238	26.0	14.5	90.0	47.0	9.4	0.0	0.0	24.0	3.9
27-Jul-03	239	29.5	15.0	94.0	36.0	7.8	0.0	0.0	24.0	3.9
28-Jul-03	240	30.0	16.5	83.0	34.0	11.1	0.0	0.0	24.0	4.8
29-Jul-03	241	23.5	13.5	94.0	53.0	12.8	9.8	0.0	24.0	3.9
30-Jul-03	242	25.0	16.5	96.0	55.0	13.5	0.0	0.0	24.0	4.0
31-Jul-03	243	28.0	15.5	93.0	43.0	6.5	0.0	0.0	24.0	3.5
1-Aug-03	244	29.0	14.0	99.0	31.0	5.1	0.0	0.0	24.0	3.2
2-Aug-03	245	29.0	15.5	100.0	37.0	5.2	0.0	0.0	24.0	3.0
3-Aug-03	246	26.0	18.0	85.0	50.0	12.2	0.4	0.0	24.0	4.0
4-Aug-03	247	25.0	20.0	88.0	67.0	6.6	1.4	0.0	24.0	3.1
5-Aug-03	248	20.0	15.5	89.0	54.0	15.5	0.0	0.0	24.0	3.9
6-Aug-03	249	23.0	10.0	93.0	46.0	8.5	0.0	0.0	24.0	2.9
7-Aug-03	250	26.0	12.5	93.0	55.0	10.0	15.6	0.0	24.0	3.0
8-Aug-03	251	24.0	17.0	99.0	73.0	7.4	3.0	0.0	24.0	2.6

9-Aug-03	252	26.0	16.5	90.0	47.0	11.8	0.0	0.0	24.0	3.7
10-Aug-03	253	25.5	13.5	100.0	45.0	7.7	0.0	0.0	24.0	2.9
11-Aug-03	254	27.5	19.0	87.0	59.0	10.3	0.0	0.0	24.0	3.4
12-Aug-03	255	27.5	16.5	90.0	48.0	7.2	0.0	0.0	24.0	3.1
13-Aug-03	256	33.0	18.5	92.0	39.0	7.3	0.0	0.0	24.0	3.4
14-Aug-03	257	29.5	19.5	60.0	32.0	15.5	0.0	0.0	24.0	5.9
15-Aug-03	258	28.5	16.0	79.0	35.0	5.6	0.0	0.0	24.0	3.1
16-Aug-03	259	30.5	20.0	72.0	37.0	10.0	0.0	0.0	24.0	4.3
17-Aug-03	260	28.5	23.5	58.0	38.0	14.8	0.0	0.0	24.0	6.1
18-Aug-03	261	29.0	17.5	64.0	27.0	10.6	0.0	0.0	24.0	4.7
19-Aug-03	262	31.5	19.0	60.0	27.0	15.8	0.0	0.0	24.0	6.0
20-Aug-03	263	19.0	14.0	94.0	65.0	11.9	3.0	0.0	24.0	2.9
21-Aug-03	264	24.0	12.5	82.0	39.0	16.8	0.4	0.0	24.0	4.2
22-Aug-03	265	26.5	13.5	86.0	47.0	13.2	0.0	0.0	24.0	3.5
23-Aug-03	266	21.0	18.0	90.0	65.0	15.4	1.2	0.0	24.0	3.4
24-Aug-03	267	24.0	12.5	80.0	22.0	15.2	0.0	0.0	24.0	4.5
25-Aug-03	268	22.5	11.5	61.0	28.0	20.6	0.2	0.0	24.0	5.8
26-Aug-03	269	19.5	11.5	78.0	48.0	15.8	0.0	0.0	24.0	3.8
27-Aug-03	270	20.0	9.0	83.0	46.0	8.4	0.0	0.0	24.0	2.5
28-Aug-03	271	19.5	10.0	94.0	45.0	12.2	0.0	0.0	24.0	2.8
29-Aug-03	272	20.0	5.5	91.0	36.0	12.7	0.0	0.0	24.0	2.8
30-Aug-03	273	24.5	10.5	79.0	34.0	12.3	0.8	0.0	24.0	3.3
31-Aug-03	274	19.0	8.0	98.0	45.0	7.9	0.0	0.0	24.0	2.1
1-Sep-03	275	19.5	10.5	95.0	58.0	14.7	19.8	0.0	24.0	2.5
2-Sep-03	276	18.5	10.0	97.0	46.0	22.0	11.4	0.0	24.0	3.0
3-Sep-03	277	20.5	5.5	100.0	45.0	10.8	0.0	0.0	24.0	1.9
4-Sep-03	278	27.0	12.5	85.0	41.0	11.0	0.0	0.0	24.0	2.6
5-Sep-03	279	22.0	10.0	93.0	39.0	6.6	0.0	0.0	24.0	1.9
6-Sep-03	280	24.0	12.0	88.0	46.0	7.8	0.0	0.0	24.0	2.1
7-Sep-03	281	24.0	12.5	96.0	54.0	9.0	0.0	0.0	24.0	2.0
8-Sep-03	282	27.5	15.5	80.0	55.0	12.3	0.0	0.0	24.0	2.8
9-Sep-03	283	25.0	17.5	78.0	52.0	13.2	0.4	0.0	24.0	3.1
10-Sep-03	284	17.0	13.5	75.0	64.0	30.1	0.4	0.0	24.0	4.3
11-Sep-03	285	21.0	10.5	88.0	35.0	12.5	0.0	0.0	24.0	2.6
12-Sep-03	286	17.0	11.5	80.0	69.0	8.2	9.6	0.0	24.0	1.9
13-Sep-03	287	13.0	10.0	95.0	69.0	20.2	0.2	0.0	24.0	2.1
14-Sep-03	288	17.0	3.0	100.0	42.0	4.0	0.0	0.0	24.0	1.1
15-Sep-03	289	15.5	10.5	87.0	66.0	8.8	2.6	0.0	24.0	1.7
16-Sep-03	290	9.5	6.5	89.0	69.0	16.4	0.0	0.0	24.0	1.9
17-Sep-03	291	9.0	4.5	99.0	89.0	13.1	12.8	0.0	24.0	1.1
18-Sep-03	292	9.0	4.5	97.0	74.0	17.8	0.6	0.0	24.0	1.4
19-Sep-03	293	9.5	1.5	100.0	64.0	7.8	0.2	0.0	24.0	1.1
20-Sep-03	294	12.0	4.5	86.0	64.0	7.5	1.2	0.0	24.0	1.3
21-Sep-03	295	11.0	8.0	99.0	88.0	4.2	2.2	0.0	24.0	1.1
22-Sep-03	296	12.5	4.0	93.0	50.0	8.4	0.0	0.0	24.0	1.3
23-Sep-03	297	8.0	4.5	97.0	80.0	12.4	17.2	0.0	24.0	1.1
24-Sep-03	298	9.5	1.5	96.0	64.0	16.5	0.6	0.0	24.0	1.3
25-Sep-03	299	8.0	4.0	94.0	76.0	10.6	3.8	0.0	24.0	1.1
26-Sep-03	300	8.0	5.5	95.0	80.0	11.9	0.0	0.0	24.0	1.2
27-Sep-03	301	10.0	4.0	96.0	71.0	4.4	0.6	0.0	24.0	0.9
28-Sep-03	302	7.5	3.5	83.0	47.0	16.1	0.0	0.0	24.0	1.9

29-Sep-03	303	6.5	0.5	94.0	54.0	14.1	1.4	0.0	24.0	1.3
30-Sep-03	304	5.5	-0.5	86.0	49.0	9.9	0.0	0.0	24.0	1.2
1-Oct-03	305	9.5	-1.5	77.0	51.0	13.1	0.0	0.0	24.0	1.4
2-Oct-03	306	15.5	2.5	99.0	44.0	10.8	0.0	0.0	24.0	1.4
3-Oct-03	307	18.5	6.0	84.0	43.0	8.5	0.0	0.0	24.0	1.6
4-Oct-03	308	21.0	3.0	99.0	46.0	4.2	0.0	0.0	24.0	0.8
5-Oct-03	309	20.0	5.5	100.0	49.0	5.4	0.0	0.0	24.0	1.0
6-Oct-03	310	22.5	4.0	100.0	41.0	7.0	0.0	0.0	24.0	1.0
7-Oct-03	311	13.0	6.0	97.0	68.0	9.8	0.0	0.0	24.0	1.1
8-Oct-03	312	12.0	3.5	93.0	65.0	12.6	0.2	0.0	24.0	1.2
9-Oct-03	313	16.0	7.0	99.0	68.0	8.8	0.2	0.0	24.0	1.1
10-Oct-03	314	16.5	5.5	87.0	41.0	12.5	0.2	0.0	24.0	1.8
11-Oct-03	315	12.5	5.0	94.0	56.0	10.2	0.0	0.0	24.0	1.2
12-Oct-03	316	13.5	0.5	100.0	57.0	3.5	0.0	0.0	24.0	0.6
13-Oct-03	317	7.5	1.5	93.0	54.0	14.8	0.0	0.0	24.0	1.4
14-Oct-03	318	5.0	0.0	89.0	49.0	16.7	0.2	0.0	24.0	1.6
15-Oct-03	319	2.0	0.0	87.0	54.0	15.8	0.0	0.0	24.0	1.6
16-Oct-03	320	5.5	0.5	79.0	46.0	4.0	0.0	0.0	24.0	0.9
17-Oct-03	321	4.5	0.5	97.0	68.0	12.8	2.2	0.0	24.0	1.0
18-Oct-03	322	6.0	0.0	94.0	68.0	5.5	0.0	0.0	24.0	0.7
19-Oct-03	323	8.0	3.5	88.0	71.0	12.5	2.6	0.0	24.0	1.2
20-Oct-03	324	7.5	3.0	98.0	91.0	6.9	0.6	0.0	24.0	0.6
21-Oct-03	325	9.0	1.5	99.0	66.0	6.9	0.8	0.0	24.0	0.7
22-Oct-03	326	8.0	4.5	78.0	65.0	23.1	0.2	0.0	24.0	2.2
23-Oct-03	327	1.0	0.0	96.0	81.0	13.5	6.0	0.0	24.0	0.9
24-Oct-03	328	-0.5	-2.5	94.0	79.0	21.8	3.4	0.0	24.0	0.0
25-Oct-03	329	0.5	-6.0	92.0	80.0	11.1	0.6	0.0	24.0	0.0
26-Oct-03	330	0.5	-1.5	92.0	74.0	7.5	5.2	0.0	24.0	0.0
27-Oct-03	331	0.5	-0.5	99.0	97.0	7.6	12.4	0.0	24.0	0.0
28-Oct-03	332	0.5	-0.5	97.0	88.0	6.1	1.6	0.0	24.0	0.0
29-Oct-03	333	-1.5	-2.5	94.0	88.0	12.7	1.6	0.0	24.0	0.0
30-Oct-03	334	-2.5	-5.0	93.0	72.0	13.3	0.8	0.0	24.0	0.0
31-Oct-03	335	-7.5	-9.5	90.0	61.0	8.7	1.6	0.0	24.0	0.0
1-Nov-03	336	-6.0	-13.0	90.0	70.0	18.9	1.4	0.0	24.0	0.0
2-Nov-03	337	-9.0	-16.0	80.0	70.0	22.0	0.0	0.0	24.0	0.0
3-Nov-03	338	-7.0	-15.5	98.0	80.0	2.1	2.2	0.0	24.0	0.0
4-Nov-03	339	-7.5	-17.0	96.0	64.0	2.4	0.0	0.0	24.0	0.0
5-Nov-03	340	-8.0	-17.0	91.0	66.0	14.4	1.2	0.0	24.0	0.0
6-Nov-03	341	-13.0	-16.5	82.0	61.0	18.7	0.4	0.0	24.0	0.0
7-Nov-03	342	-12.0	-23.5	79.0	53.0	9.8	0.0	0.0	24.0	0.0
8-Nov-03	343	-2.5	-14.0	89.0	61.0	12.3	0.0	0.0	24.0	0.0
9-Nov-03	344	-2.0	-15.5	98.0	69.0	8.6	0.0	0.0	24.0	0.0
10-Nov-03	345	-2.0	-10.0	88.0	69.0	14.0	0.0	0.0	24.0	0.0
11-Nov-03	346	-1.5	-5.0	91.0	65.0	12.5	0.0	0.0	24.0	0.0
12-Nov-03	347	-4.0	-11.0	78.0	58.0	15.8	0.0	0.0	24.0	0.0
13-Nov-03	348	3.5	-16.0	84.0	63.0	11.8	0.0	0.0	24.0	0.0
14-Nov-03	349	6.5	-7.0	96.0	51.0	7.8	0.0	0.0	24.0	0.0
15-Nov-03	350	3.0	-5.5	87.0	62.0	5.3	0.0	0.0	24.0	0.0
16-Nov-03	351	-1.5	-11.5	98.0	92.0	8.0	0.0	0.0	24.0	0.0
17-Nov-03	352	-0.5	-6.5	96.0	88.0	7.1	1.2	0.0	24.0	0.0
18-Nov-03	353	-1.5	-3.0	93.0	85.0	9.5	0.0	0.0	24.0	0.0

19-Nov-03	354	-2.0	-5.0	94.0	89.0	4.2	2.0	0.0	24.0	0.0
20-Nov-03	355	-9.5	-14.0	84.0	69.0	19.3	0.0	0.0	24.0	0.0
21-Nov-03	356	-12.5	-16.5	78.0	69.0	12.8	0.0	0.0	24.0	0.0
22-Nov-03	357	-11.5	-20.5	90.0	70.0	3.2	0.0	0.0	24.0	0.0
23-Nov-03	358	-13.0	-21.5	78.0	63.0	8.8	0.0	0.0	24.0	0.0
24-Nov-03	359	-11.0	-18.0	81.0	66.0	14.8	1.2	0.0	24.0	0.0
25-Nov-03	360	-9.5	-13.5	92.0	83.0	3.2	0.4	0.0	24.0	0.0
26-Nov-03	361	-7.5	-21.0	93.0	62.0	0.8	0.4	0.0	24.0	0.0
27-Nov-03	362	-8.5	-12.0	90.0	79.0	10.7	0.4	0.0	24.0	0.0
28-Nov-03	363	-4.5	-23.0	80.0	70.0	14.5	1.0	0.0	24.0	0.0
29-Nov-03	364	-6.0	-10.5	80.0	64.0	14.7	0.0	0.0	24.0	0.0
30-Nov-03	365	-9.5	-14.5	70.0	54.0	16.4	0.0	0.0	24.0	0.0

Table B-7. Flin Flon climate - average year.

Date	Day	Temp (°C)		RH (%)		Wind	Precip	Precip Period		P.E.
		Max	Min	Max	Min	(m/s)	(mm)	Start	End	(mm/day)
1-Dec-01	1	-8.9	-16.1	80.5	62.3	9.0	8.0	0.0	24.0	0.0
2-Dec-01	2	-8.0	-17.6	85.5	75.3	8.8	1.0	0.0	24.0	0.0
3-Dec-01	3	-8.1	-14.1	85.0	76.0	10.1	3.6	0.0	24.0	0.0
4-Dec-01	4	-13.1	-19.4	78.3	63.8	11.7	0.2	0.0	24.0	0.0
5-Dec-01	5	-10.8	-23.1	80.8	73.0	7.4	0.3	0.0	24.0	0.0
6-Dec-01	6	-9.5	-16.6	84.3	66.3	9.3	1.2	0.0	24.0	0.0
7-Dec-01	7	-12.3	-19.8	77.5	65.0	9.2	0.2	0.0	24.0	0.0
8-Dec-01	8	-9.0	-22.6	82.3	67.8	10.9	0.1	0.0	24.0	0.0
9-Dec-01	9	-9.8	-18.6	92.0	68.8	10.2	0.3	0.0	24.0	0.0
10-Dec-01	10	-12.0	-19.4	78.8	67.8	12.9	0.5	0.0	24.0	0.0
11-Dec-01	11	-12.6	-17.8	80.0	72.3	7.5	1.9	0.0	24.0	0.0
12-Dec-01	12	-14.8	-19.3	79.3	71.3	5.1	0.1	0.0	24.0	0.0
13-Dec-01	13	-11.3	-18.5	82.0	76.8	8.1	0.8	0.0	24.0	0.0
14-Dec-01	14	-11.8	-20.3	83.5	70.0	8.0	0.2	0.0	24.0	0.0
15-Dec-01	15	-13.4	-20.9	78.0	69.5	12.0	0.2	0.0	24.0	0.0
16-Dec-01	16	-12.1	-21.5	78.5	64.3	10.2	0.2	0.0	24.0	0.0
17-Dec-01	17	-10.4	-17.0	79.3	71.8	9.6	0.3	0.0	24.0	0.0
18-Dec-01	18	-11.6	-17.8	80.8	66.8	8.0	2.2	0.0	24.0	0.0
19-Dec-01	19	-12.6	-22.6	76.8	64.3	16.3	1.4	0.0	24.0	0.0
20-Dec-01	20	-17.1	-23.6	72.0	64.0	12.0	0.5	0.0	24.0	0.0
21-Dec-01	21	-16.0	-23.1	73.0	68.0	9.4	0.5	0.0	24.0	0.0
22-Dec-01	22	-12.4	-24.1	76.8	64.3	7.9	0.0	0.0	24.0	0.0
23-Dec-01	23	-13.5	-22.1	80.0	74.0	5.9	0.1	0.0	24.0	0.0
24-Dec-01	24	-8.4	-21.9	80.8	69.0	7.8	0.2	0.0	24.0	0.0
25-Dec-01	25	-7.1	-19.9	71.8	61.5	12.7	0.0	0.0	24.0	0.0
26-Dec-01	26	-11.6	-20.9	82.0	70.3	9.1	1.3	0.0	24.0	0.0
27-Dec-01	27	-7.5	-18.4	82.5	72.0	14.3	1.0	0.0	24.0	0.0
28-Dec-01	28	-10.1	-14.6	84.0	75.3	10.2	2.2	0.0	24.0	0.0
29-Dec-01	29	-14.0	-19.3	79.5	67.0	9.7	3.2	0.0	24.0	0.0
30-Dec-01	30	-15.0	-19.5	76.8	63.0	8.9	0.9	0.0	24.0	0.0
31-Dec-01	31	-15.0	-23.4	74.3	65.5	9.0	0.0	0.0	24.0	0.0
1-Jan-02	32	-14.5	-23.6	81.3	70.8	7.9	0.0	0.0	24.0	0.0
2-Jan-02	33	-13.0	-22.8	87.0	74.8	5.6	0.0	0.0	24.0	0.0
3-Jan-02	34	-10.8	-18.4	82.5	77.3	5.0	0.3	0.0	24.0	0.0
4-Jan-02	35	-9.0	-19.4	84.5	69.8	8.3	0.0	0.0	24.0	0.0
5-Jan-02	36	-13.9	-21.5	77.0	68.5	7.9	1.8	0.0	24.0	0.0
6-Jan-02	37	-7.1	-18.4	82.8	74.0	8.4	0.1	0.0	24.0	0.0
7-Jan-02	38	-4.0	-13.9	88.8	70.8	7.2	0.7	0.0	24.0	0.0
8-Jan-02	39	-1.8	-13.1	87.8	65.8	11.9	0.9	0.0	24.0	0.0
9-Jan-02	40	-4.6	-13.0	86.8	70.0	12.6	0.6	0.0	24.0	0.0
10-Jan-02	41	-12.0	-18.8	77.5	67.5	11.4	0.2	0.0	24.0	0.0
11-Jan-02	42	-12.6	-22.5	75.3	61.0	6.3	0.1	0.0	24.0	0.0
12-Jan-02	43	-14.5	-23.8	75.8	64.0	9.0	0.0	0.0	24.0	0.0
13-Jan-02	44	-16.1	-24.4	72.5	62.8	6.1	1.2	0.0	24.0	0.0
14-Jan-02	45	-14.9	-22.6	68.8	58.5	8.7	0.3	0.0	24.0	0.0
15-Jan-02	46	-15.5	-23.1	73.0	56.0	7.8	0.2	0.0	24.0	0.0
16-Jan-02	47	-11.6	-28.5	73.5	55.8	7.8	0.7	0.0	24.0	0.0

17-Jan-02	48	-12.4	-21.0	78.5	62.3	15.9	0.3	0.0	24.0	0.0
18-Jan-02	49	-15.8	-26.8	70.0	60.0	9.2	0.1	0.0	24.0	0.0
19-Jan-02	50	-17.3	-30.1	72.3	61.0	9.2	0.0	0.0	24.0	0.0
20-Jan-02	51	-19.8	-27.3	73.8	61.3	10.6	0.1	0.0	24.0	0.0
21-Jan-02	52	-19.8	-27.9	72.0	63.8	8.1	0.6	0.0	24.0	0.0
22-Jan-02	53	-18.0	-25.8	71.3	58.8	11.0	0.5	0.0	24.0	0.0
23-Jan-02	54	-17.3	-29.6	73.5	57.3	8.4	0.3	0.0	24.0	0.0
24-Jan-02	55	-14.9	-28.4	69.0	54.5	10.7	0.1	0.0	24.0	0.0
25-Jan-02	56	-13.8	-26.0	72.5	59.5	15.6	0.0	0.0	24.0	0.0
26-Jan-02	57	-13.5	-26.4	74.5	61.0	7.3	0.9	0.0	24.0	0.0
27-Jan-02	58	-14.6	-24.4	77.8	63.0	7.9	0.0	0.0	24.0	0.0
28-Jan-02	59	-12.4	-25.3	78.8	55.8	9.4	0.0	0.0	24.0	0.0
29-Jan-02	60	-11.4	-24.6	78.5	65.5	6.4	1.0	0.0	24.0	0.0
30-Jan-02	61	-12.6	-21.1	72.3	56.8	8.6	0.8	0.0	24.0	0.0
31-Jan-02	62	-15.9	-23.0	74.3	65.8	8.2	0.0	0.0	24.0	0.0
1-Feb-02	63	-12.9	-25.9	80.5	65.5	8.3	2.2	0.0	24.0	0.0
2-Feb-02	64	-9.8	-19.6	83.3	67.3	9.6	0.2	0.0	24.0	0.0
3-Feb-02	65	-10.5	-20.9	77.8	63.3	9.0	0.4	0.0	24.0	0.0
4-Feb-02	66	-6.0	-18.6	81.0	64.0	9.4	0.6	0.0	24.0	0.0
5-Feb-02	67	-11.9	-20.6	79.3	63.5	9.6	1.4	0.0	24.0	0.0
6-Feb-02	68	-11.4	-22.4	75.0	60.3	10.6	1.4	0.0	24.0	0.0
7-Feb-02	69	-10.4	-23.3	77.8	53.8	9.3	0.6	0.0	24.0	0.0
8-Feb-02	70	-11.8	-24.5	69.5	49.3	11.2	1.4	0.0	24.0	0.0
9-Feb-02	71	-17.5	-27.4	63.5	48.8	12.0	0.0	0.0	24.0	0.0
10-Feb-02	72	-15.3	-31.1	64.3	48.5	10.4	1.6	0.0	24.0	0.0
11-Feb-02	73	-13.4	-24.3	64.0	47.3	13.1	0.2	0.0	24.0	0.0
12-Feb-02	74	-15.8	-27.0	67.8	50.3	6.6	0.5	0.0	24.0	0.0
13-Feb-02	75	-11.5	-28.6	71.0	54.3	8.4	0.4	0.0	24.0	0.0
14-Feb-02	76	-11.5	-21.8	77.0	52.3	10.5	1.1	0.0	24.0	0.0
15-Feb-02	77	-13.4	-23.1	72.3	52.0	12.2	1.2	0.0	24.0	0.0
16-Feb-02	78	-13.3	-22.8	76.5	59.0	8.8	0.2	0.0	24.0	0.0
17-Feb-02	79	-6.0	-21.3	80.8	56.5	11.8	0.0	0.0	24.0	0.0
18-Feb-02	80	-10.0	-19.1	73.5	49.0	7.4	0.3	0.0	24.0	0.0
19-Feb-02	81	-12.1	-22.6	73.3	58.8	11.6	0.4	0.0	24.0	0.0
20-Feb-02	82	-11.4	-22.5	69.5	45.8	9.3	0.0	0.0	24.0	0.0
21-Feb-02	83	-8.1	-25.0	78.0	44.5	8.0	0.0	0.0	24.0	0.0
22-Feb-02	84	-7.1	-20.4	74.3	43.8	8.1	0.1	0.0	24.0	0.0
23-Feb-02	85	-11.6	-24.3	77.0	50.8	10.3	0.2	0.0	24.0	0.0
24-Feb-02	86	-9.5	-19.1	69.5	50.8	9.3	0.5	0.0	24.0	0.0
25-Feb-02	87	-10.4	-20.1	74.5	53.0	9.1	0.2	0.0	24.0	0.0
26-Feb-02	88	-7.4	-19.6	73.8	46.5	11.5	0.2	0.0	24.0	0.0
27-Feb-02	89	-8.3	-22.0	75.8	46.0	8.8	0.4	0.0	24.0	0.0
28-Feb-02	90	-8.4	-20.3	76.5	53.3	10.9	2.2	0.0	24.0	0.0
1-Mar-02	91	-9.6	-19.4	76.0	55.5	13.7	0.6	0.0	24.0	0.0
2-Mar-02	92	-8.0	-26.5	80.0	51.8	6.9	0.1	0.0	24.0	0.0
3-Mar-02	93	-6.9	-20.1	83.3	48.5	10.5	0.6	0.0	24.0	0.0
4-Mar-02	94	-6.3	-16.9	73.3	42.0	12.5	0.0	0.0	24.0	0.0
5-Mar-02	95	-6.0	-21.5	77.0	42.8	8.2	0.1	0.0	24.0	0.0
6-Mar-02	96	-8.5	-17.5	74.3	44.5	11.7	0.0	0.0	24.0	0.0
7-Mar-02	97	-7.4	-20.0	75.3	40.5	8.2	0.0	0.0	24.0	0.0
8-Mar-02	98	-6.9	-21.0	77.0	56.8	13.5	1.9	0.0	24.0	0.0

9-Mar-02	99	-8.0	-21.4	74.0	43.0	13.7	0.0	0.0	24.0	0.0
10-Mar-02	100	-10.4	-27.0	68.0	37.5	6.5	0.5	0.0	24.0	0.0
11-Mar-02	101	-8.8	-19.1	76.0	55.3	10.6	0.4	0.0	24.0	0.0
12-Mar-02	102	-6.6	-22.0	75.3	44.5	8.1	0.3	0.0	24.0	0.0
13-Mar-02	103	-5.5	-18.1	74.5	42.8	10.6	0.3	0.0	24.0	0.0
14-Mar-02	104	-6.5	-18.6	70.3	47.5	9.7	1.1	0.0	24.0	0.0
15-Mar-02	105	-5.4	-17.4	84.5	64.0	6.2	3.6	0.0	24.0	0.0
16-Mar-02	106	-6.8	-16.8	80.8	58.0	6.9	0.1	0.0	24.0	0.0
17-Mar-02	107	-5.6	-18.6	78.8	54.8	8.3	0.0	0.0	24.0	0.0
18-Mar-02	108	-0.1	-13.5	83.5	49.5	10.5	1.4	0.0	24.0	0.0
19-Mar-02	109	-0.1	-13.1	79.5	51.3	8.8	2.2	0.0	24.0	0.0
20-Mar-02	110	-1.3	-17.0	81.3	39.5	12.8	0.0	0.0	24.0	0.0
21-Mar-02	111	-1.3	-12.8	73.3	45.8	14.0	0.1	0.0	24.0	0.0
22-Mar-02	112	0.8	-10.6	77.5	43.5	13.4	0.0	0.0	24.0	0.0
23-Mar-02	113	-1.0	-9.9	76.5	41.8	15.2	0.3	0.0	24.0	0.0
24-Mar-02	114	-1.4	-12.3	74.5	47.5	15.2	0.0	0.0	24.0	0.0
25-Mar-02	115	-0.4	-12.4	77.3	47.8	9.1	0.2	0.0	24.0	0.0
26-Mar-02	116	2.4	-9.3	78.0	51.8	9.5	0.0	0.0	24.0	0.0
27-Mar-02	117	-0.5	-8.6	82.3	60.0	11.2	1.2	0.0	24.0	0.0
28-Mar-02	118	-1.8	-9.5	84.0	60.8	11.9	0.1	0.0	24.0	0.0
29-Mar-02	119	-1.6	-9.0	88.0	67.5	13.9	2.1	0.0	24.0	0.0
30-Mar-02	120	0.3	-12.8	85.8	52.3	12.8	1.2	0.0	24.0	0.0
31-Mar-02	121	2.0	-7.5	89.5	51.0	13.0	0.1	0.0	24.0	0.0
1-Apr-02	122	-1.3	-11.1	91.0	64.5	10.3	0.2	0.0	24.0	0.0
2-Apr-02	123	0.8	-12.3	84.3	46.3	9.0	0.1	0.0	24.0	0.0
3-Apr-02	124	0.0	-11.5	78.0	39.3	9.8	0.1	0.0	24.0	0.0
4-Apr-02	125	0.9	-10.8	74.3	36.3	8.2	0.5	0.0	24.0	0.0
5-Apr-02	126	0.1	-11.0	83.3	43.5	8.6	0.1	0.0	24.0	0.0
6-Apr-02	127	1.0	-10.3	80.5	38.5	11.2	1.4	0.0	24.0	0.0
7-Apr-02	128	2.0	-10.4	85.3	37.8	6.0	0.0	0.0	24.0	0.0
8-Apr-02	129	3.9	-10.4	87.3	42.3	8.0	0.1	0.0	24.0	0.0
9-Apr-02	130	4.8	-8.9	91.8	38.3	7.8	0.2	0.0	24.0	0.0
10-Apr-02	131	4.4	-9.4	76.8	42.5	12.0	0.0	0.0	24.0	0.0
11-Apr-02	132	5.6	-5.0	88.5	51.8	9.0	1.5	0.0	24.0	0.0
12-Apr-02	133	2.8	-4.5	81.5	56.8	10.8	1.9	0.0	24.0	0.0
13-Apr-02	134	4.9	-4.4	87.5	58.0	8.9	0.4	0.0	24.0	0.0
14-Apr-02	135	0.9	-7.8	84.8	46.8	15.2	2.0	0.0	24.0	0.0
15-Apr-02	136	-0.1	-10.4	74.5	46.0	12.6	0.1	0.0	24.0	0.0
16-Apr-02	137	2.3	-11.1	78.3	39.3	9.4	1.9	0.0	24.0	0.0
17-Apr-02	138	5.0	-5.4	79.8	54.0	9.6	1.0	0.0	24.0	0.0
18-Apr-02	139	8.5	-3.4	85.5	50.0	9.2	0.5	0.0	24.0	0.0
19-Apr-02	140	8.6	-4.3	89.5	44.3	7.0	0.9	0.0	24.0	0.0
20-Apr-02	141	9.8	-6.6	86.0	42.0	11.8	3.1	0.0	24.0	0.0
21-Apr-02	142	11.5	-5.5	81.8	33.5	9.2	0.0	0.0	24.0	0.0
22-Apr-02	143	14.6	-2.9	78.5	30.0	9.2	0.5	0.0	24.0	0.0
23-Apr-02	144	10.6	-1.9	86.5	50.3	9.0	3.7	0.0	24.0	0.0
24-Apr-02	145	10.0	-2.0	81.3	47.3	14.1	0.7	0.0	24.0	0.0
25-Apr-02	146	8.3	-2.6	76.3	47.5	14.7	2.6	0.0	24.0	0.0
26-Apr-02	147	8.8	-3.3	89.8	43.8	9.8	1.2	0.0	24.0	0.0
27-Apr-02	148	11.8	-4.1	88.3	29.5	8.0	0.0	0.0	24.0	0.0
28-Apr-02	149	10.4	-0.1	80.3	44.3	11.6	0.7	0.0	24.0	0.0

29-Apr-02	150	12.9	-1.4	88.3	35.5	11.5	0.1	0.0	24.0	0.0
30-Apr-02	151	11.6	-0.9	86.3	33.5	11.4	0.4	0.0	24.0	0.5
1-May-02	152	11.0	-2.6	84.5	34.0	12.7	0.0	0.0	24.0	0.6
2-May-02	153	10.1	-1.9	82.3	47.5	13.1	0.2	0.0	24.0	0.6
3-May-02	154	13.8	-1.3	88.3	42.8	7.7	2.7	0.0	24.0	0.5
4-May-02	155	14.8	-0.8	84.0	31.5	10.9	0.6	0.0	24.0	0.6
5-May-02	156	13.1	1.0	79.3	48.0	11.0	3.8	0.0	24.0	0.6
6-May-02	157	13.8	0.9	89.5	39.8	8.4	0.0	0.0	24.0	0.5
7-May-02	158	11.6	-0.1	87.5	42.8	11.6	2.8	0.0	24.0	0.6
8-May-02	159	11.5	0.3	87.8	49.8	12.0	2.0	0.0	24.0	0.6
9-May-02	160	7.1	-1.3	82.8	54.3	12.7	2.1	0.0	24.0	0.5
10-May-02	161	9.6	-1.6	83.3	45.0	9.3	1.1	0.0	24.0	0.5
11-May-02	162	14.1	-0.8	83.5	36.5	10.3	0.3	0.0	24.0	0.6
12-May-02	163	14.5	1.3	71.8	35.3	12.2	0.0	0.0	24.0	0.7
13-May-02	164	15.9	2.3	81.3	37.0	10.4	1.5	0.0	24.0	0.7
14-May-02	165	18.3	2.8	88.0	33.3	9.6	0.0	0.0	24.0	0.7
15-May-02	166	12.1	2.9	81.3	48.5	12.1	2.6	0.0	24.0	0.7
16-May-02	167	11.5	1.3	88.0	49.8	10.6	3.7	0.0	24.0	0.6
17-May-02	168	14.4	2.8	80.5	30.8	16.3	0.1	0.0	24.0	0.9
18-May-02	169	12.3	0.6	75.5	30.5	12.0	0.0	0.0	24.0	0.7
19-May-02	170	12.4	0.5	73.0	33.5	11.1	2.2	0.0	24.0	0.7
20-May-02	171	14.1	3.4	85.0	51.3	10.0	2.7	0.0	24.0	0.6
21-May-02	172	15.4	2.6	85.3	40.5	13.8	2.3	0.0	24.0	0.8
22-May-02	173	14.5	1.8	81.8	37.3	15.0	0.1	0.0	24.0	0.8
23-May-02	174	16.6	2.5	82.0	35.3	9.7	0.5	0.0	24.0	0.7
24-May-02	175	14.3	3.3	92.3	53.5	7.7	0.8	0.0	24.0	0.6
25-May-02	176	18.1	4.6	88.5	38.3	9.4	0.5	0.0	24.0	0.7
26-May-02	177	20.8	6.0	88.8	34.5	10.6	0.8	0.0	24.0	0.8
27-May-02	178	22.3	9.3	87.8	38.8	13.9	1.0	0.0	24.0	0.9
28-May-02	179	19.0	8.0	78.3	41.0	12.7	1.8	0.0	24.0	0.9
29-May-02	180	16.6	7.3	78.8	51.5	14.4	5.8	0.0	24.0	0.9
30-May-02	181	17.6	7.0	84.3	36.3	15.3	0.4	0.0	24.0	0.9
31-May-02	182	15.4	4.8	82.8	44.0	15.2	1.1	0.0	24.0	0.8
1-Jun-02	183	17.0	5.6	87.8	43.3	9.3	0.1	0.0	24.0	3.5
2-Jun-02	184	20.1	4.8	88.8	29.0	7.3	0.0	0.0	24.0	3.5
3-Jun-02	185	18.5	6.5	84.3	41.3	8.5	0.4	0.0	24.0	3.6
4-Jun-02	186	20.1	6.9	89.5	40.0	7.2	4.0	0.0	24.0	3.5
5-Jun-02	187	21.0	8.8	91.0	48.3	7.7	6.4	0.0	24.0	3.5
6-Jun-02	188	18.3	8.1	90.5	44.8	13.9	2.9	0.0	24.0	4.3
7-Jun-02	189	14.9	7.8	83.5	57.0	8.4	1.0	0.0	24.0	3.4
8-Jun-02	190	16.6	7.3	95.0	54.3	8.1	2.7	0.0	24.0	3.2
9-Jun-02	191	19.6	7.6	89.5	39.0	7.1	0.0	0.0	24.0	3.5
10-Jun-02	192	18.3	9.3	69.5	43.8	11.3	5.0	0.0	24.0	4.6
11-Jun-02	193	15.0	9.1	76.8	51.3	14.6	2.0	0.0	24.0	4.6
12-Jun-02	194	18.4	7.8	81.0	47.3	10.2	3.0	0.0	24.0	4.0
13-Jun-02	195	21.8	7.6	90.8	43.0	9.7	1.2	0.0	24.0	3.9
14-Jun-02	196	20.5	10.4	94.0	49.8	10.1	5.4	0.0	24.0	3.9
15-Jun-02	197	18.6	9.5	84.3	43.5	10.7	0.0	0.0	24.0	4.2
16-Jun-02	198	17.6	7.1	81.3	41.8	12.9	0.0	0.0	24.0	4.4
17-Jun-02	199	19.6	8.3	76.8	36.0	12.3	2.2	0.0	24.0	4.8
18-Jun-02	200	19.3	6.1	82.0	43.8	10.7	0.3	0.0	24.0	4.0

19-Jun-02	201	20.4	9.3	80.5	42.0	11.3	0.6	0.0	24.0	4.4
20-Jun-02	202	21.8	8.6	91.5	49.3	8.3	5.4	0.0	24.0	3.7
21-Jun-02	203	22.0	11.0	82.3	56.0	14.9	3.2	0.0	24.0	4.7
22-Jun-02	204	22.5	13.1	85.5	50.3	15.3	1.5	0.0	24.0	5.1
23-Jun-02	205	22.5	12.4	81.3	44.3	11.4	1.5	0.0	24.0	4.7
24-Jun-02	206	20.9	10.0	88.5	45.3	10.1	0.6	0.0	24.0	4.1
25-Jun-02	207	22.3	10.6	90.5	47.0	8.0	7.2	0.0	24.0	3.8
26-Jun-02	208	22.6	9.4	88.8	41.8	10.7	0.9	0.0	24.0	4.2
27-Jun-02	209	22.6	11.5	89.5	42.3	10.8	4.8	0.0	24.0	4.4
28-Jun-02	210	25.1	13.4	82.5	42.8	12.0	1.8	0.0	24.0	4.9
29-Jun-02	211	23.4	12.1	86.5	44.8	12.3	1.7	0.0	24.0	4.7
30-Jun-02	212	19.6	10.8	90.8	51.5	14.6	0.9	0.0	24.0	4.5
1-Jul-02	213	21.5	10.8	86.8	44.3	14.9	3.6	0.0	24.0	4.7
2-Jul-02	214	19.6	11.5	90.5	55.8	12.2	6.4	0.0	24.0	3.9
3-Jul-02	215	20.8	9.3	91.5	38.8	13.4	0.0	0.0	24.0	4.4
4-Jul-02	216	20.6	10.0	87.3	49.3	11.3	3.2	0.0	24.0	4.0
5-Jul-02	217	21.6	12.8	85.3	55.3	13.9	1.7	0.0	24.0	4.4
6-Jul-02	218	21.8	12.1	83.0	50.8	18.6	0.0	0.0	24.0	5.2
7-Jul-02	219	23.6	13.3	80.5	44.0	12.2	1.6	0.0	24.0	4.7
8-Jul-02	220	24.4	11.9	86.5	37.5	11.4	0.9	0.0	24.0	4.5
9-Jul-02	221	23.4	13.8	82.3	49.3	12.4	8.0	0.0	24.0	4.5
10-Jul-02	222	24.5	12.6	93.8	47.0	9.7	1.2	0.0	24.0	3.9
11-Jul-02	223	26.1	14.8	83.3	42.8	10.2	0.0	0.0	24.0	4.5
12-Jul-02	224	27.5	16.0	82.5	50.3	12.6	6.7	0.0	24.0	4.8
13-Jul-02	225	26.6	15.4	94.8	40.5	11.2	0.3	0.0	24.0	4.4
14-Jul-02	226	25.5	15.0	82.8	48.3	9.9	1.3	0.0	24.0	4.2
15-Jul-02	227	27.9	16.0	86.5	39.8	14.5	0.5	0.0	24.0	5.3
16-Jul-02	228	25.3	14.4	79.5	42.3	12.6	0.9	0.0	24.0	4.9
17-Jul-02	229	20.9	12.0	87.3	57.0	13.4	1.1	0.0	24.0	4.0
18-Jul-02	230	22.3	13.5	91.0	52.3	9.3	6.1	0.0	24.0	3.7
19-Jul-02	231	22.3	13.8	87.8	51.5	9.1	0.7	0.0	24.0	3.8
20-Jul-02	232	22.5	13.3	88.0	50.0	10.2	1.9	0.0	24.0	3.9
21-Jul-02	233	22.9	11.8	91.0	47.3	9.3	0.4	0.0	24.0	3.6
22-Jul-02	234	23.6	12.1	92.5	43.3	12.9	3.1	0.0	24.0	4.2
23-Jul-02	235	26.0	13.5	90.3	42.8	11.2	0.6	0.0	24.0	4.2
24-Jul-02	236	26.3	14.4	82.5	39.0	7.7	1.1	0.0	24.0	3.9
25-Jul-02	237	25.6	14.0	86.8	43.3	8.3	0.1	0.0	24.0	3.8
26-Jul-02	238	25.5	14.6	86.8	50.8	8.8	5.0	0.0	24.0	3.7
27-Jul-02	239	25.6	16.3	90.5	51.5	8.0	0.7	0.0	24.0	3.6
28-Jul-02	240	27.8	14.5	91.3	46.5	9.4	0.7	0.0	24.0	3.8
29-Jul-02	241	25.4	16.3	90.0	46.5	12.8	13.0	0.0	24.0	4.4
30-Jul-02	242	25.6	16.0	88.8	47.5	17.6	1.1	0.0	24.0	5.0
31-Jul-02	243	25.5	15.1	80.0	42.5	11.5	0.1	0.0	24.0	4.4
1-Aug-02	244	23.8	14.4	85.5	41.5	11.6	0.0	0.0	24.0	3.9
2-Aug-02	245	24.6	12.9	89.5	38.3	10.4	0.0	0.0	24.0	3.6
3-Aug-02	246	25.1	13.9	84.5	41.5	12.1	0.1	0.0	24.0	3.9
4-Aug-02	247	23.1	16.0	84.3	58.3	9.0	1.5	0.0	24.0	3.3
5-Aug-02	248	22.6	15.3	89.5	52.0	11.0	0.2	0.0	24.0	3.4
6-Aug-02	249	23.9	13.0	90.8	48.8	8.5	0.4	0.0	24.0	3.0
7-Aug-02	250	25.9	14.4	88.3	48.5	8.3	4.1	0.0	24.0	3.2
8-Aug-02	251	22.6	15.5	90.5	64.0	9.2	1.4	0.0	24.0	3.0

9-Aug-02	252	22.9	14.3	91.0	50.8	10.5	1.6	0.0	24.0	3.2
10-Aug-02	253	24.0	13.4	92.3	49.3	10.8	0.2	0.0	24.0	3.2
11-Aug-02	254	22.0	12.9	87.3	52.8	10.1	1.3	0.0	24.0	3.1
12-Aug-02	255	23.4	13.9	83.8	49.3	12.1	0.1	0.0	24.0	3.5
13-Aug-02	256	25.3	12.6	89.8	40.3	10.7	1.3	0.0	24.0	3.4
14-Aug-02	257	24.1	14.3	82.8	43.3	9.8	2.7	0.0	24.0	3.4
15-Aug-02	258	21.0	13.3	89.0	53.5	8.8	1.7	0.0	24.0	2.9
16-Aug-02	259	23.0	13.5	82.8	50.5	11.3	4.0	0.0	24.0	3.3
17-Aug-02	260	21.8	14.1	80.8	49.5	12.6	1.3	0.0	24.0	3.6
18-Aug-02	261	20.1	11.6	83.5	50.3	10.0	0.2	0.0	24.0	3.0
19-Aug-02	262	24.4	12.0	81.3	42.3	15.1	0.2	0.0	24.0	3.9
20-Aug-02	263	21.1	12.1	85.0	47.5	13.6	7.5	0.0	24.0	3.4
21-Aug-02	264	21.5	12.0	91.0	50.5	9.4	1.7	0.0	24.0	2.7
22-Aug-02	265	25.1	12.5	87.3	42.0	12.5	0.2	0.0	24.0	3.3
23-Aug-02	266	23.4	14.4	87.0	51.0	12.9	1.9	0.0	24.0	3.3
24-Aug-02	267	28.1	13.8	86.0	30.5	11.5	0.0	0.0	24.0	3.6
25-Aug-02	268	24.4	13.1	67.8	34.3	13.9	0.1	0.0	24.0	4.3
26-Aug-02	269	22.0	11.8	78.0	41.5	11.7	0.3	0.0	24.0	3.3
27-Aug-02	270	23.4	10.8	86.8	46.8	8.8	0.4	0.0	24.0	2.6
28-Aug-02	271	23.6	12.6	88.8	44.8	10.0	0.3	0.0	24.0	2.8
29-Aug-02	272	20.4	11.4	87.3	52.8	13.0	7.5	0.0	24.0	2.9
30-Aug-02	273	20.8	11.1	83.8	49.5	11.8	13.9	0.0	24.0	2.8
31-Aug-02	274	18.8	9.5	95.5	52.5	8.4	1.0	0.0	24.0	2.1
1-Sep-02	275	20.0	9.5	91.0	50.0	10.1	11.3	0.0	24.0	2.1
2-Sep-02	276	16.8	9.8	94.5	62.8	15.3	21.4	0.0	24.0	2.2
3-Sep-02	277	18.6	8.4	90.0	48.0	10.8	0.8	0.0	24.0	2.2
4-Sep-02	278	19.1	10.0	87.0	49.0	12.2	0.5	0.0	24.0	2.4
5-Sep-02	279	19.1	10.4	87.8	49.8	8.4	0.2	0.0	24.0	2.0
6-Sep-02	280	19.0	11.4	93.3	57.3	6.8	0.9	0.0	24.0	1.8
7-Sep-02	281	19.4	11.6	91.8	60.8	7.2	2.2	0.0	24.0	1.8
8-Sep-02	282	19.9	12.1	88.8	55.0	11.3	3.0	0.0	24.0	2.2
9-Sep-02	283	21.4	11.9	89.0	47.3	11.2	0.1	0.0	24.0	2.3
10-Sep-02	284	18.5	10.9	86.5	57.0	13.7	2.5	0.0	24.0	2.3
11-Sep-02	285	17.6	9.6	87.3	49.0	13.3	2.2	0.0	24.0	2.3
12-Sep-02	286	15.5	8.0	81.8	51.8	9.3	2.4	0.0	24.0	1.9
13-Sep-02	287	13.1	5.9	94.8	62.0	11.8	2.4	0.0	24.0	1.6
14-Sep-02	288	17.5	6.4	91.3	45.3	10.5	0.2	0.0	24.0	1.8
15-Sep-02	289	19.6	8.8	84.3	50.0	10.7	0.8	0.0	24.0	2.0
16-Sep-02	290	15.9	9.3	85.8	61.8	13.4	0.0	0.0	24.0	2.0
17-Sep-02	291	14.3	6.9	90.0	59.8	10.1	3.2	0.0	24.0	1.6
18-Sep-02	292	13.6	7.4	94.5	59.5	9.9	2.1	0.0	24.0	1.5
19-Sep-02	293	13.6	6.8	96.0	71.5	9.6	10.9	0.0	24.0	1.3
20-Sep-02	294	11.9	7.1	94.0	82.3	11.3	8.0	0.0	24.0	1.3
21-Sep-02	295	10.1	6.3	93.3	67.0	13.7	0.9	0.0	24.0	1.5
22-Sep-02	296	9.0	2.3	88.3	49.0	11.4	0.3	0.0	24.0	1.5
23-Sep-02	297	8.3	1.5	83.5	57.3	13.4	4.4	0.0	24.0	1.6
24-Sep-02	298	9.9	1.6	83.0	50.0	16.3	0.2	0.0	24.0	1.8
25-Sep-02	299	11.0	2.9	87.5	53.5	9.7	1.3	0.0	24.0	1.3
26-Sep-02	300	10.5	3.9	89.5	62.8	11.6	0.4	0.0	24.0	1.4
27-Sep-02	301	10.4	2.6	83.5	51.5	9.3	0.2	0.0	24.0	1.3
28-Sep-02	302	11.8	1.6	81.5	49.8	12.5	0.0	0.0	24.0	1.5

29-Sep-02	303	13.4	5.5	86.3	54.5	11.7	0.5	0.0	24.0	1.5
30-Sep-02	304	11.3	2.6	91.0	49.0	12.5	0.0	0.0	24.0	1.4
1-Oct-02	305	10.0	1.5	78.8	60.0	11.4	2.0	0.0	24.0	1.6
2-Oct-02	306	13.1	3.0	86.3	41.8	13.8	0.1	0.0	24.0	2.0
3-Oct-02	307	10.0	4.1	82.0	55.3	16.6	3.5	0.0	24.0	2.1
4-Oct-02	308	7.6	0.3	87.0	52.5	14.5	0.6	0.0	24.0	1.6
5-Oct-02	309	6.6	-0.1	92.3	49.3	9.5	0.4	0.0	24.0	1.1
6-Oct-02	310	8.8	-2.6	89.8	49.3	9.0	0.0	0.0	24.0	0.9
7-Oct-02	311	7.8	0.5	86.5	60.3	10.2	1.3	0.0	24.0	1.2
8-Oct-02	312	10.6	0.9	89.0	51.3	11.6	0.1	0.0	24.0	1.4
9-Oct-02	313	14.6	4.4	81.3	49.0	11.0	0.2	0.0	24.0	1.6
10-Oct-02	314	13.8	2.6	86.8	47.3	7.3	0.3	0.0	24.0	1.1
11-Oct-02	315	11.6	2.1	89.5	56.8	9.2	2.0	0.0	24.0	1.1
12-Oct-02	316	9.1	-0.3	94.5	58.5	8.9	0.1	0.0	24.0	0.9
13-Oct-02	317	6.9	-2.4	93.8	51.5	8.9	0.3	0.0	24.0	0.8
14-Oct-02	318	5.6	0.4	89.3	56.0	13.8	0.2	0.0	24.0	1.3
15-Oct-02	319	2.0	-2.4	86.5	57.5	12.9	0.0	0.0	24.0	1.2
16-Oct-02	320	3.9	-2.8	86.8	57.0	9.5	0.0	0.0	24.0	0.9
17-Oct-02	321	5.9	-2.3	91.8	64.5	11.2	1.2	0.0	24.0	0.6
18-Oct-02	322	5.6	-1.1	83.5	53.3	11.6	0.1	0.0	24.0	1.0
19-Oct-02	323	4.5	-1.9	87.8	58.8	12.3	1.1	0.0	24.0	0.8
20-Oct-02	324	5.1	-2.0	88.8	66.8	10.9	0.3	0.0	24.0	0.5
21-Oct-02	325	3.5	-2.0	89.5	58.5	8.3	0.2	0.0	24.0	0.4
22-Oct-02	326	4.1	-1.3	79.0	58.8	14.0	0.2	0.0	24.0	0.5
23-Oct-02	327	2.9	-2.9	89.0	60.0	13.9	1.6	0.0	24.0	0.0
24-Oct-02	328	3.5	-1.6	82.3	67.8	14.8	0.9	0.0	24.0	0.3
25-Oct-02	329	3.9	-2.8	93.3	64.3	8.9	0.6	0.0	24.0	0.2
26-Oct-02	330	2.6	-2.6	92.0	64.0	8.6	1.3	0.0	24.0	0.1
27-Oct-02	331	1.1	-3.5	88.8	68.0	9.8	3.3	0.0	24.0	0.0
28-Oct-02	332	0.6	-4.0	89.3	67.5	11.2	0.6	0.0	24.0	0.0
29-Oct-02	333	2.0	-4.3	84.5	64.0	11.6	0.7	0.0	24.0	0.0
30-Oct-02	334	2.5	-2.9	91.5	69.0	10.1	0.6	0.0	24.0	0.0
31-Oct-02	335	0.1	-5.3	94.0	76.3	5.5	3.7	0.0	24.0	0.0
1-Nov-02	336	-1.0	-4.1	89.8	75.5	12.0	2.9	0.0	24.0	0.0
2-Nov-02	337	-2.0	-6.0	88.0	80.8	9.7	0.1	0.0	24.0	0.0
3-Nov-02	338	0.3	-6.3	90.8	69.0	9.6	0.6	0.0	24.0	0.0
4-Nov-02	339	0.3	-6.3	87.8	63.8	7.3	0.2	0.0	24.0	0.0
5-Nov-02	340	1.8	-7.6	90.5	60.8	12.8	1.3	0.0	24.0	0.0
6-Nov-02	341	-4.6	-10.9	80.8	59.5	15.2	1.6	0.0	24.0	0.0
7-Nov-02	342	-6.5	-13.6	85.0	62.3	12.2	0.2	0.0	24.0	0.0
8-Nov-02	343	-4.4	-11.6	87.0	67.0	12.1	1.8	0.0	24.0	0.0
9-Nov-02	344	-4.3	-11.4	93.0	76.5	11.1	3.0	0.0	24.0	0.0
10-Nov-02	345	-4.0	-8.8	89.8	78.5	11.4	0.2	0.0	24.0	0.0
11-Nov-02	346	-5.0	-10.3	84.3	69.0	9.4	0.1	0.0	24.0	0.0
12-Nov-02	347	-5.0	-10.9	85.5	75.3	12.9	0.0	0.0	24.0	0.0
13-Nov-02	348	-2.6	-10.4	87.0	73.5	12.3	0.2	0.0	24.0	0.0
14-Nov-02	349	-1.6	-8.9	92.3	70.8	6.8	0.1	0.0	24.0	0.0
15-Nov-02	350	-1.6	-11.8	89.5	73.8	8.3	0.3	0.0	24.0	0.0
16-Nov-02	351	-1.9	-8.1	93.5	85.3	13.0	0.1	0.0	24.0	0.0
17-Nov-02	352	-1.6	-5.6	96.5	85.5	9.2	0.4	0.0	24.0	0.0
18-Nov-02	353	-1.9	-5.1	88.3	73.3	9.9	0.1	0.0	24.0	0.0

19-Nov-02	354	-2.9	-8.4	89.8	76.0	8.1	1.3	0.0	24.0	0.0
20-Nov-02	355	-6.3	-10.1	86.5	76.3	10.1	0.7	0.0	24.0	0.0
21-Nov-02	356	-7.0	-11.6	89.3	79.0	9.3	0.0	0.0	24.0	0.0
22-Nov-02	357	-6.5	-12.4	92.0	80.0	8.9	0.6	0.0	24.0	0.0
23-Nov-02	358	-7.3	-13.8	87.3	78.0	10.6	0.1	0.0	24.0	0.0
24-Nov-02	359	-6.4	-14.9	90.0	76.3	12.1	1.1	0.0	24.0	0.0
25-Nov-02	360	-7.8	-13.5	89.0	78.3	9.7	0.2	0.0	24.0	0.0
26-Nov-02	361	-6.5	-16.4	86.3	67.3	8.8	0.3	0.0	24.0	0.0
27-Nov-02	362	-5.9	-11.9	87.3	75.8	8.8	0.3	0.0	24.0	0.0
28-Nov-02	363	-2.1	-14.0	85.5	63.5	13.9	0.8	0.0	24.0	0.0
29-Nov-02	364	-7.9	-13.1	83.8	69.3	13.6	0.2	0.0	24.0	0.0
30-Nov-02	365	-8.4	-13.8	83.3	71.8	10.1	0.3	0.0	24.0	0.0

Table C-1. Daily column fluxes for low evaporation test.

Date	Day	Daily Flux (mm)*			
		Column 1	Column 2	Column 3	Column 4
22-Nov-04	0	0.00	0.00	0.00	0.00
23-Nov-04	1	-0.16	0.00	-0.49	0.00
24-Nov-04	2	-0.49	0.00	-1.46	0.00
25-Nov-04	3	-0.81	1.30	-0.81	0.00
26-Nov-04	4	-1.13	-0.97	-1.78	-1.30
27-Nov-04	5	-0.81	-0.32	0.49	0.32
28-Nov-04	6	-1.46	-0.65	-2.43	-0.65
29-Nov-04	7	-1.46	-0.97	-2.43	-0.97
30-Nov-04	8	-0.49	-0.32	-1.13	-0.32
1-Dec-04	9	-0.81	-0.65	-1.13	-0.32
2-Dec-04	10	-0.81	-0.32	-1.13	-0.32
3-Dec-04	11	-0.49	-0.32	-1.13	-0.32
4-Dec-04	12	-0.81	-0.32	-1.13	-0.32
5-Dec-04	13	-0.49	-0.32	-1.13	-0.32
6-Dec-04	14	-0.81	-0.32	-1.13	-0.32
7-Dec-04	15	-1.13	-0.65	-1.13	-0.32
8-Dec-04	16	-0.16	-0.32	-0.16	-0.32
9-Dec-04	17	-1.46	-1.30	-0.81	-0.32
10-Dec-04	18	-0.81	0.00	-0.49	0.00
11-Dec-04	19	0.81	1.30	0.16	-0.97
12-Dec-04	20	-1.13	-0.97	-1.13	-0.32
13-Dec-04	21	-1.13	-0.65	-0.81	-0.32
14-Dec-04	22	0.81	0.32	-0.49	-0.32
15-Dec-04	23	-0.16	0.00	-0.49	-0.32
16-Dec-04	24	-0.16	0.00	-0.49	-0.32
17-Dec-04	25	-0.49	0.00	-0.49	-0.32
18-Dec-04	26	-0.81	-0.32	-0.49	0.00
19-Dec-04	27	3.73	1.62	0.49	0.00
20-Dec-04	28	-0.49	-1.30	-0.81	-0.65
21-Dec-04	29	-1.13	-0.97	-0.49	-0.32
22-Dec-04	30	0.16	0.32	-0.16	0.32
23-Dec-04	31	-0.49	0.00	-0.49	0.00
24-Dec-04	32	2.11	0.65	-0.16	0.00
30-Dec-04	33	-0.49	0.00	-1.13	-0.65
31-Dec-04	34	-0.49	0.00	0.16	-0.32
1-Jan-05	35	-0.49	0.00	-0.16	-0.32
2-Jan-05	36	-0.16	0.00	-0.16	-0.32
3-Jan-05	37	-0.16	0.00	-0.16	-0.32
4-Jan-05	38	-0.16	0.00	-0.16	-0.65

5-Jan-05	39	2.11	0.00	0.16	-0.65
6-Jan-05	40	3.08	1.62	0.49	-0.65
7-Jan-05	41	-0.49	-0.32	0.16	-0.32
8-Jan-05	42	1.13	0.00	0.81	0.00
9-Jan-05	43	0.49	0.00	0.16	0.00
10-Jan-05	44	0.49	0.32	0.81	-0.32
11-Jan-05	45	0.49	0.32	0.81	-0.32
12-Jan-05	46	0.49	0.32	0.81	-0.65
13-Jan-05	47	-0.16	0.00	0.49	-0.65
14-Jan-05	48	0.81	0.00	0.81	0.00
15-Jan-05	49	0.49	0.00	0.49	0.00
16-Jan-05	50	0.81	0.00	0.49	-0.32
17-Jan-05	51	1.13	0.32	0.49	-0.32
18-Jan-05	52	1.78	0.32	2.11	-0.65
19-Jan-05	53	1.13	0.00	1.13	0.00
20-Jan-05	54	1.13	0.32	0.81	-0.32
21-Jan-05	55	1.46	0.32	0.81	-0.32
22-Jan-05	56	2.43	0.00	1.46	0.00
23-Jan-05	57	2.11	0.32	1.13	0.32
24-Jan-05	58	1.78	0.32	1.78	-0.32
25-Jan-05	59	2.43	0.32	1.13	0.32
26-Jan-05	60	2.75	0.97	2.43	-0.32
27-Jan-05	61	3.40	0.97	1.13	0.65
28-Jan-05	62	2.43	1.30	4.05	0.97
29-Jan-05	63	3.08	0.65	3.73	0.65
30-Jan-05	64	3.40	1.30	4.05	1.30
31-Jan-05	65	3.08	0.97	3.40	0.65
1-Feb-05	66	3.40	1.30	3.73	1.62
2-Feb-05	67	4.70	1.62	3.08	1.30
3-Feb-05	68	4.70	1.30	6.32	1.62
4-Feb-05	69	1.78	1.30	2.75	0.65
5-Feb-05	70	5.02	1.94	5.99	1.62
6-Feb-05	71	2.11	0.32	2.43	1.30
7-Feb-05	72	1.78	0.97	2.43	1.30
8-Feb-05	73	4.37	1.30	3.73	0.97
9-Feb-05	74	3.73	1.62	2.11	0.65
10-Feb-05	75	4.37	1.62	5.02	1.94
11-Feb-05	76	3.08	1.30	5.02	0.97
12-Feb-05	77	3.73	0.97	4.37	0.97
13-Feb-05	78	1.78	0.97	4.05	0.65
14-Feb-05	79	1.78	0.65	1.78	0.97
15-Feb-05	80	1.46	0.65	3.73	0.97

* negative denotes evaporative flux, positive denotes infitration

Table C-2. Daily column fluxes for low evaporation test.

Date	Day	Daily Flux (mm)*			
		Column 1	Column 2	Column 3	Column 4
15-Sep-04	0	0.00	0.00	0.00	0.00
16-Sep-04	1	0.00	-1.27	-1.95	-1.30
17-Sep-04	2	0.65	0.00	-2.92	-0.32
18-Sep-04	3	0.00	1.27	-3.24	-0.65
19-Sep-04	4	-0.32	0.85	0.32	-0.97
20-Sep-04	5	-1.62	-3.40	7.13	-2.27
21-Sep-04	6	1.95	-2.12	2.59	-1.62
22-Sep-04	7	2.92	2.97	0.00	0.65
23-Sep-04	8	0.97	1.27	-1.62	-0.32
24-Sep-04	9	-0.32	1.27	-2.92	0.32
26-Sep-04	11	-2.59	0.85	-4.86	0.00
27-Sep-04	12	-3.24	-1.70	-4.86	-1.30
28-Sep-04	13	-0.65	0.00	-4.86	0.00
29-Sep-04	14	-2.27	-0.42	-1.95	-0.65
30-Sep-04	15	-1.95	0.00	-4.86	0.00
1-Oct-04	16	-3.89	-2.97	-1.30	-2.27
2-Oct-04	17	-2.92	-1.70	-0.65	-1.30
3-Oct-04	18	-2.92	-1.27	-1.62	-1.62
4-Oct-04	19	-1.95	-0.85	-2.92	-0.97
5-Oct-04	20	1.30	0.85	-1.30	0.32
6-Oct-04	21	1.30	1.27	0.32	-0.97
7-Oct-04	22	0.00	0.85	0.32	0.97
8-Oct-04	23	-1.95	-1.27	-1.30	-0.97
9-Oct-04	24	-1.30	-1.70	-1.30	0.00
10-Oct-04	25	-1.30	-2.12	-1.62	-0.97
11-Oct-04	26	-1.95	-1.70	-1.62	-0.97
12-Oct-04	27	-1.30	-0.42	-0.97	-0.32
13-Oct-04	28	-1.95	-2.12	-0.32	-1.62
14-Oct-04	29	0.00	1.27	1.95	0.65
15-Oct-04	30	-0.97	-1.27	-0.32	-0.97
16-Oct-04	31	5.19	0.00	2.27	0.00

* negative denotes evaporative flux, positive denotes infitration

Table C-3. Gravimetric water contents for low evaporation test

Elevation above w.t. (cm)	Day 0	Day 14	Day 25	Day 38	Day 58	Day 80
Column 1						
150.0	0.24	0.26	0.21	0.24	0.22	0.24
145.0	0.23	0.25	0.23	0.23	0.19	0.23
140.0	0.21	0.24	0.21	0.21	0.17	0.22
135.0	0.24	0.26	0.21	0.23	0.22	0.27
130.0	0.26	0.24	0.21	0.25	0.24	0.25
125.0	0.17	0.14	0.17	0.15	0.15	0.15
120.0	0.18	0.13	0.16	0.15	0.13	0.15
115.0	0.14	0.15	0.14	0.16	0.12	0.14
110.0	0.15	0.18	0.15	0.14	0.13	0.16
105.0	0.16	0.16	0.15	0.15	0.13	0.15
95.0	0.13	0.14	0.12	0.13	0.13	0.12
90.0	0.11	0.16	0.12	0.12	0.13	0.13
85.0	0.15	0.16	0.12	0.14	0.14	0.13
80.0	0.14	0.14	0.13	0.14	0.15	0.16
75.0	0.19	0.15	0.14	0.16	0.18	0.19
70.0	0.16	0.16	0.14	0.15	0.15	0.14
65.0	0.20	0.18	0.17	0.17	0.16	0.16
60.0	0.19	0.17	0.17	0.17	0.18	0.17
55.0	0.22	0.20	0.18	0.18	0.19	0.22
50.0	0.23	0.21	0.19	0.20	0.19	0.21
45.0	0.24	0.23	0.20	0.21	0.20	0.23
40.0	0.24	0.21	0.21	0.19	0.22	0.24
30.0	0.20	0.22	0.21	0.22	0.20	0.26
20.0	0.26	0.23	0.25	0.20	0.23	0.32
10.0	0.28	0.24	0.26	0.23	0.22	0.24
Column 2						
150.0	0.15	0.14	0.14	0.14	0.17	0.18
145.0	0.15	0.14	0.14	0.12	0.12	0.16
140.0	0.17	0.16	0.13	0.15	0.16	0.18
135.0	0.19	0.18	0.15	0.18	0.16	0.19
130.0	0.19	0.19	0.15	0.17	0.17	0.19
125.0	0.18	0.15	0.17	0.17	0.18	0.19
120.0	0.18	0.18	0.16	0.17	0.20	0.19
115.0	0.19	0.19	0.16	0.18	0.17	0.18
110.0	0.19	0.18	0.15	0.17	0.18	0.20
105.0	0.19	0.18	0.18	0.16	0.16	0.20
95.0	0.13	0.13	0.13	0.12	0.12	0.14

90.0	0.14	0.15	0.14	0.12	0.11	0.11
85.0	0.11	0.15	0.14	0.13	0.14	0.14
80.0	0.13	0.16	0.15	0.15	0.15	0.10
75.0	0.14	0.15	0.15	0.15	0.16	0.15
70.0	0.16	0.16	0.14	0.14	0.17	0.15
65.0	0.19	0.19	0.18	0.17	0.16	0.19
60.0	0.19	0.17	0.17	0.18	0.16	0.20
55.0	0.21	0.19	0.19	0.21	0.19	0.18
50.0	0.21	0.20	0.19	0.20	0.18	0.20
45.0	0.21	0.21	0.20	0.21	0.19	0.19
40.0	0.21	0.21	0.20	0.20	0.21	0.19
30.0	0.24	0.25	0.23	0.23	0.22	0.21
20.0	0.23	0.30	0.22	0.23	0.22	0.22
10.0	0.26	0.27	0.25	0.23	0.24	0.24
Column 3						
120.0	0.18	0.20	0.20	0.18	0.17	0.20
115.0	0.21	0.20	0.17	0.16	0.19	0.20
110.0	0.21	0.20	0.19	0.16	0.17	0.19
105.0	0.19	0.23	0.17	0.17	0.18	0.18
95.0	0.16	0.14	0.14	0.16	0.15	0.16
90.0	0.16	0.15	0.16	0.16	0.15	0.15
85.0	0.17	0.16	0.19	0.17	0.15	0.16
80.0	0.18	0.17	0.19	0.17	0.17	0.19
75.0	0.18	0.15	0.20	0.18	0.20	0.17
70.0	0.18	0.16	0.19	0.18	0.15	0.18
65.0	0.19	0.18	0.18	0.18	0.17	0.17
60.0	0.22	0.18	0.21	0.20	0.19	0.20
55.0	0.19	0.20	0.21	0.22	0.19	0.19
50.0	0.22	0.20	0.20	0.21	0.21	0.21
45.0	0.27	0.21	0.21	0.20	0.22	0.26
40.0	0.22	0.22	0.22	0.23	0.26	0.28
30.0	0.21	0.22	0.27	0.23	0.25	0.27
20.0	0.27	0.24	0.25	0.25	0.23	0.24
10.0	0.24	0.22	0.26	0.27	0.25	0.25
Column 4						
120.0	0.17	0.13	0.09	0.11	0.17	0.22
115.0	0.17	0.12	0.11	0.11	0.19	0.21
110.0	0.17	0.15	0.11	0.11	0.17	0.19
105.0	0.20	0.16	0.10	0.13	0.18	0.23
95.0	0.14	0.15	0.15	0.15	0.15	0.13
90.0	0.16	0.20	0.17	0.17	0.15	0.14
85.0	0.17	0.16	0.16	0.13	0.15	0.16

80.0	0.17	0.15	0.15	0.15	0.17	0.15
75.0	0.16	0.15	0.16	0.14	0.15	0.16
70.0	0.19	0.15	0.15	0.16	0.15	0.14
65.0	0.19	0.16	0.16	0.16	0.17	0.15
60.0	0.18	0.16	0.16	0.16	0.17	0.17
55.0	0.19	0.17	0.17	0.17	0.17	0.16
50.0	0.19	0.18	0.18	0.18	0.20	0.19
45.0	0.21	0.21	0.19	0.18	0.21	0.22
40.0	0.23	0.22	0.21	0.20	0.22	0.21
30.0	0.22	0.23	0.22	0.21	0.22	0.26
20.0	0.26	0.27	0.24	0.23	0.23	0.30
10.0	0.25	0.22	0.25	0.25	0.25	0.29

Table C-4. Gravimetric water contents for high evaporation test

Elevation above w.t. (cm)	Day 0	Day 7	Day 14	Day 21	Day 31
Column 1					
150.0	0.25	0.24	0.22	0.21	0.20
145.0	0.26	0.23	0.22	0.20	0.19
140.0	0.25	0.22	0.23	0.24	0.22
135.0	0.26	0.22	0.19	0.19	0.19
130.0	0.26	0.22	0.22	0.22	0.22
125.0	0.19	0.20	0.13	0.10	0.13
120.0	0.18	0.12	0.12	0.11	0.12
115.0	0.20	0.16	0.12	0.12	0.11
110.0	0.16	0.13	0.14	0.16	0.16
105.0	0.17	0.13	0.13	0.17	0.15
95.0	0.15	0.11	0.11	0.11	0.11
90.0	0.20	0.13	0.11	0.12	0.12
85.0	0.20	0.14	0.11	0.13	0.11
80.0	0.16	0.14	0.14	0.14	0.13
75.0	0.17	0.15	0.15	0.16	0.16
70.0	0.19	0.13	0.17	0.15	0.15
65.0	0.18	0.16	0.15	0.17	0.16
60.0	0.21	0.18	0.16	0.19	0.17
55.0	0.19	0.20	0.17	0.21	0.19
50.0	0.20	0.20	0.20	0.19	0.20
45.0	0.25	0.22	0.21	0.21	0.21
40.0	0.23	0.23	0.21	0.21	0.22
30.0	0.22	0.26	0.23	0.24	0.24
20.0	0.26	0.26	0.22	0.23	0.24
10.0	0.27	0.21	0.23	0.28	0.27
Column 2					
150.0	0.16	0.14	0.10	0.10	0.10
145.0	0.21	0.15	0.15	0.10	0.11
140.0	0.21	0.18	0.19	0.15	0.16
135.0	0.21	0.17	0.16	0.16	0.16
130.0	0.20	0.18	0.18	0.16	0.16
125.0	0.18	0.18	0.20	0.16	0.16
120.0	0.21	0.19	0.18	0.14	0.14
115.0	0.23	0.18	0.19	0.18	0.17
110.0	0.18	0.17	0.20	0.15	0.16
105.0	0.21	0.21	0.17	0.14	0.15
95.0	0.11	0.14	0.12	0.12	0.12

90.0	0.14	0.12	0.12	0.14	0.13
85.0	0.12	0.14	0.12	0.12	0.12
80.0	0.13	0.14	0.14	0.13	0.13
75.0	0.16	0.14	0.14	0.14	0.14
70.0	0.16	0.15	0.15	0.14	0.15
65.0	0.17	0.17	0.16	0.18	0.18
60.0	0.15	0.17	0.16	0.18	0.18
55.0	0.19	0.18	0.19	0.20	0.20
50.0	0.19	0.18	0.21	0.20	0.21
45.0	0.21	0.19	0.20	0.22	0.22
40.0	0.19	0.20	0.20	0.22	0.21
30.0	0.23	0.21	0.24	0.24	0.23
20.0	0.25	0.21	0.25	0.27	0.25
10.0	0.24	0.22	0.24	0.23	0.25
		Column 3			
120.0	0.18	0.19	0.18	0.17	0.18
115.0	0.19	0.22	0.18	0.20	0.19
110.0	0.18	0.20	0.18	0.21	0.18
105.0	0.14	0.20	0.20	0.20	0.20
95.0	0.14	0.15	0.15	0.16	0.16
90.0	0.14	0.15	0.16	0.16	0.16
85.0	0.15	0.16	0.17	0.14	0.16
80.0	0.15	0.18	0.17	0.18	0.17
75.0	0.12	0.18	0.19	0.21	0.20
70.0	0.15	0.19	0.23	0.18	0.19
65.0	0.16	0.20	0.24	0.18	0.20
60.0	0.17	0.20	0.23	0.19	0.20
55.0	0.19	0.22	0.24	0.19	0.22
50.0	0.16	0.20	0.26	0.20	0.21
45.0	0.20	0.23	0.23	0.21	0.21
40.0	0.24	0.25	0.24	0.21	0.21
30.0	0.26	0.28	0.25	0.23	0.24
20.0	0.26	0.27	0.26	0.27	0.24
10.0	0.28	0.27	0.26	0.24	0.24
		Column 4			
120.0	0.16	0.18	0.16	0.16	0.17
115.0	0.15	0.20	0.15	0.16	0.15
110.0	0.16	0.19	0.17	0.14	0.15
105.0	0.15	0.18	0.15	0.13	0.15
95.0	0.12	0.14	0.14	0.14	0.14
90.0	0.13	0.14	0.14	0.15	0.14
85.0	0.13	0.17	0.13	0.13	0.14

80.0	0.13	0.15	0.13	0.14	0.15
75.0	0.14	0.16	0.14	0.15	0.16
70.0	0.16	0.15	0.16	0.15	0.16
65.0	0.16	0.15	0.18	0.16	0.17
60.0	0.18	0.17	0.22	0.23	0.20
55.0	0.17	0.17	0.21	0.19	0.20
50.0	0.18	0.18	0.22	0.22	0.22
45.0	0.22	0.23	0.23	0.22	0.23
40.0	0.22	0.22	0.23	0.27	0.23
30.0	0.19	0.25	0.25	0.26	0.25
20.0	0.26	0.27	0.26	0.24	0.24
10.0	0.25	0.25	0.21	0.28	0.26

Table C-5. Suctions for low evaporation test

	Tensiometer Location	Day 0	Day 7	Day 14	Day 21	Day 28	Day 39	Day 46	Day 53	Day 60	Day 67	Day 74	Day 80
Column 1	Above interface	11.5	11.5	12.0	12.0	12.5	11.5	11.0	10.0	9.0	fail	fail	fail
	Below interface	9.0	fail	fail	fail	fail	fail	fail	fail	fail	fail	fail	fail
Column 2	Above interface	10.0	10.0	10.0	11.0	11.0	10.0	9.5	9.5	fail	fail	fail	fail
	Below interface	9.0	9.0	9.0	9.0	fail	fail	fail	fail	fail	fail	fail	fail
Column 3	Above interface	11.0	fail	fail	fail	fail	fail	fail	fail	fail	fail	fail	fail
	Below interface	10.0	10.0	10.5	10.5	10.0	9.5	9.0	9.0	8.0	8.0	8.0	8.0
Column 4	Above interface	fail	fail	fail	fail	fail	fail	fail	fail	fail	fail	fail	fail
	Below interface	9.0	9.0	9.0	fail	fail	fail	fail	fail	fail	fail	fail	fail

Table C-6. Suctions for high evaporation test

	Tensiometer Location	Day 0	Day 3	Day 7	Day 11	Day 14	Day 21	Day 26	Day 31
Column 1	Above interface	11.0	11.0	8.0	12.0	14.0	14.0	13.0	11.5
	Below interface	9.5	9.5	10.0	10.0	9.0	11.0	10.0	9.0
Column 2	Above interface	10.5	10.5	9.0	14.0	15.0	18.0	17.0	14.0
	Below interface	9.0	9.0	8.0	9.5	8.5	8.0	8.0	8.0
Column 3	Above interface	11.0	8.0	4.0	4.0	5.0	4.0	4.0	4.0
	Below interface	10.0	10.0	10.0	11.5	12.0	14.0	12.0	10.0
Column 4	Above interface	12.0	12.0	10.0	20.0	25.0	fail	fail	fail
	Below interface	9.5	10.0	10.0	10.5	11.0	11.0	10.5	10.0